

# **Modelling Urban Travel Times**

Fangfang Zheng



# **Modelling Urban Travel Times**

## **Proefschrift**

ter verkrijging van de graad van doctor  
aan de Technische Universiteit Delft,  
op gezag van de Rector Magnificus prof.ir. K.C.A.M. Luyben,  
voorzitter van het College voor Promoties,  
in het openbaar te verdedigen op dinsdag 12 juli 2011 om 10:00 uur

door

Fangfang ZHENG (郑芳芳)

Master of Science in Traffic Engineering, Southwest Jiaotong University, Chengdu  
geboren te Pujiang, Zhejiang Province, P.R. China

Dit proefschrift is goedgekeurd door de promotor:

Prof. dr. H.J. Van Zuijlen

Samenstelling promotiecommissie:

Rector Magnificus	Voorzitter
Prof. dr. H.J. van Zuijlen	Delft University of Technology, promotor
Prof. dr. ir. S.P. Hoogendoorn	Delft University of Technology
Prof. dr. ir. B. van Arem	Delft University of Technology
Prof. dr. B. Hellinga	University of Waterloo
Prof. dr. P. Vortisch	Karlsruhe University
Dr. ir. C. van de Weijer	Eindhoven University of Technology
Dr. F. Viti	Katholieke Universiteit Leuven

This dissertation is the result of a Ph.D. study carried out from 2008 to 2011 at Delft University of Technology, Faculty of Civil Engineering and Geosciences, Transport & Planning Department. The research was supported by the Universiteits fonds Delft, Chinese Scholarship Council and Southwest Jiaotong University, China.

**TRAIL Thesis Series T2011/9, the Netherlands TRAIL Research School**

TRAIL  
P.O.Box 5017  
2600 GA Delft  
The Netherlands  
Phone: +31 (0) 152 786 046  
Fax: +31 (0) 152 784 333  
E-mail: [info@rsTRAIL.nl](mailto:info@rsTRAIL.nl)

ISBN: 978-90-5584-145-5

Copyright © 2011 by Fangfang Zheng

All rights reserved. No part of the material protected by this copyright notice may be reproduced or utilized in any form or by any means, electronic or mechanical, including photocopying, recording or by any information storage and retrieval system, without written permission from the author.

Printed in the Netherlands

Dedicated to my parents



# Preface

In March 2008, I started my PhD research in Delft University of Technology. I was first planning to do just one year research in the Netherlands, then go back to China and finish my PhD study in Southwest Jiaotong University, Chengdu. During the first year, my promoter, Professor Henk van Zuylen discussed with me about the possibilities to continue in TUD. Now, I'm glad that I made a wise decision to finish my PhD research here.

The PhD life in Delft is absolutely a wonderful and precious experience. I enjoyed many, many things here: independent research, free discussion, training courses (especially TRAIL courses), visiting conferences, and also many times nice dinner with colleagues and friends which we had so much fun every time. Here, I would like to take this opportunity to thank my colleagues and friends.

First of all, I would like to express my gratitude to my dear promoter, Henk. I am so happy that you chose me as your PhD student. I still remember that four years ago I sent you an email to ask whether I could do my PhD research in your group. You replied very fast and the answer is 'yes', which made me so excited. Through my PhD research, you put so much effort discussing about problems I encountered. You always give me very useful advice and deep insight into a problem. You always support me and give me confidence, especially when writing my thesis. Without your support, I would not be able to finish my thesis with the same quality. From you, I learned that a person can be so energetic both in his work and life. I would also like to thank other committee members for their useful comments and suggestions on my thesis. In particular, the detailed comments from Francesco Viti and Bruce Hellinga are very helpful.

Special thanks to Changsha Science and Technology Commission for providing me with field data such that my research results are more convincing for real life application.

During my stay in TUD, I got to know colleagues at Transport and Planning. We had many times nice discussion about research and other topics (culture, food, politics, etc.). I would like to give my special thanks to Adam and Erik Sander. Adam, thank you very much for helping me with the translation of the English summary into Dutch. We had very nice conversation about different topics which I enjoyed very much. Erik Sander, thank

you for translating my propositions. Kees, thank you for helping repair my stuff (bicycle, laptop). Nicole, Dehlaila and Priscilla, thank you for your daily support in the office. I would also like to thank my Chinese colleagues and friends (Yusen, Hao&Huizhao, Meng&Yanyan, Yufei, Jie (Lucas), Jie (girl), Feifei, Yaqing, Haiyang & Ran, Hui) for their help through these years.

I would like to thank my (former) roommates: Claire, Tamara, Yufei, Jie (Lucas) and Feifei. I feel very comfortable working in room 4.19. Claire, thank you for helping me with English words. I would like to apologize that we talked too much Chinese though we tried to talk in English more often.

Finally, I would like to thank my family. I'm really lucky that I have a very nice family. Thank you so much for your love, understanding, encouraging and tolerance. Without your support, I will not be able to finish my PhD.

Fangfang Zheng

Delft, July 2011

# Contents

<b>Preface</b>	<b>i</b>
<b>Contents</b>	<b>iii</b>
<b>List of Notations</b>	<b>vii</b>
<b>1 Introduction</b>	<b>1</b>
1.1 Problem statement .....	1
1.2 Research questions and objectives .....	7
1.3 Research scope .....	9
1.4 Main Research contributions .....	10
1.4.1 Scientific contributions .....	10
1.4.2 Practical relevance .....	11
1.5 Thesis outline .....	12
<b>2 State-of-the-Art of Travel Time Modelling on Urban Signalized Roads</b>	<b>15</b>
2.1 Introduction .....	15
2.2 Urban travel time estimation and prediction .....	16
2.2.1 Model-based methods .....	17
2.2.2 Data-driven approaches .....	21
2.3 Delays on urban signalized roads .....	25
2.3.1 Delay models for signalized intersections .....	26
2.3.2 Delay variability at signalized intersections .....	34
2.4 Travel time distribution models .....	36
2.5 Summary .....	37
<b>3 Measuring urban travel times</b>	<b>39</b>
3.1 Introduction .....	39
3.2 Empirical methods of measuring urban travel times .....	40
3.2.1 Automatic Number Plate Recognition (ANPR).....	40
3.2.2 Probe vehicles (GPS/Mobile phone).....	41
3.2.3 Bluetooth.....	45

3.3 Comparison of urban link travel time estimation models based on probe vehicle data (PVD) .....	49
3.3.1 Link travel time allocation.....	49
3.3.2 Description of Link travel time estimation models .....	51
3.3.3 Experimental setup .....	55
3.3.4 Sensitivity analysis in Hellinga's model.....	58
3.3.5 Results.....	59
3.3.6 Conclusions.....	63
3.4 Summary and discussions .....	64
<b>4 Delay distribution for signalized intersections</b> .....	<b>67</b>
4.1 Introduction .....	67
4.2 Delay distribution at signalized intersections.....	68
4.2.1 Delay distribution in the undersaturated condition with a fixed overflow queue .....	68
4.2.2 Delay distribution in the oversaturated condition with a fixed overflow queue.....	70
4.2.3 Delay distribution with a stochastic overflow queue.....	74
4.2.4 Comparison between the Poisson arrival and Binomial arrival processes .....	76
4.2.5 Comparison between the delay model and VISSIM simulation in undersaturated conditions.....	77
4.3 Delay uncertainty at signalized intersections .....	79
4.4 Summary .....	81
<b>5 Model development for urban travel time distribution</b> .....	<b>83</b>
5.1 Introduction .....	83
5.2 Travel time distribution for a link with one signalized intersection.....	84
5.2.1 Definition of the link travel time .....	84
5.2.2 Components of urban link travel time .....	84
5.2.3 Derivation of a single link travel time distribution.....	85
5.2.4 Comparison with VISSIM .....	86
5.2.5 Comparison with field data.....	87
5.3 Travel time distribution for an urban corridor.....	92
5.3.1 Basic notations and assumptions .....	92
5.3.2 Delay at two adjacent intersections .....	94
5.3.3 Travel time distribution for two adjacent intersections .....	100
5.3.4 Trip travel time distribution.....	109
5.3.5 Comparison with VISSIM simulation .....	111
5.4 Conclusions and discussion.....	116
<b>6 Urban travel time distribution estimation based on traffic measurements</b> .....	<b>119</b>
6.1 Introduction .....	119
6.2 Parameter estimation methods for the delay distribution model.....	120
6.2.1 Parameters in the delay distribution model.....	120
6.2.2 Parameter estimation methods.....	121

6.3	Experiment setup .....	124
6.3.1	Scenarios .....	124
6.3.2	Simulation runs .....	124
6.3.3	Sampling strategies for ground truth simulation data .....	125
6.3.4	Implementation of GA .....	126
6.3.5	Performance measures .....	126
6.3.6	Results .....	127
6.4	Conclusions and discussion .....	133
<b>7</b>	<b>Application of the model for link travel time distribution prediction</b>	<b>135</b>
7.1	Introduction .....	135
7.2	Methodology .....	136
7.2.1	Traffic flow prediction .....	136
7.2.2	Cycle length and green split prediction using a Neural Network model .....	136
7.2.3	Link travel time distribution prediction .....	138
7.3	Experiment with VISSIM simulation data .....	139
7.3.1	Experiment setup .....	139
7.3.2	Results .....	140
7.4	Experiment with field data .....	143
7.4.1	Data preparation .....	143
7.4.2	Cycle time and green splits prediction using SCATS data .....	144
7.4.3	Results .....	144
7.5	Conclusions and discussion .....	150
<b>8</b>	<b>Conclusions and future research</b>	<b>153</b>
8.1	Conclusions .....	153
8.1.1	Conclusions from the state-of-the-art review .....	153
8.1.2	Empirical analysis of urban travel times .....	154
8.1.3	New insight into travel time variability .....	155
8.1.4	Urban travel time distribution model .....	156
8.1.5	Model calibration .....	156
8.1.6	Model validation .....	157
8.1.7	Model prediction .....	158
8.2	Practical usability of the results .....	159
8.3	Policy implications .....	159
8.4	Recommendation for future research .....	160
8.4.1	Recommendation for model development .....	160
8.4.2	Recommendation for model calibration and validation .....	161
8.4.3	Recommendation for research direction .....	161
	<b>Bibliography</b>	<b>163</b>
	<b>Appendix</b>	<b>173</b>

<b>A</b>	<b>GPS position and speed accuracy</b>	<b>173</b>
A.1	GPS position accuracy <sup>1</sup> .....	173
A.2	GPS speed accuracy.....	177
<b>B</b>	<b>Formulation of overflow queue distribution</b>	<b>179</b>
<b>C</b>	<b>Derivation of boundary delays in the trip travel time distribution function in oversaturated conditions</b>	<b>181</b>
C.1	Mismatch 1 (early green).....	181
C.2	Mismatch 2 (late green).....	188
<b>D</b>	<b>Comparison of link travel time in case of a vertical queue and shock wave</b>	<b>191</b>
D.1	Delay calculation in case of shock wave.....	191
D.2	Comparison of link travel time between a vertical queue and shock wave.....	195
<b>E</b>	<b>Test area</b>	<b>199</b>
<b>F</b>	<b>Complete link travel time estimation from GPS data</b>	<b>201</b>
	<b>Summary</b>	<b>203</b>
	<b>Samenvatting</b>	<b>207</b>
	<b>Summary (Chinese)</b>	<b>211</b>
	<b>About the author: curriculum vitae and list of publications</b>	<b>215</b>
	<b>TRAIL Thesis Series</b>	<b>219</b>

# List of Notations

## Statistical symbols

MAPE	: Mean Absolute Percentage Error
RMSE	: Root Mean Square Error
MSE	: Mean Square Error

## Abbreviations

ANPR	: Automatic Number Plate Recognition
GPS	: Global Positioning System
ANN	: Artificial Neural Network
MEMS	: Micro-Electro-Mechanical System
CTM	: Cell Transmission Model
ARMA	: Autoregressive Moving Average
ARIMA	: Autoregressive Integrated Moving Average
K-NN	: K-Nearest Neighbour
LOWESS	: Locally Weighted Scatter plot Smoothing
SSNN	: State Space Neural Network
HCM	: Highway Capacity Manual
CoV	: Coefficient of Variation
MAC	: Machine Access Control
PVD	: Probe Vehicle Data
DTA	: Dynamic Traffic Assignment
RS	: Random Sampling
LHS	: Latin Hypercube Sampling
LS	: Least Squares
ML	: Maximum Likelihood
GA	: Genetic Algorithm
KS	: Kolmogorov-Smirnov
SCATS	: Sydney Coordinated Adaptive Traffic System
SCOOT	: Split, Cycle and Offset Optimisation Technique
DS	: Degree of Saturation

## Symbols, variables and parameters

$TT$	: travel time
$TT^{O-D}(t)$	: travel time from origin O to destination D at the departure time instant $t$
$TT_f$	: free flow travel time
$TT_f^{i \rightarrow i+1}$	: free flow travel time from the upstream intersection $i$ to the downstream intersection $i+1$
$D_q^i(t)$	: queuing delay encountered by the vehicle arriving at intersection $i$ at time instant $t$
$D_s^i(t)$	: signal delay encountered by the vehicle arriving at intersection $i$ at time instant $t$
$t_{arrive}^i$	: arrival time instant at intersection $i$
$t_{departure}^i$	: departure time instant from intersection $i$
$N_i$	: holding capacity of cell $i$
$n_i(t)$	: number of vehicles in cell $i$ waiting to enter cell $i+1$ at time step $t$
$N_Q$	: number of vehicles in queue
$q_i(t)$	: inflow into cell $i$ at time step $t$
$Q_i$	: inflow capacity of cell $i$
$d_i(t)$	: total delay in cell $i$ at time step $t$
$d_u$	: average delay in the undersaturated condition
$d_o$	: average delay in the oversaturated condition
$d_1$	: uniform delay
$d_2$	: incremental delay accounting for the stochastic arrivals and oversaturation queues
$d_3$	: residual delay for oversaturation queues that may have existed before the analysis period
$f_{PF}$	: progression adjustment factor accounting for signal coordination
$f_r$	: adjustment factor for residual delay
$f_P$	: adjustment factor for situations when platoon arrives during the green interval
$P$	: proportion of vehicles arriving during the effective green interval
$P_1, P_2, P_3$	: percentage positions on links 1, 2 and 3, respectively
$k$	: traffic density
$k_j$	: jam density
$L_Q$	: the length of queue
$L_m$	: maximum queue length
$L$	: length of link/road segment
$u_f$	: free flow speed
$q$	: arrival rate
$s$	: saturation flow rate
$\tau_r$	: effective red time
$\tau_g$	: effective green time
$\tau_C$	: cycle time
$\tau_i$	: travel time of target vehicle $i$
$tt_{ik}$	: time difference between the target vehicle $i$ and the following vehicle $k$
$\Delta_c$	: tolerance time
$c = s \cdot \tau_g / \tau_C$	: signal capacity

---

$\lambda$	: effective green to cycle time ratio
$x$	: degree of saturation
$x_{min}$	: minimum of (1.0, $x$ )
$x_{max}$	: maximum of (1.0, $x$ )
$I$	: variance-to-mean
$T$	: evaluation time period
$A(t)$	: cumulative number of arrivals during period [0, t]
$D(t)$	: cumulative number of departures during period [0, t]
$W(k)$	: average delay during cycle $k$
$W_1(k)$	: total delay accumulated within cycle $k$ by all vehicles arriving during cycle $k$ and vehicles already waiting at the intersection at the start of cycle $k$
$W_2(k)$	: total delay experienced by only vehicles waiting at the intersection at the beginning of cycle $k$
$W_3(k)$	: total delay experienced by vehicles arriving during cycle $k$ and caused by the presence of the residual queue
$Q_k$	: overflow queue at cycle $k$
$Q(t)$	: overflow queue at time $t$
$Q_0$	: overflow queue
$Q_e$	: equilibrium value of queue under steady-state conditions
$P(Q=j, t)$	: probability of observing queue $j$ at time $t$
$H_{ij}$	: transition matrix
$\alpha(t), \beta(t), \gamma(t)$	: time-dependent parameters in Van Zuylen-Viti model
$\alpha, \beta$	: parameters in the delay distribution model
$\eta$	: coefficient vector
$\theta$	: parameter matrix
$\mu$	: mean value
$\sigma$	: variance
$\varepsilon$	: error term
$X(\cdot)$	: input layer in the neural network model
$H(\cdot)$	: hidden layer
$Y(\cdot)$	: output layer
$L(\cdot)$	: likelihood function
$W(t/n)$	: delay at time instant $t$ given certain queue $n$
$n_0$	: initial overflow queue
$n$	: number of vehicles in the queue
$\delta(\cdot)$	: Dirac delta function
$B(\cdot)$	: box shaped function in the delay distribution model
$P_d(\cdot)$	: delay probability function
$P_f(\cdot)$	: free flow travel time probability function
$P(t)$	: probability of travel time $t$
$P(W/n_0)$	: probability of delay $W$ given an deterministic overflow queue $n_0$
$P(n_0)$	: probability of queue $n_0$

$P_m$	: probability distribution of measured delays
$D_U$	: delay uncertainty
$N$	: number of extra red time an arriving vehicle needs to wait at an intersection
$N_{min}$	: minimum number of extra red time an arriving vehicle needs to wait at an intersection
$N_{max}$	: maximum number of extra red time an arriving vehicle needs to wait at an intersection
$\tau_{off}$	: offset between two signalized intersections
$\tau_m$	: mismatch time between two intersections in case of signal coordination
$t_n$	: transition moment within one cycle when vehicles need to wait extra $n$ red times

# Chapter 1

## Introduction

### 1.1 Problem statement

Over the past decades, traffic congestion has increased significantly both on freeways and urban road networks. As a consequence, travellers experience higher travel times during their daily commuting activities and fuel consumption has increased due to traffic congestion. The urban mobility report 2009 (Schrank et al., 2009) shows that in 2007, congestion caused urban Americans to travel 4.2 billion hours more and to purchase an extra 2.8 billion gallons of fuel for a congestion cost of \$87.2 billion – an increase of more than 50% over the previous decade. These negative aspects of traffic congestion have been receiving a lot of attention. Therefore, different traffic management strategies, for instance, ramp metering, peak lanes, speed limit, traffic signal control at intersections, traveller information system, have been applied to improve traffic conditions both on freeways and urban roads. One important quality of mobility on the road network is the travel time. On one hand, the total travel time of vehicles can be used to reflect the performance of road networks and is of great interest for the road authorities who are trying to improve the mobility on the road network level. On the other hand, individual travel time is an important quality of a journey for travellers who need to make decisions on their choices, e.g. route choice, mode choice and departure time choice.

Different monitoring techniques, for instance, Automatic Number Plate Recognition (ANPR) camera, Bluetooth scanners, mobile sensors (GPS integrated in-car devices, mobile phones, etc.), speed sensors (e.g., radar detectors) have been applied to measure travel times over the last decades. Some of these techniques (e.g., ANPR, Bluetooth devices) have been proved to be very promising, especially on freeways (Bertini et al., 2005; KMJ Consulting, 2010; Yegor et al., 2010). Mobile sensors, especially GPS equipped probe vehicles, have been widely used to collect traffic information both on freeways and urban roads in recent years. At the meantime, scientists have proposed

different mathematical models to estimate travel times (Chu et al., 2005; OH et al., 2003; Vanajakshi et al., 2009; Yeon et al., 2008) or predict travel times (Clark, 2003; Innamaa, 2005; van Hinsbergen et al., 2009; van Lint, 2004; You et al., 2000) and these models perform quite well on freeways. However, compared with freeways, very few models have been developed for urban networks and most estimation or prediction results are not so satisfactory (Liu, 2008). The reason behind this is that the traffic mechanisms on urban roads are very different from those on freeways. Traffic flows on freeways are often treated as uninterrupted flows, while traffic flows on urban roads are in general interrupted flows. Travel time varies with the fluctuations in traffic demand (e.g. due to time of day, day of the week, weather, seasonal effects, population characteristics, traffic information and user responses) and supply (e.g. due to incidents, road works, weather conditions, road geometry) on freeways, while on urban arterials, besides the fluctuations in traffic demand and supply, travel time can be influenced by other factors. Figure 1.1 schematically describes factors contribute to the travel time on the urban signalized roads.

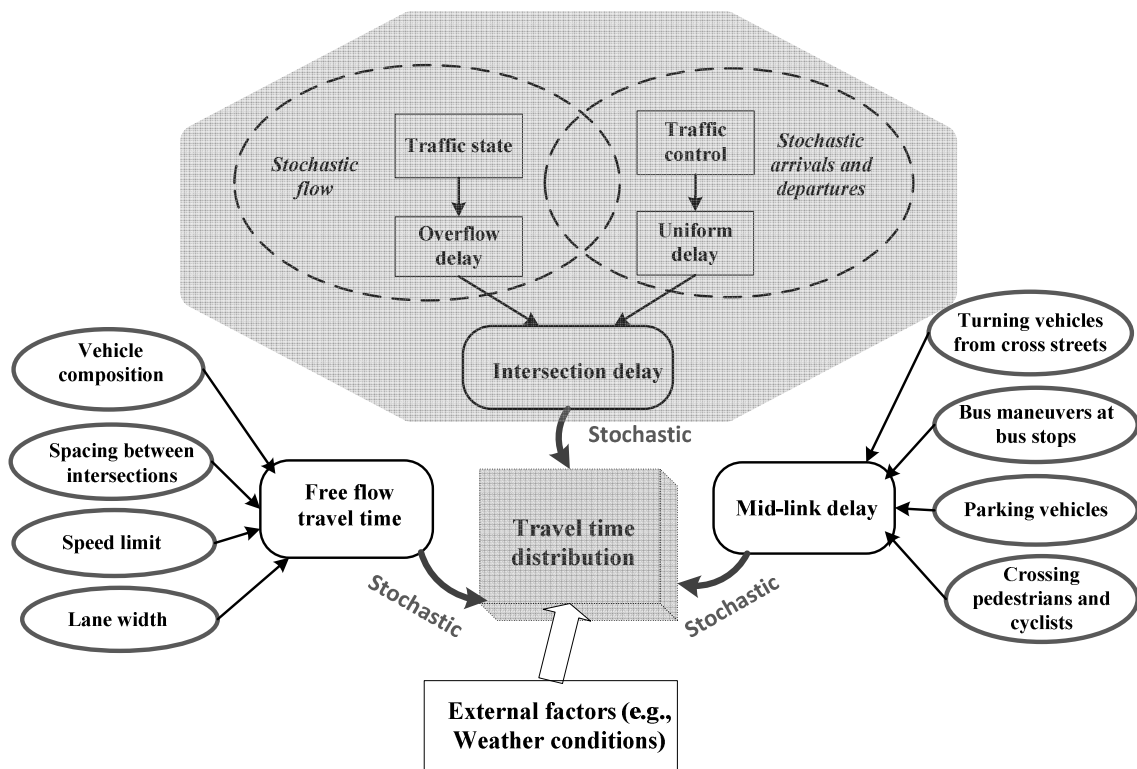


**Figure 1.1: Schematic representation of factors contributing to the link travel time on the urban road**

Travel times vehicles experience on the urban road can be decomposed into free flow travel times and delays. Vehicles travelling on the urban road are subject to intersection delays due to queues and traffic control and mid-link delay caused by turning vehicles from cross streets, bus manoeuvres at bus stops, parking vehicles along the roadside, crossing pedestrians and cyclists, etc. However, intersection delays vary with effects of stochastic properties of traffic flow, stochastic arrivals and departures at the signalized

intersection and variations in the traffic control. These partly stochastic factors are not independent but rather overlap. As a result, delays are uncertain given known traffic condition (traffic flow) and traffic control. The free flow travel time is basically determined by the distance and the free flow speed. The free flow speed is determined by the speed limit, vehicle composition, spacing between intersections, lane width (TSENG et al., 2005). Therefore, the free flow travel time is not a constant value but variable given known travel distance. The result of all these factors is that for a given link or route within a certain time period, travel times are variable and a certain travel time distribution can be observed.

Figure 1.2 illustrates the empirical travel time-flow relationship derived from local 10min aggregated measurements of time-mean flow and median travel time for each 10min on an urban arterial road 'Kruithuisweg' in March 2010 in the Netherlands. There is almost no influence of public transit, cyclists and pedestrians since no bus stops, bicycle lanes and pedestrian lanes were designed along the road. The delay vehicles experienced on this road is mainly caused by intersections. The region 'A' illustrates the uncongested condition and region 'B' shows the oversaturated condition. It can be clearly seen in the Figure 1.2 that there is no one-one correspondence relationship between travel time and flow over the whole range of traffic flow. Even in the uncongested condition (region 'A'), for a certain traffic flow, there is a big range of travel time corresponding to it. In the congested condition, a large variation of travel times can be observed. The variation of travel times in Figure 1.2 can be attributed to the factors discussed above. Many of these factors are stochastic, which result in variable travel times. Among all these factors, traffic control has a special effect on the variability of travel times as illustrated in Figure 1.3. Two consecutive vehicles that enter the network at nearly the same time can have completely different travel times when the first vehicle just passes an intersection in the end of the green phase and the following vehicle has to stop. This may have impact on the delay at next intersections so that the first vehicle may have a much shorter travel time than the second one. This gives bifurcation (van Geenhuizen et al., 1998) in the development of the status of vehicles: even when the initial status is the same, the development of the status in time can be very different.

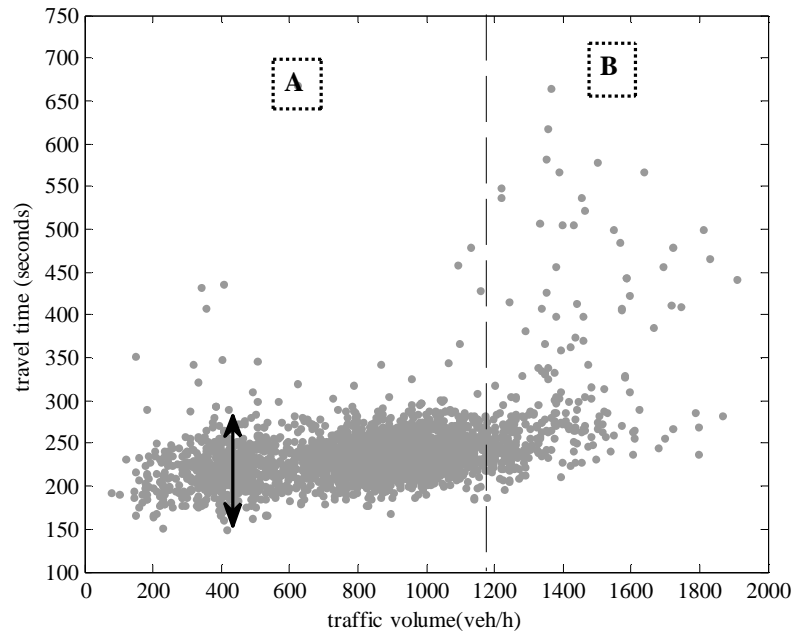


**Figure 1.2: Travel time-outflow relationships on an urban arterial road ‘Kruithuisweg’ in March 2010 (Flow and travel time are both measured in 10min aggregation) in the Netherlands.**

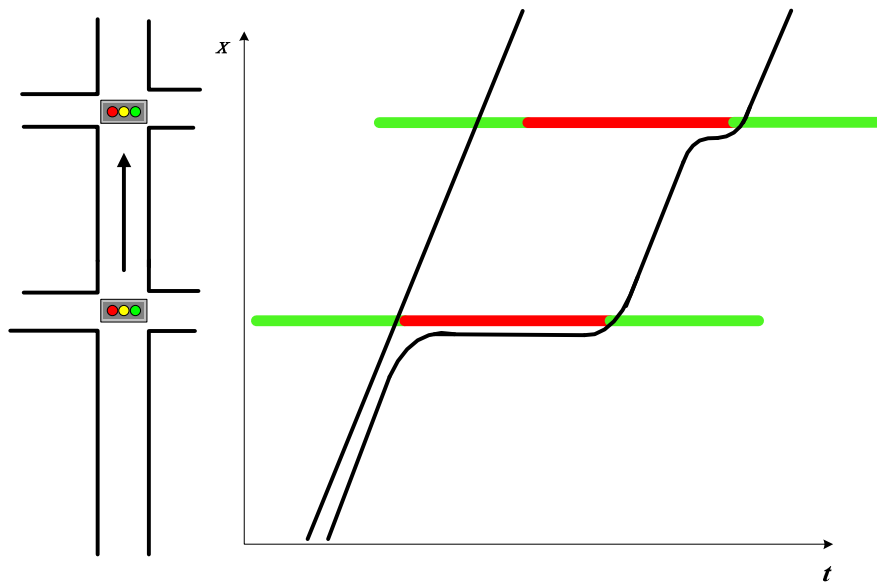


**Figure 1.3: Bifurcation phenomenon of vehicles passing signalized intersections**

A thorough analysis of all these factors influencing travel time variability seems impossible so far. If the frequency of bus manoeuvres at stops is known and also the frequency of parking manoeuvres, the effect on link travel times can be determined by analytical models, simulations or heuristic methods like Artificial Neural Networks (ANN). The time spent in queues is less predictable because the queue length at arrival on a link is not deterministic. The stochastic character of the arrivals makes it difficult or even unfeasible to predict the queue length for a longer time horizon (van Zuylen et al.,

2007; Viti, 2006). In the case that the traffic condition is undersaturated and there is no initial queue, depending on the arrival moment at the signalized intersection, the effect of the traffic control is basically that vehicles have delays that are nearly uniformly distributed between zero second and the duration of the red phase. As a result, what we can observe in urban travel time is three time scales, corresponding to the following three different mechanisms:

1. Slow variations with a time scale of about ten to twenty minutes, corresponding to variations on the average traffic flow (Figure 1.4);
2. Medium fast variations with a time scale of minutes, corresponding to stochastic variations in the arrivals at bottlenecks and corresponding overflow queues (Figure 1.5);
3. Fast variations in the time scale of seconds, caused by the random arrival moment at the signalized intersections. As shown in Figure 1.6, the difference between the maximum travel time and minimum travel time can be as large as 162 seconds even within a small departure time period of 1min.

As discussed in (van Hinsbergen et al., 2009), travel times can be de-noised as the ‘underlying trend’ travel times (low-frequency component) and noisy travel times (high-frequency component). The method proposed by these authors can better predict the so-called ‘underlying trend’ urban travel times. However, the so-called noisy component of travel times is probably caused by the random arrival moment at the signalized intersections and stochastic variations in the arrivals at bottlenecks and corresponding overflow queues, which is yet a challenging subject for research.

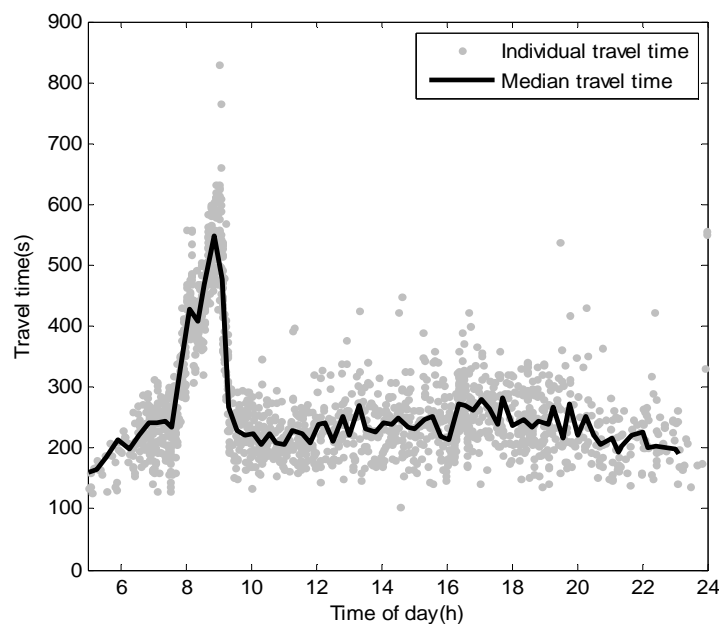


**Figure 1.4: Slow variation of travel time with 15 min aggregation. The individual travel times are collected from an urban arterial road ‘Kruithuisweg’, the Netherlands on March 2<sup>nd</sup>, 2010**

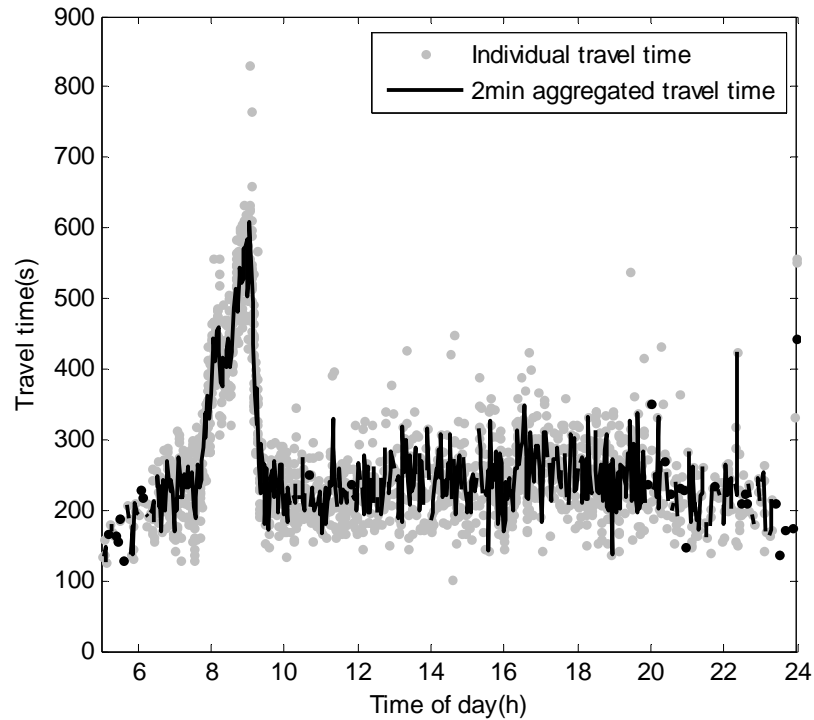


**Figure 1.5: Median fast variation of travel time with 2min aggregation. The individual travel times are collected from an urban arterial road ‘Kruithuisweg’, the Netherlands on March 2<sup>nd</sup>, 2010**

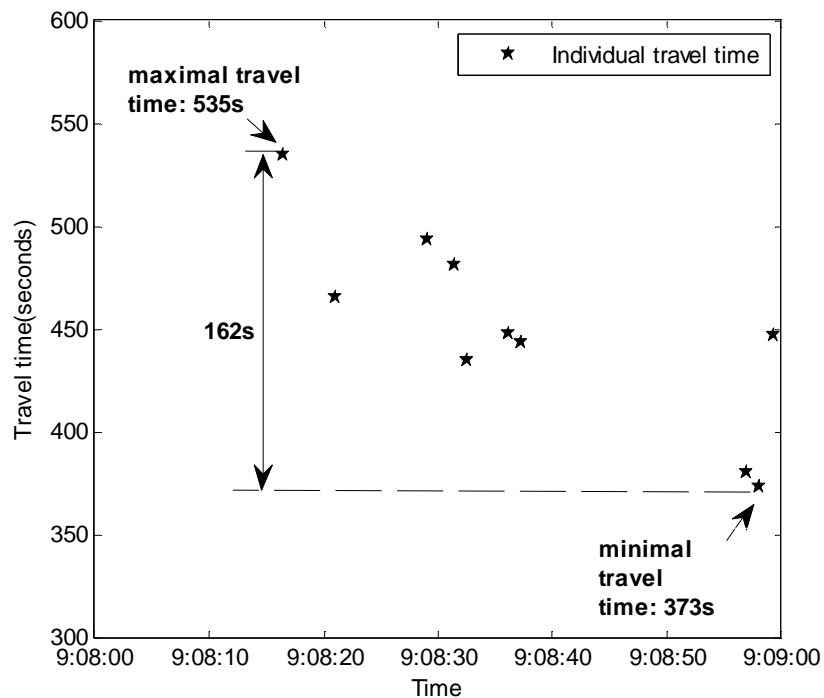


**Figure 1.6: Fast variation of travel time within a small departure period of 1 minute from 9:08AM to 9:09 AM. The individual travel times are collected from an urban arterial road ‘Kruithuisweg’, the Netherlands on March 2<sup>nd</sup>, 2010**

The importance of travel time variability (uncertainty) in urban networks has received a lot of attention during past years. As suggested by Bates (Bates et al., 2001), for many travellers, the reduction in variability of travel time is as important as, if not more important than, the reduction in expected travel time. However, the investigation of travel time variability as done by most researchers is just in a phenomenological way by calibrating some distribution functions (e.g., log-normal, Gamma) with observed travel times. The problem arises when applying these distributions to different traffic conditions since they are only calibrated for a certain traffic condition. The character of urban travel times is represented by a specific distribution which can be influenced by different traffic processes (e.g., traffic flow, traffic control). The understanding of fundamental mechanisms of urban travel times can help better deal with travel time variability, predict travel time variability and furthermore influence travel time variability. Therefore, it is important to develop a theoretical travel time distribution model which can explain these mechanisms and can be generalized for different traffic conditions. This thesis focuses on the investigation of the travel time and its variability based on an analytical travel time distribution model, furthermore, estimating and predicting the travel time distribution for urban signalized arterials. As for urban arterials, a large part of travel time uncertainty is due to the uncertainty of delays at intersections. By analysing the stochastic properties of traffic flows, stochastic arrivals and departures at intersections and signal control, a better understanding of travel time uncertainty on urban arterials can be achieved. The knowledge of travel time uncertainty (variability) can help different types of travellers make better route choice for different purposes. Risk-averse travellers tend to choose more reliable routes even if they have higher travel times. For opportunity-seekers, routes with lower travel times but higher uncertainty are more appealing.

The remainder of this chapter is organized as follows. The research questions and objectives are specified in section 1.2. Section 1.3 defines the research scope in this dissertation. Then, the main contributions to the existing knowledge and practical relevance are described in section 1.4. Finally, the outline of this thesis is given in section 1.5.

## 1.2 Research questions and objectives

This thesis focuses on the development of an analytical travel time distribution model, calibrating and validating the model and furthermore, applying this model for prediction. In this section, research questions are given and each research question is followed by the research objective.

Observed travel times are essential for solid calibration and validation of any travel time estimation or prediction models. During the past decades, different monitoring techniques have been applied for monitoring road traffic. This raises our first research question:

**Research question 1:** Regarding many different monitoring techniques, are these monitoring techniques qualified for measuring urban travel times?

In order to answer this question, we set our research objective as:

**Research objective 1:** Investigate different monitoring techniques and specify their advantages and disadvantages in terms of measuring urban travel times.

Among all travel time measuring techniques, probe vehicles with GPS as monitoring sensors has become a popular technique to obtain information about travel times. . However, very little research has been devoted to look into detailed problems with measuring urban travel times, e.g., travel times derived from two GPS measurements are usually not complete link travel times or route travel times. Then our second research question comes up:

**Research question 2:** How can we use GPS measurements to derive complete link or route travel times?

**Research objective 2:** Develop a model to estimate complete link travel times based on GPS data and compare this model with other existing models.

From field travel time data, we can observe that urban travel times are very variable. In most research about travel time distribution, a single statistical distribution or a combination of different distributions is usually applied to fit field travel time data(EL FAOUZI et al., 2006; Guo et al., 2010). There is no physical meaning about these distributions. Therefore the third research question is as follows:

**Research question 3:** Travel times are very variable on urban signalized roads, how can we model travel time variability in an analytical way such that it can be applied to describe travel time distributions for different traffic conditions?

**Research objective 3:** Develop *travel time distribution* models for a single link as well as for an urban corridor and investigate travel time variability based on travel time distribution models.

The traffic process on an urban road is rather stochastic. The number of vehicles arriving at the intersection within a certain time period is not constant but rather variable. Besides, vehicle arrival moments at the intersection are not deterministic as well. Therefore, our research question is formulated as:

**Research question 4:** Do these stochastic properties of traffic flow, stochastic arrivals and departures influence the travel time variability? If so, how do these factors influence travel time variability?

**Research objective 4:** Investigate the impact of different arrival processes and stochastic capacities on the travel time variability under different traffic conditions.

Traffic is interrupted by signal control at intersections on urban roads. Vehicles need to wait at the intersection when the traffic light is red. This causes delay to arriving vehicles

at the intersection. Besides, vehicles passing the upstream intersection either can pass the downstream intersection without delay or vehicles need to wait at the downstream intersection due to the queue or traffic control (red phase). This puts forward our fifth research question:

**Research question 5:** How does signal control influence the travel time distribution for an urban corridor?

**Research objective 5:** Model the impacts of signal coordination on the travel time distribution for different traffic conditions.

Modelling dynamics of queues at intersections is still a challenging topic. Queues are not deterministic but rather stochastic as already discussed by (Viti, 2006). For a given traffic condition and traffic control, a queue distribution can be observed. The queue has a direct impact on the delay and therefore on the travel time. In undersaturated conditions, the overflow queue distribution can be derived analytically and there is always an equilibrium distribution which can be achieved by a certain time period, regardless of the initial condition (e.g., no overflow queue or a certain length of the overflow queue). However, in oversaturated conditions, the queue distribution is rather time dependent and no equilibrium distribution exists. Then, the related research question is:

**Research question 6:** Can we estimate the overflow queue distribution from sample travel time measurements and furthermore reconstruct the travel time distribution?

**Research objective 6:** Estimate parameters (overflow queue distribution in this case) in the travel time distribution model based on measured travel times (delays), subsequently reconstruct the travel time distribution from estimated parameters.

If a travel time distribution can be reconstructed based on the estimated parameters, then the following question is:

**Research question 7:** Can we predict travel time distribution from the network state?

**Research objective 7:** Develop a model to predict travel time distribution with sufficient accuracy for practical applicability.

### 1.3 Research scope

The previous section discussed research questions that will be tackled throughout this thesis and research objectives that need to be achieved. The aim of this section is to define the research scope.

This research focuses on urban arterials with fixed-time controlled intersections. Urban roads with dynamic controlled intersections, as well as unsignalized urban roads and urban streets with roundabouts are not addressed. However, some widely applied dynamic traffic

signal control systems, e.g., SCATS or SCOOT (SCATS, 2006; Hunt, et al., 1981), fall back to fixed time control, for instance, in peak flow situations. The variation of cycle time and green splits is small within a short time period under the similar traffic condition. Unsignalized urban roads can be modelled in a similar way, but more complicated and therefore not the subject of research yet. No special attention is given to different vehicle classes and therefore heterogeneity of traffic composition is not considered in this research.

Many factors can influence the urban travel time and its variability as discussed in section 1.1. A thorough analysis of all these factors on resulting travel times seems unrealistic. On urban signalized roads, delay at intersections constitutes a large part of the total delay vehicles experience and therefore has a significant impact on the travel time. In this thesis, the focus is on the stochastic traffic processes at intersections and traffic control on urban arterials as shown in figure 1.1 (grey hexagon box). When developing the travel time distribution model, the free flow speed is assumed not to be a constant value, but to have a certain probability distribution (e.g., normal distribution). The influence of the variation of free flow travel time on the travel time distribution is also discussed. Other factors, such as bus manoeuvres at bus stops, crossing pedestrians and cyclists, turning vehicles from cross streets, are not explicitly considered but can be included in the phenomenological free travel time distribution.

## **1.4 Main Research contributions**

### **1.4.1 Scientific contributions**

The scientific contributions of this thesis to the state-of-the-art of understanding modelling urban travel time can be summarized as follows:

The discussion and comparison between different technologies of measuring urban travel times give more insight into the application of these technologies in the urban network context. Especially with GPS probe vehicle system, the fundamental problem related to deriving complete link or route travel times from recorded time stamps of two arbitrary positions on the link/route is not explicitly addressed in most research. In chapter 3, a model to derive the complete link travel time is proposed and this model outperforms other existing models.

- A new analytical link travel time distribution model is presented. It takes into account the stochastic properties of traffic flow, stochastic arrivals and departures at the signalized intersection both for undersaturated conditions and oversaturated conditions.
- The comparison of delay (travel time) distributions with different arrival processes (Poisson, Binomial) at intersections has been performed, which provides more insights into how different arrival processes influence delay (travel time) distributions under different traffic conditions
- The delay (travel time) uncertainty analysis based on the developed delay (travel time)

distribution model provides new knowledge on the evolution of travel time uncertainty among different traffic conditions.

- An analytical travel time distribution model for an urban corridor, which takes into account of the signal coordination between consecutive intersections, is for the first time developed in this thesis. Different from other research about travel time distribution on urban roads, which mainly focuses on applying statistical distributions to the real data, the proposed model (chapter 5) provides more insight into travel time variability on urban arterials and it can be applied in different traffic conditions.
- Heuristic methods are proposed to estimate the overflow queue distribution from a sample of measured travel times. Based on the estimated queue distribution, the travel time distribution is well reconstructed using the proposed travel time distribution model.

### 1.4.2 Practical relevance

Besides the scientific contributions listed in the previous subsection, the work done in this thesis is also relevant to some practical applications, which can be elaborated in five aspects:

- ***Assessment of traffic state:*** Monitoring link/route travel times is an important topic in traffic management. Nowadays, GPS equipped probe vehicles are widely used to monitor traffic conditions. The average speed estimated from GPS data is used to reflect traffic conditions on the road in most practical applications. However, it is not the best option to use the average speed on the urban signalized roads to characterize the traffic situation. While on freeways the average speed from probe vehicles gives more useful information regarding the traffic state. The models discussed in chapter 3 and the proposed neural network model to estimate the complete link travel times from probe vehicle data provides the possibility to monitor traffic states for urban links using estimated travel times from GPS data.
- ***Travel time assessment:*** The present navigation systems provide mean travel times for urban routes based on average traffic conditions or only a few probes (e.g., Tomtom does that). The model proposed in this thesis makes it possible to give a better estimation and even prediction of the whole range of travel times and inform drivers better about routes with highest reliability.
- ***Travel time reliability:*** The travel time distribution model developed in this thesis gives the possibility to assess travel time reliability in urban areas, which is one of issues in the policy goals (at least in the Netherlands).
- ***Travel time prediction:*** Instead of predicting the mean travel time, this thesis proposes a travel time distribution prediction model which is more meaningful for the urban network with a lot of uncertainties involved.

- **Route choice models:** In route choice models, travel time reliability is considered as an important aspect which influences choice behaviour. The travel time distribution model provides the possibility to better incorporate travel time reliability into route choice models.
- **Influence uncertainty:** By understanding fundamental mechanisms of urban travel times, for instance, impacts of different traffic processes (e.g., traffic flow and traffic control) on the travel time distribution, it provides possibilities to influence the travel time distribution (uncertainty) on urban roads.

## 1.5 Thesis outline

Figure 1. 7 shows the structure of this thesis and the connection between different chapters.

Chapter 2 provides a state-of-the-art overview of modelling urban travel times. Three distinguishable yet interrelated parts of modelling urban travel times are covered in this chapter, namely, modelling delay at intersections, travel time estimation and prediction models, modelling travel time variability. Both advantages and disadvantages of these existing models or modelling approaches are discussed. Existing delay models mainly look at the expectation or standard deviation of delay, which just partially explain the delay uncertainty at intersections. Most travel time estimation or prediction models mainly estimate or predict average travel times, while they tend to overlook the variability of travel time. The stochastic properties of the traffic process on urban roads are not explicitly modelled in most cases. All these limitations in the existing models make urban travel time estimation and prediction less accurate.

Chapter 3 compares different traffic monitoring techniques for measuring urban travel times. Special attention is given to the GPS probe vehicle system. A neural network model is proposed to estimate complete link travel times from partial travel times recorded by probe vehicles. The proposed model is compared with two other models and the results show that our model outperforms the other models.

Chapter 4 describes the development of the delay distribution model for an isolated, fixed-time controlled intersection. The model considers the stochastic properties of traffic flow, stochastic arrivals and departures at intersections. Based on the delay distribution model, the delay uncertainty is investigated under different traffic conditions (from undersaturation to oversaturation).

Chapter 5 is a further extension of chapter 4. It provides an analytical travel time distribution model for an urban corridor with fixed-time controlled intersections. The model explicitly takes account of signal coordination between two consecutive intersections. Different offset settings (well-coordinated, different levels of mismatch) are

investigated under different traffic conditions. The comparison of the model and simulation results as well as the field data is presented in this chapter.

Chapter 6 proposes heuristic methods to estimate parameters (e.g., overflow queue distribution) in the travel time distribution model based on sample measured travel times. Afterwards, the travel time distribution is reconstructed using estimated parameters.

Chapter 7 describes the link travel time distribution prediction procedure and how this model is applied to predict the travel time distribution with field data.

Chapter 8 summarizes conclusions from this research and provides future research directions.

Apart from main chapters, appendixes A to D provide more detailed derivation of model equations and analysis.

Travel times derived from GPS data are used as the ground-truth in our research. The discussion of the GPS positioning and speed information accuracy is provided in Appendix A.

The delay distribution model developed in chapter 4 considers stochastic overflow queues. Appendix B provides the detailed formulation of overflow queue distribution based on Markov chain process.

In chapter 5, the delay distribution model for an urban trip is presented. The detailed derivation of boundary delays in the delay distribution function can be found in Appendix C.

Appendix D compares the formulation of link travel time function in the case of a vertical queue with that of shock wave.

Appendix E provides more detailed information about the field test area we chose for our research.

Appendix F gives the estimation process of real-life GPS travel times, which were used for the validation of the proposed model in chapter 5 and 7.

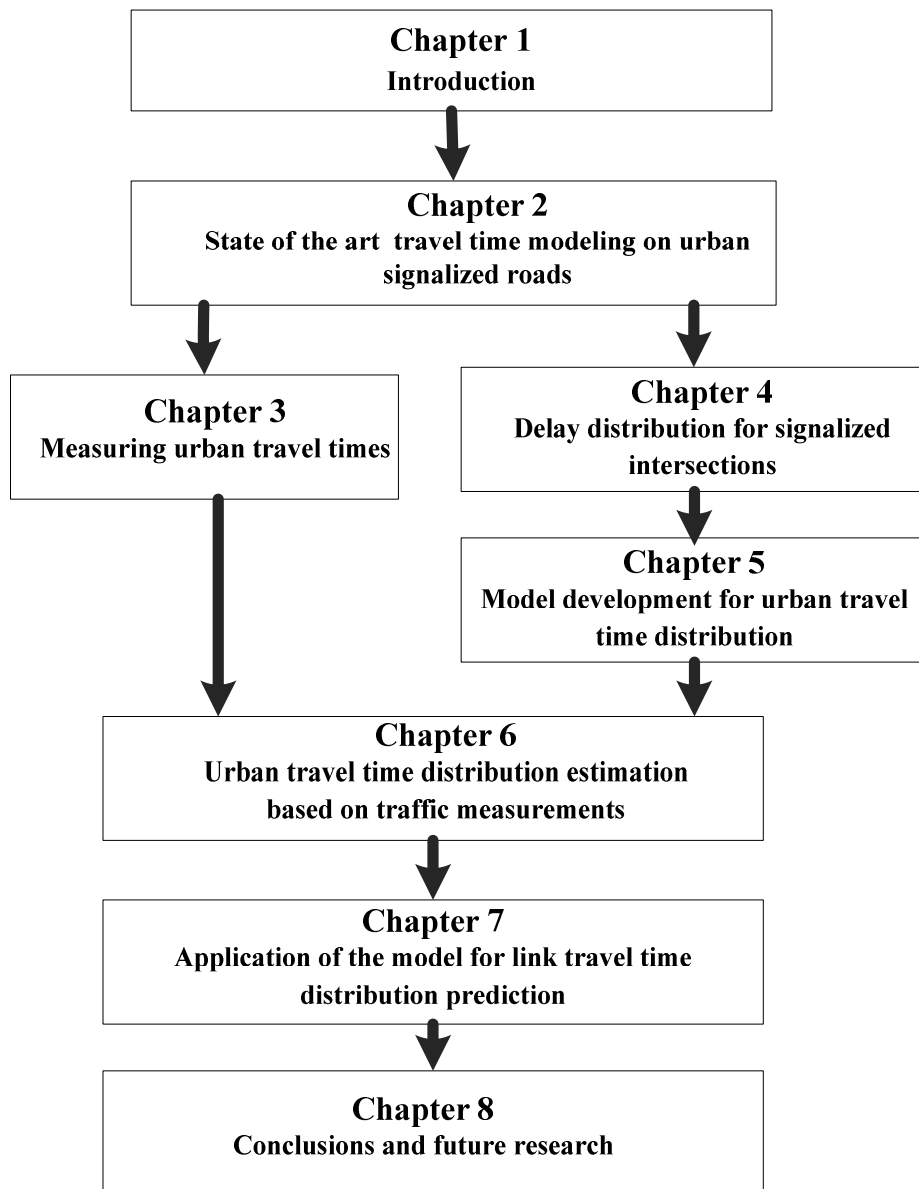


**Figure 1. 7: Outline of the thesis**

# Chapter 2

## State-of-the-Art of travel time modelling on urban signalized roads

### 2.1 Introduction

Modelling travel time on freeways has been intensively discussed in the literature, from travel time estimation and prediction models (Dharia et al., 2003; Innamaa, 2005; van Hinsbergen et al., 2008; van Lint et al., 2005; Wei et al., 2007; Yeon et al., 2008) to travel time reliability models (Asakura et al., 1991; Loustau et al., 2010; Tu et al., 2007; 2008). A lot of these models have shown relatively good results either in estimating or predicting travel times on freeways. In this thesis, the focus is on the travel time at signalized urban roads, which has attracted relatively less attention due to the increased complexity brought by the traffic process at the intersections. The traffic characteristics of urban roads are significantly different from those of freeways. The travel time is mainly determined by three distinctive elements:

1. Minimum driving time, mainly determined by the travel distance and the free flow speed characteristics;
2. Waiting time at the junction(s), determined by the traffic control imposed (signalized, unsignalized intersections or roundabouts);
3. Lost time due to secondary operations, such as parking movements, (un)loading vehicles and buses at stops, crossing pedestrians and cyclists, turning vehicles from cross streets;

The free flow speed on urban roads is mainly determined by the speed limit. It can be influenced by the vehicle composition, different driving behaviour, lane width, number of lanes, spacing between two intersections and etc. (TSENG et al., 2005; Yusuf, 2010). The mid-link delay is mainly caused by the movements of e.g. buses at bus stops, vehicles

parking along the road, pedestrians and cyclists crossing the road. The time spent in queues is determined by the queue lengths and the effective capacity of the bottleneck in front of the queue. Since this is in most cases a signalized intersection, this part of the travel time has a strong relation with traffic signals. The delay at a signalized intersection is determined by the regular process of the green and red status of the signal and by the queuing process. However, some irregular behaviour, e.g., visiting a shop during the trip along the roadside, is difficult to be modelled. This gives outliers if travel times are measured and this is one of the problems in predicting travel times from observed values.

It is widely reported that the delay at signalized intersections constitutes the largest part of the total delay in urban networks. For this reason from now on in this thesis we will focus on signalized roads. According to the above listed three elements, travel times - excluding intermediate stops for shopping etc. - on urban signalized roads can be subdivided into two parts: time spent for traversing links with desired speed and delay due to the queue process at traffic signals. Since delays at signalized intersections play a dominant role in the travel times that vehicles experience on urban roads, modeling delay is not only important for real-time traffic control but also for urban travel time estimation and prediction. In this chapter, firstly, section 2.2 gives a state-of-art overview of urban travel time estimation and prediction models and their limitations in real applications are discussed. Thereafter, section 2.3 describes analytical delay and delay variability models at signalized intersections. In section 2.4, urban travel time variability measures and urban travel time variability models are presented. Finally, section 2.5 summarizes this chapter and provides the motivations for this thesis.

## 2.2 Urban travel time estimation and prediction

In literature, researchers propose different ways of categorizing travel time estimation and prediction models. For instance, a first distinction can be made according to different traffic data sources: travel time estimation and prediction models can be classified into fixed sensor-based (e.g., loop detectors, cameras, Bluetooth), mobile sensor-based (e.g., probe vehicles equipped with GPS devices or mobile phones) and multiple data source-based (e.g., combining of the fixed sensor data and the mobile sensor data). From the modelling approach point of view, these methods can be classified into model-based methods and pure data-driven approaches. Among all, model-based methods and pure data-driven methods are two commonly used classes. Model-based methods make use of traffic flow models to estimate or predict traffic states along the route of interest. Based on the traffic states, travel times can be estimated or predicted. The data is used in these methods to calibrate the model parameters and for determining the actual traffic states. While pure data-driven approaches just look in the data for relationships, trends analogies between certain parameters (e.g., speeds and flows) and the (future) travel times without physical models behind. The overview provided in this section only covers the model-based approaches for travel time estimation and prediction on urban roads.

## 2.2.1 Model-based methods

### Queuing theory based models

#### 1. Sandglass model

Queuing theory is widely used for analysing congested systems. One famous model based on queuing theory is called the ‘Sandglass travel time model’ which is an analogy of vehicle discharging at an intersection with sand flowing to the bottom of the sandglass. In this model, travel time is defined as:

$$TT = \frac{N_Q}{c} + \frac{L - L_Q}{u_f} \quad (2.1)$$

Where  $TT$  is the travel time;  $N_Q$  and  $L_Q$  are number of vehicles in queue and the length of queue, respectively;  $L$  is the length of road segment;  $u_f$  is the link free flow speed and  $c$  is the link capacity.

The first component is the time spent in queuing at the intersection. The second component is the free flow travel time on the uncongested section of the link. This model is therefore a deterministic queuing model.

(Takaba et al., 1991) extended the sandglass model by defining a procedure for estimating the number of vehicles in the queue. The link travel time is further expressed as:

$$TT = \frac{k_j L_Q}{c} - L_Q \left( \frac{k_j}{s} - \frac{1}{u} \right) + \frac{L - L_Q}{u_f} \quad (2.2)$$

Where  $u$  is the travel speed;  $k_j$  is the jam density;  $s$  is the saturation flow rate.

The application of this model requires extensive estimation and calibration of model parameters such as saturation flow rate, jam density, free flow speed and queue length. Furthermore, the model is based on the steady state condition which implies that the probability distribution for the number of vehicles does not vary with time. This is obviously an unrealistic assumption for the oversaturated condition in which there is no equilibrium state of overflow queue.

#### 2. Liu et al. model

As the development of traffic data collection techniques, more and more traffic data become available for traffic performance analysis and model development. (Liu et al., 2006) proposed a time-dependent arterial travel time estimation model by utilizing high-resolution detector and signal status data. According to this model, travel time is composed of three parts: free flow travel time, queuing delay and signal delay. Therefore, the time-dependent travel time can be calculated as:

$$TT^{O-D}(t) = \sum_{i=0}^n TT_f^{i \rightarrow i+1} + \sum_{i=1}^n D_q^i(t_{arrive}^i) + \sum_{i=1}^n D_s^i(\hat{t}_{arrive}^i) \quad (2.3)$$

where,  $TT^{O-D}(t)$  denotes the estimated travel time from origin O to destination D at the departure time instant  $t$ ;  $TT_f^{i \rightarrow i+1}$  denotes the free flow travel time from the upstream intersection  $i$  to the downstream intersection  $i+1$ ;  $D_q^i(t)$  denotes the queuing delay encountered by the vehicle arriving at intersection  $i$  at time instant  $t$ ;  $D_s^i(t)$  denotes the signal delay encountered by the vehicle arriving at intersection  $i$  at time instant  $t$ ;  $t_0$  is the departure time instant at the origin O;  $t_{arrive}^i$  is the arrival time instant at intersection  $i$ , which can be derived as:

$$t_{arrive}^i = t_{departure}^{i-1} + TT_f^{i-1 \rightarrow i} \quad (2.4)$$

$t_{departure}^i$  is the departure time instant at intersection  $i$ , which is calculated from:

$$t_{departure}^i = t_{arrive}^i + D_q^i(t_{arrive}^i) + D_s^i(\hat{t}_{arrive}^i)$$

$\hat{t}_{arrive}^i$  is the adjusted arrival time at intersection  $i$  for calculating signal delay; it depends on the signal and flow status at the intersection.

This model was further improved in (Liu et al., 2009) by integrating probe vehicle data. The good performance of this model is at the cost of accurate high resolution data (e.g., second-to-second detector data and signal control data) which are unavailable in most cases in reality.

### **Traffic flow theory based models**

The first order traffic flow model proposed by (Lighthill et al., 1955), as well as (Richards, 1956) (which is widely known as ‘LWR’ model) has been successfully applied in describing traffic flow dynamics on freeways. According to LWR model, the traffic flow can be characterized by flow, density and speed using the following equations:

$$\frac{\partial q(x,t)}{\partial x} + \frac{\partial k(x,t)}{\partial t} = 0 \quad (2.5a)$$

$$q = Q(k) \quad (2.6a)$$

Where,  $q(x, t)$  and  $k(x, t)$  is the flow and density at time instant  $t$  and location  $x$ , respectively. The first equation is also termed as principle of conversation of vehicles. The second equation represents the so-called the fundamental diagram, which describes the relationship between flow and density. Different forms and equations can be used to specify this relationship. The application of LWR model for travel time estimation on freeways has been investigated by several researchers (NAM et al., 1999; OH et al., 2003). This type of model requires either no on-ramp and off-ramp or detectors on every on-ramp and off-ramp. However, it is difficult to apply the LWR model on the urban road due to the fact that it is unlikely that all traffic streams merging and diverging are monitored.

On the urban signalized roads, the kinematic (shock) wave theory is widely used to describe the queue forming and discharging process over time and space. Different from the queuing theory which considers vertical queues without occupying space, the shock wave theory considers horizontal queues, which is more realistic. One of these models was proposed by (Skabardonis et al., 2005), which applies kinematic wave theory to model the spatial and temporal queuing at the traffic signals considering the signal coordination in estimating traffic arrivals at the intersection. The model estimates the travel time as the sum of the free flow time and the delay at the traffic signal. The delay is further decomposed of three parts:

- Delay of a single vehicle due to the traffic signal;
- Delay due to the queue formed at the intersection;
- Oversaturation delay caused when the number of arrivals is larger than the number of departures at the intersection.

This model considers different processes and the effect of signal offsets and platooning is also taken into account. However, the application of this model requires the estimation and calibration of a lot of parameters such as parameters for the fundamental diagram (free flow speed, capacity, jam density and congested wave speed), parameters for the driver behaviour (acceleration and deceleration rate).

### **Cell Transmission Models**

The cell transmission model (CTM) was first proposed by (Daganzo, 1994; 1995). It is a finite difference numerical approximation of the LWR hydrodynamic model. In CTM, the road section is divided into homogeneous sections called ‘cells’. The length of each cell is equal to the distance travelled by a vehicle in one time step at the free flow speed so that no vehicle can pass more than one cell during one simulation time step under free flow conditions. In addition, each cell has a holding capacity  $N_i$  determined by the following equation:

$$N_i = k_j n_i L \quad (2.7)$$

where  $k_j$  is the jam density;  $n_i$  is the number of lanes in cell  $i$  and  $L$  is the cell length.

The CTM has two basic equations that are applied at each time step  $t$  for each cell  $i$ . The inflow into cell  $i+1$  (or outflow from cell  $i$ ) at time step  $t$  is given by:

$$q_{i+1}(t) = \min\{n_i(t), Q_{i+1}, w/v_f (N_{i+1} - n_{i+1}(t))\} \quad (2.8)$$

Where  $n_i(t)$  is the number of vehicles in cell  $i$  waiting to enter cell  $i+1$ ;  $Q_{i+1}$  is the inflow capacity (vehicle) of cell  $i+1$  per time step;  $N_{i+1} - n_{i+1}(t)$  is the available space in cell  $i+1$  and  $w/v_f$  is the ratio of the backward shockwave speed and the free flow speed.

Once the aforementioned flows for each cell  $i$  at time step  $t$  have been determined, the number of vehicles at the next time step in cell  $i$  can be updated as:

$$n_i(t+1) = n_i(t) + q_i(t) - q_{i+1}(t) \quad (2.9)$$

The CTM has been initially proposed to model traffic flow on highways. The application of CTM for traffic state estimation and prediction has been discussed in (Tampere et al., 2007), which shows that the CTM can be used in a general Extended Kalman Filtering framework to do the traffic state estimation and prediction on motorways.

Lo et al. (Lo, 1999; 2001; Lo et al., 2004) also show that the CTM can be extended for network scenarios, e.g., signalized intersections. By formulating the inflow capacity  $Q_{i+1}(t)$  as a binary variable that fluctuates between null and saturation flow  $Q_m$ , the effects of a traffic signal can be simulated.

$$Q_{i+1}(t) = \begin{cases} Q_m & \text{if } t \in \text{green phase} \\ 0 & \text{if } t \in \text{red phase} \end{cases} \quad (2.10)$$

The application of the CTM for traffic control purpose has been proposed by (Lo, 1999; 2001). The delay in CTM can be estimated at the cell level by subtracting a cell's outflow from its current occupancy for each time step as:

$$d_i(t) = n_i(t) - q_{i+1}(t) \quad (2.11)$$

Once the delay has been determined at a cell level, it can be aggregated at link or network level and used as the performance measure for control strategies.

The CTM has the ability to capture the macroscopic features of traffic, e.g., shockwave, queue formation and dissipation in both congested and uncongested conditions. However, in CTM, the queue forms in a deterministic way which is not realistic in the urban context. Vehicle arrival and departure at intersections are not deterministic but rather stochastic, following certain distributions (e.g., Poisson, Binomial). Therefore, the observed queue is also not deterministic but more stochastic.

### **Other model**

Traffic counts from loop detectors are often displayed by means of cumulative vehicle plots. Cumulative vehicle plots have a number of applications, among which they can be used to determine the travel time in between two road sections. As shown in Figure 2.1,

$A(t)$  is the cumulative arrival curve at the entry of a road section and  $D(t)$  is the cumulative curve at the exit of a road section. The travel time of the  $N^{th}$  vehicle can be determined as:

$$TT(N) = D^{-1}(N) - A^{-1}(N) \quad (2.12)$$

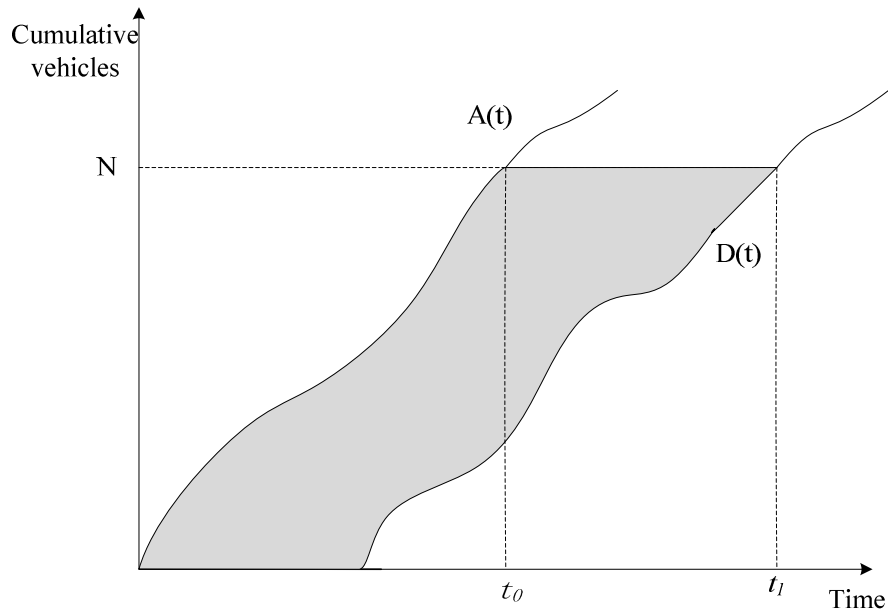


**Figure 2.1: Cumulative arrivals and departures**

Travel time estimation based on cumulative plots is done mainly for freeways. The cumulative traffic counts at the upstream and downstream of links can be recorded by detectors. As a result, the estimation results are very sensitive to the accuracy of detector counts. As for urban roads, due to the intersections and mid-link sinks and sources, there is relative deviation amongst cumulative plots which has been intensively discussed by Bhaskar et al. (Bhaskar et al., 2009). By integrating different data sources including traffic counts from loop detectors, signal settings and probe vehicle data, Bhaskar et al. (Bhaskar et al., 2009) proposed a travel time estimation model for urban roads based on cumulative plots. The cumulative plot measured from the upstream intersection is redefined by utilizing the probe vehicle data and the cumulative plot at the downstream intersection. This model improves the estimation accuracy by correcting the miscounting at the upstream intersection and mid-link sinks and sources. However, on one hand, the miscounting problem at the upstream intersection is considered and on the other hand, the model assumes that there is no counting error at the downstream intersection which is obviously unrealistic.

In general, model-based methods can describe the traffic process explicitly and provide full insight into the locations and causes of delays on the road network. Furthermore, these model-based methods are generic in the sense that they are not location-specific and system-dependent. However, these models are very complex to implement in practice due to the estimation or prediction requirements of traffic demand and supply at the model boundaries as inputs.

### 2.2.2 Data-driven approaches

Different from model-based approaches, data-driven approaches consider the traffic processes which generate travel times as black boxes and exploit purely inductive

techniques to either directly or indirectly estimate or predict travel times without explicitly addressing the physical traffic processes. Basically, two types of data-driven approaches can be found in literature. The first type is pure statistical methods which are more conventional approaches by assuming specific statistical properties of input parameters and outcomes (e.g., Gaussian noise around the means). The second type here we call Artificial Intelligence based approaches, which are more advanced methods though they can also be statistical methods, such as clustering (k-Nearest Neighbour, Fuzzy C-means), neural network models.

### **Pure statistical approaches**

#### **1. Regression methods**

Regression analysis is widely used for prediction and is also used to understand which of the independent variables are related to the dependent variable, and to explore the forms of these relationships. Many researchers (Gault et al., 1981; Sisiopiku et al., 1994; Takayuki et al., 2004) have developed travel time prediction models based on regression. The main advantage of these models is that they are simple and easy to implement in practice. The factors such as degree of saturation and signal offsets can be easily incorporated into these models. The drawbacks of Gault's model and Sisiopiku's model lie in the fact that they are only for urban segment travel time prediction. Whether it is possible to extend these regression models to a route trip has not been investigated. Furthermore, these regression models are valid for relatively small deviations from those used for calibrating the regression line.

#### **2. Time series methods**

Time series models such as autoregressive moving average (ARMA) and autoregressive integrated moving average (ARIMA) models (Billings et al., 2006; Davis et al., 1990) are widely used for travel time prediction. One advantage of these models is that the traffic state (speed, flow, occupancy) or travel time in previous time intervals can be incorporated to predict travel time in the next time interval, especially for trend prediction. However, this can also be a limitation of such models that have the tendency to focus on the trend of data and miss the extreme. Therefore, these models have the difficulty of capturing non-recurrent traffic behaviour or the transition from congestion to free flow condition. Furthermore, these models require a historical database which is not always available in practice.

### **Pattern recognition based approaches**

Pattern recognition is used for classifying data (patterns) based either on a priori knowledge or on statistic information extracted from the patterns. Different pattern recognition based techniques such as k-Nearest Neighbor (k-NN), fuzzy C-means and neural network are applied to match traffic patterns for travel time estimation or prediction.

## 1. k-Nearest Neighbour based approaches

The k-Nearest Neighbour (k-NN) is a method for classifying objects based on closest training examples in the feature space. The basic idea behind it is that by matching the current set of input variables with historical observations, a set of  $k$  historical observations that are similar to the current input can be obtained. The current output can be defined as a function of the values from the obtained set of  $k$  historical observations.

You et al. (You et al., 2000) applied k-NN method to estimate travel time on urban roads based on the travel times obtained by probe vehicles. Their model is based on segregating the non-linear time series of travel time data into local linear trend. The estimation results showed that the model could perform well with a MAPE in the region of 8% to 10%.

Bajwa et al. (Bajwa et al., 2003) used the inverse of time-mean speed aggregated over 5 minutes obtained from ultrasonic detectors as feature vectors. The traffic pattern was identified as a function of distance weighted by these feature vectors. A genetic algorithm was applied to determine the optimal number of nearest neighbours. By minimizing the squared difference between the predicted traffic pattern and historical traffic patterns in the database, nearest neighbours are obtained.

Based on the flow and occupancy data collected by the loop detectors, Robinson (Robinson, 2005) applied the k-NN method to estimate urban link travel time. The Automatic Number Plate Recognition (ANPR) cameras were used to collect link travel times for the historical database. The key parameters which include attributes to be included in the feature vector, Distance Metric, value of  $k$  and Local Estimation Method in the k-NN method were identified. The value of  $k$  is determined by minimizing the mean squared error between the predicted traffic pattern and the historical pattern. Then the final travel time is estimated using LOWESS (LOcally WEighted Scatter plot Smoothing) method. Robinson also compared the k-NN method with other existing models. Results showed that the proposed model outperforms other existing models with the optimum parameter setting, especially at low and very high levels of actual travel time.

The advantage of k-NN is that it has a solid theoretical foundation with a lot of available research relating to the implementation of this method. However, there are several disadvantages related to this method. First, the k-NN method requires a large historical database which can cover different traffic patterns. However, increasing the size of the data also increases the computation time. In case that a non-recurrent incident happens, the model tends to be incapable of capturing such a traffic phenomenon since it is not stored in the historical database. Secondly, the performance of this method highly depends on the selection of parameters as discussed by (Robinson, 2005). There is no standard rule to select the attributes to be included in the feature vector. An insufficient size can result in an incomplete image of traffic searched in historical data. The value of  $k$  is difficult to determine and dependent on the size of the historical database as well.

## 2. Fuzzy logic based approaches

Li et al. (Li et al., 2002) applied fuzzy logic to estimate link travel time by using a single GPS equipped probe vehicle. The driving patterns were determined by combining the average speed of the probe vehicle and a variable called maximum continuous acceleration (MCA). The output is the ratio of travel time of the probe vehicle to the mean travel time which is estimated from camera data. The membership function values are determined by historical traffic data of the tested road segment. Based on the output ratio, the travel time is estimated for different driving patterns (slow/very slow, medium, fast/very fast). Though only a single GPS probe vehicle can provide the travel time estimation, the formation of membership functions requires a large amount of historical data. In addition, Li et al. did not discuss the question how to determine the range of output ratio for different driving pattern in order to estimate travel time.

The advantage of using fuzzy logic is that it allows imprecise input data for estimation or prediction. The employment of fuzzy logic might be helpful, for very complex processes, when there is no simple mathematical model for highly nonlinear processes (e.g., the traffic process on the urban road is highly nonlinear). However, applying fuzzy logic requires the determination of the number of membership functions. There is no standard rule about this. Furthermore, how well these membership functions can represent different traffic patterns directly determines how accurate the estimation or prediction results would be. As a result, fuzzy logic based methods require a large historical database that can cover different traffic patterns and a sufficient expert knowledge for the formulation of different rules for fuzzification and defuzzification.

## 3. Neural network based approaches

Neural networks have been widely applied for short-term traffic and travel time prediction on freeways. Models based on neural networks have the potential to learn complex nonlinear relationship between variables by identifying the patterns in the data. Different neural network models such as spectral basis neural network (SNN) (Park et al., 1999), state-space neural network (SSNN) (van Hinsbergen et al., 2008; van Hinsbergen et al., 2009; van Lint et al., 2005) have been successfully applied to predict travel time on freeways. The idea behind all these models is that travel times are determined by the traffic states along the route. Whereas on the urban road, the application of neural network is less successful due to the difficulties in predicting turning fractions at intersections and highly complex traffic conditions along the road as discussed by (Liu, 2008).

The clear advantages of neural network models include the fact that they do not require extensive expertise on traffic flow modelling, that they are fast and easy to implement and ready-to-use software packages for model design and calibration are available (van Lint, 2004). However, there are three main problems related to neural network models:

- *Over-fitting*: it is one of the problems that occur during neural network training. The estimation or prediction error on the training set is very small, but when new data is applied to the network the error becomes large. The network has memorized the training examples instead of generalizing to new situations, especially when the training data set is small. In this case, there is a trade-off between the complexity of the network and training error though there are some techniques, for instance, early stopping and regularization to improve the over-fitting problem.
- *Generalizability*: It has been recognized that the neural network tends to have poor generalizability. For instance, the network trained for predicting travel times in the morning peak hour could not directly be used for predicting travel times in other time periods (e.g., off-peak hour).
- *Transferability*: Most neural network models developed for travel time estimation and prediction are location specific. The model developed for a certain route or link cannot be applied to other routes or links with different geometric conditions and traffic conditions. Therefore, results from one location are not transferable to another.

## 2.3 Delays on urban signalized roads

The previous sections provided different travel time estimation and prediction methods, some based on physical models inspired by hydrodynamic and queuing theories, others on statistical models, from more conventional to more advanced AI approaches. These methods, however, do not model explicitly the traffic process and delays at the signalized intersections, i.e. they account implicitly for these delays when extracting and processing the data but do not relate the data to the traffic process at each signal. By doing so they overcome the extra complexity brought by modelling explicitly the traffic control mechanism. On the other hand they fail to provide full insight into the relationship between the latter and the resulting travel time dynamics and variability.

The delay vehicles experience at signalized intersections accounts for a large part of the delay that vehicles would experience on the urban road compared with that caused by other factors, e.g., bus stops and parking along the road. The importance of vehicle delay at signalized intersections lies in the use of this parameter for both evaluation practices and traffic management applications, e.g., determining the optimal signal control scheme by delay minimization, estimating urban link travel time by integrating delay models. The thesis mainly deals with delays at signalized intersections, and more specifically, how traffic processes and traffic control mechanisms influence delay distributions and in turn to travel time distributions on urban roads. Therefore, in the following of this chapter we will give an overview of the delay models and modelling approaches that are available in literature.

The delay at signalized intersections is usually defined as the difference between the travel time a vehicle experiences when passing the intersection and the travel time experienced

by this vehicle if travelling at desired speed. Figure 2.2 illustrates an example of hypothetical trajectory of a vehicle passing two signalized intersections. The total delay experienced at the downstream signal is composed of the stopped delay due to signal operations and queues, deceleration delay and acceleration delay.

Any of the components constituting the total delay contribute to its dynamic and stochastic behavior, and in turn to vehicles travel time variability, e.g., the arrival times, their position in the queue, etc. In the following of this section we describe how these components are modeled and how their variability is addressed at the signal level, while later we extend this overview to the travel time variability.

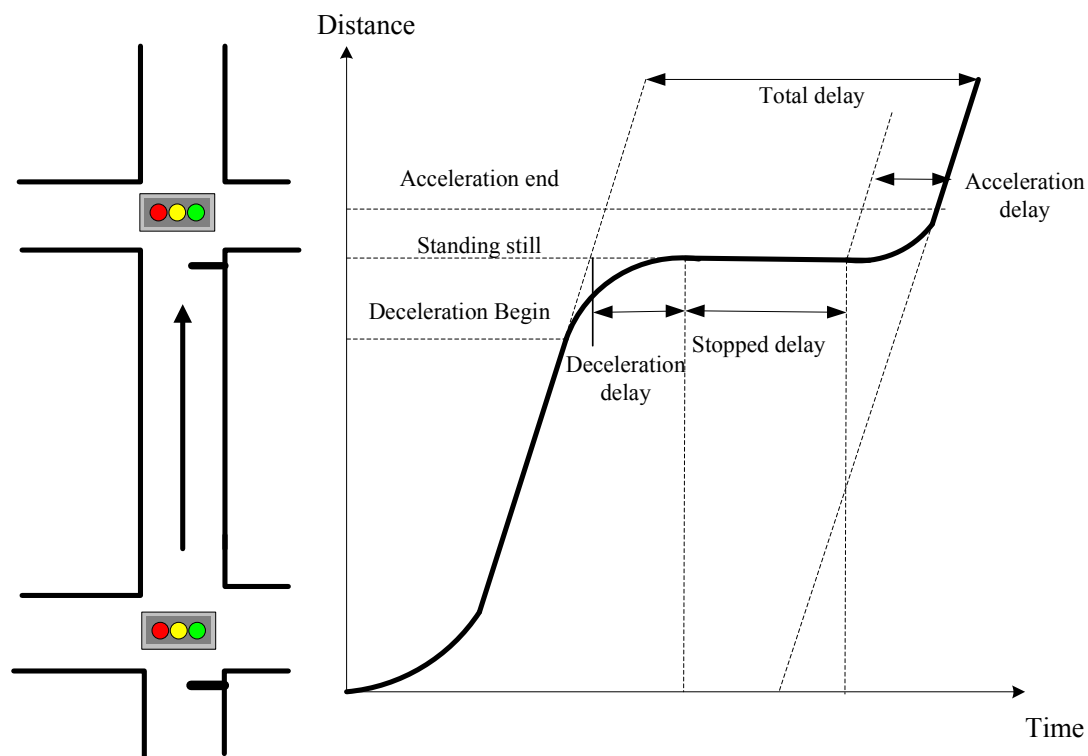


Figure 2.2: Trajectory of a vehicle travelling on the urban signalized road

### 2.3.1 Delay models for signalized intersections

#### Deterministic queuing model

The deterministic queuing model assumes that vehicles arrive at the intersection and depart from the intersection with uniform and constant rates. Figure 2.3 illustrates expected cumulative arrivals and departures for both under-saturated and oversaturated conditions. In reality, vehicles are not continuous but discrete. Therefore, the cumulative curves should have steps. The conversion from the discrete time step to the continuous time step has been clarified by (Van Zuylen et al., 2006). Therefore, the continuous cumulative plots are used for analysis. In the under-saturated condition, during the red phase, the arriving vehicles queue up linearly and they will be served within the next green phase. The delay in the area of the triangular bordered in bold is called the uniform delay

as shown in Figure 2.3(a). In the oversaturated condition as illustrated in Figure 2.3(b), a zero initial queue is assumed in this case. The average arriving flow rate is larger than the average departure rate. The overflow delay is calculated by the area between the line which represents the arrivals at capacity and the line representing the actual arrivals. Equations (2.7) and (2.8) can be derived to calculate the average uniform delay and the average delay in the oversaturated condition, respectively.

$$d_u = \begin{cases} \frac{\tau_c(1-\lambda)^2}{2(1-x\lambda)} & x \leq 1.0 \\ 0.5(\tau_c - \tau_g) & x > 1.0 \end{cases} \quad (2.7)$$

$$d_o = 900T((x-1) + \sqrt{(x-1)^2}) \quad (2.8)$$

Where,

$d_u$ : average uniform delay

$d_o$ : average overflow delay during evaluation period  $T$

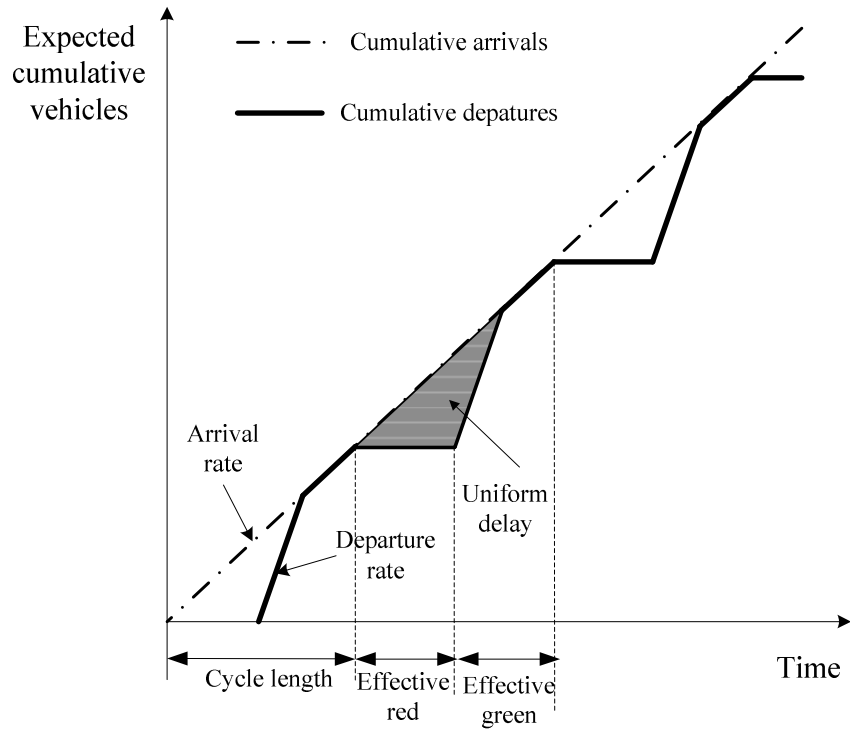
$\tau_c$ : signal cycle

$\lambda$ : effective green to cycle time ratio

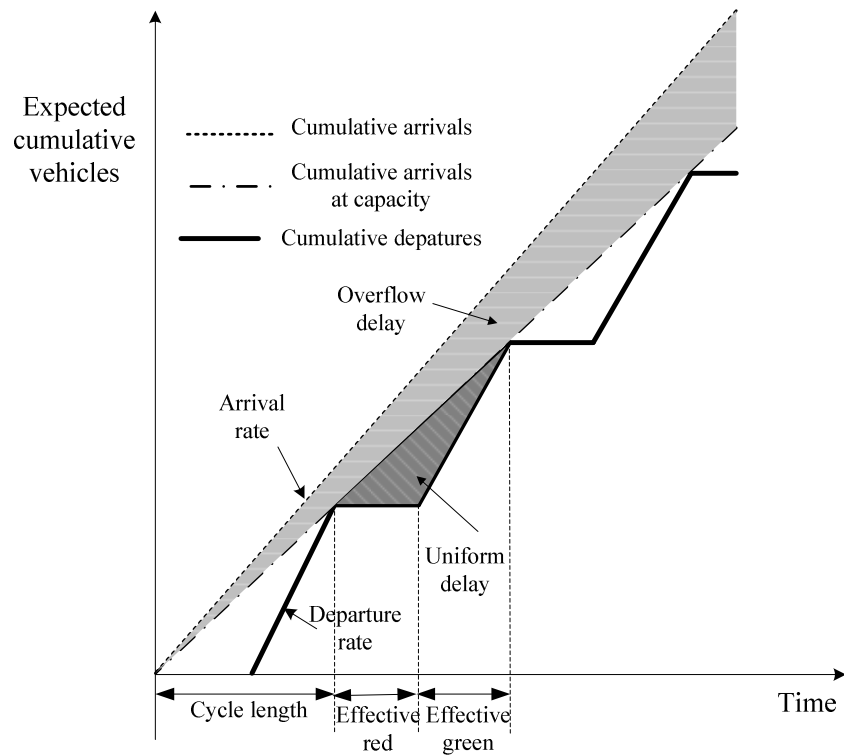
$x$ : degree of saturation

$T$ : evaluation period in the oversaturated condition

The assumption made for Equation (2.7) is that vehicles arrive at a uniform and constant flow rate. The queue can always be cleared before the start of the next red time. However, in reality, due to random effects in certain cycles, it is likely that some vehicles will remain queued at the end of the green phase even when the average arriving flow is smaller than the capacity. This phenomenon occurs at random, depending on which cycle happens to experience higher-than-capacity flow rates, especially at intersections operating near capacity. Equation (2.8) considers only the deterministic overflow delay caused by sustained periods of oversaturation, and this equation does not include the delay due to the initial queue at the start of analysis period. Viti (Viti, 2006) showed that the probabilistic phenomenon contributes to obtain a smooth transition between the uniform and the oversaturated delay components, as it will be shown in the next sections. Moreover, he proposed a delay model that can be used for both under-saturated and oversaturated conditions and for modelling the transition between these two states and also for the case of initial queue.



(a) Cumulative arrivals and departures in the undersaturated condition



(b) Cumulative arrivals and departures in the oversaturated condition

**Figure 2.3: Deterministic components of delay in undersaturated and oversaturated conditions with uniform arrivals and departures**

Figure 2.4 illustrates the relationship among three delay components. The first component  $W_1(k)$  represents the total delay accumulated within cycle  $k$  by all vehicles arriving during cycle  $k$  and vehicles already waiting at the intersection at the start of cycle  $k$ . The second component  $W_2(k)$  denotes the total delay experienced by only vehicles waiting at the intersection at the beginning of the cycle  $k$  and  $W_3(k)$  denotes the total delay experienced by vehicles arriving during cycle  $k$  and caused by the presence of the residual queue  $Q_k$ . Given the total arrival vehicles  $A_k$  within cycle  $k$ , the average delay experienced by a vehicle arriving during the cycle  $k$  is calculated as:

$$W(k) = \frac{W_1(k) - W_2(k) + W_3(k)}{A_k} \quad (2.9)$$

Viti (Viti, 2006) gave a more general expression, following earlier works on this subject by Olszewski (Olszewski, 1990; Olszewski, 1994) as:

$$W(k) = \frac{W_1(k) - \Phi(Q_k) + \Phi(Q_{k+1})}{A_k} \quad (2.10)$$

with

$$W_1(k) = \begin{cases} \frac{(2Q_k + A_k)\tau_c - n_d \cdot \tau_g}{2} & \text{if } Q_k + A_k \geq d \\ \frac{(2Q_k + A_k)\tau_c - n_d \cdot \tau_g}{2} + \frac{(n_d - Q_k - A_k)^2}{2(n_d / \tau_g - A_k / \tau_c)} & \text{otherwise} \end{cases} \quad (2.11)$$

$$\Phi(Q_k) = \frac{Q_k^2 \cdot \tau_g}{2 \cdot d} + (k+1)(Q_k - \frac{k \cdot d}{2}) \cdot \tau_r \quad (2.12)$$

where  $A_k$  is the total arrivals within cycle  $k$ ;  $n_d$  denotes the constant value of departures for each cycle;  $k$  is the minimum number of cycles needed to serve  $Q_k$  vehicles such that  $Q - k \cdot d \leq 0$ ;

Therefore, given a non-zero overflow queue length at the beginning of a cycle, the above formulas allow one to calculate the delay experienced in the following cycles due to this overflow queue.

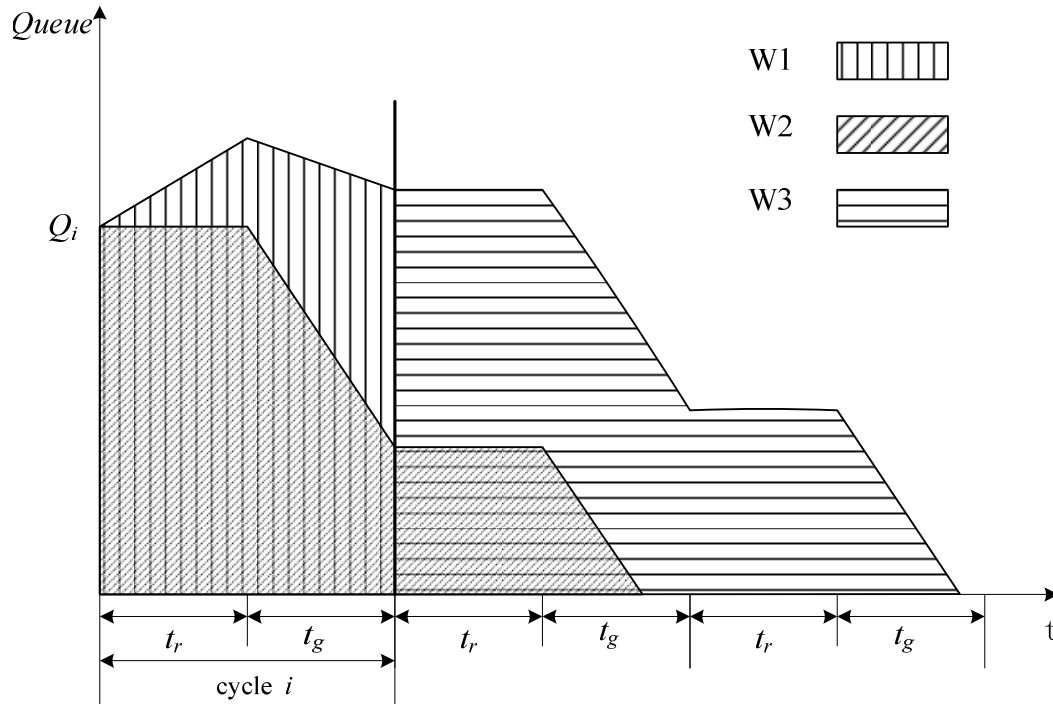


**Figure 2.4: Schematic display of cycle delay when overflow queue is present (cited from Viti 2006)**

### Steady-state delay models

The deterministic queuing model assumes that vehicles arrive uniformly at the intersection, while steady-state delay models take the randomness of arrivals into account. The steady state models are developed under the assumption of stationary conditions for the overflow queue which indicates that these models are applicable only for the cases of undersaturation. The most widely used delay formula was proposed by (Webster, 1958):

$$d = \frac{\tau_c(1-\lambda)^2}{2[1-\lambda x]} + \frac{x^2}{2q(1-x)} - 0.65\left(\frac{\tau_c}{q^2}\right)^{1/3} x^{2+5\lambda} \quad (2.13)$$

The first term is the estimation of uniform delay. The second term considers the effect of the random nature of arrivals. It is known as the ‘random delay’ which was derived analytically assuming a Poisson arrival process and constant departure rate. The third term is an empirical correction term to reduce the discrepancy with the simulation data.

Besides Webster’s model, other steady-state models were proposed under different assumptions for the arrival and departure distribution. (Miller, 1963) developed a model indirectly estimating delays through the estimation of average overflow queue, thus not limited by a specific distribution for the arrivals. (Newell, 1965) proposed a delay model in which he used an index of variability that is not limited by the assumed arrival distribution (e.g., Poisson, as in the case of Webster).

### **Time-dependent delay models**

All steady-state delay models assume that the stochastic equilibrium can be achieved after a certain period of time. When the degree of saturation is low, this equilibrium can be reached within a reasonable time period. However, when the traffic flow is close to the capacity, the time to achieve the steady state can exceed the evaluation period. In this case, the system should allow a long time period to run until the equilibrium state is reached. Further, as the traffic demand exceeds capacity, steady-state models could not handle this situation.

In order to limit the assumption of steady-state conditions, a lot of research has been carried out during the past several decades to develop time-dependent delay models. Compared with the steady-state models where the arrivals and departures are assumed to follow known distributions and they do not change over time, the time-dependent models deal with arrivals and departures as a function of time. (May et al., 1967) proposed a delay model by applying a trapezoidal-shaped arrival profile and constant departure rate. One assumption in the model is that the random queue fluctuations can be neglected. This model could provide acceptable results in highly undersaturated conditions and oversaturated conditions. However, when the traffic flow approaches the capacity, the model underestimates queues and delays because the extra queues caused by the random fluctuations are not considered. How to estimate the delay properly when the traffic intensity approaches the capacity remained a problem until (Kimber et al., 1979). They used the coordinate transformation technique such that the steady-state model can be asymptotic to the deterministic model in case of oversaturated conditions. This approach overcomes the gap between steady-state models and deterministic models. However, there is no rigorous theoretical basis for this approach but only a heuristic method, though Viti (Viti, 2006) compared his model, which has more rigorous theoretical bases, with Kimber and Hollis' model and showed some similarities. Nevertheless, a number of time-dependent models have been developed based on the coordinate transformation technique (Akcelik, 1980; 1988; Akcelik et al., 1993; Brilon et al., 1990) and later on have incorporated into some capacity guides, e.g., the Highway Capacity Manual (TRB, 1997), the Canadian Capacity Guide (ITE, 1995) and the Australian Capacity Guide (ARR, 1995). A general form of these capacity guide delay models is given by (Dion et al., 2004):

$$D = d_1 \times f_{PF} + d_2 + d_3 \times f_r \quad (2.14)$$

with:

$$d_1 = 0.5\tau_c \left[ \frac{\left(1 - \frac{\tau_g}{\tau_c}\right)^2}{1 - \frac{\tau_g}{\tau_c} \cdot \min(x, 1.0)} \right]$$

$$d_2 = 900x^n T \left[ (x-1) + \sqrt{(x-1)^2 + \frac{mkI}{cT}(x-x_0)} \right]$$

$$f_{PF} = \frac{(1-P)f_P}{1 - \frac{\tau_g}{\tau_c}}$$

Where  $d_1$  is the uniform delay;  $d_2$  is the incremental delay accounting for the stochastic arrivals and oversaturation queues;  $d_3$  is the residual delay for oversaturation queues that may have existed before the analysis period;  $f_{PF}$  denotes the adjustment factor accounting for the quality of progression in coordinated systems;  $f_r$  denotes the adjustment factor for residual delay component;  $f_p$  denotes the adjustment factor for situations in which the platoon arrives during the green interval;  $P$  is the proportion of vehicles arriving during the effective green interval;  $k$  denotes the incremental delay factor accounting for pre-timed or actuated signal controller settings;  $I$  denotes the adjustment factor for upstream filtering/metering;  $T$  is the evaluation period;  $c$  is the capacity of intersection approach (veh/h);  $m$  and  $n$  denote capacity guide parameters;  $x_0$  denotes the degree of saturation below which the overflow delay is negligible.

While Kimber and Hollis' model lacks the theoretical basis, Viti (2006) proposed an analytical time-dependent model which can well describe the dynamics of the queue in both cases of decrease of the overflow queue and increase of the overflow queue based on Markov process. The formulation of this model is as follows:

$$E[Q(t)] = \sum_{j=0}^{Q_{\max}} j \cdot P(Q = j, t) \quad (2.15)$$

$$P(Q = j, t) = \sum_{i=0}^{Q_{\max}} P(Q = i, t-1) H_{ij}(t) \quad (2.16)$$

where  $E[Q(t)]$  is the time-dependent expected value of overflow queue;  $P(Q=j, t)$  is the probability of observing queue  $j$  at time  $t$ ;  $H_{ij}(t)$  is the transition matrix which represents the probability that the queue length moves from state  $i$  at time  $t-1$  to state  $j$  at time  $t$ . Viti further derived a heuristic formula which can well capture the behaviour of the expected overflow queue from Markov simulation (Equations (2.15) and (2.16)):

$$Q(t) = \alpha(t) \cdot [Q_0 + (x-1) \cdot N_c \cdot t] + (1-\alpha(t)) \cdot [Q_e + \gamma(t) \cdot e^{-\beta(t)t}] \quad (2.17)$$

Where  $N_c$  represents the average number of departures per cycle;  $Q_e$  denotes the equilibrium value of queue under steady-state conditions;  $\alpha$ ,  $\beta$ ,  $\gamma$  are time-dependent model parameters.

One difficulty in all these delay models is how to model the arrivals such that the model can better represent the real situation. The Poisson arrival distribution is known to be

applicable only in the case of an isolated intersection with low traffic volume. As discussed in (Dion, 2004), various capacity guide models attempt to consider non-Poisson arrivals, e.g., platoon arrivals.

### **Shock wave delay model**

Michalopoulos and Stephanopoulos (Michalopoulos et al., 1981) derived an analytical model based on shock wave theory to estimate delays at signalized intersections. The main difference between this model and the steady state delay model lies in the fact that the latter assumes that the queue is building vertically without considering space on the link while the former considers that vehicles queue horizontally. The advantages of this shock wave delay model is that it describes the evolution of queues in both time and space rather than time alone and density variations along time and space during the dissipation period are taken into account.

Figure 2.5 illustrates the shock waves at a signalized intersection in the undersaturated condition. The maximum queue length can be determined more realistically by considering the horizontal extent of a queue. The total travel time spent by all vehicles can be estimated using the density and flow rate associated with each region. Therefore, the total delay within one signal cycle is calculated as the difference between the total travel time with traffic signals and the total travel time without traffic signals (Dion et al., 2004):

$$TT_D = TT_{sig} - TT_{no\_sig} \quad (2.18)$$

The average delay for individual vehicles can be estimated as:

$$d = 3600 \frac{|L_m|}{2q\tau_c} \left[ \tau_r (k_B - k_A) + (\tau_{mQ} + \tau_{cQ})(k_C - k_A) \right] \quad (2.19)$$

where  $L_m$  is the maximum queue length;  $q$  is the arrival flow rate;  $\tau_r$  is the effective red phase interval;  $k_A$ ,  $k_B$ ,  $k_C$  are densities of area A, B and C;  $\tau_{mQ}$  is the time interval between the beginning of the green phase and the time instant when the maximum queue length reaches;  $\tau_{cQ}$  is the time spent on clearing the queue of vehicles.

The maximum queue length in this model is assumed to be deterministic. However, as shown in (Viti, 2006), the overflow queue is not deterministic but rather stochastic. Van Zuylen, and Hoogendoorn (van Zuylen et al., 2007) proposed a probabilistic model by combining the Markov chain process with shock wave theory. Due to the stochastic properties arrivals and departures, the maximum queue length is not deterministic but stochastic with a certain distribution. The expected value of the maximum queue length by this model is much longer than that from other models.

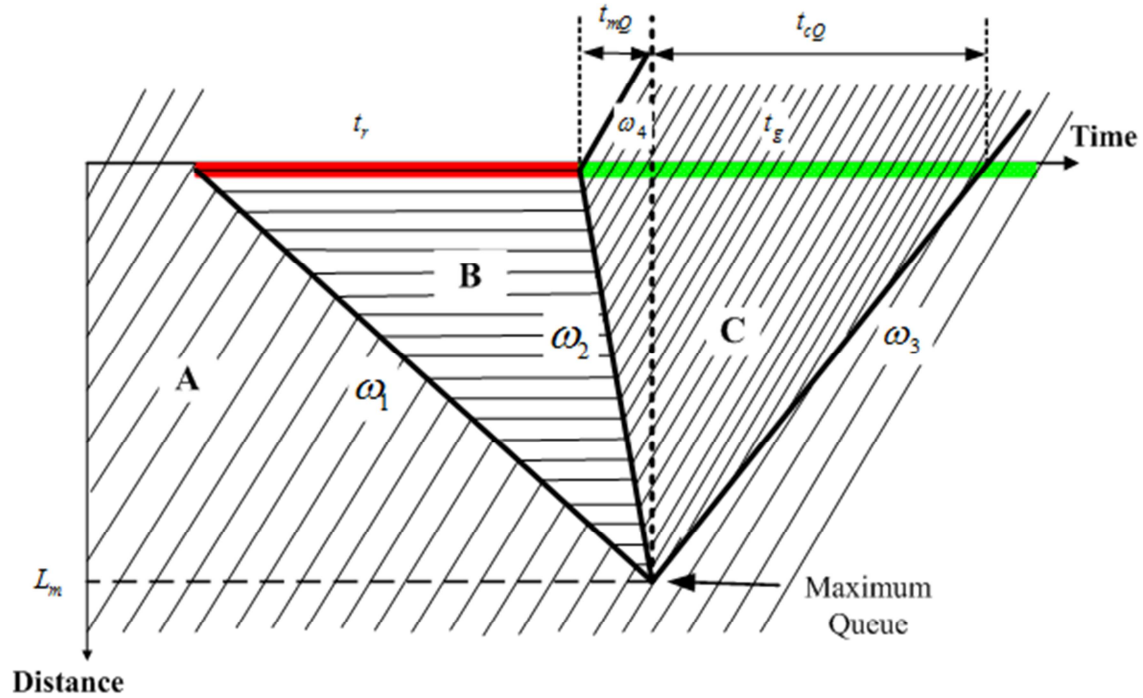


Figure 2.5: Shock waves at the signalized intersection in under-saturated conditions

### 2.3.2 Delay variability at signalized intersections

#### Delay variance models

The delay models as discussed in the previous sections focus on estimating the mean delay at intersections. However, due to the random fluctuations of arrivals and departures and interruptions caused by traffic controls, delays have a high variation among vehicles at the signalized intersection. (Fu et al., 2000) developed a delay variability model to quantify the variation of delays in highly undersaturated and highly oversaturated conditions. The model is composed of two parts: the variance of the uniform delay and the variance of the random delay and analytical expression is the summation of these two parts:

$$\text{Var}(d(t)) = \frac{\tau_c(1-\lambda)^3(1+3\lambda-4\lambda x_{\min})}{12(1-\lambda x_{\min})} + \left\{ \frac{I_a T x}{2c} + \frac{T^2(1-x_{\max})^2}{12} \right\} e^{-\left(\frac{x_0}{x}\right)^\beta} \quad (2.20)$$

Where  $\text{Var}(d(t))$  = time-dependent variance of delay

$\tau_c$  = cycle time (seconds)

$\lambda$  = effective green to cycle time ratio

$I_a$  = variance-to-mean vehicle arrivals. If the vehicle arrivals follow a Poisson distribution,  $I_a$  is equal to 1

$c$  = capacity (pcu/second) which is determined by the saturation flow rate  $s$  and effective green to cycle time ratio  $\lambda$

$x$  = degree of saturation

$x_{min}$  = minimum of (1.0,  $x$ )

$x_{max}$  = maximum of (1.0,  $x$ )

$T$  = evaluation time

$x_0$  and  $\beta_1$  are model parameters and calibrated from a simulation model

$$x_0 = 0.947 + 1.330 \times 10^{-6} T / q_c + 0.157 \lambda$$

$$\beta_1 = 8.294 + 6.080 \times 10^{-4} T / q_c$$

The validity of Fu's model under the entire range of degree of saturations is questionable since the model was only developed and calibrated under two extreme traffic conditions which are highly undersaturation and highly oversaturation. Gu and Lan (Gu et al., 2009) proposed an approximation model which is able to predict the delay variability for different degrees of saturation with assumptions that no initial queue is present at the beginning of the evaluation period, vehicle arrivals follow a known distribution and the average arrival rate is constant during the evaluation period. The model contains two components including the expected conditional variance of individual delay and the variance of mean delay. The analytical model was further simplified using the Taylor expansion and the approximation formula is:

$$\begin{aligned} Var(d(t)) \cong & \frac{t_c^2 (1-\lambda)^3 (1+3\lambda-4\lambda x_{min})}{12(1-\lambda x_{min})^2} \\ & + \left\{ \frac{T^2 (1-x_{max})^2}{12} + \frac{t_c^2 (1-\lambda)}{12} (-1+2x_{max}+3\lambda-4\lambda x_{max}) + \frac{T^2}{3q_c^2} Var(v) \right\} \frac{1}{1+e^{\alpha-\beta x}} \end{aligned} \quad (2.21)$$

Where  $Var(v)$  is the variance of arrivals,  $\alpha$  and  $\beta$  are model parameters need to be calibrated.

Gu compared the results from their model with those from a Monte Carlo simulation model and those from Fu's model. They claimed that Fu's model underestimates the overall delay variability over middle to high degrees of saturation which were not explicitly investigated in Fu's model.

### **Delay distribution model**

Besides the delay variance, another effective way to model the variability of delay is the delay probability distribution. Due to the randomness of traffic flow process and uncertainty associated with factors affecting intersection capacity, the actual delay

incurred in any cycle may be very different from the expected mean delay. Instead, a certain probability distribution can be observed. Unfortunately, research in developing delay probability distribution models is very limited in the past decades. Olszewski (Olszewski, 1994) proposed a cycle-average delay probability distribution model based on the sequential calculation of queue length probabilities. Influence of different arrival processes, different degrees of saturation and control schemes were investigated and they concluded that the effect of arrival variability on the cycle-average delay probability distribution is significant. The shape of probability distribution at an undersaturated approach resembles a shifted exponential distribution, with a high probability of delay equal to the uniform delay component. For the oversaturated conditions, the probability distributions become more dispersed over time. This model can capture the uncertainty of the average cycle delay while in most research only point estimates of delay were provided. However, this model didn't explicitly deal with the uncertainty or variability of delay among individual arriving vehicles within one cycle time.

## 2.4 Travel time distribution models

The travel time distribution is commonly used to quantitatively evaluate travel time uncertainty and its spatial and temporal variations. Emam and AI-Deek (Emam et al., 2006) compared different distributions for modelling the traffic data on freeways, e.g., log-normal, Gamma, Weibull and exponential distributions. They concluded that the log-normal distribution provided the best fit. However, this single-mode travel time distribution couldn't well represent the travel time distribution on urban roads due to the complex traffic conditions. Therefore, a multi-state (multi-mode) travel time distribution model was proposed by (Guo et al., 2010). The model provides the connection between the travel time distributions and the underlining traffic states.

$$f(TT|\eta, \theta) = \sum_{i=1}^N \eta_i f_i(TT|\theta_i) \quad (2.22)$$

Where  $TT$  is the travel time;  $f(TT|\eta, \theta)$  denotes the probability density function for  $TT$ ;  $\eta = (\eta_1, \eta_2, \dots, \eta_N)$  is a vector of mixture coefficients which relate to different traffic states and  $\sum_{i=1}^N \eta_i = 1$ ;  $\theta = (\theta_1, \dots, \theta_N)$  is a matrix of model parameters for each component distribution;  $f_i(\cdot)$  stands for different distributions, e.g., normal, log-normal or Weibull;  $f(TT_i|\eta, \theta_i)$  represents the distribution of travel time corresponding to a specific traffic condition, e.g., congested state and free flow state can have their own distinct component distribution.

One advantage of applying this model is that model parameters and the underlining traffic state can be connected. The similar work can also be found in (Loustau et al., 2010), in which a combination of three lognormal distributions was proposed to model the travel time distribution for different traffic conditions.

Up to now, most research on travel time distribution mainly focuses on applying certain statistical distributions (e.g., normal, log-normal) to the observed travel times. The influence of different traffic processes and traffic control schemes on travel time variability is not explicitly considered or modelled. On urban roads, the dynamic and stochastic behaviour has a significant influence on the delay uncertainty and in turn to the travel time variability. Therefore, a travel time distribution model which explicitly takes into account stochastic traffic processes and the traffic control mechanism is proposed in chapter 4 and 5.

## 2.5 Summary

The subject of modelling travel times on freeways has received a lot of attention in the past decades. Compared with that of freeways, less research has been dedicated to this subject on urban roads, though more and more urban travel time estimation and prediction models have been developed in recent years. In this chapter, three aspects of modelling urban travel times are discussed, namely, urban travel time estimation and prediction models, modelling delays at signalized intersections and modelling urban travel time variability.

First of all, this chapter gives a state-of-the-art overview on urban travel time estimation and prediction models. The advantages and disadvantages of these models are discussed. It appears that most of existing models didn't take into account of stochastic processes (e.g., stochastic queuing process at intersections) on the urban road. Besides, most existing models including both model-based and heuristic models aim at estimating or predicting the mean travel time. However, travellers take travel time variability into consideration sometimes even more than mean travel time itself. Therefore, if the travel time distribution is very large and skewed, providing the mean travel time to road users can be useless, especially when time constraints are involved (e.g. an important appointment). Therefore, it is more meaningful to model urban travel times in terms of distribution. In chapter 5 and 6, how travel time distribution can be modelled and furthermore how these distributions can be estimated and predicted are discussed.

Secondly, different delay models including deterministic and time-dependent models are discussed. Since delay vehicles experience at intersections is an important component of the travel time on urban roads, how delays are estimated has a significant influence on the final travel times. However, delay models have been developed mainly for the purpose of improving traffic controls at intersections. Therefore, these models try to estimate or predict the mean delay vehicles experience at intersections. As shown in (Viti, 2006), due to the stochastic overflow queues at intersections, delays are uncertain. Given the known average traffic demand and capacity, a range of delay (a certain delay distribution) can be found. The derivation of the delay distribution at the signalized intersection and travel time uncertainty based on the analysis of the delay distribution will be discussed in chapter 4. An extension of delay distribution for an urban trip will be introduced in chapter 5.

Finally, this chapter also discusses the research on travel time distribution models. The limitation of the current research is that the investigation of travel time variability is just in a phenomenological way, e.g., by calibrating some distribution functions (e.g., log-normal, Gamma) to the observed travel times. The stochastic traffic processes and traffic control schemes are not explicitly considered in these models. Therefore, these models fail in provide full insight into the relationship between traffic processes, traffic control on urban roads and the resulting travel time variability.

# Chapter 3

## Measuring urban travel times

### 3.1 Introduction

Travel times are widely accepted as very useful information both for travellers and road authorities. A number of models have been developed to estimate or predict urban travel times as discussed in chapter 2. At the meantime, more and more traffic monitoring techniques have been developed to measure link or route travel times. Basically, there are two types of traffic sensors for measuring travel times:

- *Fixed sensors:* This type of sensors is installed along the roadside at specific locations. When vehicles pass a pair of sensor locations, both time stamps are recorded and travel times between these two locations can be derived. E.g., Automatic Number Plate Recognition (ANPR) cameras, Bluetooth scanners, speed detectors.
- *Mobile sensors:* Position detection equipment such as GPS sensors, cell phone sensors can provide direct travel time from point-to-point on the route traversed by probe vehicles.

In this chapter, different monitoring techniques for measuring urban travel time are discussed in section 3.2. Especially, mobile sensors are regarded as very promising means to measure urban travel times. However, there are some limits applying these techniques. For instance, one limit of GPS travel time data in most real applications is that travel times collected at present by probe vehicles are obtained with rather low frequencies (e.g., 30s, 1min), and therefore, do not originate from a single complete link but are experienced by probe vehicles from a certain position on one link to a certain position on another link. Now the question is how to decompose travel times into individual links such that complete link travel times or route travel times can be derived. In section 3.3, different models to decompose travel times recorded by GPS probe vehicles into individual links are discussed and the performance of these models is compared with each other using both

the simulation data and empirical data. Finally, some important conclusions are presented in section 3.4.

## 3.2 Empirical methods of measuring urban travel times

### 3.2.1 Automatic Number Plate Recognition (ANPR)

Automatic Number Plate Recognition (ANPR) systems have been widely applied to measure freeway travel times. ANPR systems normally consist of two components: cameras that detect passing vehicles and continuously send the images to a computer and software that recognizes number plates with its characters and stores them in a database. By matching number plates recorded at two camera locations with time stamps, travel times of passing vehicles between these two locations can be estimated.

One advantage of using ANPR is that travel times between two specific locations can be calculated accurately. For instance, as long as the start and end of links are defined at the ANPR camera locations, link travel times can be measured. The second advantage of ANPR systems is the high recognition rate. Although, the recognition rate can vary depending on different factors including vehicle characteristics, quality of installation and weather condition. The average recognition rate on freeways as reported in the literatures can be as high as 85%-90% (Friedrich et al., 2008). However, the recognition rate is likely to be lower on the urban road, especially close to intersections or in case of congestion where vehicles drive at closer distance to each other. Therefore, the number plate of cars can be obscured by larger vehicles, e.g., buses or trucks. Besides, due to a lot of turning movements at intersections, vehicles recognized in one camera location may not pass the second camera location or vice versa. This would cause a low matching rate.

The major concern about ANPR system in urban environment is that it is difficult to determine whether a vehicle has travelled exactly along the route between A and B without making unexpected stops en-route or choosing alternative routes which have similar or less travel time than the average travel time of this route. For this case, statistical data cleaning methods such as percentiles, standard deviation may fail to detect travel times which are not experienced by vehicles on the route of interest. Nevertheless, as suggested by (Robinson, 2005), it is possible to detect whether a vehicle has 'reasonably' travelled along the route of interest by comparing the travel time of individual vehicle with those immediately ahead of and behind it at the first camera. An overtaking rule approach was proposed by comparing the travel time of the current vehicle against the travel time of a certain number of immediately following vehicles. The travel time of a target vehicle  $i$  is identified as valid if its travel time meets the criteria given by:

$$\tau_i \leq \tau_k + tt_{ik} + \Delta_C \quad \forall k \in FV(i) \quad (3.1)$$

where  $\tau_i$  represents the travel time of the target vehicle;  $\tau_k$  denotes the travel time of the following vehicle;  $FV(i)$  denotes the set of following vehicles;  $tt_{ik}$  is the time difference between the target vehicle and the following vehicle passing the start point, which takes into account that the target vehicle might be stopped by traffic lights, enabling the following vehicle to catch it up;  $\Delta_c$  is the tolerance time which allows for the target vehicle to be overtaken by the following vehicle by a certain amount of time before it is identified as invalid.

This method is basically a dynamic way of cutting long travel times. Applying this method requires two parameters, namely, the number of following vehicles and tolerance time, to be properly determined. It is difficult to prove whether this method could work well in urban situations or not. If these two parameters are not well determined, e.g., the tolerance time is too large, the consequence is that the outliers of long travel times cannot be properly filtered.

### 3.2.2 Probe vehicles (GPS/Mobile phone)

Basically, probe vehicles are those vehicles which are equipped with certain sensors, e.g., GPS integrated navigation devices or mobile phones, travelling along the road and regularly reporting their positions on the route, travel speeds, directions and etc. In this subsection, two types of probe vehicles: Probe vehicles equipped with GPS integrated navigation devices and probe vehicles equipped with mobile phones are discussed.

#### Probe vehicles equipped with GPS integrated navigation devices

Vehicles (e.g., taxis, trucks, buses) equipped with GPS devices are widely used to collect traffic information (speeds or travel times) both on freeways and urban roads. There are three main issues related to GPS probe vehicles for collecting travel times in the urban environment including positioning, transmission frequency and sample size.

##### 1. Positioning

###### ● Stand-alone GPS positioning system

Concerning the positioning issue, GPS requires at least four satellites to estimate the location. In urban areas with overhanging trees, tunnels and tall buildings, this requirement might not be met and GPS systems will fail to estimate its position. This phenomenon is called 'urban canyon effect' which does exist in most cities. Due to unavailability of GPS signals or communication error, there are instances when data is not recorded by GPS equipment and link travel times in the urban area with this effect cannot be obtained by GPS systems. In addition, the reflection of satellite signals has a significant impact on the accuracy of GPS positioning (Modsching et al., 2006). E.g. in Figure 3.1, the satellite signal is reflected 3 times before reaching the receiver. The delay of the signal is extended by the length of  $t$  which is the sum of all additional paths the signal takes due to reflection. Due to the fact that the GPS receiver is unaware of the built-up in its

environment, it would determine its own position to  $Pos_{(GPS)}$  which is located at the opposite side of the building.

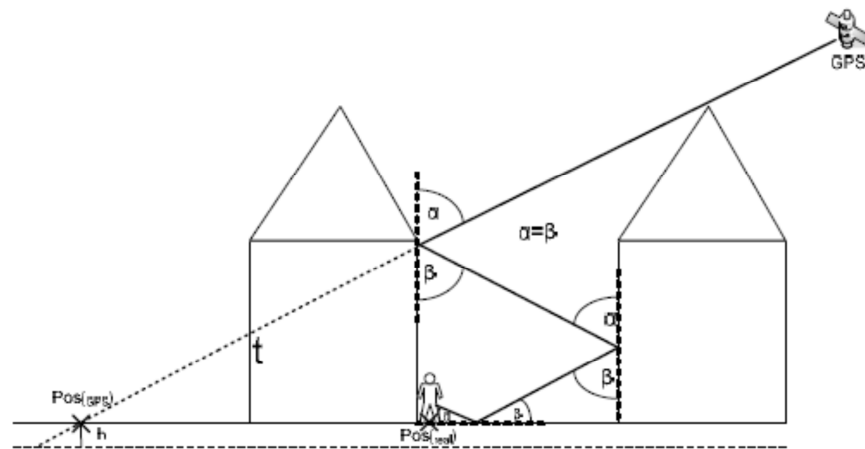


**Figure 3.1: GPS signal reflection (Modsching et al., 2006)**

- **GPS/MEMS INS integrated system**

The stand-alone GPS positioning system suffers signal masking, reflection of signal from buildings, large vehicles and GPS signal outages in the urban environment, which limits its capability to deliver the required level of availability, accuracy and reliability of positioning. The integration of GPS positioning system with other complementary navigation technologies, such as MEMS (Micro-Electro-Mechanical System) based inertial navigation system (INS), has shown a significant improvement in the positioning accuracy (Godha et al., 2007; Davidson et al., 2009). An inertial system consisting of inertial sensors (e.g., gyros, accelerometers) can provide continuous estimation of the position and the velocity, which can be used to augment GPS data when the signal is weak or short GPS signal outages. This GPS/MEMS INS integrated system has been applied in car navigation devices, e.g., Tomtom, Garmin.

## 2. *Transmission frequency*

Another issue about using GPS systems is the data transmission frequency which determines how frequently GPS systems receive positions of vehicles on the road. The higher the transmission frequency is, the more accurate link travel times can be estimated. Recently, some car navigation systems collect GPS data every second, which provides very detailed information about vehicle positions and speeds. Travel times can be easily derived from this high resolution GPS data. However, due to data processing and storage cost, a lot of commercial GPS solutions rarely record positions of vehicles with temporal interval smaller than 30s. For instance, taxis equipped with GPS devices are widely used to collect traffic information with polling intervals longer than 30s (e.g., 60s, 300s) in Chinese cities. The low temporal resolution makes it difficult to determine the precise times vehicles enter and exit a certain link. This also implies that travel times recorded by GPS probe vehicles are not complete link or route travel times but rather ‘intermediate’

travel times from a certain position on one link to a certain position on another link. This fact is overlooked by a lot of research that proposes to use GPS probe vehicles to collect link travel time data. It is necessary to re-estimate complete link or route travel times from the travel times recorded by GPS probe vehicles. Therefore, three methods to reallocate travel times collected by GPS probe vehicles into individual links are discussed in section 3.3 and the performance of each method in different traffic conditions is also presented.

### 3. Sample size

To what extent that travel times measured by probe vehicles can represent the mean population travel time is an important issue related to sample size and sample bias. The statistical sampling methodology can be used to determine the minimum required number of probe vehicles that would provide reliable link travel time estimates. For a link  $i$  and time interval  $t$ , let  $\mu_{it}$  represent the “true” mean of link travel time,  $\sigma_{it}$  represent the “true” variance of link travel time,  $n_{it}$  represent the number of probe vehicles required,  $\varepsilon_{max}$  represent the maximum relative error,  $\beta$  represent the percentage of time the absolute value of relative error is less than  $\varepsilon_{max}$ . In addition, let  $\Phi(x)$  represent the cumulative distribution function and  $\Phi^{-1}$  is the inverse. Assume that travel time on a particular link is an identically and independently distributed random variable, then the number of probe vehicles required can be calculated as:

$$n_{it} = \left[ \frac{\Phi^{-1}\left(\frac{1+\beta}{2}\right)\left(\frac{\sigma_{it}}{\mu_{it}}\right)}{\varepsilon_{max}} \right]^2 \quad (3.2)$$

Turner et al. (Turner et al., 1995) employed this statistical sampling method to obtain the minimum number of probe vehicles corresponding to a pre-specified permitted relative error and confidence level. The sample size equation can be obtained as:

$$n = \frac{z_{\alpha/2}^2 CV^2}{e^2} \quad (3.3)$$

Where  $z_{\alpha/2}$  is standard normal variables with the confidence level of  $1-\alpha$ ;  $CV$  is the coefficient of variation which is the standard deviation divided by the mean travel time;  $e$  is the permitted relative error (%). The assumption behind formulas (3.1) and (3.2) is that travel times collected by probe vehicles are valid. Outliers should be removed before applying this formula to determine whether the sample travel times collected by probe vehicles can provide a statistical representation of real travel time.

Table 3.1 gives an example of minimum sample size of GPS probe vehicles estimated using Equation (3.2) and the real sample size of GPS probe vehicles for one link during different time period on 15<sup>th</sup>, May, 2010. The field GPS data was collected in Changsha, a city in China. Every 30 seconds, speeds, time stamps and positions of GPS equipped taxis

were recorded and sent to the monitoring centre. Based on the collected time stamps, speeds and positions, the link travel time for each probe vehicle can be estimated. In order to see whether the mean link travel time estimated from probe vehicle data can statistically represent the mean travel time of all vehicles on this link, we applied the sampling method discussed above. Column 2 in table 3.1 illustrates sample size of probe vehicles derived from the field data for each time period of 15 minutes (total 2 hours). Column 3 and 4 indicate estimated sample size with different marginal error (5% and 10%). When the allowed maximum relative error is small, e.g., 5%, the required minimum sample size is larger than that measured from the field data in all time periods. In this case, it could not guarantee that the mean link travel time estimated from probe vehicles for each time period can represent the mean travel time of all vehicles on this link.

**Table 3.1: Comparison of field sample size of probe vehicles and estimated sample size with 95% confidence level**

Time period	Field GPS sample size	Estimated GPS sample size(marginal error =5%)	Estimated GPS sample size(marginal error =10%)
10:00-10:15	56	178	44
10:15-10:30	90	215	53
10:30-10:45	85	616	154
10:45-11:00	79	204	51
11:00-11:15	97	275	68
11:15-11:30	96	406	101
11:30-11:45	110	574	143
11:45-12:00	90	343	85

It can be clearly seen from equation (3.2) that for a given level of significance and permitted relative error, the sample size is directly determined by the coefficient of variation (CV) of the population. The higher the CV is, the larger the sample size is needed. Due to a number of stochastic factors on the urban road, e.g., the stochastic properties of traffic flow, the stochastic arrivals and departures at intersections, the variation of urban link travel time is larger than that of freeway travel time, the sample size needed is expected to be larger for urban link travel time estimation than for freeway travel time estimation.

In the urban area, there are two main sources causing the biased travel time estimates using probe vehicles, which are bias in the probe vehicle composition and bias in the arrival time distribution. The first source is widely accepted that only a certain type of vehicles as probe vehicles tends to have biased travel time estimates. For instance, lorries as probe vehicles are likely to be over represented within a sample of GPS travel time records since lorries are in general slower than private cars. Using taxis as probe vehicles can also lead to biased travel time estimates due to different driving behaviour of taxis which are likely to stop along the roadside for (un)loading or search for customers. The second source of bias in travel time estimates is the bias in the arrival time distribution as

discussed in (Hellenga et al., 2002). The variability of travel time that vehicles experience on the urban arterial road segment is predominately determined by the variability of delay experienced at the signalized intersection. Delay at signalized intersections can be calculated as the function of the arrival time with respect to the signal cycle. Therefore, a biased probe vehicle sample with respect to their arrival time distribution will lead to a biased travel time estimate no matter how many probe vehicles are available.

### **Probe vehicles equipped with mobile phones**

Vehicles with one or more active mobile phones have the potential to become probe vehicles. Mobile phones can be located by nearby base stations. There are different ways to calculate positions of mobile phones. One method is to estimate the position by calculating the distance from three nearby base stations. The positioning accuracy is about 50-200m. Another method is to calculate the direction the signal is coming from using special antenna arrays installed at the base stations. The typical accuracy is about 50-300m for this method (Wunnava et al., 2007). By applying mobile phone technologies, different mobile phone probe systems have been developed, such as Call Record Systems, Alink/Handoff Systems, Timing Advance Systems and Abis Measurement Report Systems (Cayford et al., 2010). In recent years, some cellular networks also use GPS to locate a mobile phone. In this method, GPS satellite system is used to calculate the position of the mobile phone. The accuracy is between 5m and 30m. Based on the information of time stamps between two located positions, Point-to-Point travel times can be directly derived. However, the first two methods (most commonly used in cellular network) of positioning have the problem of low positioning accuracy which ranges from 50m up to 300m. This might not be a serious problem on the freeway with mild traffic conditions. Whereas in the urban network with densely distributed roads, matching probe vehicle positions to the right road is very difficult. Within the distance of 200m, several parallel roads can be found in the urban area. Another problem related to mobile phone sensors is that it is difficult to distinguish whether a mobile phone is in the vehicle or outside the vehicle, especially on the urban road. For instance, mobile phone data from a user in a parallel metro or tram to the road can be misrecognized as travelling on the road, which causes an error for the travel time estimation. Similarly, when a pedestrian or cyclist uses a mobile phone on the footpath or cycle path along the road, the travel time collected by this mobile phone can be also misinterpreted as the vehicle travel time on the road, especially in congested conditions.

### **3.2.3 Bluetooth**

Bluetooth is a wireless communication platform used to connect electronic devices. The interconnection between Bluetooth devices is achieved through transmission and acceptance of a 48-bit Machine Access Control, or 'MAC' address between inquiring and receiving devices. Vehicles with one or more Bluetooth devices on board can be recognized by a Bluetooth receiver installed on the roadside and when they pass different

Bluetooth receivers on a route, the time difference between registrations at two locations can be used to estimate the travel time.

As shown in Figure 3.2, the Bluetooth device has a certain detection area with the radius about 50 to 60 meters. Vehicles with Bluetooth devices entering this circle will be detected. Therefore, a single device could collect data from both sides of the roadway.

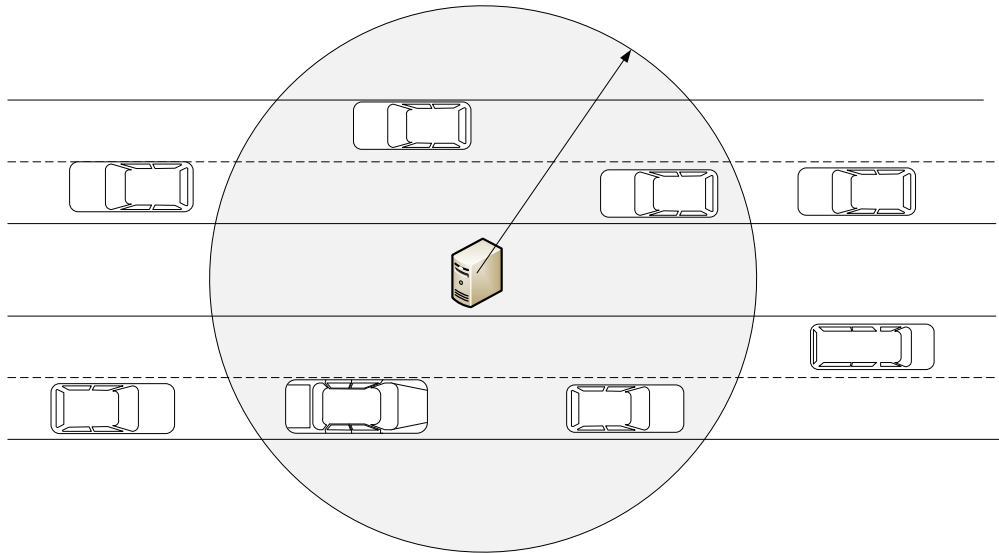


**Figure 3.2: An example of detection range of a Bluetooth scanner**

Application of Bluetooth devices for measuring travel times on freeways has shown very promising results (KMJ Consulting, 2010; Yegor et al., 2010). As discussed in (Yegor et al., 2010), travel times collected by Omni-directional antennae Bluetooth sensors even with small samples (e.g., 4%) can provide a good representative of the actual traffic condition. Another advantage of applying this technique is that the constant broadcast of MAC addresses is detectable and measurable without establishing a relationship to personal or sensitive information, keeping the travelling public and their information anonymous, which implies that the private issue is not a problem and it would be easier to implement in practice.

However, there are also some limitations related to this technique. First of all, Bluetooth devices transmit signals rather frequently. The Bluetooth-equipped vehicle could be detected at any time within the detection zone and could be detected several times when it passes a roadside Bluetooth receiver or not be detected at all depending on the driving speed and on the detection range of the Bluetooth device. The problem arises that which moments are chosen to calculate the travel time. For a longer distance, it might not be a big problem. While for a short distance, choosing inappropriate detection moments can cause large error. The estimation error is likely to be larger on the urban road if two Bluetooth devices are placed in a short distance (e.g., one link distance) or close to the intersections. Secondly, the same problem as discussed before with ANPR arises when vehicles that are detected at the beginning and at the end of a road segment may divert in

between or may stop for some time rather than being delayed by the traffic. This gives outliers and it is not always possible to distinguish the outliers from the regular trips. In order to see whether the method proposed by (Robinson, 2005) and discussed in section 3.2.1 can also be used to detect outliers from the Bluetooth data, a test was carried out. The Bluetooth data was collected in Changsha, a city in Hunan province, in China. The Bluetooth devices were placed on an urban arterial. The distance between these two devices is about 2200m and two intersections are in between. Figure 3.3 illustrates the individual travel time collected by Bluetooth devices for two directions. After applying the outlier detection method, the travel times with red circles are identified as outliers while the black dots are valid travel times. The detection results are quite sensitive to the number of following vehicles and the tolerance time as mentioned in section 3.2.1. The larger the tolerance time is, the less will travel times be identified as outliers. The travel time distribution based on all valid travel times identified by this method is compared with the travel time distribution from GPS data as shown in Figure 3.4 . Larger travel times are more frequently observed by Bluetooth devices for both directions (Southbound and Northbound) compared with those collected by GPS probe vehicles. The travel time distribution from GPS data shifts more to the left with smaller mean travel time compared with the travel time distribution from Bluetooth data. However, it is hardly to say whether the outlier detection method performs well or not since we don't have real ground truth data to validate it. Though travel time distribution from GPS data on the same link during the same time period could provide some evidence, these travel times are collected by taxis. In the uncongested condition, it is likely that taxis travel faster than other vehicles. The Kolmogorov-Smirnov test results are shown in Figure 3.5. The hypothesis that these travel time distributions (Bluetooth and GPS) come from the same distribution is rejected at 5 % significance level for both directions ( $p=2.91e-9 \ll 0.05$  and  $p=1.42e-5 \ll 0.05$ , respectively).

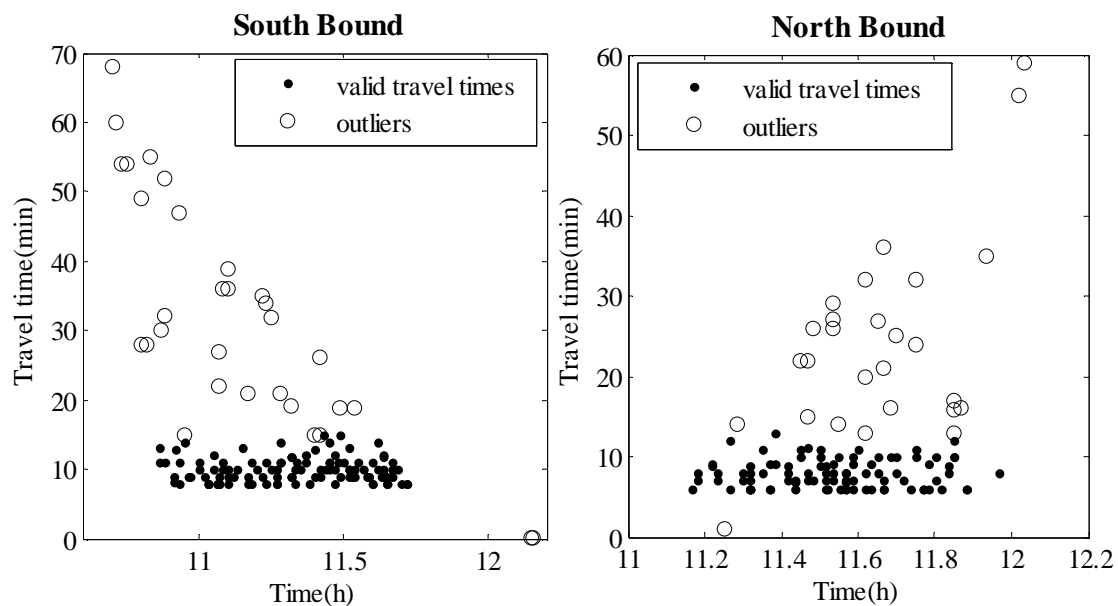


**Figure 3.3: Individual travel times collected by Bluetooth devices between time period of 10:30 and 12:05 on 15<sup>th</sup>, May, 2010**

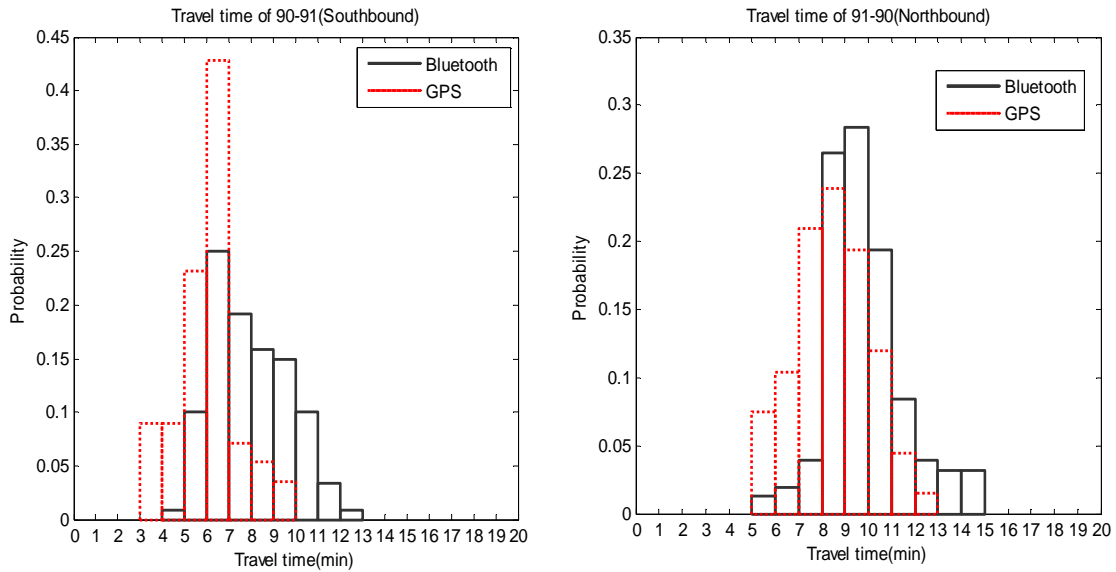


**Figure 3.4: Travel time distributions derived from Bluetooth data and GPS data**

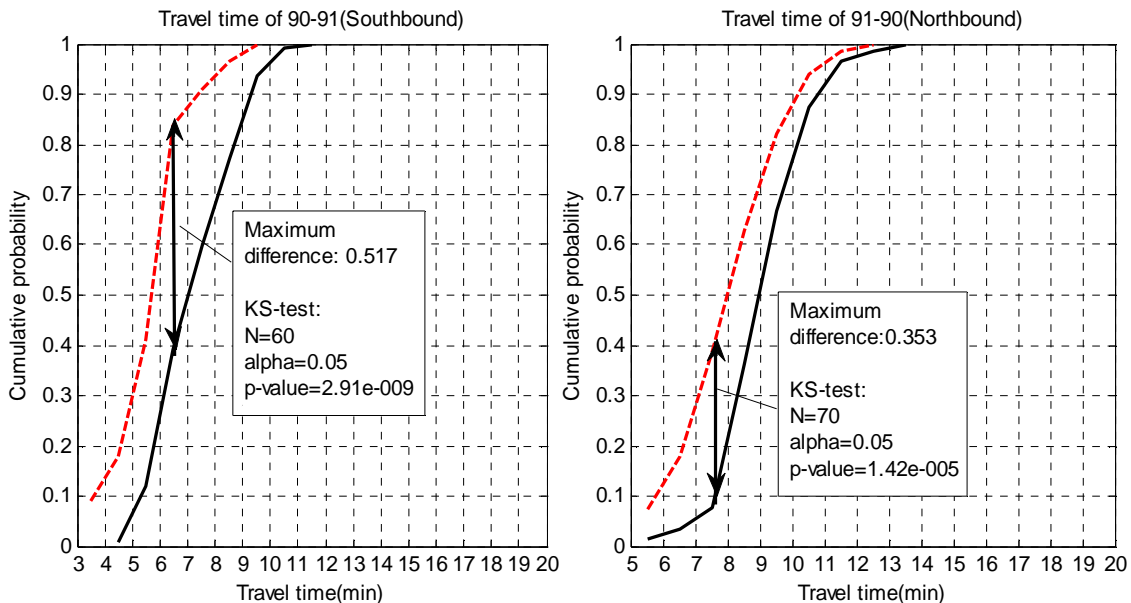


**Figure 3.5: Kolmogorov-Smirnov test for travel time distributions from Bluetooth data and GPS data**

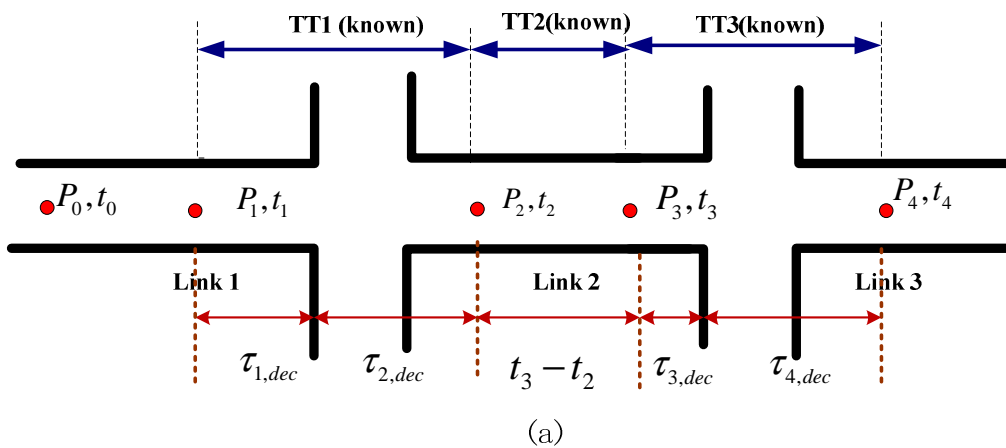
Besides, on the urban road, travel times collected by Bluetooth devices could come from cyclists or pedestrians carrying Bluetooth-enabled devices. Though, one would argue that the travel time experienced by a cyclist is much longer than that is from a vehicle. In congested conditions, this would not be the case since cyclists can experience similar travel times as vehicles within a short distance (e.g., a link of 500 meters). This type of outliers is rather difficult to distinguish in practice.

### 3.3 Comparison of urban link travel time estimation models based on probe vehicle data (PVD)

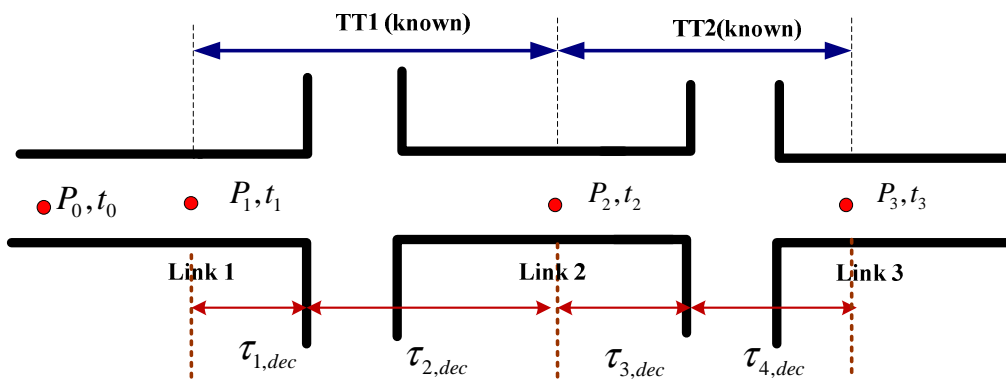
Travel times collected by probe vehicles with low polling frequencies usually does not apply to one single link and therefore cannot be directly used as travel time information for travellers or for further travel time prediction. This type of travel times is not a complete link or route travel time but rather from a certain position on one link to a certain position on the same or another link. As for travellers, when making route choices they want to know the complete link or route travel times from their origins to the destinations. It is necessary to allocate the travel times between two consecutive time stamps from probe vehicles into individual links.

#### 3.3.1 Link travel time allocation

Travel times collected by probe vehicles do not originate from a single complete link but are experienced by probe vehicles from a certain position on one link to a certain position on another link. These can be categorized into three types as illustrated in Figure 3.6 (a), (b) and (c).



(a)



(b)

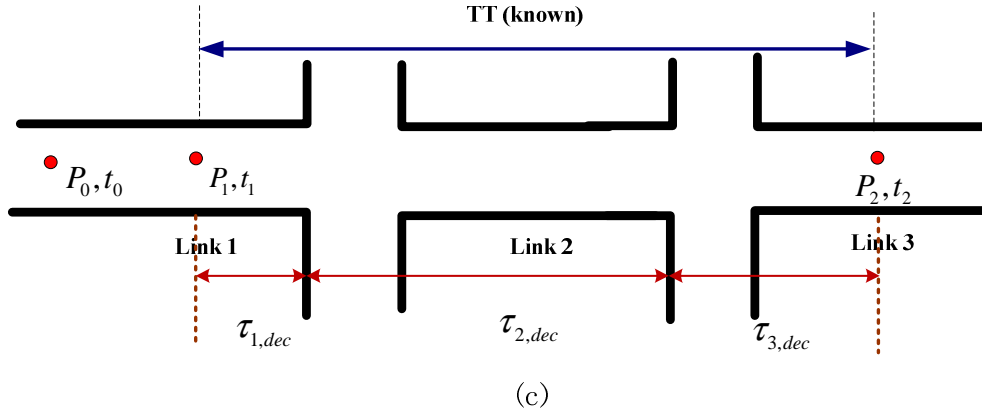


**Figure 3.6: Sketch of assignment of travel times between recorded positions to the link in the middle (taking through-going traffic as an example)**

$P_1$ ,  $P_2$ ,  $P_3$  and  $P_4$  are positions on the corresponding links and  $t_1$ ,  $t_2$ ,  $t_3$  and  $t_4$  are time stamps.  $t_{1,dec}$ ,  $t_{2,dec}$ ,  $t_{3,dec}$  and  $t_{4,dec}$  represent the reallocated link travel times based on the travel times collected by probe vehicles. The complete link travel time here is defined as the time difference between the time instant when the vehicle passes the upstream stop line and the time instant when the vehicle passes the downstream stop line.

**Type 1:** The reported positions are on the same link (e.g. Link 2) as shown in Figure 3.6 (a), the complete travel time of link 2 is composed of three parts:

$$TT_{L2} = \tau_{2,dec} + t_3 - t_2 + \tau_{3,dec} \quad (3.4a)$$

For this case, the link is long or the traffic condition on the target link is likely to be congested or vehicles need to wait for the red time since the probe vehicle experiences long travel time (at least longer than the sampling interval) on this link.

**Type 2:** The first and second reported positions are on adjacent links shown in Figure 3.6 (b), then the travel time of link 2 is estimated as:

$$TT_{L2} = \tau_{2,dec} + \tau_{3,dec} \quad (3.4b)$$

**Type 3:** At least one full link is existing between two consecutive reported positions illustrated in Figure 3.6 (c), the travel time of link 2 is:

$$TT_{L2} = \tau_{2,dec} \quad (3.4c)$$

For this case, the traffic condition on the target link is likely to be free flow or undersaturated since the probe vehicle experiences short travel time.

### 3.3.2 Description of Link travel time estimation models

#### **Model 1: Distance-proportion Model**

The basic idea of distance-proportion method is that the travel time between two time stamps is decomposed into individual links based on the distance. The link travel time based on this method can be derived according to three situations as shown in Figure 3.6. E.g., the travel time of link 2 can be estimated as:

#### **Type 1:**

$$\begin{aligned} TT_{L_2} &= \tau_{2,dec} + t_3 - t_2 + \tau_{3,dec} \\ &= (t_2 - t_1) \frac{L_2 P_2}{L_1(1-P_1) + L_2 P_2} + t_3 - t_2 + (t_4 - t_3) \frac{L_2(1-P_3)}{L_2(1-P_3) + L_3 P_4} \end{aligned} \quad (3.5a)$$

#### **Type 2:**

$$\begin{aligned} TT_{L_2} &= \tau_{2,dec} + \tau_{3,dec} \\ &= (t_2 - t_1) \frac{L_2 P_2}{L_1(1-P_1) + L_2 P_2} + (t_3 - t_2) \frac{L_2(1-P_2)}{L_2(1-P_2) + L_3 P_3} \end{aligned} \quad (3.5b)$$

#### **Type 3:**

$$TT_{L_2} = \tau_{2,dec} = (t_2 - t_1) \frac{L_2}{L_1(1-P_1) + L_2 + L_3 P_2} \quad (3.5c)$$

where  $L_1$ ,  $L_2$  and  $L_3$  denote the length of link1, link2 and link3, respectively.

This decomposition method is very simple and does not contain any other assumption than that travel times are allocated proportional to the length of the links that the probe vehicle has travelled between two registrations.

#### **Model 2: Hellinga's model**

Hellinga (Hellinga, 2008) proposed an analytical model to decompose recorded partial link or route travel time into individual links considering the stopping probability and congestion probability. On the following, a brief introduction of this method is given. More detailed information about this method is given in Hellinga's original paper.

According to the definition proposed by Hellinga, link travel times in the urban road network can be decomposed into 3 parts:

- 1) Free flow travel time;
- 2) Stopping time caused by traffic control devices (deceleration and acceleration are included);

### 3) Delay due to traffic congestion.

Therefore, the travel time between two consecutive time stamps of a probe vehicle can be expressed as:

$$t_{m,i+1} - t_{m,i} = \sum_{j=0}^{J(m,i)} \{ \tau_f(l_{m,i,j}) + \tau_s(l_{m,i,j}) + \tau_{cong}(l_{m,i,j}) \} \quad (3.6)$$

where  $t_{m,i}$ ,  $t_{m,i+1}$  are consecutive time-stamps of probe vehicle  $m$  on link  $i$  and link  $i+1$ ;  $\tau_f(l_{m,i,j})$  is the free flow travel time on link  $j$ ;  $\tau_s(l_{m,i,j})$  is the stopping time on link  $j$  and  $\tau_{cong}(l_{m,i,j})$  is the congestion time on link  $j$ .

The free flow travel time on a link is calculated as the link length divided by the free flow speed:

$$\tau_f(l(n_i, n_j)) = \frac{|l(n_i, n_j)|}{u_f(n_i, n_j)} \quad (3.7)$$

Where  $|l(n_i, n_j)|$  is the length of the complete link or partial link  $l(n_i, n_j)$ ,  $u_f(n_i, n_j)$  is the free flow speed for the complete or partial link  $l(n_i, n_j)$ . However, in reality, free flow speeds vary with driving behaviour, speed limit, weather conditions, etc. It is difficult to estimate free flow speeds. Instead, the maximum allowed speed is used to calculate the free flow travel time. In order to see how Hellinga's method performs with different free flow speeds, a sensitivity analysis of the free flow speed is discussed in section 3.3.4.

The congestion time and stopping time based on the probability function are calculated by Hellinga as:

$$\tau_{cong}(l_{m,i,J}) = \int_0^{w_{max}} \sigma_{m,i,J} \tau_{cong} \frac{\sum_{j=0}^{J(m,i)} P_w(m,i,w) P_s(l_{m,i,J},w)}{Q_s(m,i)} dw \quad (3.8)$$

$$\tau_s(l_{m,i,J}) = \int_0^{w_{max}} \tau_s \frac{P_w(m,i,w) P_s(l_{m,i,J},w)}{Q_s(m,i)} dw \quad (3.9)$$

Where  $w$  is the congestion index which is the ratio of the congestion time on the route to the sum of the congestion time and the free flow travel time on the route; The minimum value of  $w$  occurs when traffic demand is very low and the probe travels at the free speed and the maximum value  $w_{max}$  occurs when vehicles travel at a speed less than free flow speed due to traffic congestion and experience no delay caused by traffic control devices.  $\tau_{cong}$  is the total congestion time;  $\tau_s$  is the total stopping time;  $P_w(m,i,w)$  is the congestion probability which is used to capture the likelihood of a certain degree of congestion experienced by a probe vehicle  $m$  when traversing a given link. It is defined as:

$$P_w(m, i, w) = \min\left(1, \frac{T_c(m, I_p(i)) + T_c(m, i)}{t_{m, I_p(i)+1} - t_{m, I_p(i)} + t_{m, i+1} - t_{m, i}} \frac{1}{w}\right) \quad (3.10)$$

where  $T_c(m, i)$  is the maximum delay the probe vehicle  $m$  experiences due to congestion.

$P_s(l_{m,j,J}, w)$  is the stopping probability which assumes that a probe vehicle stops at most once on the route. It is defined as:

$$P_s(l_{m,i,j}, p, w) = \begin{cases} H_s(l_{m,i,0}, w) & \text{if } J(k, i) = 0 \\ H_s(l_{m,i,J}, w) \prod_{j \neq J} (1 - H_s(l_{m,i,j}, w)) & \text{otherwise} \end{cases} \quad (3.11)$$

where  $H_s(l_{m,j,J}, w)$  is the probability of stopping on a link. It is worth mentioning that there are two parameters  $c_1$  and  $c_2$  in the stopping probability function which need to be calibrated. In section 3.3.4, a sensitivity analysis regarding these two parameters is given.

### **Model 3: Artificial Neural Network model**

Basically, the traffic data collected by probe vehicles include positions, time stamps and speeds on the route. Therefore, positions, time stamps and speeds can be used as the input data in the Artificial Neural Network (ANN) model. Traffic flow and signal timings are considered optionally since on one hand, they are not always available on the urban road network and on the other hand, it is preferable to develop a model to estimate travel time as accurate as possible with least information and make the model more generic. As discussed in (Hellenga, 2008), the traffic condition the probe vehicle experiences during the recent sampling interval is considered not substantially different from that on the route traversed by the same probe vehicle during the previous sampling interval. In the ANN model, the probe vehicle information on previous sampling interval is incorporated with the information on the recent sampling interval. Figure 3.7 shows the structure of the ANN model. The mathematical description of the model is as follows:

#### ***Input layer:***

$$X(i) = \begin{bmatrix} x_1(i) \\ \vdots \\ x_n(i) \end{bmatrix} = \begin{bmatrix} p(i) \\ s(i) \\ t(i) \\ u(i) \end{bmatrix} \quad (3.12)$$

Where  $p(i)$  is the position vector of probe vehicle  $i$  on the upstream link, target link and downstream link;  $s(i)$  is the link number vector indicating on which links the probe vehicle positions are;  $t(i)$  is the time stamp vector which indicates the time instances when the probe vehicle sends the information;  $u(i)$  is the speed vector.

$$p(i) = \begin{bmatrix} p_1(i) \\ \cdot \\ \cdot \\ p_j(i) \end{bmatrix}, \quad s(i) = \begin{bmatrix} s_1(i) \\ \cdot \\ \cdot \\ s_j(i) \end{bmatrix}, \quad t(i) = \begin{bmatrix} t_1(i) \\ \cdot \\ \cdot \\ t_j(i) \end{bmatrix}, \quad u(i) = \begin{bmatrix} u_1(i) \\ \cdot \\ \cdot \\ u_j(i) \end{bmatrix}$$

The number of input neurons in our model can be determined as  $N=n*m$ ; where  $n$  is the number of information points taken into consideration for each probe vehicle;  $m$  is the categories of information, here  $m$  is chosen to be 4 (positions, link IDs, time stamps and speeds).

For the case in Figure 3.6 (a), the information on the previous sampling interval is also taken into account, so the input neurons are  $5*4$  (5 positions+5 link IDs+5 time stamps +5 speeds) for each probe vehicle. For the case in Figure 3.6 (b),  $4*4$  input neurons are used and  $3*4$  input neurons are needed for the case in Figure 3.6 (c).

#### **Hidden layer:**

$$H(i) = \begin{bmatrix} h_1(i) \\ \vdots \\ h_m(i) \end{bmatrix} = \begin{bmatrix} \varphi \left( \sum_{j=1}^n \omega_{j,1} x_j(i) + b_1 \right) \\ \vdots \\ \varphi \left( \sum_{j=1}^n \omega_{j,m} x_j(i) + b_m \right) \end{bmatrix} \quad (3.13)$$

where  $h_m(i)$  denotes the value of the  $m^{th}$  hidden neuron,  $\omega_{j,m}$  denotes the weight connecting the  $j^{th}$  input neuron and the  $m^{th}$  hidden neuron,  $b_m$  denotes a bias with a fixed value for the  $m^{th}$  hidden neuron;  $\varphi$  is the transfer function. Common forms of the transfer function are logistic sigmoid and hyperbolic tangent functions. In practice, the latter is found to give rise to faster convergence (Bishop, 1995). Thus, we chose

$$\varphi(x) = \frac{1 - e^{-2x}}{1 + e^{-2x}}$$

#### **Output layer:**

$$Y(i) = TT(i) = \phi \left( \sum_{k=1}^m \omega_k h_k(i) + b \right) \quad (3.14)$$

where  $Y(i)$  denotes the estimated travel time of probe vehicle  $i$ ;  $\omega_k$  denotes the weight connecting the  $k^{th}$  hidden neuron and the output neuron;  $b$  is the bias for the output;  $\Phi$  is the transfer function and a linear function is commonly used for the output units.

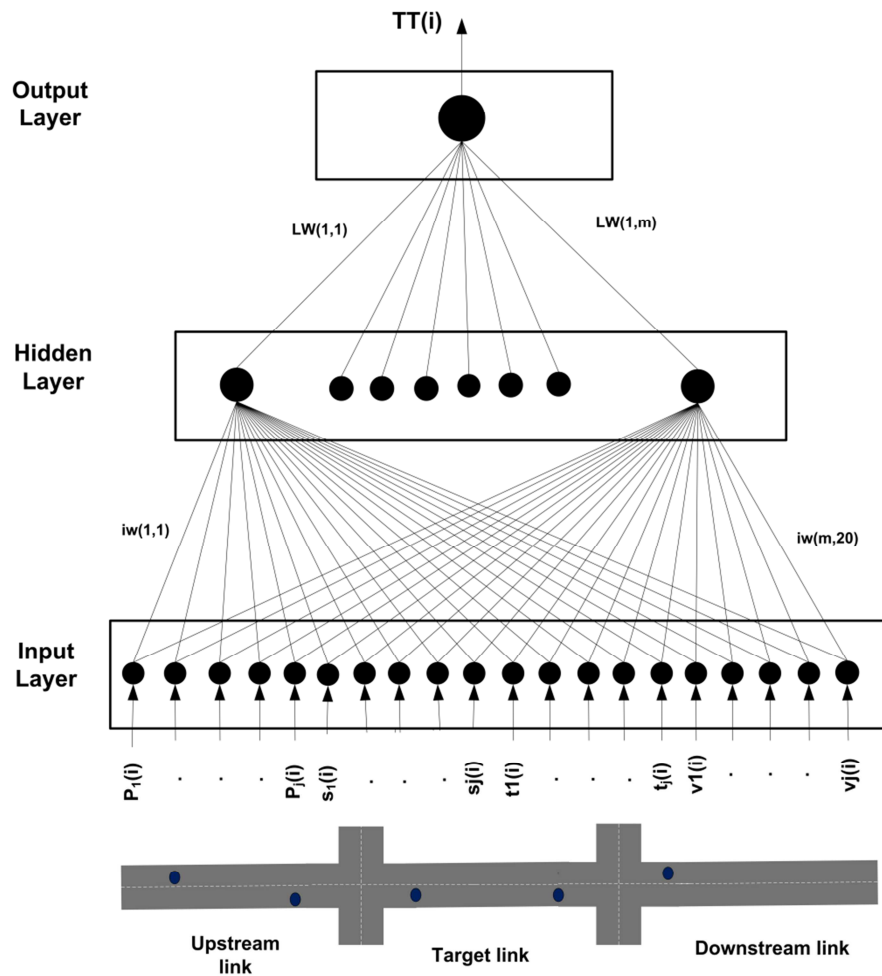
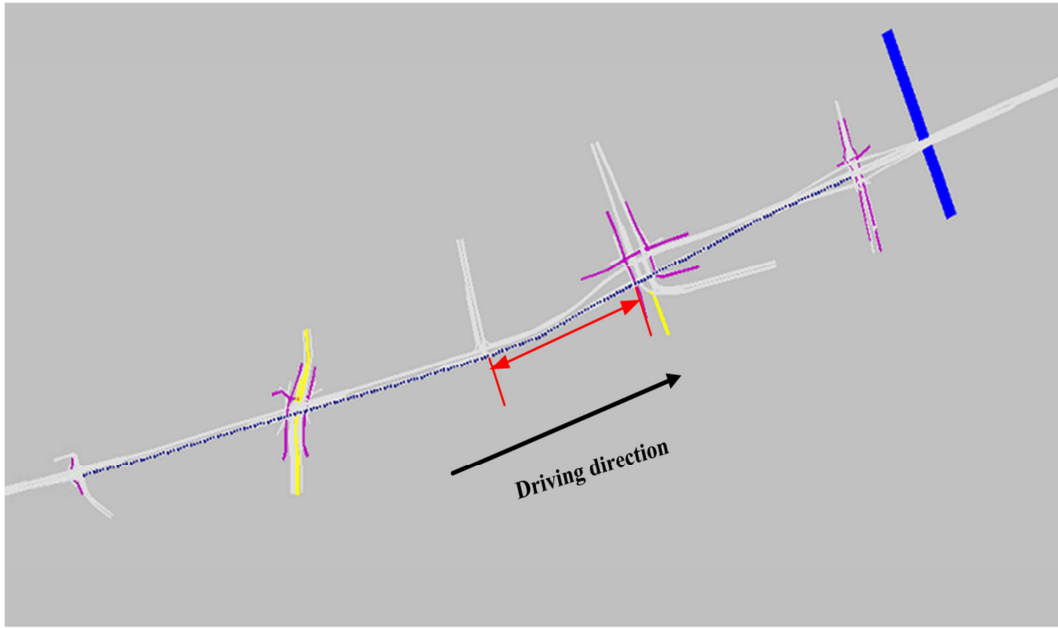


Figure 3.7: Topology of an Artificial Neural Network for link travel time estimation

### 3.3.3 Experimental setup

#### Description of the Test urban road

As shown in Figure 3.8, an urban road called ‘Kruithuisweg’ in Delft city in the Netherlands was modelled using the VISSIM simulation model. Kruithuisweg is a typical urban road with signalized intersections lying between two freeways, A4 and A13. In order to mimic the real traffic situation on this road, traffic was assigned using Dynamic Traffic Assignment (DTA) based on the dynamic OD matrix in VISSIM. All the traffic signal controllers at the intersections are vehicle actuated. The free flow speed is set to be 100km/h which is the speed limit on the real situation. The dots are the data collection points which record the information of vehicles every second. The arrow indicated in the figure is the target link for travel time estimation.



**Figure 3.8: VISSIM model of Kruithuisweg road in Delft, the Netherlands**

### **Data preparation**

#### ***Re-sampling process***

The network was simulated for a period of 65min for each simulation run. Data from the first 5min of simulation were considered to be the warm-up period and were not used in the analysis. Every second, positions, time stamps and speeds of vehicles were recorded by the data collection point. However, in real world, the sampling interval is much longer than 1s. Instead, the sampling interval of 30s or 60s is more often used in reality. Hence, a ‘Re-sampling’ procedure with 60s interval was taken to extract the data from the original simulation data set. One thing we should keep in mind is that the position of the probe vehicle can be anywhere on the link when sampling. This means that if we just take one position on the link as the initial sampling position, the estimation results will be biased. The ‘Re-sampling’ strategy can be explained by Figure 3.9. For instance, if the initial sampling moment is  $i$ , when applying 60s sampling strategy, the next moment is  $j+60$ , and then  $j+120$ ,  $j+180$ , etc. We can get different moment combinations to estimate the travel time of link 2.

**Combination 1:**  $j, j+60, j+120, j+180, j+240, \dots$

**Combination 2:**  $j+1, j+61, j+121, j+181, j+241, \dots$

Therefore, the average travel time of a probe vehicle  $i$  traversing link 2 can be calculated as:

$$TT_{L2}(i) = \frac{1}{n} \sum_{j=1}^n TT_{L2,j}(i) \quad (3.15)$$

where  $n$  is the number of different initial sampling moments,  $TT_{L2, j}(i)$  is the estimated link 2 travel time of probe vehicle  $i$  with the initial sampling moment  $j$ .

Equation (3.15) is applied for all three models (Distance-proportion model, Hellinga's model and NN model) to calculate the average estimated travel time for each probe vehicle. The true link travel time of a probe vehicle traversing the target link is recorded by data collection points located at the beginning of the link and the end of the link.

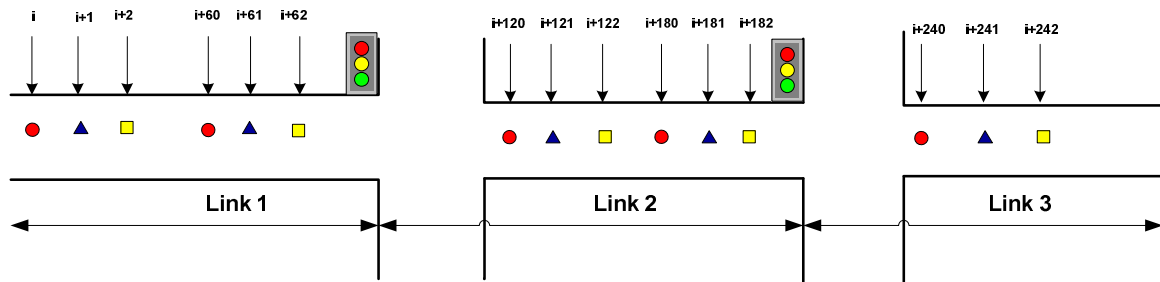


**Figure 3.9: Different moments (positions) recorded by probe vehicles on different links**

#### *Data for training and evaluation*

After the 'Re-sampling' process, the extracted data were used for training the neural network and estimating the link travel time. Total 70 random seeds were simulated and probe vehicle data from 30 random seeds, in which 20 random seeds are in the undersaturated condition and 10 random seeds are in the highly oversaturated condition, were used for the training process. The other 40 random seeds were used for the performance evaluation. Four scenarios were chosen for evaluation. The subdivision of data sets for training and evaluation is indicated in Table 3.2.

- **Scenario 1:** Original demand (undersaturated condition)
- **Scenario 2:** 20% demand increase
- **Scenario 3:** 50% demand increase
- **Scenario 4:** 100% demand increase (highly oversaturated condition)

**Table 3.2: Simulated data sets for training and evaluation**

	Training			Evaluation				
		<i>training</i>	<i>validation</i>	<i>testing</i>	<i>scenario 1</i>	<i>scenario 2</i>	<i>scenario 3</i>	<i>scenario 4</i>
<b>Number of random seeds</b>	Undersaturation	12	4	4	10	10	10	10
	Oversaturation	6	2	2				

Also a real GPS data set was extracted from original data obtained from trips along the Kruithuisweg road for validation purpose. This was done according to the re-sampling process and contained in total 7 trips.

### Neural Network training

A training process is needed before the ANN model can be applied to estimate link travel times. Three procedures including training, validation and testing were conducted in the whole training process. The total training data set was divided into three subsets which are 18 random seeds for training, 6 random seeds for validation and 6 random seeds for testing. During the training process, different hidden neurons, e.g. 10, 15, 20, 25, were chosen. The testing results show that the performance in terms of Mean Square Error(MSE) for the case of 10 and 15 neurons is not as good as that of 20 or 25 neurons. Therefore, 20 hidden neurons were used to build the network. Levenberg-Marquardt algorithm (Ranganathan, 2004) was chosen so that the over fitting phenomenon could be avoided. Besides, the Levenberg-Marquardt algorithm can provide fast convergence even for large networks that contain a few hundred weights. The trained ANN model is applied to estimate link travel times both in undersaturated conditions and oversaturated conditions.

### 3.3.4 Sensitivity analysis in Hellinga's model

In Hellinga's model, link travel time is composed of three parts including free flow travel time, congestion time and stopping time. In order to estimate free flow travel times, free flow speeds need to be determined. Besides, in the stopping likelihood function as proposed by Hellinga, two model parameters denoted by  $c_1$  and  $c_2$  were used to reflect the stopping likelihood pattern of the link. In this section, the sensitivity of the performance in terms of RMSE and MAPE of this model in both low traffic demand conditions and high traffic demand conditions are investigated.

$$RMSE = \sqrt{\frac{1}{n} \sum_{i=1}^n (t_{PVD,i} - t_{true,i})^2} \quad (3.16)$$

$$MAPE = 100 * \frac{1}{n} \sum_{i=1}^n \left| \frac{t_{PVD,i} - t_{true,i}}{t_{true,i}} \right| \quad (3.17)$$

Where,  $t_{PVD,i}$  is the estimated travel time of the  $i^{th}$  probe vehicle;  $t_{true,i}$  is the true link travel time of the  $i^{th}$  probe vehicle recorded by the data collection points.

Figure 3.10 gives an illustration of how different combinations of  $c_1$  and  $c_2$  influence the performance of the Hellinga's model in terms of RMSE and MAPE. The free flow speed was set to be the speed limit (100km/h) for this case. The best combination of  $c_1$  and  $c_2$  was then chosen and the next step is to analyse the sensitivity of the performance to the free flow speed, for which a range of speeds from 50 km/h to 150 km/h was used. The best combination of  $c_1, c_2$  and the free flow speed for each scenario is given in Table 3.3. The selected parameter values are used in Hellinga's model to estimate complete link travel times.

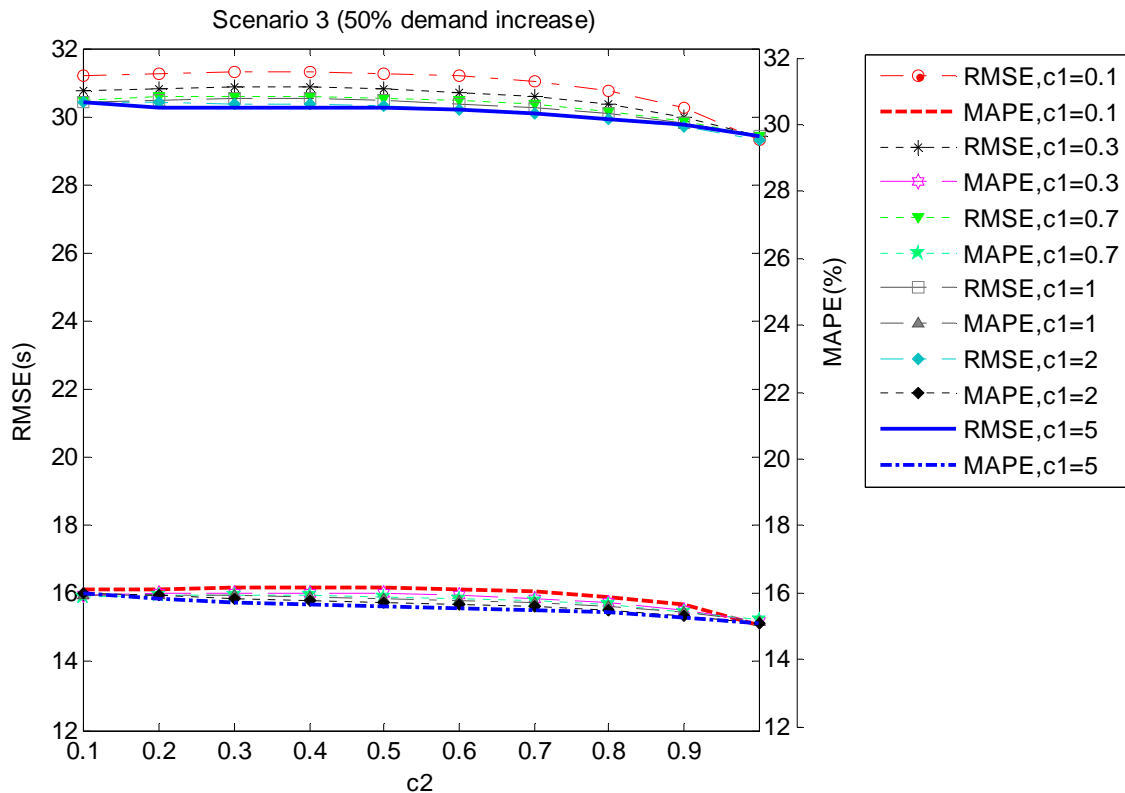


**Figure 3.10: Performance of Hellinga's model with different combinations of  $c_1$  and  $c_2$  in scenario 3**

**Table 3.3: Parameter values in Hellinga's model under different traffic conditions**

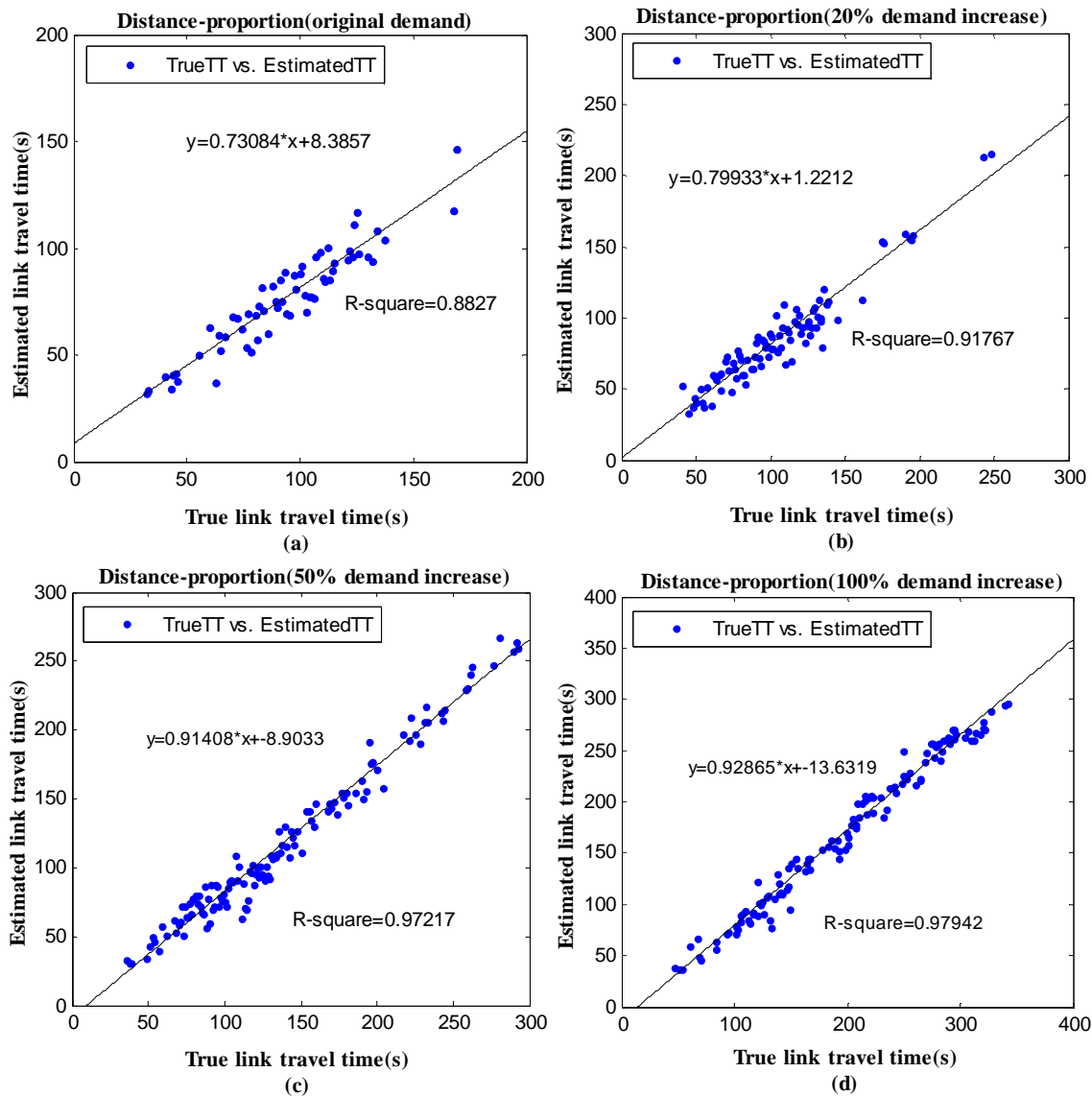
Parameters	Scenario 1	Scenario 2	Scenario 3	Scenario 4
$c_1$	5	5	0.1	0.1
$c_2$	1	1	1	1
Free flow speed (km/h)	80	80	100	110

### 3.3.5 Results

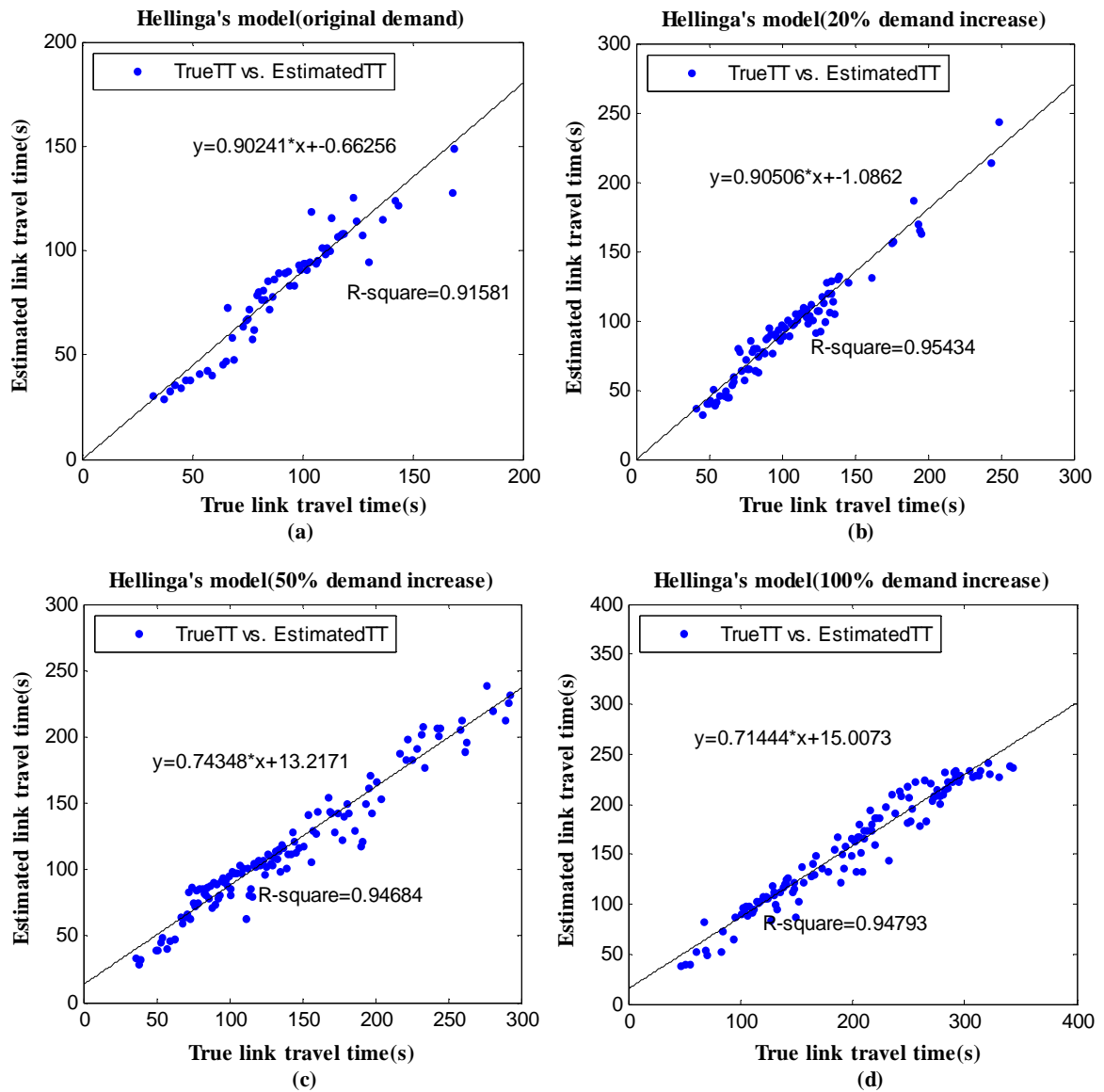
#### Results based on simulation data

Figure 3.11, Figure 3.12 and Figure 3.13 provide the comparison between the estimated link travel times based on the Distance-proportion model and true link travel times, estimated link travel times based on Hellinga's model and true link travel times, estimated link travel times based on the ANN model and true link travel times under different traffic demand conditions, respectively. The average travel time for each probe vehicle is estimated based on Equation (3.15) for all three models. Each point represents individual travel time for each probe vehicle. A linear regression is applied to compare the estimated links travel times with the true (simulated) link travel times. When traffic demand increases from original free flow condition to high demand condition, both the distance-proportion model and Hellinga's perform reasonably well with  $R^2 > 88\%$ . Among these

three models, the ANN model performs the best as can be seen in Figure 3.13 (a), (b), (c) and (d). The estimated link travel times based on ANN exhibit no apparent bias and have very high correlation with the true link travel times ( $R^2 > 96\%$ ). The performance of these three estimation methods in terms of RMSE and MAPE is indicated in Table 3.4. As for ANN model, both RMSE and MAPE increase marginally as traffic demand increases. The increase of MAPE is less than 2%. As for Hellinga's model, the MAPE increases from 12% to 20% when traffic demand increase from undersaturated conditions (Original demand and 20% demand increase) to oversaturated conditions (50% demand increase and 100% demand increase). Compared with Hellinga's model, the Distance-proportion model gives less accurate estimation results when the traffic demand is low (in the case of original demand and 20% demand increase); However, when the traffic demand increases (from 50% increase to 100% increase), the Distance-proportion method provides more accurate estimation with lower RMSE.



**Figure 3.11: Correlation between estimated link travel times and true link travel times based on Distance-proportion method (60s sampling interval)**



**Figure 3.12: Correlation between estimated link travel times and true link travel times based on Hellinga's method (60s sampling interval)**

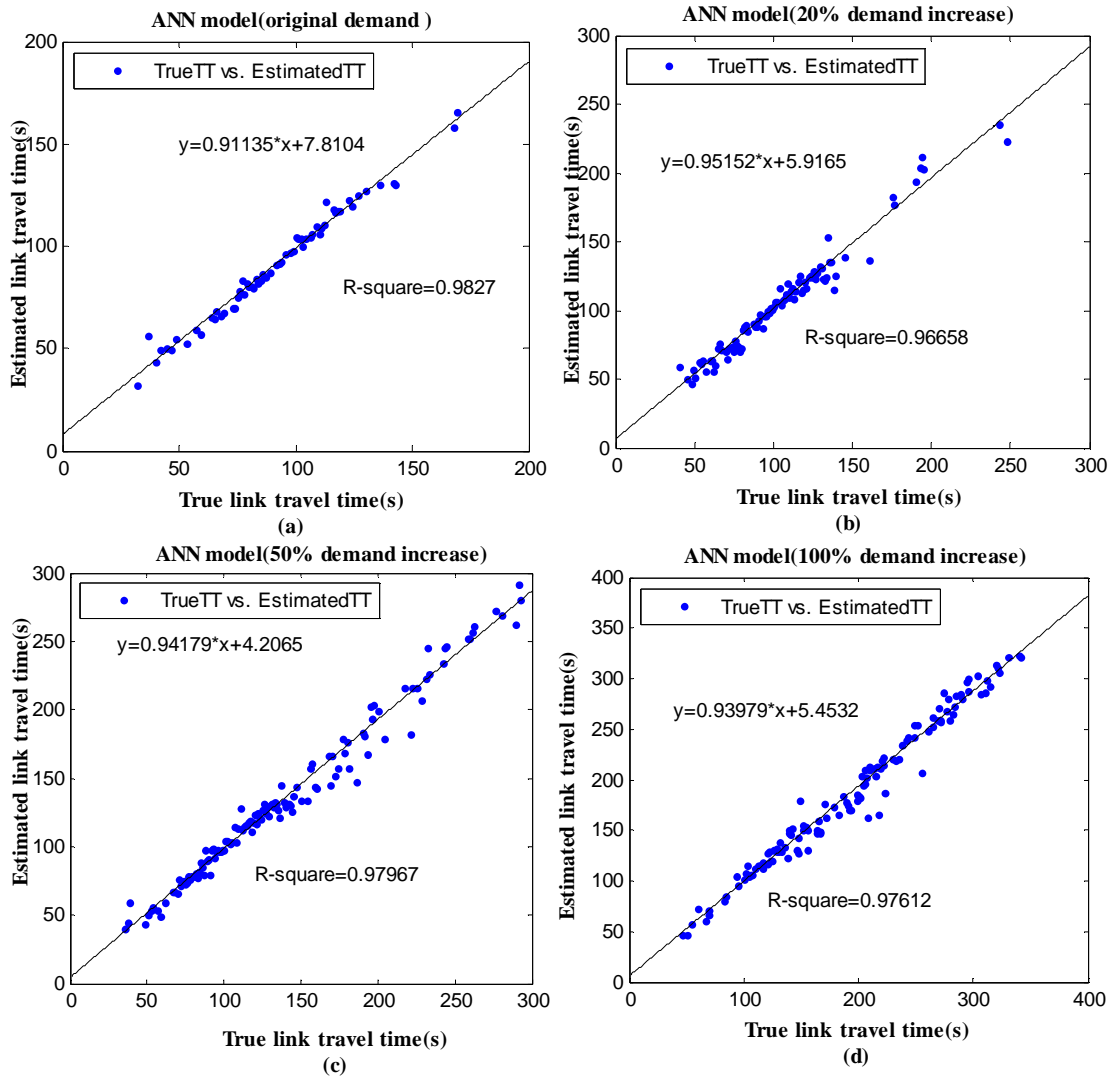


**Figure 3.13: Correlation between estimated link travel times and true link travel times based on ANN method (60s sampling interval)**

**Table 3.4: Performance measurements of Distance-proportion model, ANN model and Hellinga's model with different traffic demand**

	Scenario 1			Scenario 2		
	Distance_proportion	Hellinga	ANN	Distance_proportion	Hellinga	ANN
RMSE(s)	20.06	12.98	4.53	23.75	13.69	7.57
MAPE(%)	16.85	12.20	3.97	18.88	10.96	5.61
Average Travel time(s)	91.35			105.73		
	Scenario 3			Scenario 4		
	Distance_proportion	Hellinga	ANN	Distance_proportion	Hellinga	ANN
RMSE(s)	23.50	29.44	9.97	30.11	48.55	13.48
MAPE(%)	15.90	15.18	4.98	15.50	20.03	5.08
Average Travel time(s)	137.80			192.51		

### Results based on real GPS data

The trained ANN model was also applied to estimate travel times based on the real GPS data. A car with a GPS device was driving back and forth on the same road ‘Kruithuisweg’ 7 times and all the GPS positions were recorded every 0.3s. As discussed in the section 3.2.2, GPS positioning is not so accurate on urban roads due to tunnels, tall buildings, etc. Reflection of GPS signals has a significant impact on the accuracy of estimated positions. In our experiment, the urban road ‘Kruithuisweg’ is located in an open area. The ‘urban canyon’ is not a problem in our case.

In the sampling procedure, 60s sampling interval was applied to extract GPS data from the original data set. The estimation result is shown in Figure 3.14. Each point represents the travel time for each trip. From the regression formula in the figure, it can be seen that the trained ANN model performs reasonably well. The RMSE and MAPE are about 7.8s and 10.9%, respectively. While for the Hellinga’s model, the estimation accuracy is lower with RMSE and MAPE of 14.2s and 20.6%, respectively. Though one could argue that the real data set is too small to give a statistically sound result, it shows the possibility to apply the ANN model to the real GPS data.

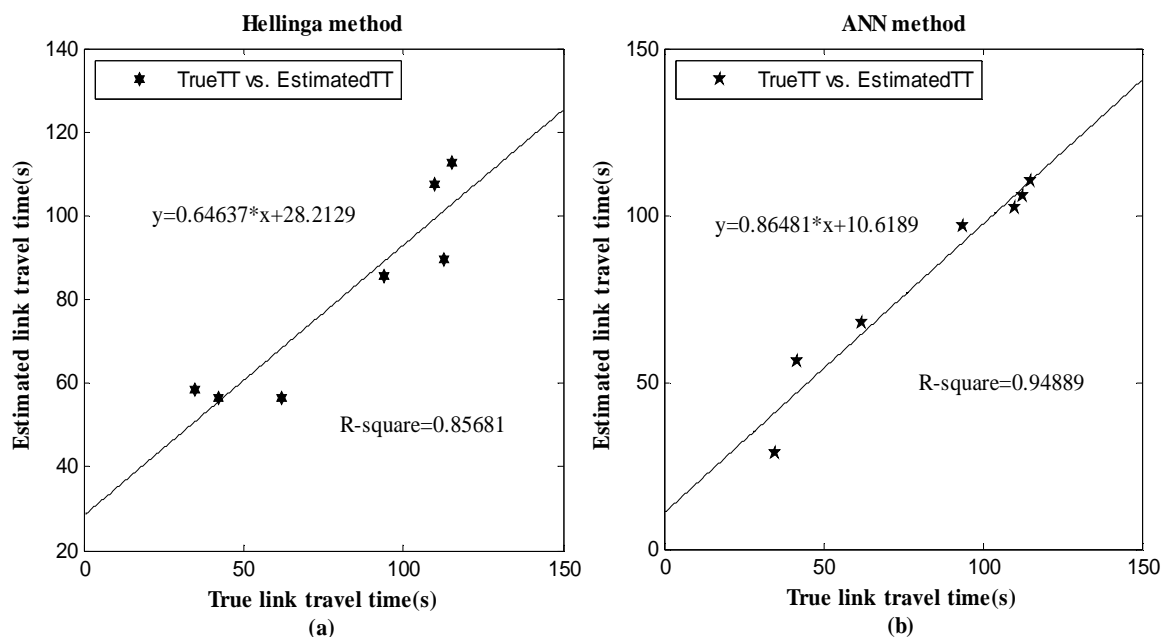


**Figure 3.14: Correlation between estimated link travel times and true link travel times based on real GPS data**

### 3.3.6 Conclusions

Link travel time estimation based on the travel times collected by probe vehicles is one important application of PVD. Up to now, there is not much research about travel time allocation using PVD. In this section, three models are applied to estimate the complete link travel time based on PVD. A three-layer Artificial Neural Network model is proposed to estimate complete link travel times. The input information in the ANN model includes

individual probe vehicle's positions, link IDs, time stamps and speeds. The estimation results are compared with those from Distance-proportion model and Hellinga's model. The ANN model performs quite well under different traffic conditions. On average, the MAPE is less than 6 %. As for Hellinga's model, the MAPE increases from 12% to 20% when the traffic demand increases. In Hellinga's model, the link travel time is composed of free flow travel time, stopping time and congestion time. When congestion occurs, stopping time and congestion time are the main components of the estimated link travel time, which also suggests that stopping probability and congestion probability should be properly calibrated, especially when dealing with signalized intersections. The delay time can be caused by either traffic control or congestion. One thing worth mentioning is that the number of parameters in the ANN model is much more than those in Hellinga's model. The higher performance of the ANN model is probably also due to the higher number of parameters.

### 3.4 Summary and discussions

Travel times are important not only for traffic management and planning, but also for the traffic guidance in the urban area. This chapter compared different techniques (ANPR cameras, probe vehicles, Bluetooth devices) developed in recent years to measure travel times on the urban road. The challenge of ANPR and Bluetooth devices for measuring urban travel times is how to properly determine outliers, which is not an easy task. Compared with ANPR and Bluetooth technologies, probe vehicles equipped with positioning (e.g., GPS, DGPS, GPS/MEMS integrated system) devices are more promising for collecting urban travel times. Especially in the case of GPS/MEMS equipped car navigation system with high polling frequency (e.g., 1s), travel times can be accurately derived. Special focus was given to the probe vehicle data (PVD) with low polling frequencies (e.g., 15s, 30s, 60s). Due to the fact that travel times directly collected by these probe vehicles are unlikely to be complete link or route travel times, in this chapter different models including Distance-proportion model, Hellinga's model and Artificial Neural Network (ANN) model to estimate complete link travel times based on PVD were discussed and compared with each other. The estimation results showed that the ANN model gives the best performance.

Travel times measured by ANPR cameras, probe vehicles and Bluetooth devices provide useful information about the traffic state on the road. First of all, measured travel times provide the ground-truth for developing any travel time estimation or prediction model. Secondly, measured travel times are valuable for building the historical travel time database for the purpose of traffic management and planning. Finally and also most importantly, from measured travel times, travel time distribution can be derived which provides more insight into travel time variability and furthermore can be used for travel time prediction purpose. However, travel time distribution derived from measured travel times could not give sufficient insight into what causes this travel time distribution, in other words, what causes the travel time variability. A model that could provide some

insight into factors that lead to a certain travel time distribution and furthermore estimate the travel time distribution would be preferable. Therefore, in chapter 4, a delay (travel time) distribution model for an isolated intersection is developed taking different stochastic factors into account. This model is further extended to an urban trip with fixed time controlled intersection in chapter 5.



# Chapter 4

## Delay distribution for signalized intersections

### 4.1 Introduction

In the previous chapter, several empirical methods to measure travel times on urban roads have been discussed and different models to estimate the complete link travel time have been introduced. The remaining question is how we can make good use of measured travel times. Providing mean travel time to travellers would lead to the problem that the actual travel time can be significantly different from the mean travel time, especially on the urban road. One important application of these travel time measurements (estimates) is that travel time variability can be investigated by looking at travel time distribution or using other statistical measures, e.g., percentiles, standard deviation, coefficient of variance. Instead of directly modelling travel time variability from measured travel times, an alternative way is to model travel time variability analytically. On urban roads, the uncertainty of delay at intersections is the main source of travel time uncertainty. The stochastic delays at the signalized intersection constitute a large part of travel times on urban links. The understanding of the vehicle delay evolution or delay variability at signalized intersections can lead to more insights into the variability of urban link travel time and gives more possibilities for travel time estimation and prediction.

Basically, delays vehicles experience at a signalized intersection include uniform delays due to traffic control and overflow delays due to high traffic demand. However, delays vary with effects of stochastic properties of traffic flow, stochastic arrivals and departures at the signalized intersection as illustrated in Figure 4.1. These stochastic factors are not independent but rather overlap. As a result, delays are uncertain given known traffic condition (traffic flow) and traffic control. Instead, a certain delay distribution can be observed.

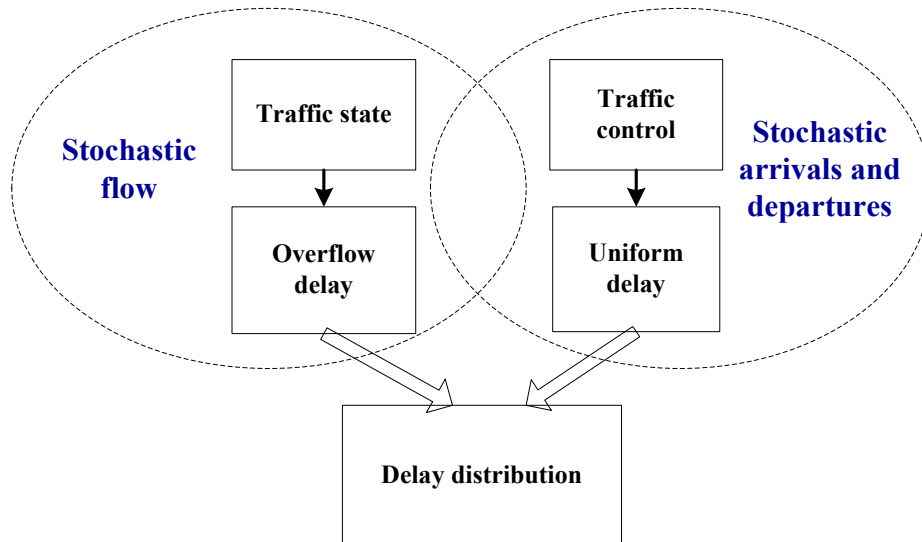


**Figure 4.1: Schematic overview of main components of delay distribution**

In this chapter, a delay distribution model for a fixed-time controlled intersection - taking stochastic properties of traffic flow, stochastic arrivals and departures into account is proposed in section 4.2. The proposed model can deal with both the undersaturated condition and oversaturated condition. Section 4.2 also investigates the influence of different arrival patterns to the delay distribution. In section 4.3, the delay (travel time) variability is quantified by looking at the delay percentile from the derived delay distribution. The statistical range method is introduced to measure the delay uncertainty at signalized intersections. Finally, section 4.4 summarizes the contribution of this chapter.

## 4.2 Delay distribution at signalized intersections

### 4.2.1 Delay distribution in the undersaturated condition with a fixed overflow queue

The delay at an approach of a signalized intersection depends on the arrivals and departures, the length of the red and green phases, and the initial queue. The queue length is a step function that increases with one at the arrival of a vehicle and decreases with one at the departure of a vehicle in one cycle. If we take the expectation value of the queue length, it becomes a continuous function of time. The expectation value of the queue length can be derived from the probability function of queue length as shown in (Viti, 2006). In order to derive the delay distribution function, we start with a simple case in the undersaturated condition. We assume that at the beginning of the red phase with  $t=0$ , no initial queue exists at the stop line of the intersection and the green phase  $\tau_g$  is not fully saturated on the average. The queue builds up proportional to the time in the red phase  $\tau_r$  and decreases proportional to the time in the green phase. The average arrival rate is  $q$  and it remains constant during the evaluation period. The delay as function of the arrival time at the stop line of the intersection (in the case of a vertical queue) for this simplified case can be derived as (van Zuylen 2006; van Zuylen et al., 2007):

$$W(t) = \tau_r - t + \frac{qt+1}{s} = \tau_r + \frac{1}{s} - t(1 - \frac{q}{s}), \text{ if } t < \tau_r \quad (4.1a)$$

$$W(t) = \frac{(qt+1-s(t-\tau_r))}{s}, \text{ if } \tau_r < t < \frac{\tau_r + \frac{1}{s}}{1 - \frac{q}{s}} \quad (4.1b)$$

$$= \tau_r + \frac{1}{s} - t(1 - \frac{q}{s})$$

$$W(t) = 0, \text{ if } t \geq \frac{\tau_r + \frac{1}{s}}{1 - \frac{q}{s}} \quad (4.1c)$$

As a next step let's assume that an initial overflow queue  $n_0$  exists at the start of the red phase and that the green phase is still long enough to handle all traffic. For this case, the delay is given by:

$$W(t | n_0) = \tau_r - t + \frac{(n_0 + 1 + qt)}{s} = \tau_r + \frac{n_0 + 1}{s} - t(1 - \frac{q}{s}), \text{ if } t < \tau_r \quad (4.2a)$$

$$W(t | n_0) = \frac{(n_0 + 1 + qt - s(t - \tau_r))}{s}, \text{ if } \tau_r < t < \frac{\tau_r + \frac{n_0 + 1}{s}}{1 - \frac{q}{s}} \quad (4.2b)$$

$$= \tau_r + \frac{n_0 + 1}{s} - t(1 - \frac{q}{s})$$

$$W(t | n_0) = 0, \text{ if } t > \frac{\tau_r + \frac{n_0 + 1}{s}}{1 - \frac{q}{s}} \quad (4.2c)$$

The delay has a maximum as experienced by a vehicle arriving just after the end of the effective green time. It is equal to the red time  $\tau_r$  plus the time necessary to release the initial queue and the arriving vehicle itself, and decreases linearly until the end of the saturated green time. Afterwards, the delay is zero. The probability that a vehicle has a delay between  $d$  and  $d + \Delta d$  is given by the chance that a vehicle arrives between  $t = W^{-1}(d)$  and  $t + \Delta t = W^{-1}(d + \Delta d)$  as shown in Figure 4.2 (a), where  $\Delta t$  can be easily obtained as:

$$\Delta t = -\Delta d \frac{dt}{dW(t)} \quad (4.3)$$

The inverse mapping of delay  $W$  to the arrival time is not a single valued function as can be seen from Figure 4.2 (b). The derivative does not exist at  $W=0$ . This can be simply solved by introducing the Dirac delta function (in fact a generalization of the function concept, only applicable in integrations) with the following properties:

$$\delta(x) = 0 \quad \text{if } x \neq 0, \quad \int_{-\infty}^{\infty} \delta(x) dx = 1$$

$$\int_{-\infty}^{+\infty} \delta(x-x_0) f(x) dx = f(x_0) \quad (4.4)$$

Therefore, the probability density function can be determined as:

$$P(W|n_0) = \alpha(n_0)\delta(W) + \beta \quad (4.5)$$

where  $\alpha = 1 - \frac{\tau_r + \frac{n_0+1}{s}}{\tau_c(1-\frac{q}{s})}$ ,  $\beta = \frac{1}{\tau_c(1-\frac{q}{s})}$ ,  $\tau_c$  is the cycle time.

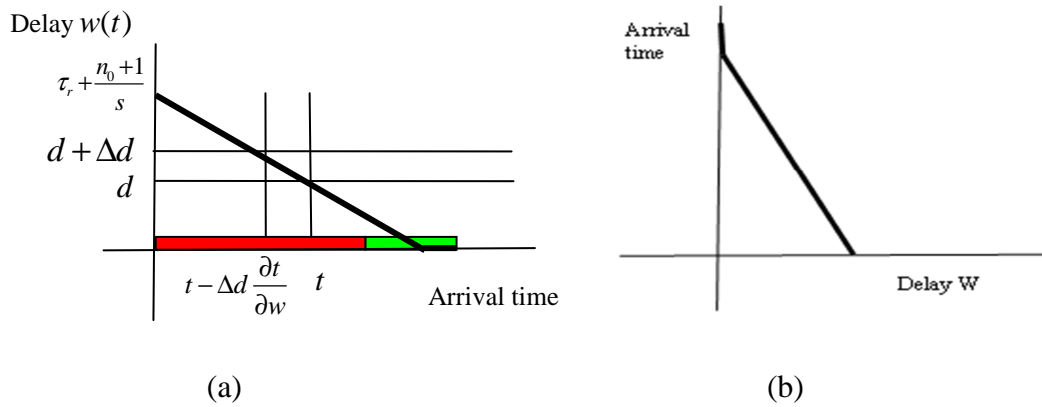


**Figure 4.2: Delay as a function of arrival time  $W(t)$  and the inverse relation  $t(W)$**

#### 4.2.2 Delay distribution in the oversaturated condition with a fixed overflow queue

When the initial queue is larger than a certain threshold, the green phase becomes oversaturated. The question whether an arriving vehicle has to wait for a next cycle to depart, depends on the number of vehicles that arrived before this one in the cycle plus the initial queue. As soon as this quantity exceeds the number of vehicles that can depart in the (remaining) green time, the vehicle has to wait for a following cycle or even more cycles. The delay becomes

$$\begin{aligned} W(t|n_0) &= (\tau_r - t) + \left\lfloor \frac{n_0 + 1 + qt}{s\tau_g} \right\rfloor \tau_c + (n_0 + 1 + qt) - \left\lfloor \frac{n_0 + qt + 1}{s\tau_g} \right\rfloor s\tau_g s^{-1} \\ &= \left\{ \tau_r + \frac{n_0 + 1}{s} + \left\lfloor \frac{n_0 + qt + 1}{s\tau_g} \right\rfloor \tau_r \right\} - t(1 - \frac{q}{s}) \quad \text{if } t < \tau_r \end{aligned} \quad (4.6a)$$

$$\begin{aligned}
W(t | n_0) &= \left\lfloor \frac{n_0 + 1 + qt}{s\tau_g} \right\rfloor \tau_c + (n_0 + 1 + qt - s(t - \tau_r)) - \left\lfloor \frac{n_0 + qt + 1}{s\tau_g} \right\rfloor s\tau_g s^{-1} \\
&= \left\{ \tau_r + \frac{n_0 + 1}{s} + \left\lfloor \frac{n_0 + qt + 1}{s\tau_g} \right\rfloor \tau_r \right\} - t \left(1 - \frac{q}{s}\right) \quad \text{if } t > \tau_r
\end{aligned} \tag{4.6b}$$

The floor  $\lfloor \cdot \rfloor$  is used to indicate the integer value of the expression inside the brackets. An example of the oversaturated condition is shown in Figure 4.3. In this example the transitions occur at four time instants:  $t_0$ ,  $t_1$ ,  $t_2$  and  $t_3$ . Vehicles arriving between  $t_0$  and  $t_1$  can leave the intersection in the next green phase, vehicles arriving between  $t_1$  and  $t_2$  can depart in the green phase of the next cycle, etc. The number of red time that the arriving vehicles need to wait for can be directly derived from Equation (4.6). The more generic expression is:

$$N = \left\lfloor \frac{qt + n_0 + 1}{s\tau_g} \right\rfloor \tag{4.7}$$

The minimum number of extra red time an arriving vehicle needs to wait for can be derived as:

$$N_{\min} = \left\lfloor \frac{n_0 + 1}{s\tau_g} \right\rfloor \tag{4.8}$$

If the initial overflow queue can depart from the intersection within the effective green time, the minimum number of extra red time that the arriving vehicle needs to wait for is zero. In this example, we assume that the initial overflow queue can be released within the effective green time.

Similarly, the maximum number of extra red times occurs when vehicles arrive at the end of cycle time given by:

$$N_{\max} = \left\lfloor \frac{q\tau_c + n_0 + 1}{s\tau_g} \right\rfloor \tag{4.9}$$

The transition moments can be expressed as:

$$t_N = \begin{cases} 0 & N = N_{\min} \\ \frac{Ns\tau_g - n_0 - 1}{q} & N_{\min} < N \leq N_{\max} \end{cases} \tag{4.10}$$

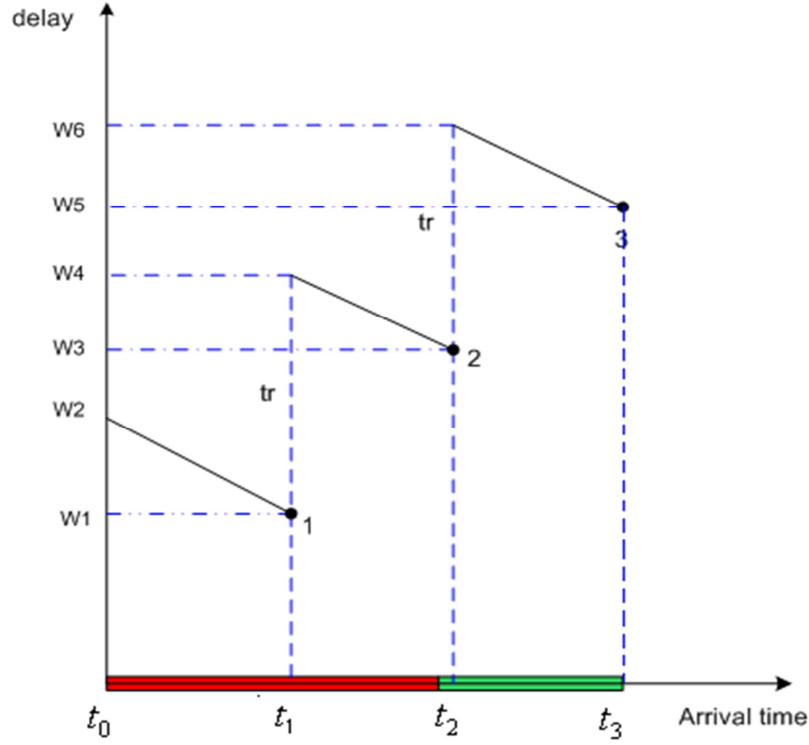


**Figure 4.3: Delay as a function of arrival time for the oversaturated condition**

**Transition point 0:**  $t_0 = 0$

$$W_2 = \tau_r + \frac{n_0 + 1}{s} = \tau_r + \frac{n_0 + 1}{s}$$

**Transition point 1:**  $t_1 = \frac{s\tau_g - n_0 - 1}{q}$

$$W_1 = \tau_r + \frac{n_0 + 1}{s} - \frac{s\tau_g - n_0 - 1}{q} \left(1 - \frac{q}{s}\right) = \tau_c + \frac{n_0 - s\tau_g + 1}{q}$$

$$W_4 = W_1 + \tau_r = \tau_c + \tau_r + \frac{n_0 - s\tau_g + 1}{q}$$

**Transition point 2:**  $t_2 = \frac{2s\tau_g - n_0 - 1}{q}$

$$W_3 = \tau_r + \frac{n_0 + 1}{s} + \tau_r - \frac{2s\tau_g - n_0 - 1}{q} \left(1 - \frac{q}{s}\right) = 2\tau_c + \frac{n_0 + 1 - 2s\tau_g}{q}$$

$$W_6 = W_3 + \tau_r = 2\tau_c + \tau_r + \frac{n_0 + 1 - 2s\tau_g}{q}$$

**Transition point 3:**  $t_3 = \frac{3s\tau_g - n_0 - 1}{q} = \tau_c$

$$W_5 = \tau_r + \frac{n_0 + 1}{s} + 2\tau_r - \tau_c \left(1 - \frac{q}{s}\right) = 3\tau_r + \frac{n_0 + 1}{s} - \tau_c \left(1 - \frac{q}{s}\right)$$

For more general expression, we can substitute  $t$  in Equation (4.6) with  $t_N$  and the delay for each transition point can be calculated as:

$$W_{2N+1} = \begin{cases} \max\left(0, (N+1)\tau_c + \frac{n_0 + 1 - (N+1)s\tau_g}{q}\right) & N \min \leq N < N \max \\ (N+1)\tau_r + \frac{n_0 + 1}{s} - \tau_c \left(1 - \frac{q}{s}\right) & n = N \max \end{cases} \quad (4.11a)$$

$$W_{2N+2} = \begin{cases} (1+N)\tau_r + \frac{n_0 + 1}{s} & N = N \min \\ N\tau_c + \tau_r + \frac{n_0 + 1 - Ns\tau_g}{q} & N \min < N \leq N \max \end{cases} \quad (4.11b)$$

The probability distribution for this case consists of some box shaped functions that may overlap as shown in Figure 4.4. The box shaped functions are defined as:

$$B(W, W_{2N+1}, W_{2N+2}) = \begin{cases} 0 & \text{if } W < W_{2N+1} \\ 1 & \text{if } W_{2N+1} \leq W \leq W_{2N+2} \\ 0 & \text{if } W > W_{2N+2} \end{cases} \quad (4.12)$$

The delay probability function can be represented as:

$$P(W|n_0) = \sum_{N=N \min}^{N \max} \beta B(W, W_{2N+1}(n_0), W_{2N+2}(n_0)) \quad (4.13)$$

where  $\beta = \frac{1}{\tau_c \left(1 - \frac{q}{s}\right)}$

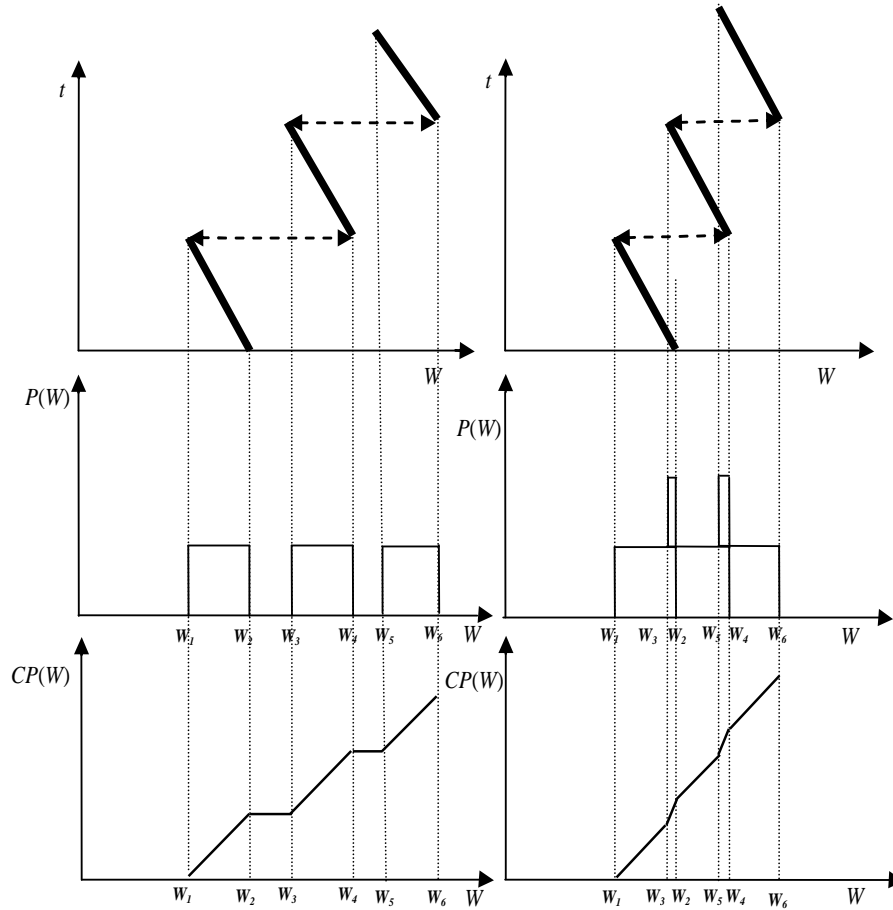


**Figure 4.4: Delay probability distribution for the oversaturated condition**

Based on Equations (4.5) and (4.13), delay probability distribution with an initial queue for both undersaturated and oversaturated conditions can be expressed in one equation:

$$P(W | n_0) = \alpha(n_0)\delta(W) + \sum_{N=N_{\min}}^{N_{\max}} \beta B(W, W_{2N+1}(n_0), W_{2N+2}(n_0)) \quad (4.14)$$

Where  $B(W, W_{2N+1}(n_0), W_{2N+2}(n_0))$  is given by Equation (4.12) and  $W_{2N+1}(n_0), W_{2N+2}(n_0)$  are given by Equation (4.11).

### 4.2.3 Delay distribution with a stochastic overflow queue

The delay probability distribution function derived in the previous section is based on the fixed overflow queue that is present at the start of the green phase. If the overflow queue is stochastic with a certain probability distribution, the expected probability distribution of the delay can be composed as a weighted sum of probability functions:

$$P(W) = \sum_{n_0=1}^{\infty} P(W | n_0)P(n_0) \quad (4.15)$$

where  $P(n_0)$  is the probability distribution of the initial queue. It can be easily derived using the Markov Chain Process by assuming a certain arrival distribution (e.g., Poisson) and departure distribution (e.g. Normal or Binominal) as explained in (Olszewski, 1994; van Zuylen et al., 2007; Viti, 2006).

Based on Equations (4.13), (4.14) and (4.15), we can numerically calculate the delay distribution with a stochastic overflow queue. Figure 4.5 (a) illustrates the delay distribution for an undersaturated condition (degree of saturation  $x = 0.833$ ) based on the function in Equation (4.15). The tail above  $W = 36$ , the red time, and the increase between 0 and 36s delay are the consequence of the stochastic overflow queue distribution. Figure 4.5 (b) compares the delay distribution among different degrees of saturation. When the degree of saturation is increasing, the shape of the delay distribution shifts to the right with a higher standard deviation. However, the delay distributions for different degrees of saturation are highly overlapping as can be clearly seen in Figure 4.5 (b). A given delay can correspond to different traffic conditions with certain probabilities. This indicates that a single delay couldn't give enough information about what is happening at the intersection. Consequently, measured delays of a single vehicle do not have much value for the prediction of delays of other vehicles travelling at the same time period.

For the case of oversaturation, as we already discussed, no equilibrium state of the queue distribution exists which also means that the delay distribution is time-dependent and shifts over time towards higher delay values. Figure 4.6 can explain this phenomenon more intuitively. The shape of delay distribution shifts from left to right cycle by cycle and spreads over with a larger range of delay from cycle to cycle. The expected value of delay continues to increase and the same for the variance of delay.

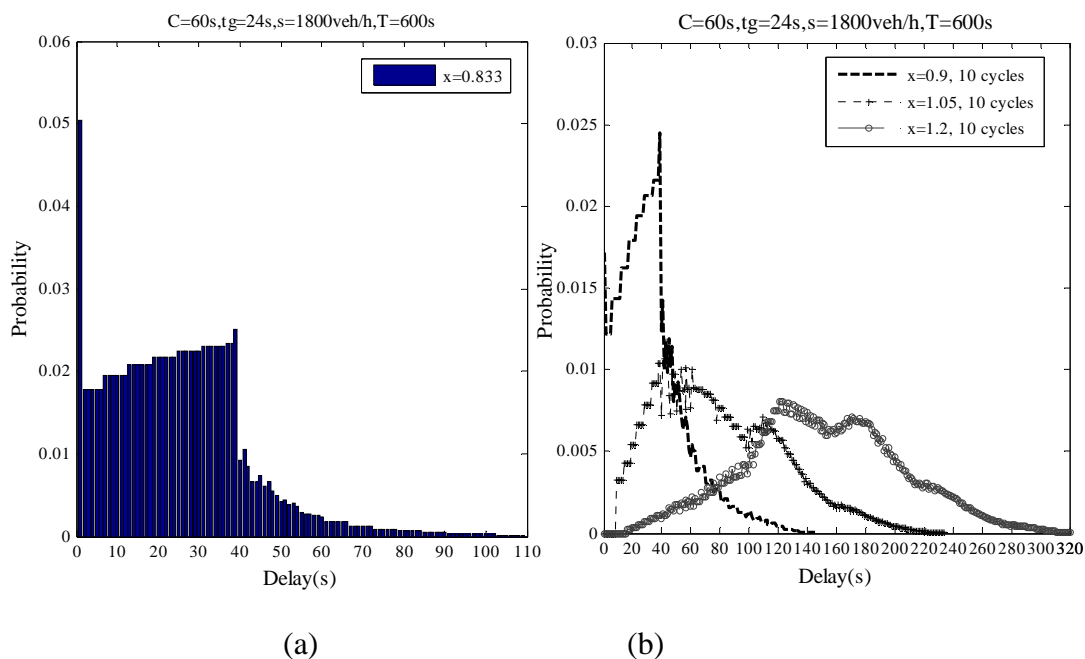


**Figure 4.5: Delay probability distribution in undersaturated and oversaturated conditions**

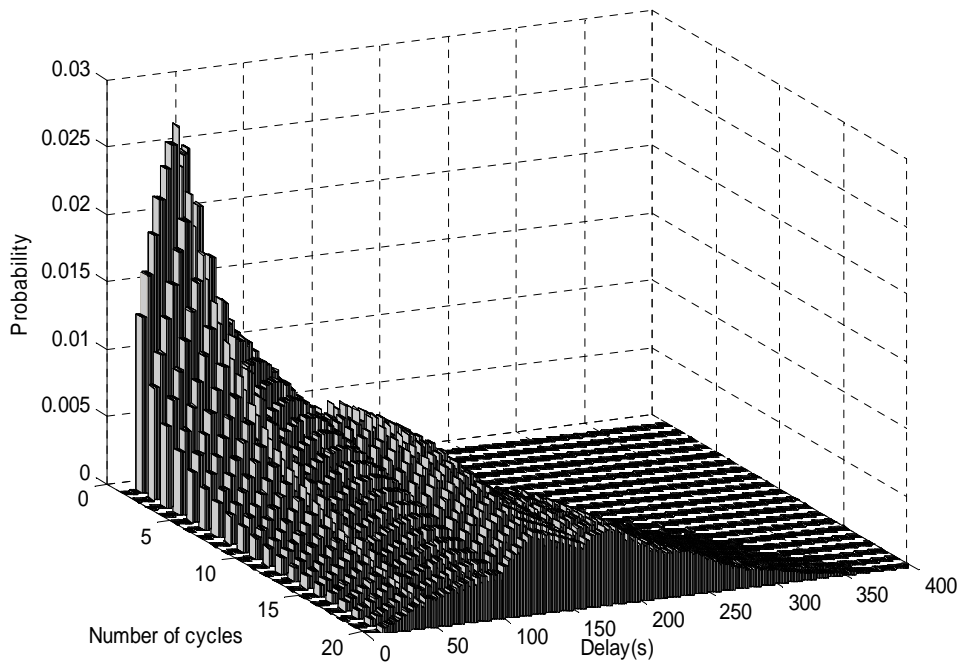


**Figure 4.6: Evolution of delay distribution in oversaturated condition ( $\tau_C = 60s$ ,  $\tau_g = 24s$ ,  $x = 1.1$ ,  $s = 1800veh/h$ )**

#### 4.2.4 Comparison between the Poisson arrival and Binomial arrival processes

Delay distribution with Poisson arrival process has been discussed in the previous section. As we know, the Poisson process is a random process which means that events occur independently of one another. For an isolated intersection with light traffic condition, vehicles can pass independently of each other. The Poisson process can be used to describe vehicle arrivals in this case. When traffic demand is increasing, vehicle headways become more uniform due to car following behaviour; On the other hand, more and more vehicles form platoons (clusters, groups). Some distributions, e.g., negative exponential, shifted negative exponential, are commonly used to describe arrival headways. However, these commonly used distributions tend to give poor predictions for the range of small headways as shown in (Akcelik et al., 1994). Instead, they proposed a bunched exponential distribution model which provides more realistic prediction of arrival headways. In our study, we still use the Binomial arrival distribution just as an example to show how different arrival distributions influence the delay distribution in different traffic conditions. Compared with the Poisson process, one property of Binomial process is that the ratio of variance over mean is smaller than 1. Here we define it as the coefficient of variance:

$$I = \frac{\sigma^2}{\mu} \quad (4.16)$$

where  $\sigma^2$  is the variance of arrivals and  $\mu$  is the average arrivals.

One condition in applying a Binomial process is that the variance needs to be determined in advance. The variance of arrivals has to be estimated based on observations and usually is intersection specific. In order to see how the coefficient of variance influences the delay distribution, the value of  $I$  is chosen to be 0.4, 0.6 and 0.9. The results are compared with that of Poisson process and shown in Figure 4.7. For the undersaturated condition ( $x=0.833$ ) as shown in Figure 4.7(a), choosing different value of  $I$  for the Binomial arrival has no significant influence on the delay distribution. Nevertheless, when the value of  $I$  increases towards an oversaturated condition ( $x=1.2$ ) as illustrated in Figure 4.7 (b), the delay distribution spreads over a larger range of delays. For this case, different arrival patterns, especially the variation in arrivals will have a significant influence on the delay distribution. Larger variance in arrivals will lead to larger variance in delay distribution. Compared with the delay distribution of Poisson arrivals, smaller variance of delay can be observed in the delay distribution with Binomial arrivals. This is explainable because in the Poisson arrival process, the arrivals are more uncertain, which leads to the larger variance of delays experienced by vehicles at that intersection.

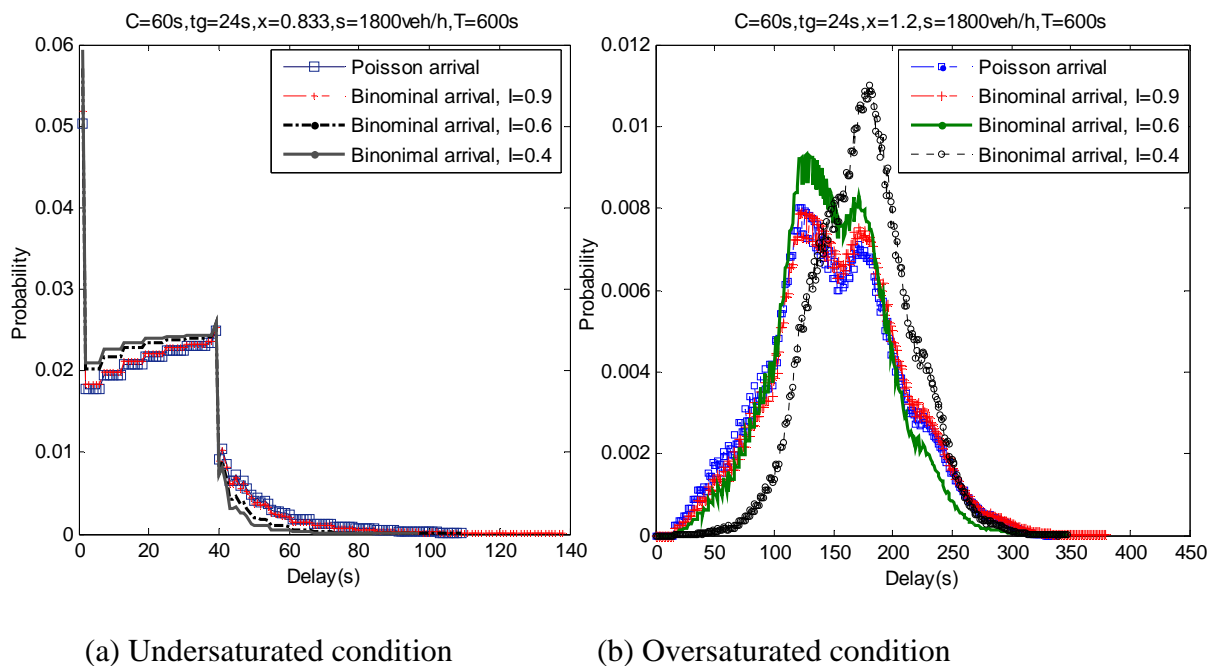
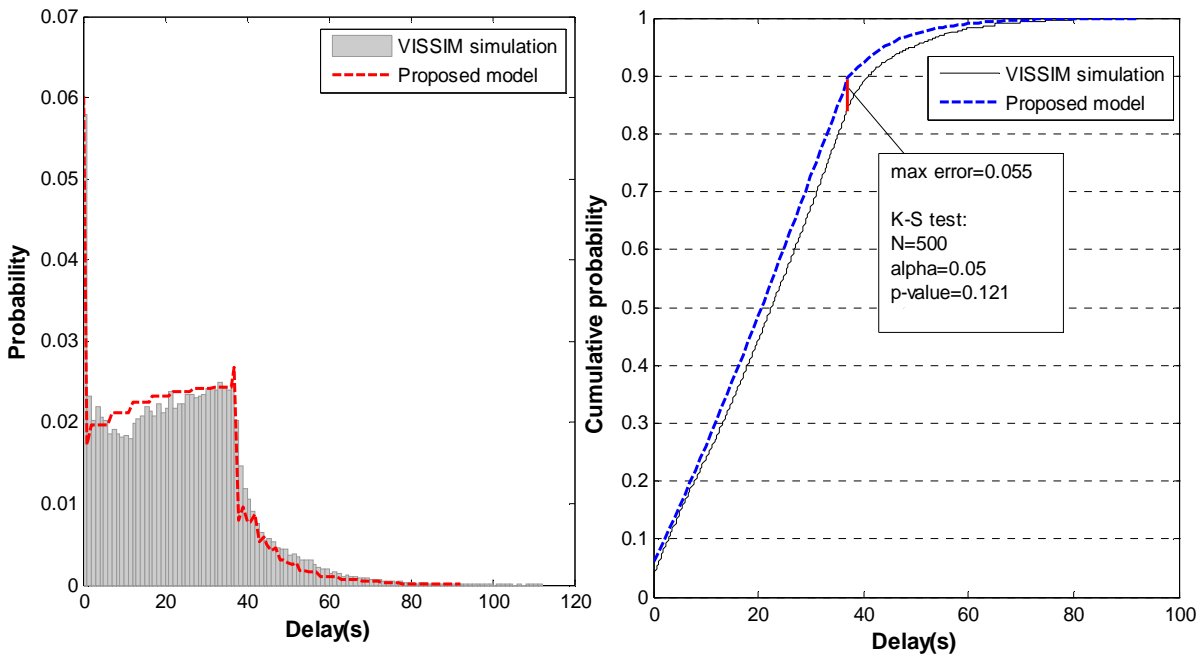


**Figure 4.7: Delay distribution with Poisson arrivals and Binomial arrivals**

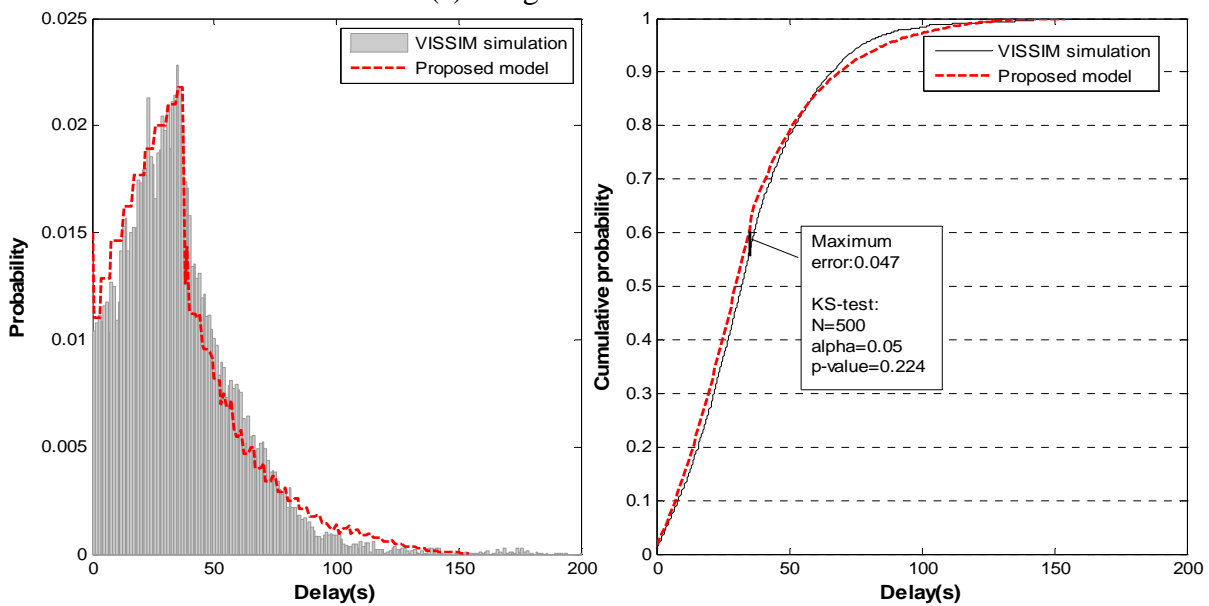
#### 4.2.5 Comparison between the delay model and VISSIM simulation in undersaturated conditions

The delay distribution model presented in previous sections has the ability to describe the evolution of delay distribution under different traffic conditions. In order to see how this analytical model works, we compared the delay distribution from the proposed model with that from VISSIM simulation. The cycle time is 60s and green time is 24s both for the

analytical model and simulation model. The saturated flow is 2200veh/h/lane. The individual delay was recorded in VISSIM and the delay distribution was derived. As illustrated in Figure 4.8 (a) (b), the delay distributions based on the analytical model match those from VISSIM simulation very well both for the degree of saturation of 0.833 and 0.917. The Kolmogorov-Smirnov test (Figure 4.8) shows that the hypothesis that the delay distribution based on the simulation data and that based on the proposed model come from the same distribution cannot be rejected with significance level of  $\alpha=5\%$ .



(a) Degree of saturation=0.833



(b) Degree of saturation=0.917

**Figure 4.8: Comparison of delay distribution between analytical model and simulation**

### 4.3 Delay uncertainty at signalized intersections

In the previous section, the delay distribution model for an isolated intersection has been proposed. It has shown that a wide range of delays can be found both in undersaturated and oversaturated conditions. Based on the delay distribution, it is easy to calculate the percentile delay, e.g. 90<sup>th</sup> percentile delay (Figure 4.9). The expected value and standard deviation also can be calculated.

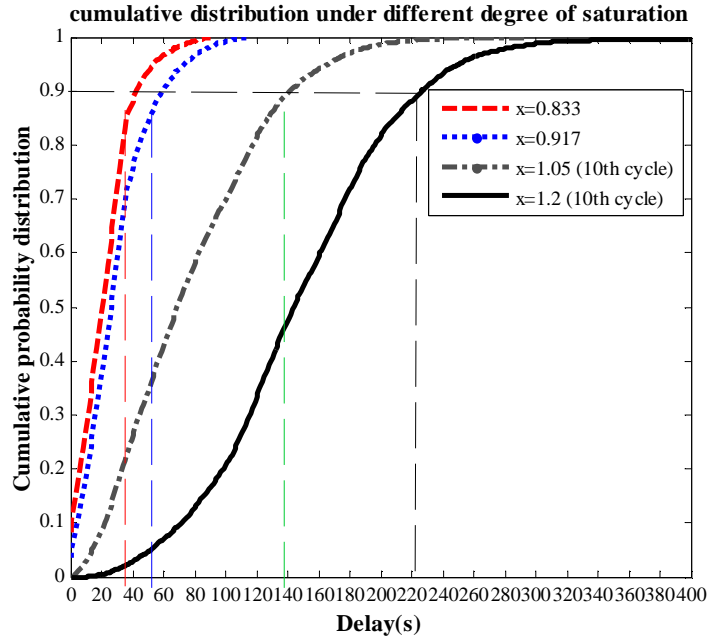


**Figure 4.9: Cumulative delay distribution for different degrees of saturation**

In literatures, the variance of delay is commonly used to quantify the uncertainty (variability) of delay at signalized intersections. Here, we use an indicator called ‘width’ to measure the uncertainty of delay. It was originally proposed in (van Lint et al., 2005; van Lint et al., 2008) to measure the reliability of travel time. The wider the travel time is, the less reliable travel times become. An example of this method is the difference between the 90<sup>th</sup> and 10<sup>th</sup> percentile relative to the median:

$$D_U = \frac{D^{90th} - D^{10th}}{D^{50th}} \quad (4.17)$$

where,  $D_U$  denotes the (relative) delay uncertainty,  $D^{90th}$ ,  $D^{50th}$  and  $D^{10th}$  denote 90<sup>th</sup>, 50<sup>th</sup> and 10<sup>th</sup> percentile delay, respectively.

Figure 4.10 shows the dynamics of delay uncertainty defined in equation (4.18) for the period of 30 cycles. Under the undersaturated condition (degree of saturation  $x=0.80$ ),  $D_U$  fluctuates for the first 5 cycles and remains nearly constant for the next 25 cycles. In a slightly oversaturated condition (e.g.,  $x=1.05$ ),  $D_U$  rapidly increases for the first 5 cycles and flattens out for the remaining 25 cycles. However, in a highly oversaturated condition (e.g.  $x=1.2$ ),  $D_U$  increases at the beginning and decreases monotonically as the number of

cycles increases.  $D_U$  is larger in low degree of saturation ( $x=0.8$ ) as can be clearly seen in Figure 4.10. Under the undersaturated condition, the most probable delay is zero and the delay is predominately determined by the arrival moment at the intersection and the red time. The stochastic characteristics at the intersection play a main role in the delay uncertainty. While under the oversaturated condition, delays are mainly determined by the overflow queue and stochastic arrivals and departures have less influence on the delay distribution. Therefore, delays are relatively more certain under oversaturated conditions even though vehicles experience larger delays.

We also investigated the delay variability under different degrees of saturation ranging from 0.5 until 2 and the analysis period  $T=600s$  (10 cycles). As shown in Figure 4.11, two different arrival processes (Poisson arrival and Binomial arrival processes) are compared with each other. The delay uncertainty can be divided into three regions. For the case of highly undersaturated conditions ( $x<0.8$ ),  $D_U$  decreases both for the Poisson and Binomial process. When the degree of saturation increases ( $0.8<x<1$ ),  $T_{DU}$  increases dramatically for Poisson arrivals. This is explainable because when the traffic condition is near saturated, traffic flow becomes unstable and a small disturbance can lead to a large variation of delay. In highly oversaturated conditions when the degree of saturation is higher than 1.1,  $D_U$  keeps on decreasing.  $D_U$  for the Binomial arrival process (the coefficient of variance is set to be 0.8) is slightly smaller than that of Poisson arrival process. Figure 4.12 illustrates the delay uncertainty under stochastic departures with standard deviation equals to 10% and 20% of average departures per cycle, respectively. Under highly undersaturated and highly oversaturated conditions, the relative uncertainties of delay for these two cases are quite similar to each other, while under traffic conditions in between, larger standard deviation of departures tends to have a larger  $D_U$ . The similar phenomenon can be observed in Figure 4.11, where a larger variance of arrivals leads to a larger  $D_U$  in middle traffic conditions.

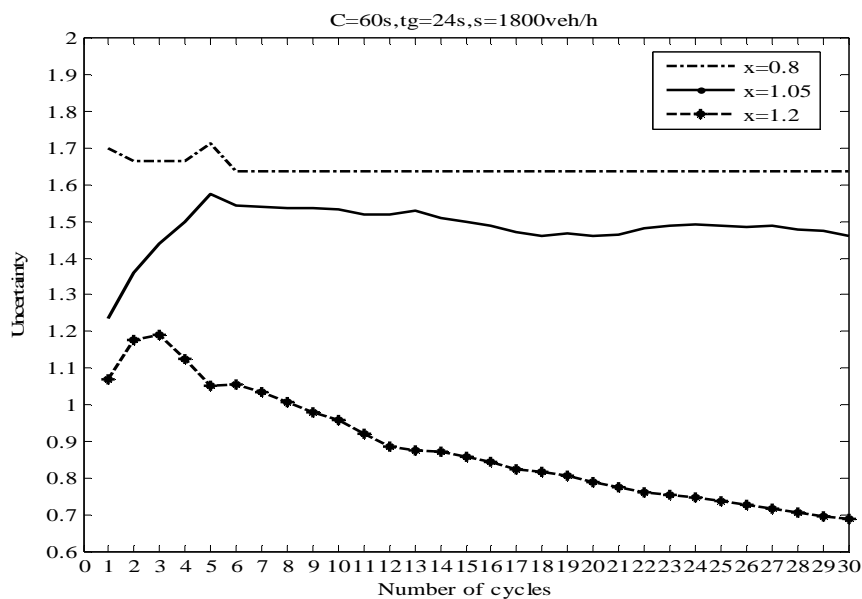


**Figure 4.10: Evolution of delay variability for the period of 20 cycles**

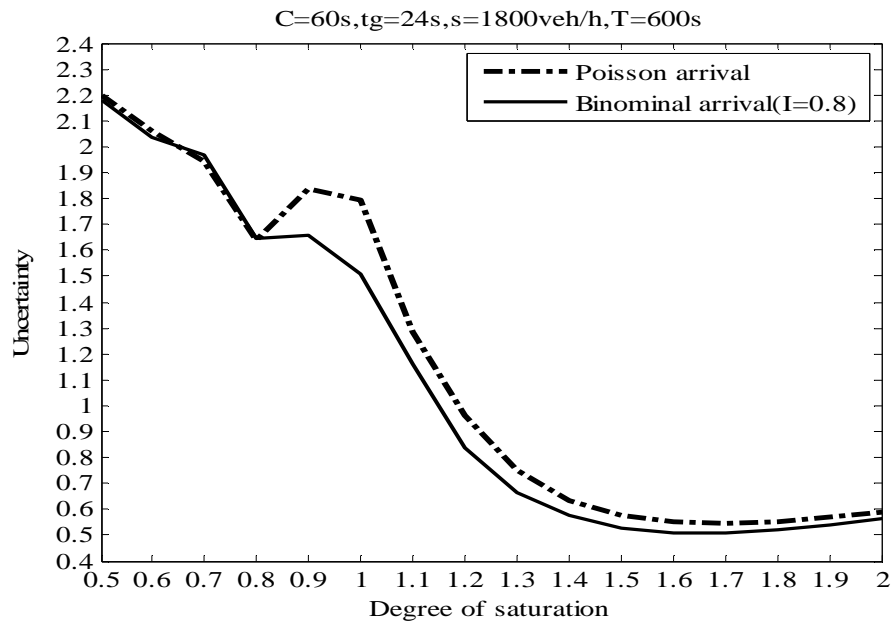


**Figure 4.11: Delay uncertainty as function of degrees of saturation for different arrival distributions (The standard deviation of saturation flow is chosen as 10% of the average saturation flow)**

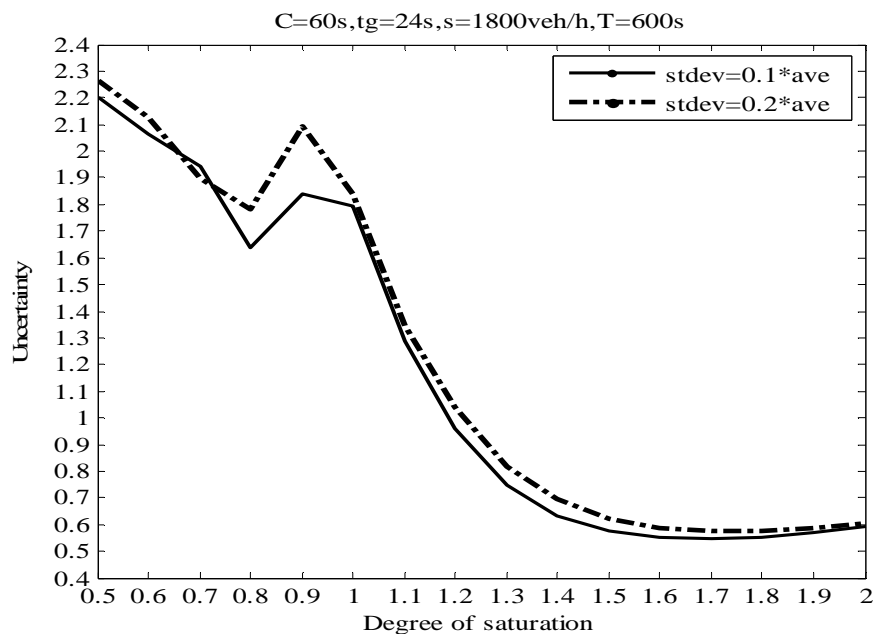


**Figure 4.12: Delay uncertainty as function of degrees of saturation for different standard deviation of the saturation flow (Poisson arrival)**

## 4.4 Summary

On the urban road, the variability (uncertainty) of travel time is largely caused by the variability (uncertainty) of delay vehicles experience at intersections. This chapter has focus on the analysis of the delay distribution for an isolated, fixed-time controlled intersection. The delay distribution model is developed and the variability of delay at

signalized intersections is investigated based on the delay distribution model taking the stochastic properties of the traffic into account.

In the proposed model, we assume that the initial queue is not deterministic but has a certain probability distribution. Both the Poisson arrival process and the Binomial arrival process are considered and the departures are assumed to be stochastic. Analysis of different arrival processes has revealed that in undersaturated conditions, the delay distribution does not significantly influenced by different arrival processes (e.g., Poisson, Binomial). The comparison of delay uncertainty in different traffic conditions has shown that the delay is more uncertain in undersaturated conditions than oversaturated conditions. This gives more insight to travel time estimation and prediction on the urban road. The uncertainty of delay in undersaturated conditions should be particularly taken into account in order to have better estimation or prediction results. This chapter also reveals that the delay distributions for different degrees of saturation are highly overlapping which indicates that a single delay can correspond to different traffic states with certain probabilities and also for a given traffic state, a range of delays can be found.

Up to this chapter, the delay distribution model is only applicable for an isolated intersection. On urban arterials, traffic process can be influenced by signal coordination between intersections. Delays (travel times) that vehicles experience on urban roads are accordingly influenced by signal coordination. This is investigated in chapter 5.

# Chapter 5

## Model development for urban travel time distribution

### 5.1 Introduction

The travel time that vehicles experience on an urban road can be decomposed into two parts: the free flow travel time and the delay. The free flow travel time is basically calculated as the distance over the free flow speed. However, estimation of delay is more difficult due to stochastic characteristics of traffic on the urban road as discussed in chapter 4. Up to now, most research about travel time estimation and prediction mainly deals with the expectation or variance of travel times. Very little attention has been paid to investigate the travel time *distribution*, though some research about using statistical distributions (e.g., normal, log-normal or combination of different distributions) to fit observed travel times and estimating parameters from these measured travel times can be found in the literature (EL FAOUZI et al., 2006; Guo et al., 2010). These models hardly have physical meaning and some parameters are difficult to interpret from the traffic point of view. Therefore, it is necessary to develop a travel time distribution model which can explain the underlying urban traffic phenomenon and can be generalized to different traffic conditions.

One important and difficult part in developing an analytical travel time distribution model is to estimate delays at intersections. Delays are rather uncertain due to a lot of stochastic factors when vehicles approaching intersections. In chapter 4, a delay distribution model for an isolated intersection has been developed. The proposed model can well capture the delay dynamics and uncertainty at intersections. In this chapter, a single link travel time distribution model is developed in section 5.2. In order to see how the proposed model performs, travel time distributions generated both from the VISSIM simulation model and

field data are compared with those estimated from the analytical model. In section 5.3, a travel time distribution model for an urban trip passing two intersections is proposed. Travel time distributions estimated based on the analytical model are compared with those derived from the VISSIM simulation model and from field data obtained from floating cars. Finally, section 5.4 presents some conclusions.

## 5.2 Travel time distribution for a link with one signalized intersection

### 5.2.1 Definition of the link travel time

In this thesis, the complete link travel time is defined as the travel time when the vehicle enters the upstream of the link of interest until it leaves the downstream intersection as illustrated in Figure 5.1. The link travel time is expressed as:

$$TT = t_{entry} - t_{exit} \quad (5.1)$$

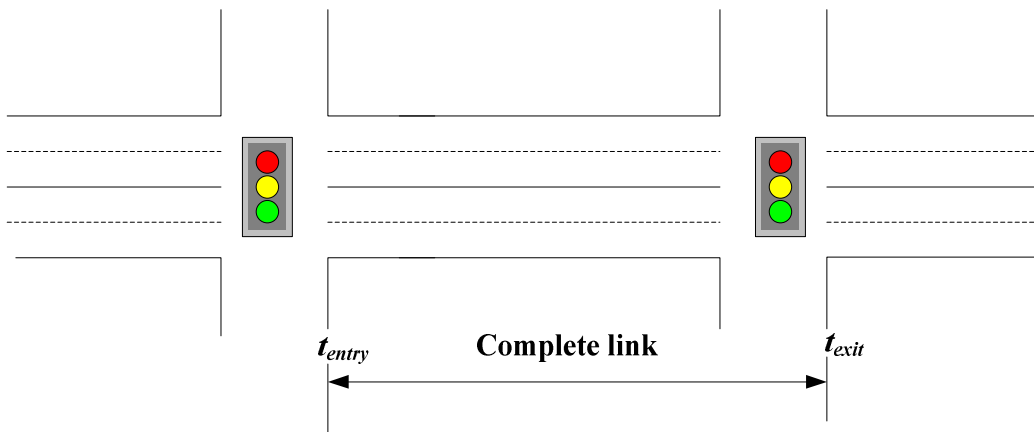


Figure 5.1: Schematic representation of an urban link

### 5.2.2 Components of urban link travel time

Basically, the travel time vehicles experience on a certain link  $i$  can be subdivided into two components:

$$TT_i(t) = TT_i^f(t) + D_i(t) \quad (5.2)$$

Where  $TT_i^f(t)$  represents the free flow travel time at time instant  $t$  on link  $i$ . It is further calculated as the link length  $L_i$  divided by the free flow speed  $u_f$ :

$$TT_i^f(t) = \frac{L_i}{u_f} \quad (5.3)$$

The free flow speed varies with different driving behaviour, speed limit, spacing between intersections, vehicle composition, weather conditions, etc. Therefore, the free flow travel time is not a constant value.  $D_i(t)$  represents the delay vehicles experience when departing at time instant  $t$ . As discussed in chapter 2 and chapter 4, delays vehicles encountered on an urban trip can be caused by different factors, e.g., bus manoeuvres at bus stops, vehicles parking along the roadside, cross pedestrians and cyclists, traffic control and queues at intersections. Among all these factors, the delay at intersections due to the queue and traffic control constitutes a large part of the total delay. In this thesis, we mainly consider the delay at intersections.

In order to apply the definition in Equation (5.2) to derive the link travel time distribution, we assume a vertical queue at the intersection. This assumption has been discussed in chapter 4 to derive the delay distribution. The second assumption is that the number of vehicles in queue is not too large such that there is no spill back in case of a horizontal queue. The reason for the second assumption is that if the queue is so large that it spills back and blocks the traffic at the upstream intersection. In this case, the vertical queue is not a reasonable assumption anymore.

### 5.2.3 Derivation of a single link travel time distribution

#### **Case 1: constant free flow travel time**

The free flow travel time can be estimated by simply assuming a constant free flow speed (e.g., speed limit). In that case, the free flow travel time is a constant value. The delay vehicles experience at the signalized intersection is derived based on the vertical queue as discussed in chapter 4. This does not have a big influence on the final calculation of the total link travel time for the case of undersaturated conditions or slightly oversaturated conditions. More detailed discussion about calculating the total link travel time in case of vertical queue and shock wave can be found in Appendix D. The probability of a certain link/trip travel time  $t$ ,  $P(t)$  can then be seen as the shifted probability of a certain delay  $w$  as:

$$P(t) = P_d(t - \tau_f) \quad (5.4)$$

where,  $\tau_f$  is the link free flow travel time;  $P(t)$  is the probability of a certain link travel time  $t$  ( $t = w + \tau_f$ );  $P_d(w)$  is the probability of a given delay  $w$  which has been derived in chapter 4 with formulas (4.16) and (4.17).

#### **Case 2: stochastic free flow travel time**

However, the free flow travel time in most cases is not a constant value. Instead, the free flow travel time has a certain probability distribution. As for an isolated intersection, the delay distribution at the intersection is independent of the travel speed. Therefore, by combining the free flow travel time distribution with the delay distribution, the link travel time distribution can be derived as:

$$P(t) = \int_0^t P_d(t-s|s)P_f(s)ds \quad (5.5)$$

Where  $P_f(s)$  denotes the free flow travel time distribution;  $P_d(w/s)$  denotes the conditional probability of the delay  $w$  given a certain free flow travel time  $s$ . For a given travel time  $t$  ( $t=w+s$ ), this conditional probability can also be formulated as:

$$P_d(w|s) = P_d(t-s|s) \quad (5.6)$$

For the case that both the delay probability distribution and free flow travel time distribution are discrete, the link travel time distribution can be modified as:

$$P(t) = \sum_{s=0}^t P_d(t-s|s)P_f(s) \quad (5.7)$$

## 5.2.4 Comparison with VISSIM

The analytical model presented in the previous section has the ability to describe the variability of travel times (travel time distribution) given the known traffic conditions (e.g., traffic demand, traffic control). One may question whether this model is able to represent the reality or not. In this section, the first validation was conducted by comparing the results from the analytical model with those from the VISSIM simulation model.

A single-lane link of 600m with one fixed time controlled intersection was modelled in VISSIM. Travel times for the complete link were recorded in VISSIM. The cycle time is 60s and effective green time is 24s. The number of simulation runs is 300 and the evaluation time for each simulation 1200s (20cycles). Two scenarios were chosen:

**Scenario 1:** The input flow is 720veh/h. The degree of saturation is about 0.833;

**Scenario 2:** The input flow is 807veh/h. The degree of saturation is about 0.917.

The free flow travel times were also recorded by letting vehicles travel through the link without interruption. The mean free flow travel time and the standard deviation were estimated based on the recorded data. A normal distribution was used as an approximation of the free flow travel time distribution in this study. Figure 5.2 compares the link travel time distributions derived from the proposed model and those from the VISSIM simulation model. The link travel time distributions derived from the analytical model can well represent those from the VISSIM simulation model for both scenarios. This can be confirmed by the Kolmogorov-Smirnov test ( $\alpha=5\%$ ) results as shown in Figure 5.3. The hypothesis that simulated travel times come from the same distribution as the model predicted is not violated with the sample size of 500.

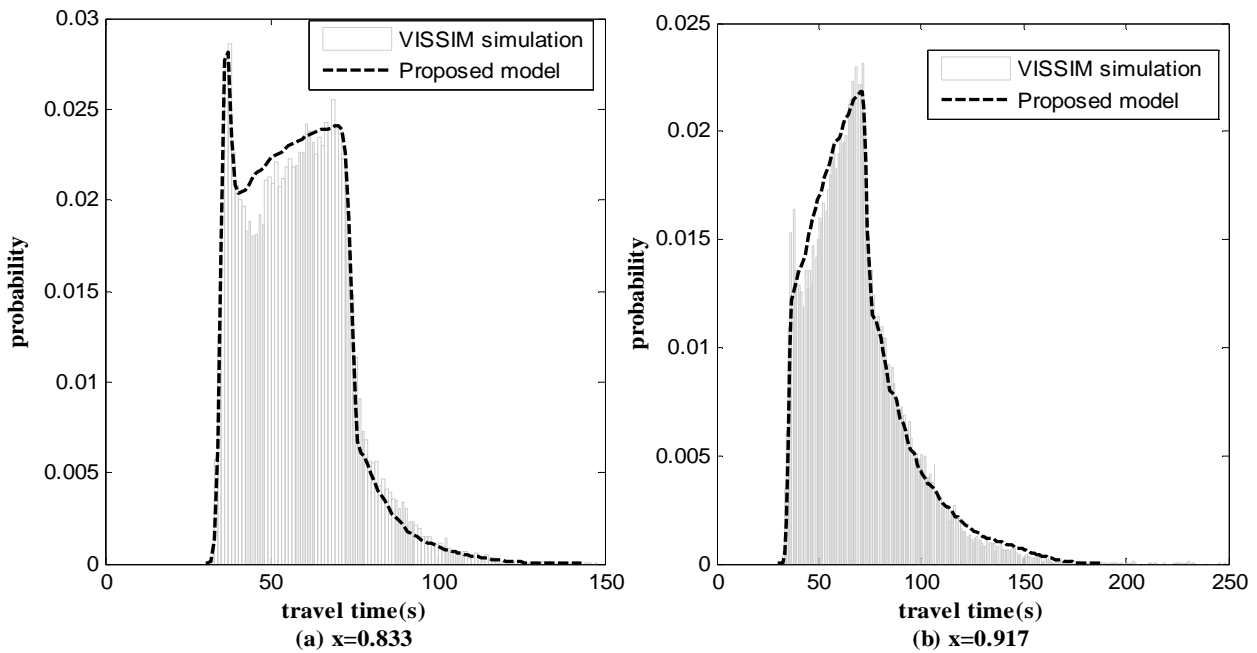


**Figure 5.2: Comparison of the link travel time distribution between the analytical model and VISSIM simulation model**

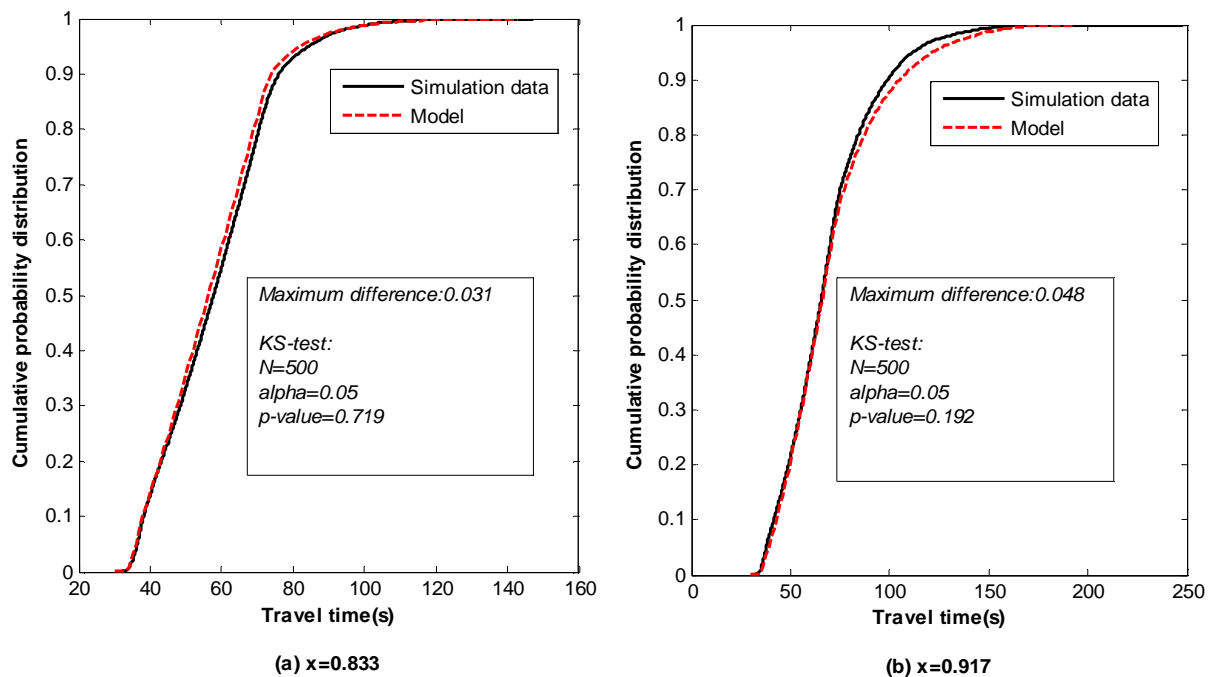


**Figure 5.3: Kolmogorov-Smirnov test**

## 5.2.5 Comparison with field data

### Test area

In the previous subsection, travel time distributions derived from the proposed model are compared with those from the VISSIM simulation data. In this section, field data were

collected in Changsha, a Chinese city in Hunan Province. More than 5000 taxis equipped with GPS devices are used as probe vehicles travelling in the urban road network. Every 30s, positions, speeds and time stamps are recorded and sent to the monitoring centre. As discussed in chapter 3, the Neural Network model can provide good estimation of complete link travel times from GPS data. However, due to the lack of ground-truth travel time data, it is infeasible to apply the NN model in this case. Instead, complete travel times were estimated by applying interpolation with speed and time stamp information when taxis pass before and after intersections for each complete link. More detailed information can be found in Appendix F. Two links with signalized intersections indicated by arrows along Shaoshan Road were chosen as the test area shown in Figure 5.4.



Figure 5.4: The test road in Changsha city

### Data and parameters

Travel times collected by GPS probe vehicles between 10:00 AM and 11:00AM on 15<sup>th</sup>, May 2010 are used for analysis and comparison. Table 5.1 indicates parameters of each link and intersection as well as the number of field travel time observations for each link. The average free flow speeds are estimated as the median speeds from GPS data after

removing zero speed, which are 23km/h, 25km/h and 24km/h for link 13-11, 11-8 and 8-3, respectively. The saturation flow rate for each intersection was estimated based on observations. From the analysis of the saturation flow for different lanes and intersections, the average saturation flow is about 1550veh/h with a standard deviation of 150veh/h. Therefore, the saturation flow rate was determined by minimizing the error between the model predicted travel time distribution with the field GPS travel time distribution using the step-wise method.

**Table 5.1: Parameters of links and intersections**

<i>Link</i>	<i>Link length(m)</i>	<i>Average infow(veh/h/lane)</i>	<i>Average free flow travel time(min)</i>	<i>Number of field travel time observations</i>
13-11	1200	500	3	104
11-8	700	350	1.7	145
8-3	600	340	1.5	84
<i>Intersection</i>	<i>Average cycle time(s)</i>	<i>Effective green time(s)</i>	<i>Saturation flow(veh/h/lane)</i>	
11	200	68	1550	
8	190	53	1580	
3	190	50	1600	

## **Results**

Figure 5.5 and Figure 5.6 illustrate the travel time distributions from GPS probe vehicle data and from the analytical model on link 13-11, link 11-8 and link 8-3 during periods 10:00AM-10:30AM and 10:30AM-11:00AM, respectively. Travel time distributions from the proposed model can represent the field travel time distributions reasonably well. However, middle range of travel times and higher travel times are more frequently observed in field GPS data than the model predicts, especially for link 11-8. This discrepancy probably due to the fact that in the test road, vehicles turning from cross streets can cause extra delay to the through-going vehicles on link 11-8 as can be seen in Figure 5.4, while the proposed model does not consider the effect of turning movements from side streets between two signalized intersections. From the Kolmogorov-Smirnov test as shown in Figure 5.5 (b) (d) (f) and Figure 5.6 (b) (d) (f), even with small GPS sample data, the hypothesis of a same distribution between the model and field data cannot be rejected except link 11-8 which has larger discrepancy between the model and observations during period 10:00AM-10:30AM.

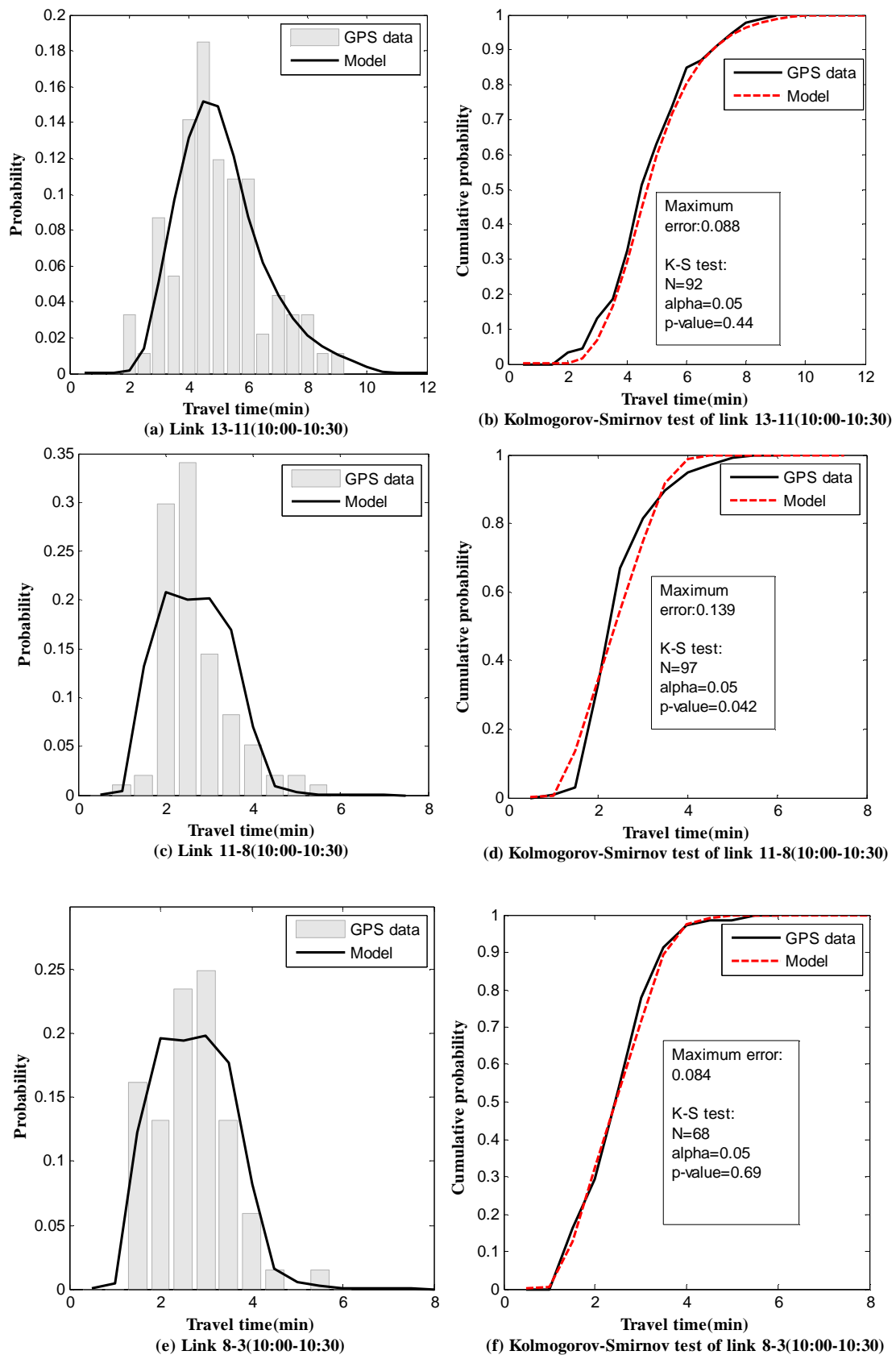


**Figure 5.5: Comparison between travel time distributions from GPS probe vehicle data and those derived from the proposed model on link 13-11, link 11-8 and link 8-3, respectively (10:00 AM-10:30 AM).**

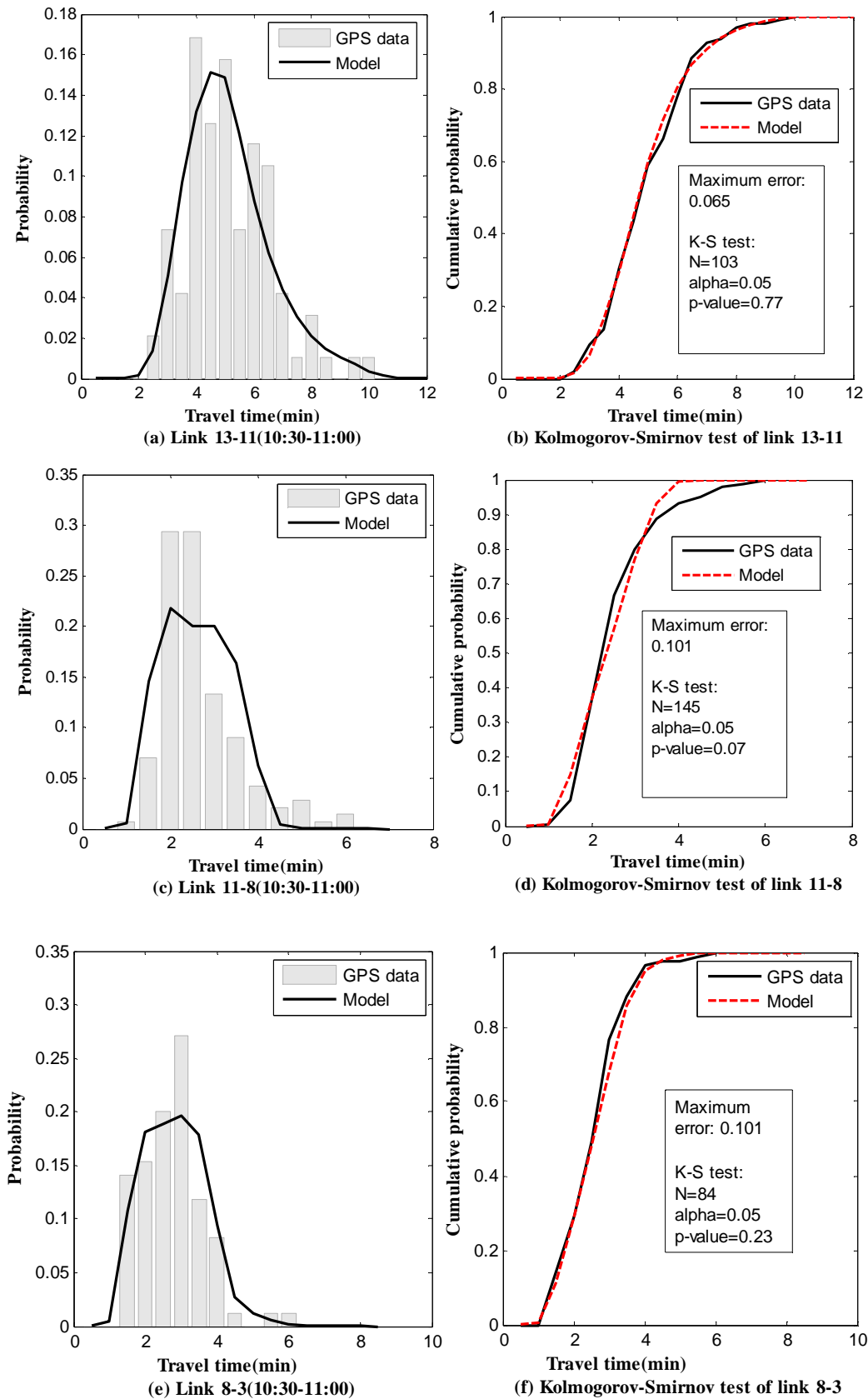


**Figure 5.6: Comparison between travel time distributions from GPS probe vehicle data and those derived from the proposed model on link 13-11, link 11-8 and link 8-3, respectively (10:30 AM-11:00 AM).**

## 5.3 Travel time distribution for an urban corridor

As already discussed, the delay vehicles experience plays a main role in the total travel time. The situation becomes even more complicated for an urban corridor with multiple intersections. The way how these intersections are coordinated has a big influence on the final delay distribution. In this section, a delay distribution model for an urban corridor is developed. By combining the delay distribution with the free flow travel time distribution, the link travel time distribution was derived.

### 5.3.1 Basic notations and assumptions

The delay distribution model for an isolated intersection has been discussed in chapter 4. In order to derive the delay distribution for an urban trip with a group of signals, we limit ourselves by the following conditions:

- 1) Two fixed-time signalized intersections are considered in a single trip. The saturation flow rate is the same for both intersections.
- 2) The acceleration and deceleration effects are not explicitly considered. The concepts of effective green and effective red are used instead.
- 3) The vehicle arrivals at the first intersection follow the Poisson distribution. The average arrival rate is assumed to be constant during the evaluation period;
- 4) The arrival times of vehicles are uniformly distributed; Departures are uniformly distributed at the saturation flow rate  $s$  when there is a queue and at the arrival rate  $q$  after the queue has disappeared.
- 5) Platoon dispersion is not considered between two adjacent intersections.
- 6) The mid-link delay caused by bus manoeuvres at bus stops and vehicles' parking etc. along the roadside is not considered.

In chapter 4, the sensitivity of a similar model for different arrival distributions is analysed and it has shown that the condition 3 is not essential. The assumption 4 can be relaxed to a more general case that departures from the upstream intersection within a cycle time is a continuous time-dependent distribution as discussed in (Viti et al., 2009). Here we consider departures are uniformly distributed for the convenience of modelling. As for fixed-time control, the coordination scheme between two intersections has a big influence on the delay vehicles experience when passing these two intersections. Figure 5.7 (a) and (b) shows different offset settings for two fixed-time controlled intersections. For the convenience of modelling, we assume that both intersections have the same cycle time  $\tau_C$ , effective green time  $\tau_g$  and red time  $\tau_r$ . These assumptions can be relaxed to different effective green times between consecutive intersections. The derivations in the following sections are all based on the assumption of the same cycle time and effective green time between two consecutive intersections. The offset  $\tau_{off}$  between two intersections is defined as:

$$\tau_{off} = t_2 - t_1 \quad (5.8)$$

where  $t_1$  is the beginning of effective green time at the upstream intersection and  $t_2$  is the beginning of effective green time at the downstream intersection. The link length between the two intersections is  $L$ ; the free flow speed is  $u_f$ . Then the average free flow link travel time is:

$$TT_f = \frac{L}{u_f} \quad (5.9)$$

If two intersections are well coordinated, there is no mismatch between these two intersections. In the case that two intersections are not well coordinated, the mismatch of green time  $\tau_m$  as illustrated in Figure 5.7 (a) (b) between the upstream intersection and the downstream intersection can be derived as:

$$\tau_m = \tau - \tau_{off} \quad (5.10)$$

Two types of mismatch can be found in reality as shown in Figure 5.7.

- 1) **Mismatch 1, early green:** As illustrated in Figure 5.7 (a), the start of the green phase at the downstream intersection is too early such that part of the green time is not utilized by the platoon. Hence, the mismatch between the two intersections is positive :

$$\tau_m = \tau - \tau_{off} > 0$$

Since the mismatch time is only utilized by the remaining queue from the previous cycle not by the vehicles departing from the upstream intersection right after the traffic light turns to green. The effective green time of the downstream intersection when vehicles can pass without delay is given by:

$$\tau'_g = \tau_g - \tau_m \quad (5.11)$$

- 2) **Mismatch 2, late green:** As illustrated in Figure 5.7 (b), the start of the green phase at the downstream intersection is too late so that vehicles departing directly after the start of the green time from the upstream intersection need to wait for the red time at the downstream intersection. Hence, the mismatch between the two intersections is negative:

$$\tau_m = \tau - \tau_{off} < 0$$

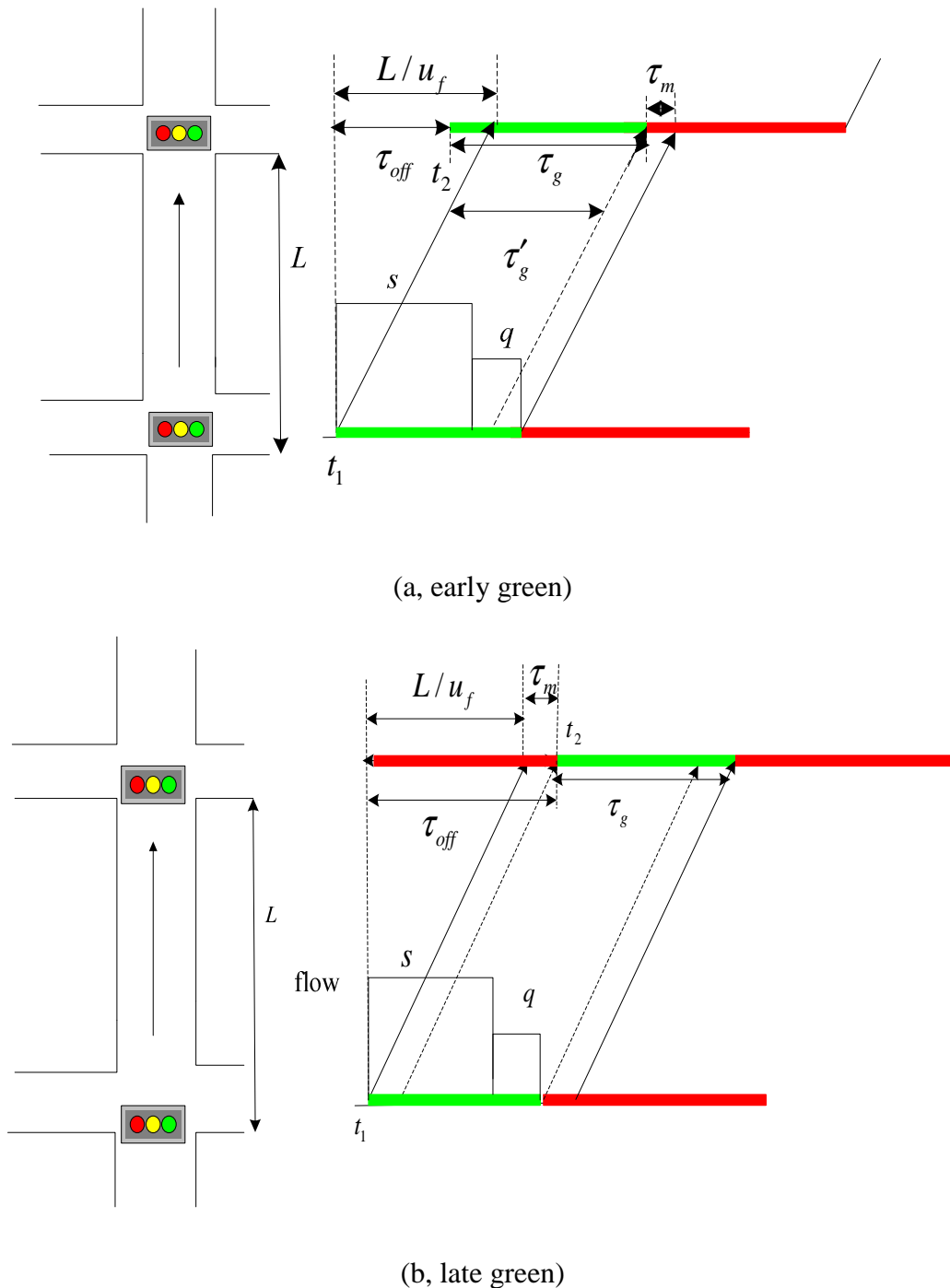


**Figure 5.7: Offsets at adjacent intersections**

### 5.3.2 Delay at two adjacent intersections

As discussed in the previous section, there are two types of mismatch (early green and late green) between the two fixed-time controlled intersections. In this section, the delay vehicles experience when traversing the two consecutive intersections is analysed and discussed according these two types of mismatch.

### **Mismatch 1, early green**

#### ***(1) When the upstream intersection is undersaturated***

Figure 5.8 illustrates the delay that vehicles experience passing two signalized intersections. We assume that there is no oversaturation (filtered by the upstream intersection) at the downstream intersection. Depending on the arrival moment at both intersections, the initial overflow queue at the upstream intersection and offsets between two intersections, delay vehicles experience can be categorized into three cases:

#### **Case 1: Figure 5.8 (a)**

As shown in Figure 5.8 (a), vehicles leaving from the upstream intersection at time  $t_l$  can pass the downstream intersection without delay. Vehicles departing from the first intersection after  $t_l + \tau_g'$  have to wait at the second intersection. The arrivals are first in a dense platoon determined by the saturation flow and after the saturated green time, the flow is determined by the arrival rate. When the vehicle arrives at the beginning of the red time  $t_0$  at the upstream intersection, delay equals to the red time plus the time to release the initial overflow queue at the upstream intersection plus the arriving vehicle itself and decreases linearly until zero at the saturated green time which is given by:

$$t_{sat} = t_0 + \frac{\tau_r + \frac{n_0 + 1}{s}}{1 - \frac{q}{s}} \quad (5.12)$$

Where  $\tau_r$  is the red time;  $n_0$  is the initial queue;  $s$  is the saturation flow rate and  $q$  is the arriving flow rate.

Vehicles arriving at the upstream intersection experience zero delay after  $t_{sat}$  up till  $t_f = t_0 + \tau_r + \tau_g'$  as shown in Figure 5.8 (a) and after  $t_f$ , vehicles have to wait for the red time at the downstream intersection. The delay as a function of arrival time at the stop line of the upstream intersection can be determined as:

$$W(t|n_0) = \begin{cases} \tau_r + \frac{n_0 + 1}{s} - (1 - \frac{q}{s})(t - t_0) & t_0 \leq t \leq t_{sat} \\ 0 & t_{sat} < t \leq t_f \\ \tau_r - (1 - \frac{q}{s})(t - t_f) & t > t_f \end{cases} \quad (5.13)$$

#### **Case 2: Figure 5.8 (b)**

As shown in Figure 5.8 (b), when the initial overflow queue becomes larger such that vehicles arriving the upstream intersection at time  $t_h$  before the end of the saturated green time  $t_{sat}$  have to wait for the red time at the downstream intersection. The moment  $t_h$  is given by:

$$n_0 + q(t_h - t_0) + 1 = s\tau'_g$$

$$\text{i.e. } t_h = t_0 + \frac{s\tau'_g - n_0 - 1}{q} \quad (5.14)$$

Vehicles arriving before  $t_h$  only have delay at the upstream intersection and after  $t_h$ , vehicles need to wait at the downstream intersection. For this case, delay as a function of arrival time at the stop line of the upstream intersection can be calculated as:

$$W(t|n_0) = \begin{cases} \tau_r + \frac{n_0 + 1}{s} - (1 - \frac{q}{s})(t - t_0), & t \leq t_h \\ 2\tau_r + \frac{n_0 + 1}{s} - (1 - \frac{q}{s})(t - t_0), & t > t_h \end{cases} \quad (5.15)$$

### Case 3: Figure 5.8 (c)

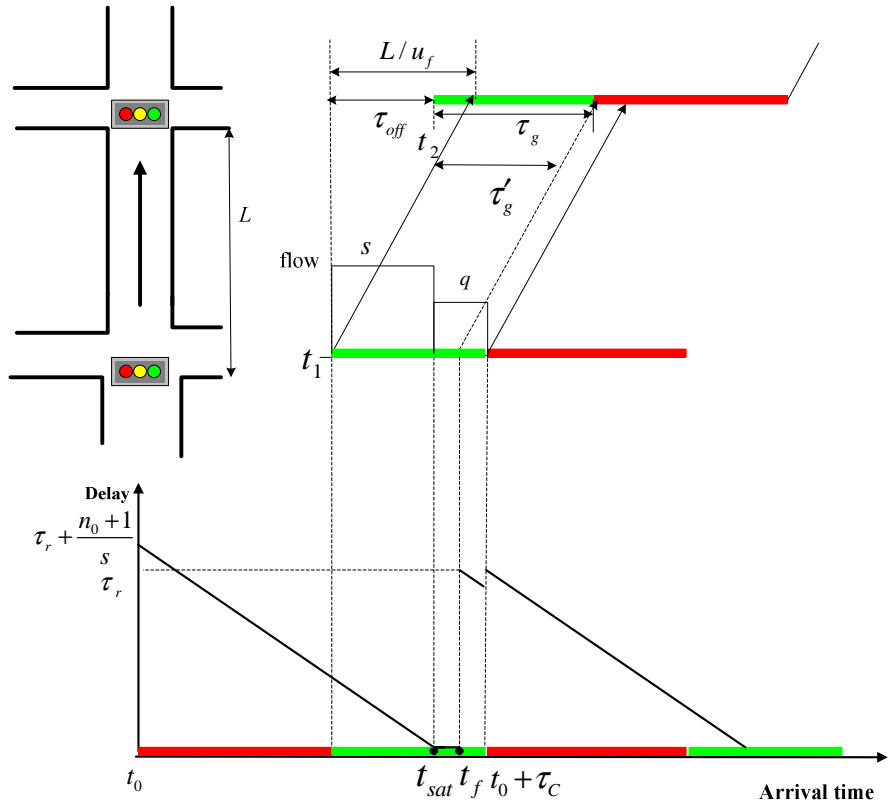
As shown in Figure 5.8 (c), if the initial overflow queue departing from the upstream intersection is so large that it can't leave the downstream intersection completely within the green time  $\tau'_g$ . For this case, the vehicle arriving right after the start of the red time at the upstream intersection needs to wait for the red time at the downstream intersection because of the long overflow queue which is given by:

$$n_0 + 1 \geq s\tau'_g$$

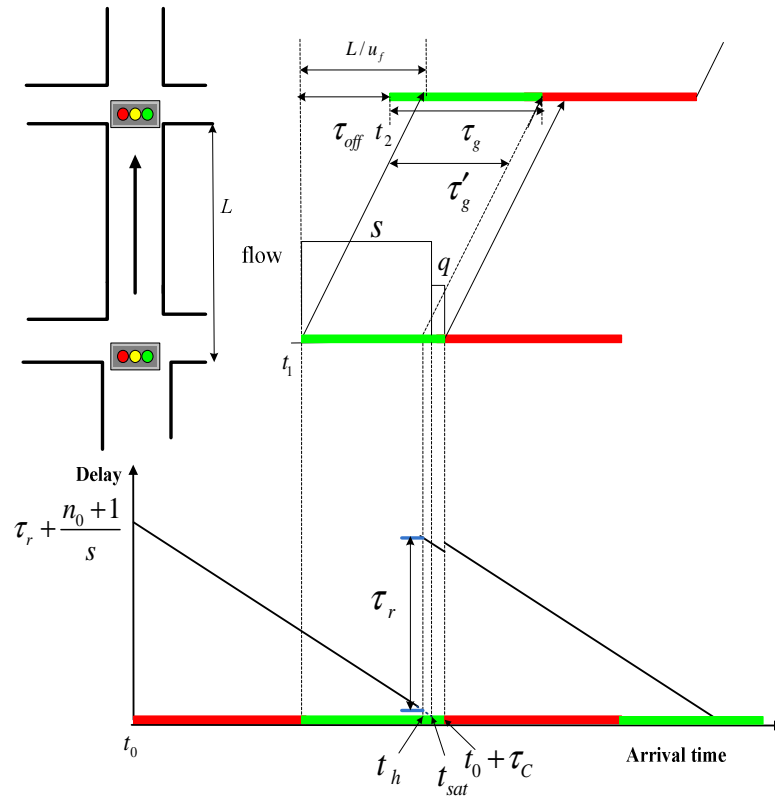
$$n_0 \geq s\tau'_g - 1$$

The delay vehicles experience can be calculated as:

$$W(t|n_0) = 2\tau_r + \frac{n_0 + 1}{s} - (1 - \frac{q}{s})(t - t_0) \quad (5.16)$$



(a)



(b)



The floor  $\lfloor \cdot \rfloor$  is used to indicate the integer value of the expression inside the brackets.

### **Mismatch 2, late green**

#### **(1) When the upstream intersection is undersaturated**

Vehicles leaving from the first intersection after  $t_l$  (the beginning of the green time) have to wait at the second intersection for a period of  $\tau_m$  as shown in Figure 5.9. The arrivals are first in a dense platoon determined by the saturation flow and after the saturated green time, the flow is determined by the arrival rate. When vehicles arrive before  $t_{sat}$ , the delay at the first and second intersection is determined by:

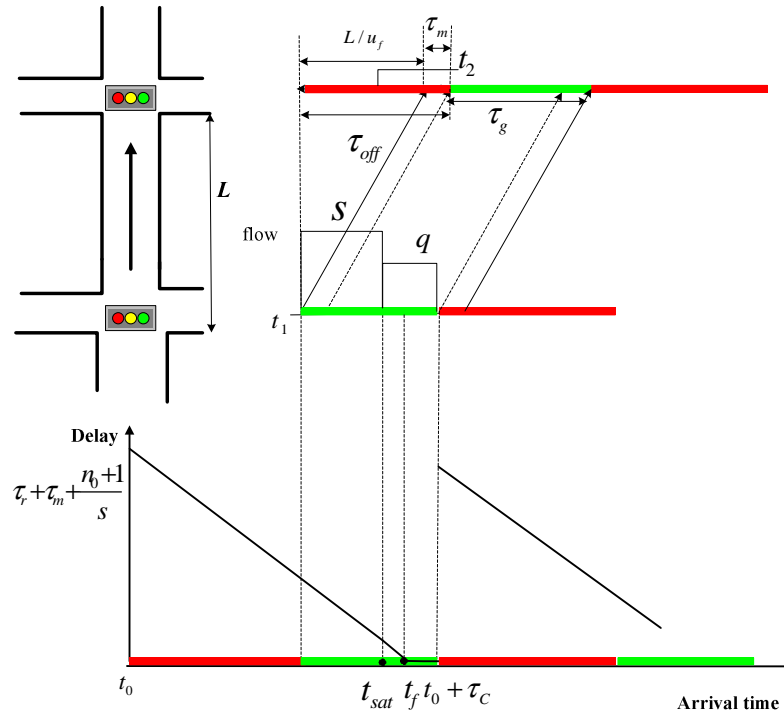
$$W(t|n_0) = \tau_r + \frac{n_0 + 1}{s} - (1 - \frac{q}{s})(t - t_0) + \tau_m, \quad t < t_{sat} \quad (5.18)$$

After  $t_{sat}$ , the delay can be calculated as:

$$\begin{aligned} W(t|n_0) &= \text{Max}\{\tau_m - (1 - \frac{q}{s})(t - t_{sat}), 0\} \\ &= \text{Max}\{\tau_r + \tau_m + \frac{n_0 + 1}{s} - (1 - \frac{q}{s})(t - t_0), 0\}, \quad t \geq t_{sat} \end{aligned} \quad (5.19)$$

By combining Equations (5.18) and (5.19), the delay as a function of arrival time at the upstream intersection can be derived as:

$$W(t|n_0) = \text{Max}\{\tau_r + \tau_m + \frac{n_0 + 1}{s} - (1 - \frac{q}{s})(t - t_0), 0\} \quad (5.20)$$



(a)

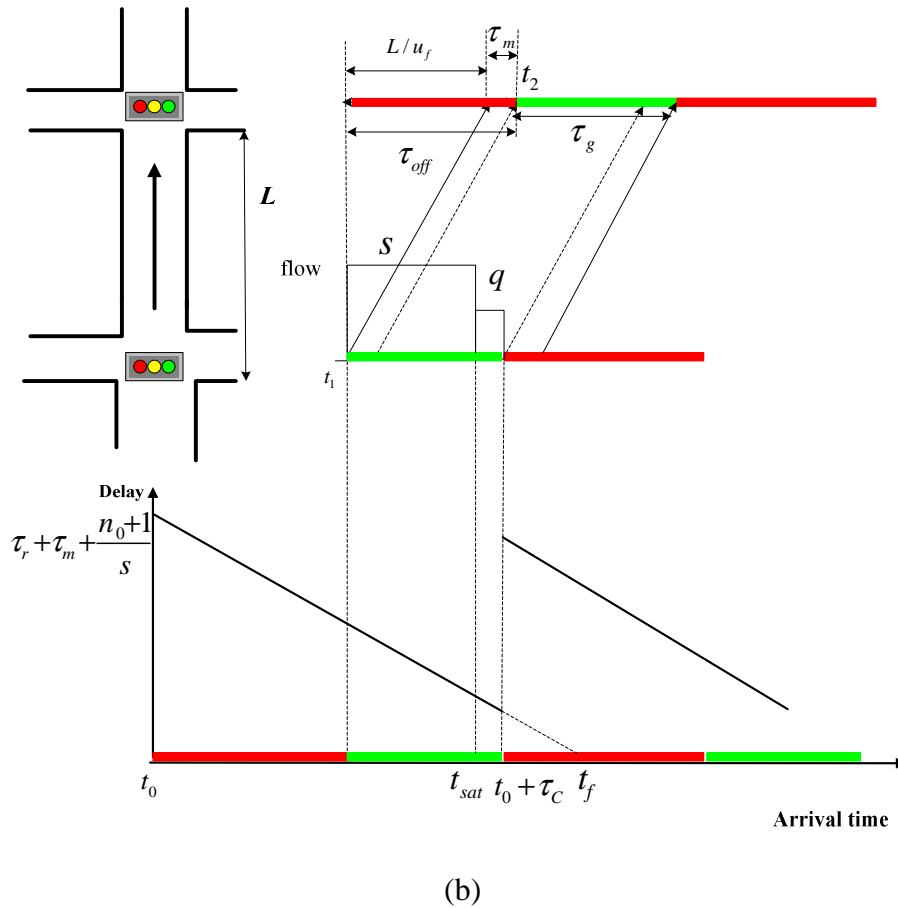


**Figure 5.9: Delay as a function of arrival time for two adjacent intersections in the undersaturated condition (Mismatch 2, late green)**

**(2) When the upstream intersection is oversaturated**

In oversaturated conditions, the arriving vehicle needs to wait for extra red times due to the large initial overflow queue and the high traffic demand. Therefore, the delay as the function of arrival time can be deduced as:

$$W(t|n_0) = \left\{ \tau_r + \tau_m + \frac{n_0 + 1}{s} + \left[ \frac{n_0 + q(t - t_0) + 1}{s\tau_g} \right] \tau_r \right\} - \left(1 - \frac{q}{s}\right)(t - t_0) \quad (5.21)$$

### 5.3.3 Travel time distribution for two adjacent intersections

The delay as function of the arrival time at the upstream intersection for two types of mismatch both in the undersaturated condition and oversaturated condition has been discussed in the previous subsection. In this subsection, the travel time distribution model for two consecutive fixed-time controlled intersections, taking the stochastic overflow queue in the first intersection and different mismatches between these two intersections into account, is developed.

### **Delay distribution with an initial deterministic queue**

#### ***(1) Mismatch 1: early green***

The delay as a function of arrival time at the upstream intersection both for the undersaturated condition and oversaturated condition can be derived according to Equations (5.15), (5.17), (5.18) and (5.19). As for the oversaturated condition, the number of extra red times that a vehicle arriving at time  $t$  needs to wait at the upstream intersection can be directly derived from Equation (5.19). The more generic expression is:

$$N = \left\lceil \frac{q(t-t_0) + n_0 + 1}{s\tau_g} \right\rceil \quad (5.22)$$

From Equation (5.19), we can see that when a vehicle arriving within the time interval of one cycle time, the minimum number of extra red times this vehicle needs to wait at the upstream intersection can be derived as:

$$N_{\min} = \left\lceil \frac{n_0 + 1}{s\tau_g} \right\rceil \quad (5.23)$$

And the maximum number of extra red times is given by:

$$N_{\max} = \left\lceil \frac{q\tau_c + n_0 + 1}{s\tau_g} \right\rceil \quad (5.24)$$

If the value within  $\lceil \cdot \rceil$  is an integer, the maximum delay will be experienced by the vehicle arriving at the end of the cycle. Otherwise, the maximum delay will appear before the end of the cycle ( $t < t_0 + \tau_c$ ) in oversaturated conditions.

When vehicles arrive at the downstream intersection, there are two cases:

- *Passing the downstream intersection without delay;*
- *Passing the downstream intersection with a certain delay.*

Whether vehicles need to wait for the red time at the downstream intersection depends on whether the number of vehicles in front of this vehicle plus the vehicle itself can be released within the green time  $\tau_g'$  at the downstream intersection.

1) If  $0 \leq n_0 + q(t-t_0) + 1 - \left\lceil \frac{n_0 + q(t-t_0) + 1}{s\tau_g} \right\rceil s\tau_g < s\tau_g'$ , vehicles experience no delay at the

downstream intersection. Vehicles just experience delays at the upstream intersection. Given the initial moment of the calculation  $t_0$ , in our approach, it is the beginning of the red time. For this case, the transition moments (discontinuity of the delay as function of  $t_n$ ) appear when:

$$n_0 + q(t_N - t_0) + 1 - Ns\tau_g = 0$$

Each transition moment can be derived as:

$$t_N = \begin{cases} t_0 & N = N_{\min} \\ t_0 + \frac{Ns\tau_g - n_0 - 1}{q} & N_{\min} < N \leq N_{\max} \end{cases} \quad (5.25)$$

2) If  $n_0 + q(t - t_0) + 1 - \left\lfloor \frac{n_0 + q(t - t_0) + 1}{s\tau_g} \right\rfloor s\tau_g \geq s\tau'_g$  vehicles experience delays at both the upstream and downstream intersections, the transition moments appear when:

$$n_0 + q(t'_N - t_0) + 1 - Ns\tau_g = s\tau'_g$$

Each transition moment can be expressed as:

$$t'_N = t_0 + \frac{Ns\tau_g + s\tau'_g - n_0 - 1}{q} \quad (5.26)$$

An example is shown in Figure 5.10. The ‘star’ points are the transition moments when vehicles arriving at the stop line of the upstream intersection need to wait for another red phase at the upstream intersection. The dots are transition moments when vehicles arrive at the stop line of the upstream intersection will experience an extra delay of ‘red phase’ at the downstream intersection. The star transition moments lie on the decreasing trend line starting from the dot transition moments in case two intersections have the same red time. However, if the upstream intersection and the downstream intersection have different red times, the star transition moments can be above or below the trend line. Figure 5.11 illustrates trajectories of vehicles passing two intersections. The bold solid lines indicate trajectories of vehicles arriving at the ‘transition moments’ which are ‘dots’ and ‘stars’ as shown in Figure 5.10. In the case of a vertical queue, the ‘transition arrival moments’  $t'_I$ ,  $t_I$  are extrapolated and the dotted lines are virtual trajectories of vehicles arriving at the stop line of the upstream intersection.

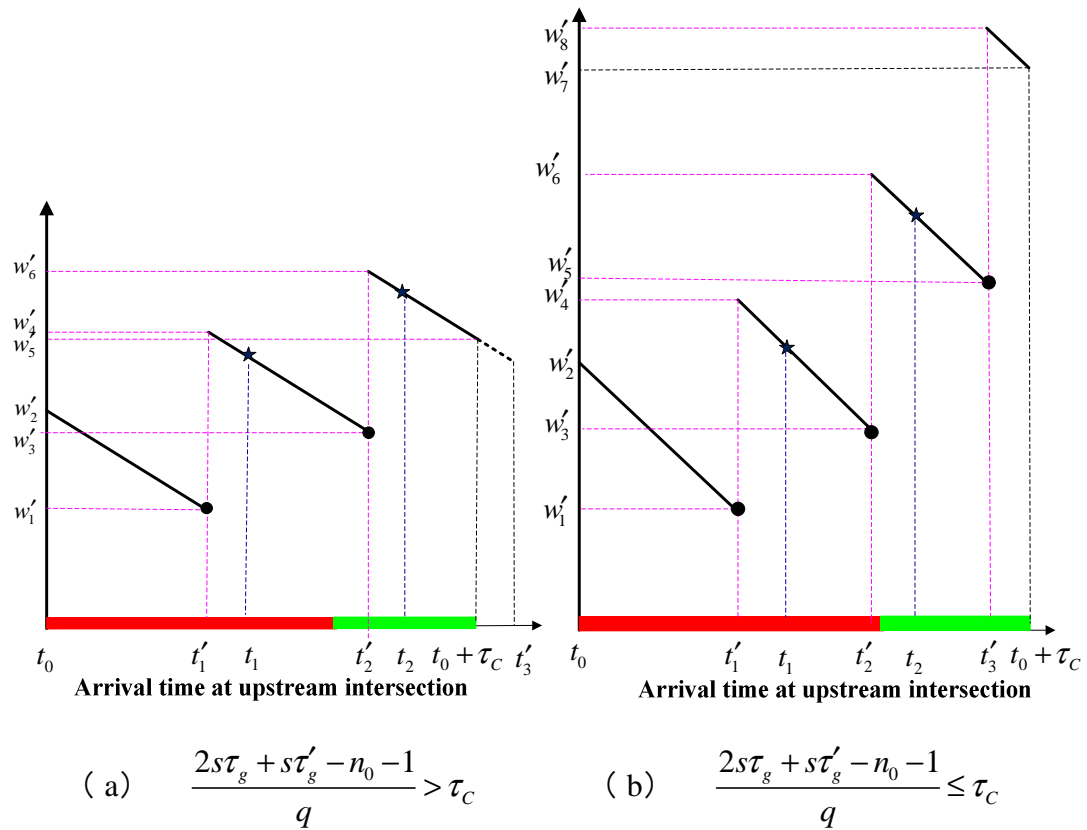


**Figure 5.10:** Delay as a function of arrival time (at the stop line of the upstream intersection in the case of a vertical queue) in the oversaturated condition with the same red time for both intersections (Mismatch 1, early green)

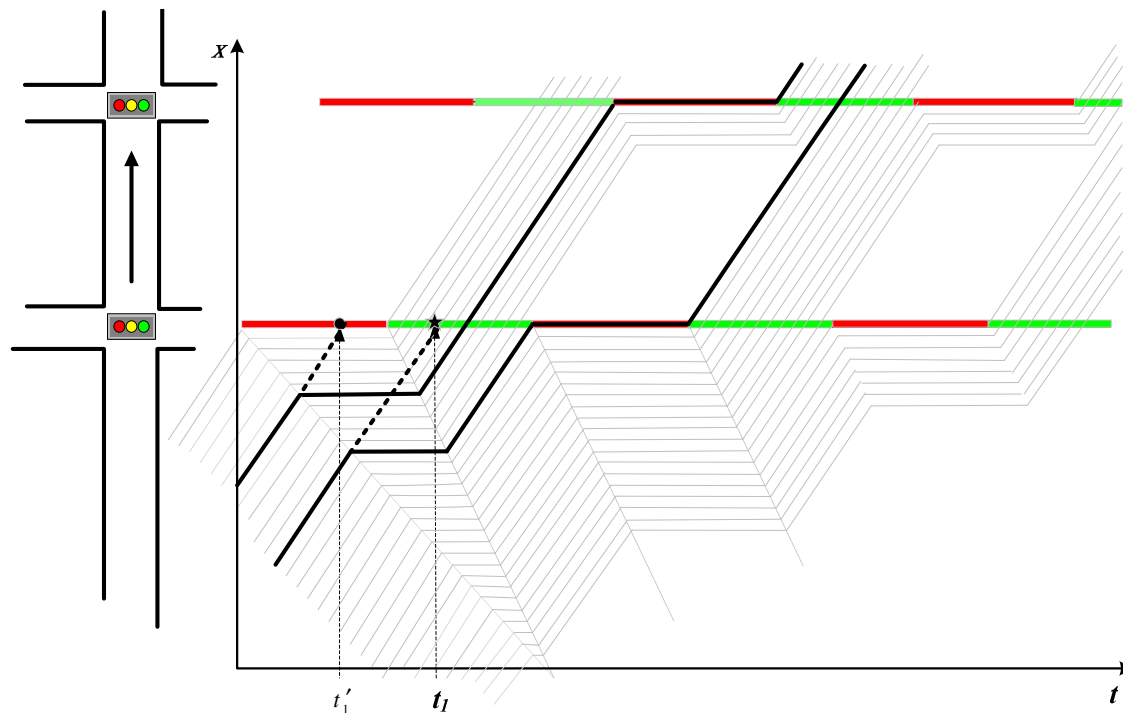


**Figure 5.11:** Trajectories of vehicles passing two intersections (Mismatch 1, early green)

## (2) Mismatch 2: late green

In case of mismatch 2, vehicles departing from the upstream intersection right after the traffic light turns to green will experience extra delay due to the late start of green phase at the downstream intersection. The transition moments can be derived from Equation (5.21) as:

$$t_N = \begin{cases} t_0 & N = N_{\min} \\ t_0 + \frac{Ns\tau_g - n_0 - 1}{q} & N_{\min} < N \leq N_{\max} \end{cases} \quad (5.27)$$

$N_{\min}$ ,  $N_{\max}$  are the minimum number of extra red time and maximum number of extra red time that vehicles need to wait at the upstream intersection, respectively, which are given by Equations(5.23) and (5.24).

Figure 5.12 illustrates the delay as a function of arrival time at the upstream intersection (In case of a vertical queue, the arrival time refers to the arrival moment at the stop line) in the oversaturation condition. The ‘star’ points are the transition moments when vehicles arriving at the stop line of the upstream intersection need to wait for an extra red phase at the upstream intersection. Trajectories of vehicles passing two intersections and the ‘transition arrival moment’  $t_l$  at the stop line of the upstream intersection are shown in Figure 5.13. The dotted line is the virtual trajectory of the vehicle arriving at the stop line of the upstream intersection in the case of a vertical queue.

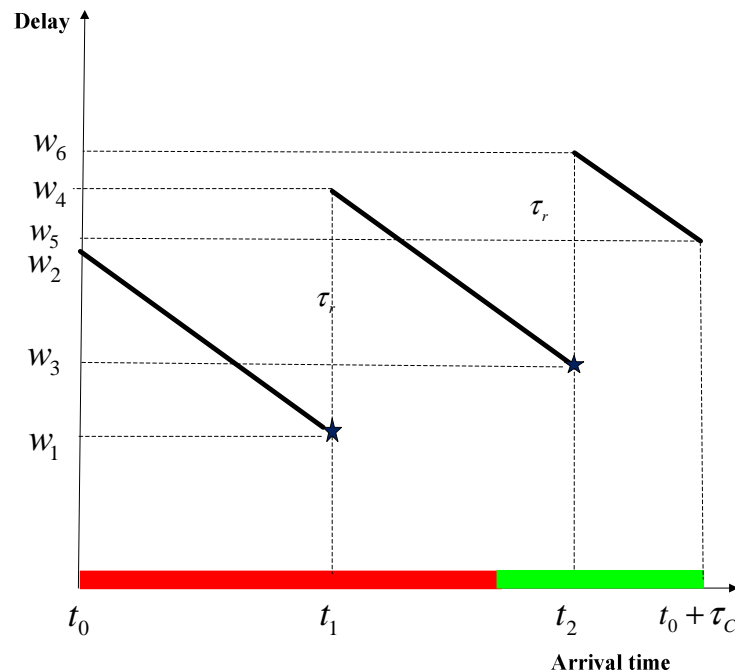


**Figure 5.12: Delay as a function of arrival time for two adjacent intersections in the oversaturated condition with the same red time for both intersections (Mismatch 2, late green)**

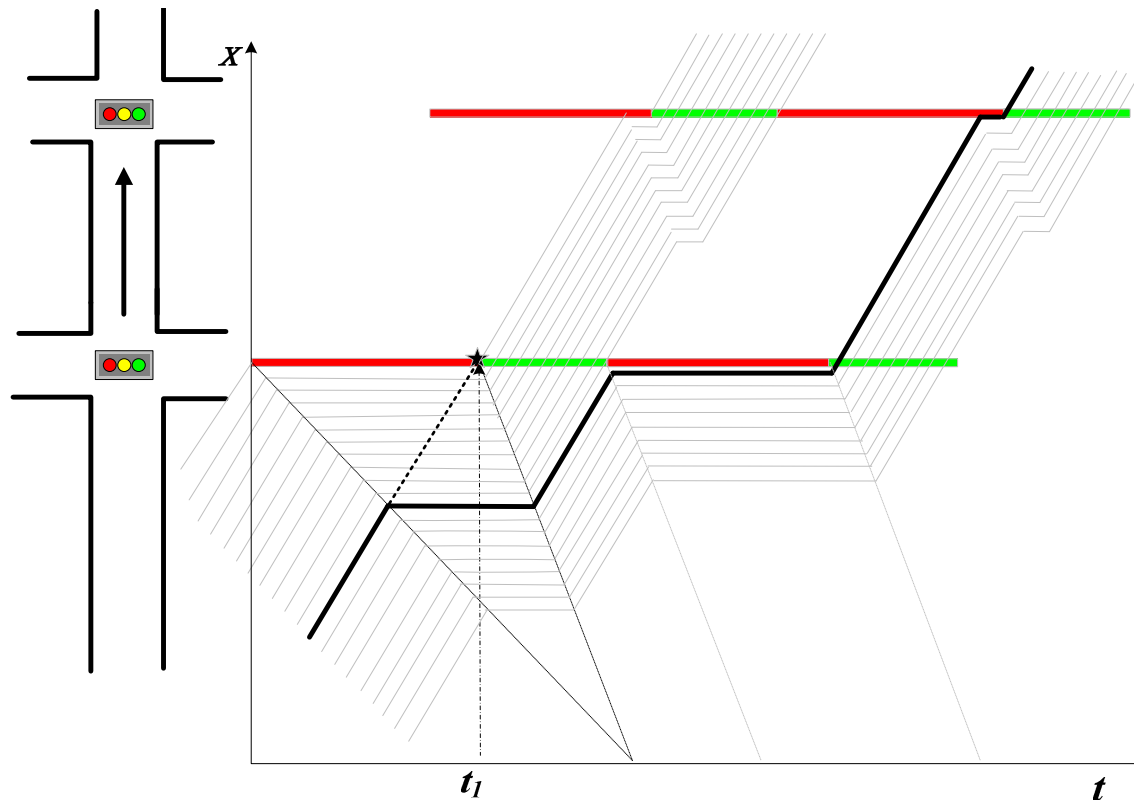


**Figure 5.13: Trajectories of vehicles passing two intersections with mismatch 2 (The bold solid line indicates the trajectory of the vehicle arriving at the ‘transition moment’  $t_I$  as shown in figure 5.12)**

The influence of shockwave on delay calculation is discussed in Appendix D and it shows that the shock wave does not have influence on the final delay calculation as long as there is no spill back. According to Equations (5.17) and (5.21), delay at these transition moments can be calculated. Due to the complexity, the detailed deduction process of delays for different transition moments under all the cases described in previous sections is not discussed in this chapter but can be found in Appendix C. The general expressions of delay for these transition moments and the initial moment are given according to two types of mismatch.

**Mismatch 1:**

(1) If  $n_0 + 1 - \left\lfloor \frac{n_0 + 1}{s\tau_g} \right\rfloor s\tau_g < s\tau'_g$  &  $\frac{N_{\max} s\tau_g + s\tau'_g - n_0 - 1}{q} > \tau_c$ : The first vehicle arriving

right after the beginning of the red time can leave the downstream without delay and the last transition moment according to Equation (5.26) is larger than the cycle time (shown in Figure 5.10 a), then delays at the transition moments are given by the following equations:

$$W_{2N+1} = \begin{cases} N\tau_C + \tau_r + \tau'_g - \frac{Ns\tau_g + s\tau'_g - n_0 - 1}{q} & N_{\min} \leq N < N_{\max} \\ (N+1)\tau_r + \frac{n_0 + 1}{s} - \tau_C(1 - \frac{q}{s}) & N = N_{\max} \end{cases} \quad (5.28a)$$

$$W_{2N+2} = \begin{cases} (N+1)\tau_r + \frac{n_0 + 1}{s} & N = N_{\min} \\ (N-1)\tau_C + 2\tau_r + \tau'_g - \frac{(N-1)s\tau_g + s\tau'_g - n_0 - 1}{q} & N_{\min} < N \leq N_{\max} \end{cases} \quad (5.28b)$$

- (2) If  $n_0 + 1 - \left\lfloor \frac{n_0 + 1}{s\tau_g} \right\rfloor s\tau_g < s\tau'_g$  &  $\frac{N_{\max}s\tau_g + s\tau'_g - n_0 - 1}{q} \leq \tau_C$ : The first vehicle arriving

right after the beginning of the red time can leave the downstream without delay and the last transition moment according to Equation (5.26) is within the cycle time (shown in Figure 5.10 b), then delays at the transition moments are given by the Equations (5.29a) and (5.29 b) as:

$$W_{2N+1} = \begin{cases} N\tau_C + \tau_r + \tau'_g - \frac{Ns\tau_g + s\tau'_g - n_0 - 1}{q}, & N_{\min} \leq N \leq N_{\max} \\ (N+1)\tau_r + \frac{n_0 + 1}{s} - \tau_C(1 - \frac{q}{s}) & N = N_{\max} + 1 \end{cases} \quad (5.29a)$$

$$W_{2n+2} = \begin{cases} (N+1)\tau_r + \frac{n_0 + 1}{s} & N = N_{\min} \\ (N-1)\tau_C + 2\tau_r + \tau'_g - \frac{(N-1)s\tau_g + s\tau'_g - n_0 - 1}{q} & N_{\min} < N \leq N_{\max} + 1 \end{cases} \quad (5.29b)$$

- (3) If  $n_0 + 1 - \left\lfloor \frac{n_0 + 1}{s\tau_g} \right\rfloor s\tau_g \geq s\tau'_g$  &  $\frac{N_{\max}s\tau_g + s\tau'_g - n_0 - 1}{q} > \tau_C$ : The initial overflow queue

is so large that the first vehicle arriving right after the start of the red time at the upstream intersection has to wait for the red time at the downstream intersection plus the condition that the last transition moment according to Equation (5.26) is larger than the cycle time (shown in Figure 5.10 a). For this case, then delays at the transition moments are calculated as:

$$W_{2N+1} = \begin{cases} N\tau_C + \tau_r + \tau'_g - \frac{Ns\tau_g + s\tau'_g - n_0 - 1}{q} & N_{\min} + 1 \leq N < N_{\max} \\ (N+1)\tau_r + \frac{n_0 + 1}{s} - \tau_C(1 - \frac{q}{s}) & N = N_{\max} \end{cases} \quad (5.30a)$$

$$W_{2N+2} = \begin{cases} (N+1)\tau_r + \frac{n_0+1}{s} & N = N_{\min} + 1 \\ (N-1)\tau_c + 2\tau_r + \tau'_g - \frac{(N-1)s\tau_g + s\tau'_g - n_0 - 1}{q} & N_{\min} + 1 < N \leq N_{\max} \end{cases} \quad (5.30b)$$

(4) If  $n_0 + 1 - \left\lfloor \frac{n_0 + 1}{s\tau_g} \right\rfloor s\tau_g \geq s\tau'_g$  &  $\frac{N_{\max}s\tau_g + s\tau'_g - n_0 - 1}{q} \leq \tau_c$ : The initial overflow queue is

so large that the first vehicle arriving right after the start of the red time at the upstream intersection has to wait for the red time at the downstream intersection plus the condition that the last transition moment according to Equation (5.26) is within the cycle time (shown in Figure 5.10b). The delays at the transition moments for this case are given by:

$$W_{2N+1} = \begin{cases} N\tau_c + \tau_r + \tau'_g - \frac{Ns\tau_g + s\tau'_g - n_0 - 1}{q} & N_{\min} + 1 \leq N \leq N_{\max} \\ (N+1)\tau_r + \frac{n_0+1}{s} - \tau_c(1 - \frac{q}{s}) & N = N_{\max} + 1 \end{cases} \quad (5.31a)$$

$$W_{2N+2} = \begin{cases} (N+1)\tau_r + \frac{n_0+1}{s} & N = N_{\min} + 1 \\ (N-1)\tau_c + 2\tau_r + \tau'_g - \frac{(N-1)s\tau_g + s\tau'_g - n_0 - 1}{q} & N_{\min} + 1 < N \leq N_{\max} + 1 \end{cases} \quad (5.31b)$$

### Mismatch 2:

$$W_{2N+1} = \begin{cases} (N+1)\tau_c + \tau_m - \frac{(N+1)s\tau_g - n_0 - 1}{q} & N_{\min} \leq N < N_{\max} \\ (N+1)\tau_r + \tau_m + \frac{n_0+1}{s} - \tau_c(1 - \frac{q}{s}) & N = N_{\max} \end{cases} \quad (5.32a)$$

$$W_{2N+2} = \begin{cases} (N+1)\tau_r + \tau_m + \frac{n_0+1}{s} & N = N_{\min} \\ N\tau_c + \tau_m + \tau_r - \frac{Ns\tau_g - n_0 - 1}{q} & N_{\min} < N \leq N_{\max} \end{cases} \quad (5.32b)$$

As shown in chapter 4, for an isolated intersection, the delay probability distribution in the undersaturated condition consists of a Dirac delta function and a box shaped function. While for the oversaturated condition, the probability distribution is the sum of some box shaped functions that may overlap. For the case of two adjacent intersections, once the delay at transition points is determined, by inverse mapping the delay to the arrival time and taking the derivative, the delay distribution can be derived similarly as shown in

Figure 5.14 (a) (b). The probability distribution function for both the undersaturated and oversaturated condition is given by:

$$P_d(W|n_0) = \alpha(n_0)\delta(W) + \sum_N \beta B(W, W_{2N+1}(n_0), W_{2N+2}(n_0)) \tag{5.33}$$

Where  $\alpha$  and  $\beta$  are model parameters with

$$\alpha = \max\left(\frac{s\tau'_s - n_0 - 1}{q\tau_c} - \frac{\tau_r + \frac{(n_0 + 1)}{s}}{\tau_c(1 - \frac{q}{s})}, 0\right), \beta = \frac{1}{\tau_c(1 - \frac{q}{s})}$$

The definition of  $\delta(W)$  and  $B(W, W_{2N+1}, W_{2N+2})$  are given by Equations (4.4) and (4.14) in chapter 4, respectively.  $W_{2N+1}, W_{2N+2}$  are delays at transition moments, which are given by Equations (5.28) - (5.32).

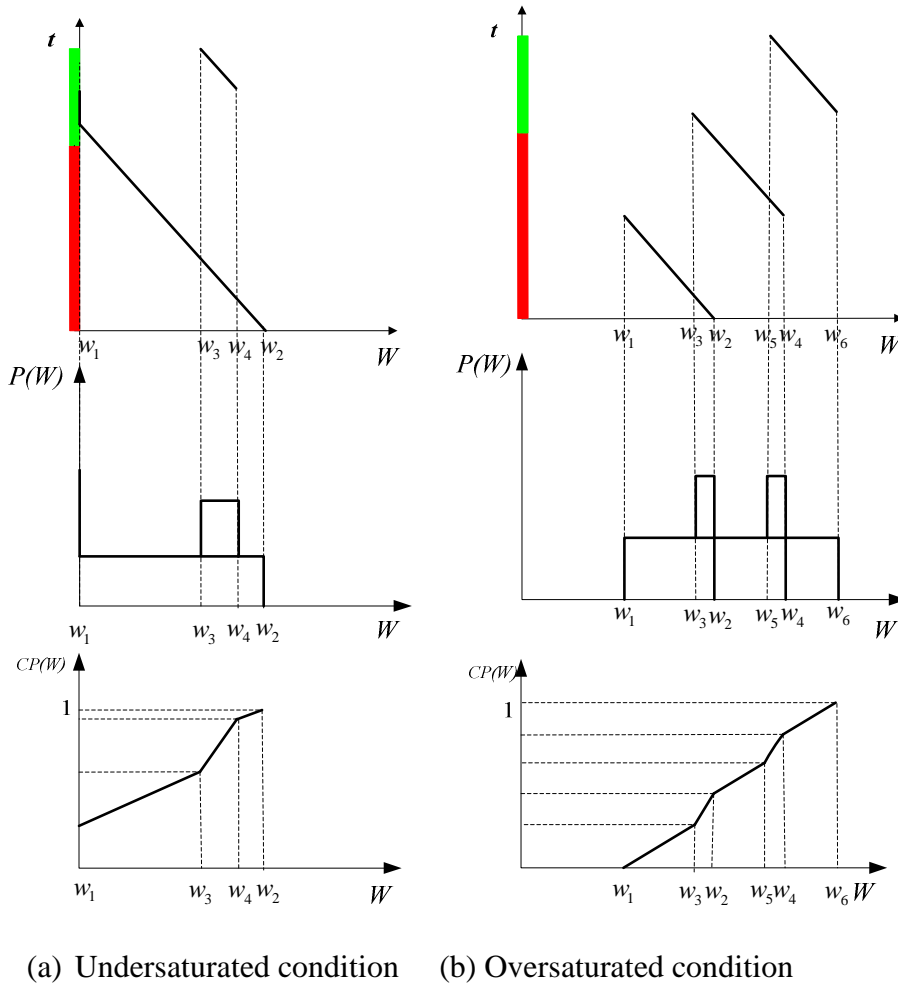


**Figure 5.14: Delay probability distribution and cumulative distribution for both undersaturated and oversaturated conditions**

### **Delay distribution with a stochastic overflow queue**

The delay probability distribution function derived in the previous subsection is based on the fixed initial queue that is present at the beginning of the green phase at the upstream (initial) intersection. If the initial queue is stochastic with a certain probability distribution, the expected probability distribution of the delay  $P_d(W)$  can be calculated as a weighted sum of probability functions:

$$P_d(W) = \sum_{n_0=0}^{\infty} P_d(W | n_0) P(n_0) \quad (5.34)$$

where  $P(n_0)$  is the probability of the overflow queue  $n_0$ .

### **5.3.4 Trip travel time distribution**

In section 5.2.3, the single link travel time distribution has been derived by combining the free flow travel time with the delay distribution. However, for an urban trip with two intersections or more, the delay is dependent on the free flow travel time. Fast drivers may encounter green waves along the trip while slow drivers may be stopped by the red light. The delay distributions for these two types of drivers are different. Furthermore, variable free flow travel time enables vehicles to take over each other. Therefore, for a given travel time  $t$  ( $t = w + s$ ), the probability of a certain delay  $w$  can be formulated as:

$$P'_d(w, s | s) = P'_d(t - s, s | s) \quad (5.35)$$

In this case, the trip travel time distribution  $P(t)$  ( $t = w + s$ ) can be calculated as:

$$P(t) = \int_0^t P'_d(t - s, s | s) P_f(s) ds \quad (5.36)$$

Where  $P'_d(w, s | s)$  denotes the probability of a certain delay  $w$  given a certain free flow travel time  $s$  and it takes into account that slow vehicles are taken over by faster ones so that slow vehicles join a larger queue at the downstream intersection;  $P_f(s)$  denotes the probability of a certain free flow travel time  $s$ . If the variation of the free flow speed is very small such that vehicles cannot take over each other or in case of one lane traffic, Equation (5.36) can be approximated by the following equation:

$$P(t) \approx \int_0^t P_d(t - s | s) P_f(s) ds \quad (5.37)$$

$P_d(w/s)$  ( $t=w+s$ ) denotes the probability of a certain delay  $w$  given a certain free flow travel time  $s$  with assumptions that vehicles cannot take over each other.

### **Numerical example: Trip travel time distribution with two intersections**

In order to see how the proposed trip travel time distribution model works under different traffic conditions, a hypothetical corridor of 1200m with two fixed time controlled

intersections is used for analysis. The distance between two intersections is 500m. The cycle time for both the upstream intersection and the downstream intersection is 60s with the effective green time of 24s. The saturation flow rate is assumed to be 1800veh/h. The total evaluation period is 600s (10 cycles). The average free flow speed is assumed to be 60km/h. Therefore, the average free flow travel time between two intersections is about 30s. Two different traffic conditions, for instance, undersaturation ( $x=0.85$ ) and oversaturation ( $x=1.2$ ), are investigated under different offsets between two intersections:

- *Mismatch=0s*: The offset equals to the average free flow travel time between two intersections. The average mismatch between two intersections is zero. In this case, two intersections are well coordinated. Most vehicles experience zero delay at the downstream intersection.
- *Mismatch=10s*: The average mismatch of traffic signals between two intersections is about 10 seconds. Some vehicles will experience delay at the downstream intersection.
- *Mismatch=20s*: The average mismatch of traffic signals between two intersections is about 20 seconds. Two intersections are badly coordinated.

Figure 5.15 and Figure 5.16 compare the travel time distributions for different degrees of saturation of mismatch 1 and mismatch 2, respectively. The travel time distributions are derived at the 10<sup>th</sup> cycle. For the case of mismatch 1 as shown in Figure 5.15, as the level of mismatch increases (from well-coordinated to badly coordinated), the delay distribution for the low degree of saturation ( $x=0.85$ ) changes significantly. When two intersections are well coordinated, the travel time distribution is skewed to low values. However, the distribution tends to be skewed towards high values as the level of mismatch increases and the whole distribution shifts more to the high travel times. This indicates that the coordination between two intersections has a large influence on the travel time distribution in low degree of saturation. As for the high degree of saturation (e.g. 1.2), the travel time distribution shifts from the left to the right which implies that more and more vehicles will experience longer travel times. The similar phenomenon can be observed for the type of mismatch 2 as shown in Figure 5.16. When the level of mismatch increases, the travel time distribution keeps the similar shape and shifts towards higher values.

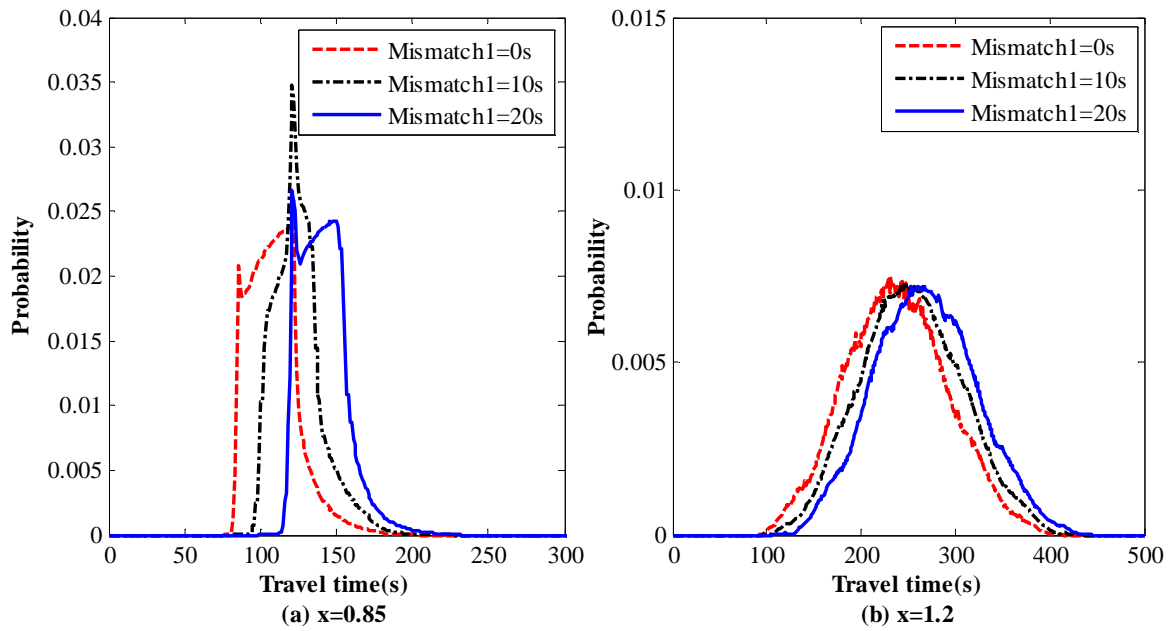


**Figure 5.15:** Trip travel time distribution with different levels of Mismatch 1 in the undersaturated condition (left) and the oversaturated condition (right) ( $x$  is the degree of saturation) calculated with the analytic model

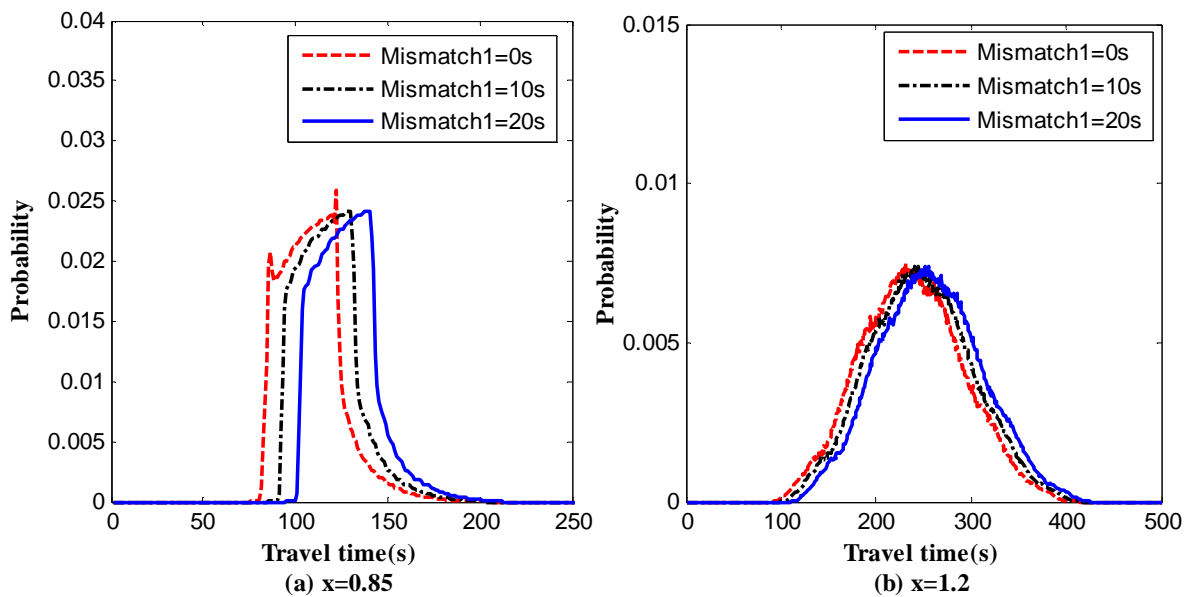


**Figure 5.16:** Trip travel time distribution with different levels of Mismatch 2 in the undersaturated condition (left) and the oversaturated condition (right) ( $x$  is the degree of saturation)

### 5.3.5 Comparison with VISSIM simulation

An urban corridor composed of two fixed-time controlled intersections was built in VISSIM. The total length of the corridor is about 1200m and the desired speed is 60km/h. The cycle time and effective green time for the through-going approach are the same for both intersections with 60s and 24s, respectively. The inflow is 800veh/h/lane. The

simulation period is 1200s and a total of 300 realizations were simulated for each level of mismatch between two intersections (Four levels of mismatch: 0s, 5s, 15s and 20s). Travel times were recorded for each simulation run. Figure 5.17 and Figure 5.19 compare travel time distributions from the analytical model and those from the VISSIM simulation under the undersaturated condition ( $x = 0.917$ ). As can be seen from these figures, the travel time distributions from the analytical model can well represent those from the simulation model under different levels of mismatch except that there is small discrepancy in low travel times and high travel times. This discrepancy could be the result of both the variable free flow travel time in VISSIM and stochastic arrivals and departures at the upstream intersection. Different free flow travel times modify vehicles' arrival moments at the downstream intersection. For instance, in case of early green mismatch, the first vehicle departing from the upstream intersection with smaller free flow travel time can decrease the level of mismatch for this vehicle. As a consequence, the vehicle experiences smaller delay compared with the delay estimated by assuming the average free flow travel time. The variation of inflow (stochastic arrivals) and outflow (stochastic departures) for each cycle at the upstream intersection influences the delay both at the upstream intersection and the downstream intersection. The discrepancy in the high travel times could be caused by the stochastic overflow queues due to stochastic arrivals and departures at the upstream intersection. Nevertheless, from the Kolmogorov-Smirnov test as illustrated in Figure 5.18 (Mismatch1) and Figure 5.20 (Mismatch 2), the hypothesis that the sample travel time distribution generated in VISSIM and the travel time distribution from proposed model are drawn from the same distribution holds for different levels of mismatch and different types of mismatch.

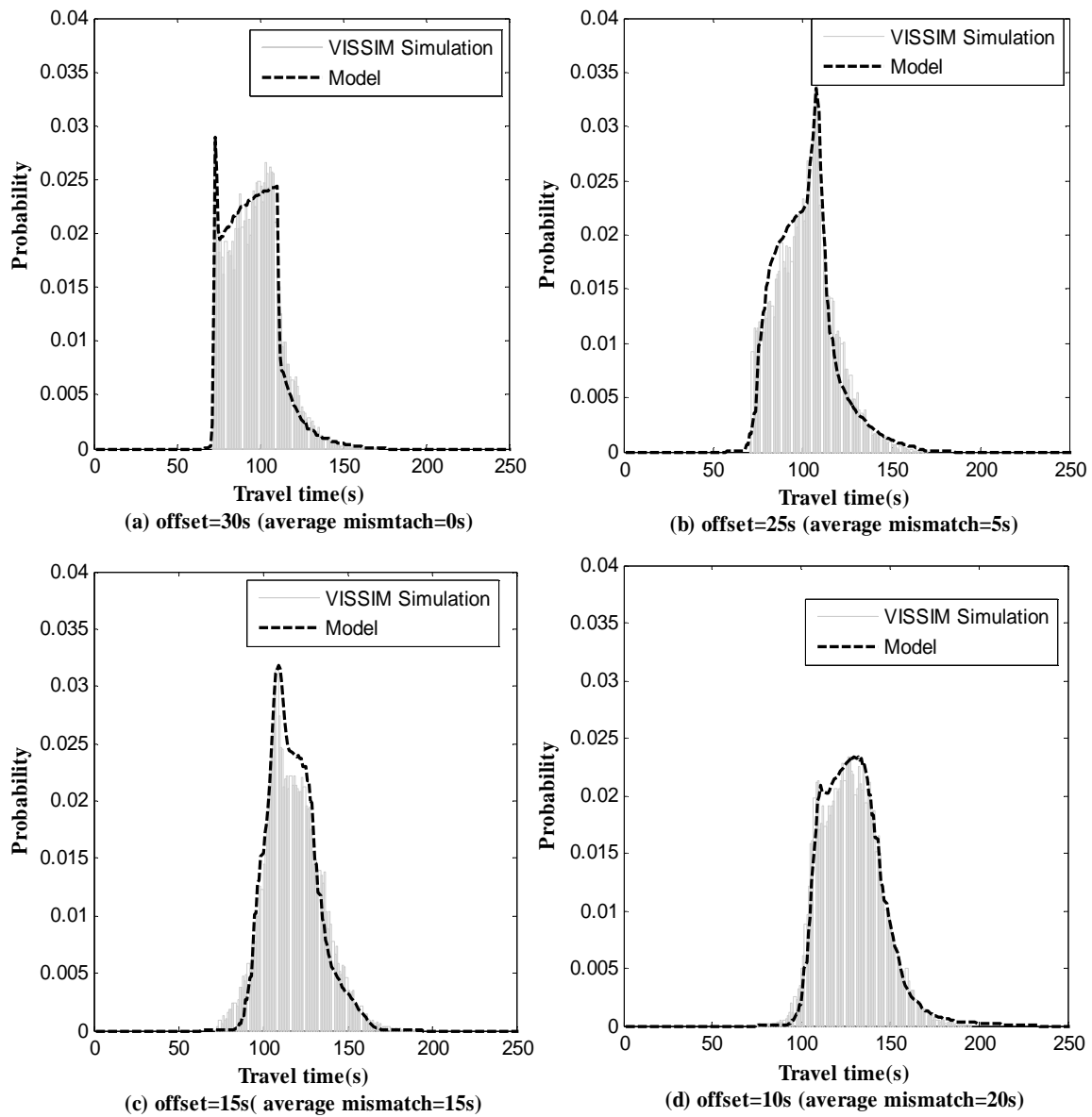


**Figure 5.17: Trip travel time distributions derived from the analytical model and VISSIM simulation data with different level of mismatch 1 ( $q=800\text{veh/h/lane}$ ,  $L=500\text{m}$ )**

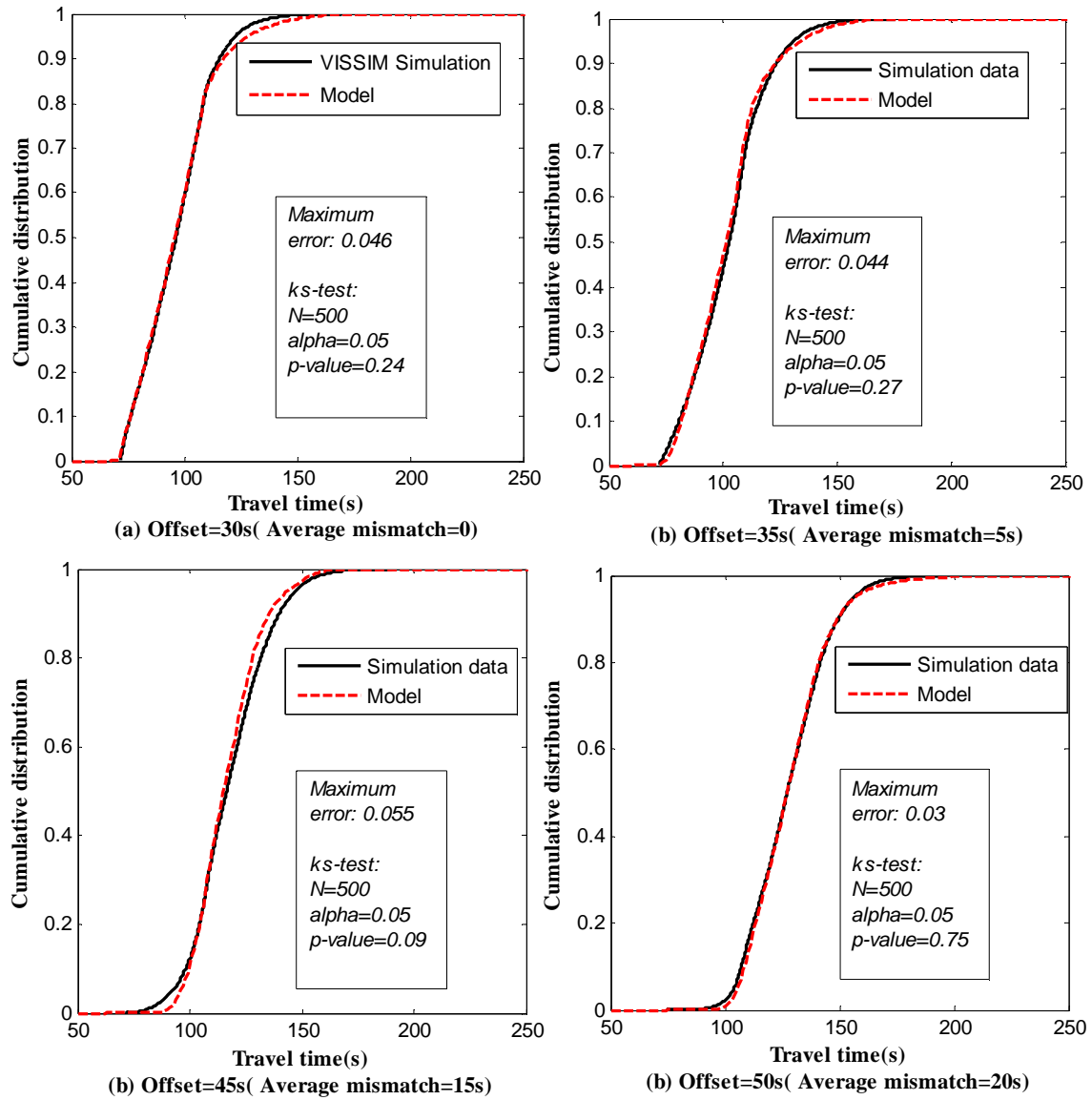


**Figure 5.18: Kolmogorov-Smirnov test for different level of mismatch 1**

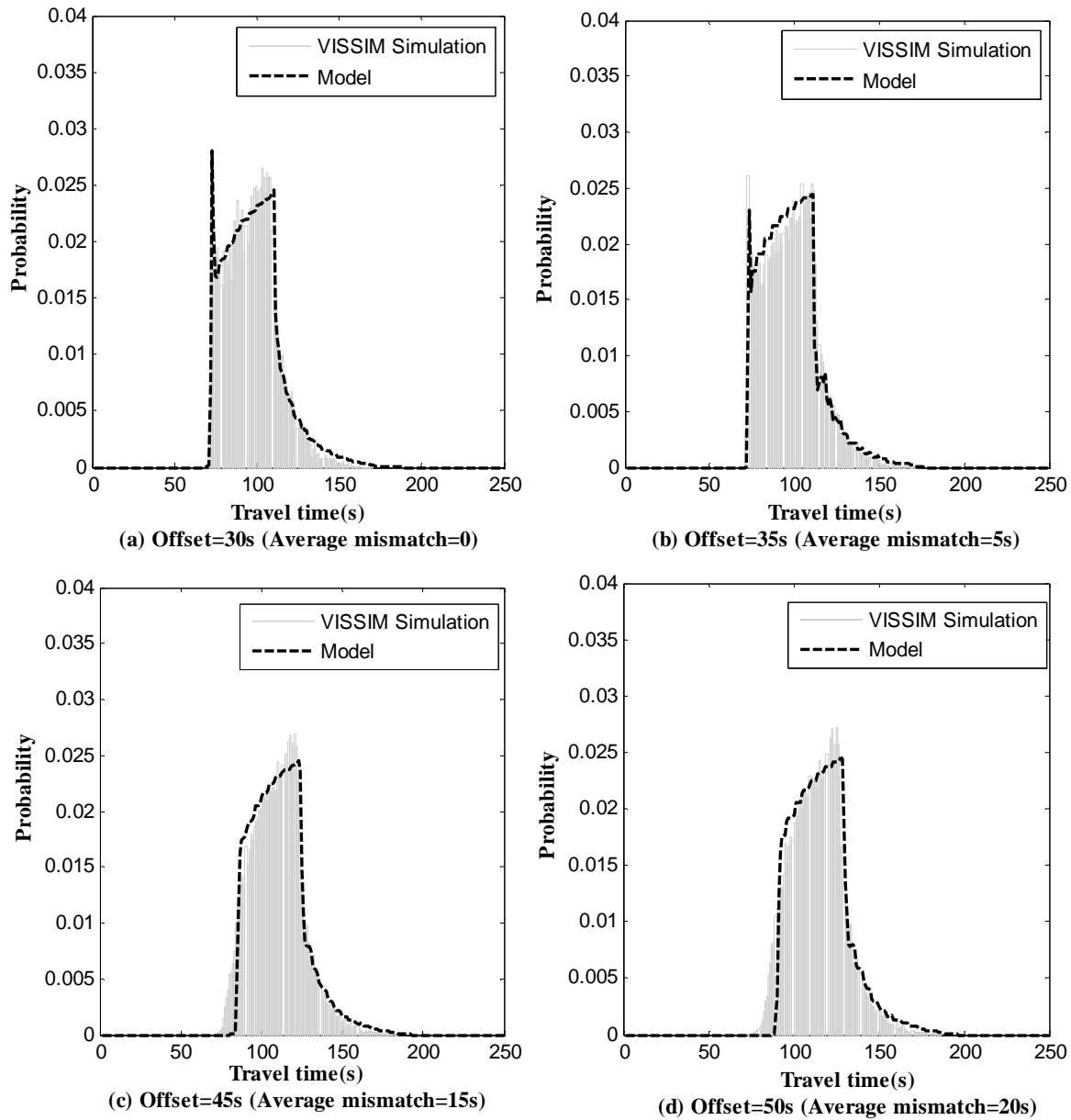


**Figure 5.19: Trip travel time distributions derived from the analytical model and VISSIM simulation data with different levels of mismatch 2 ( $q = 800\text{veh/h/lane}$ ,  $L = 500\text{m}$ )**

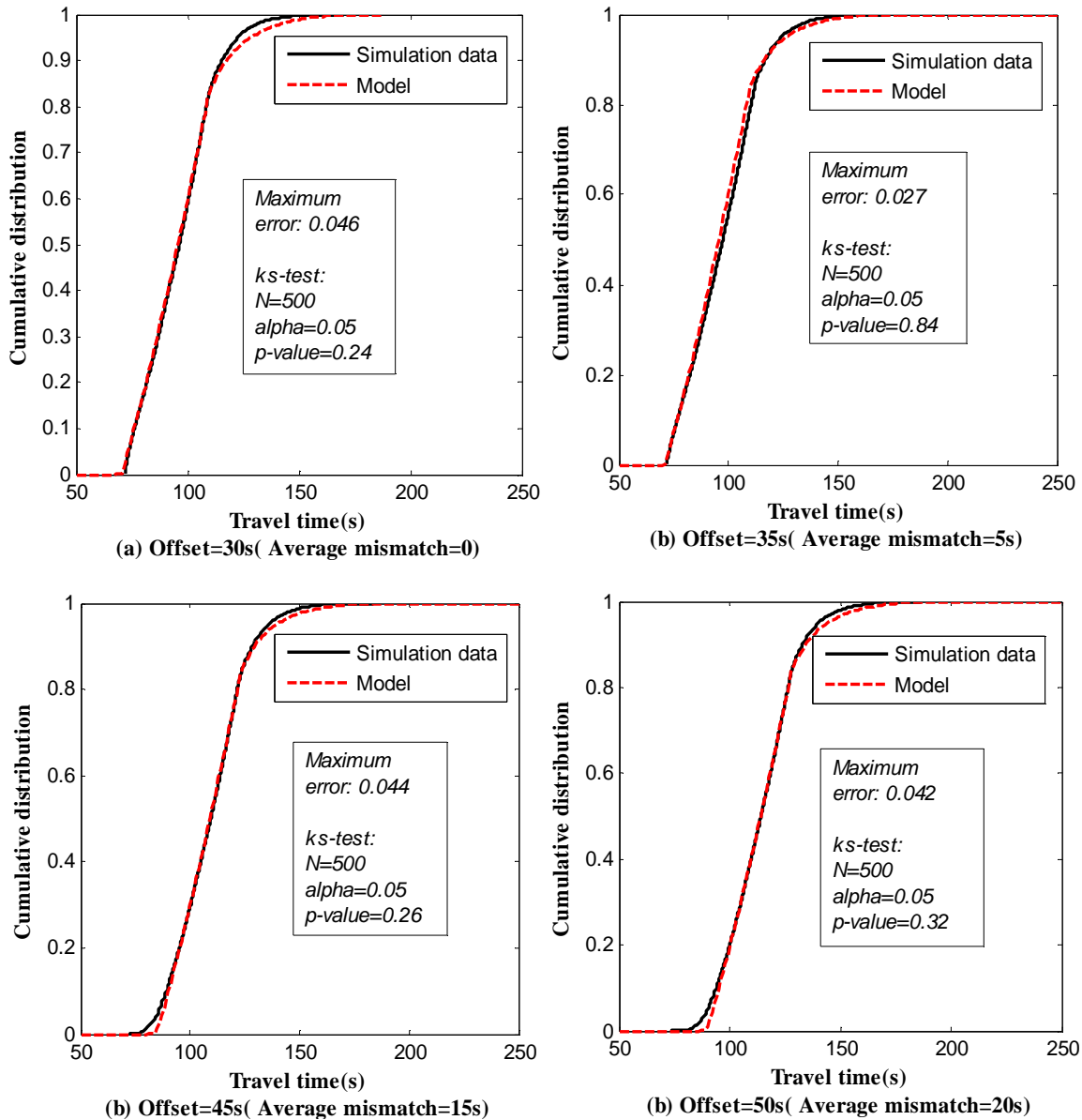


Figure 5.20: Kolmogorov-Smirnov test for different level of mismatch 2

## 5.4 Conclusions and discussion

The ability to measure the variability of travel time for an urban trip is important for urban link travel time estimation and prediction. Given the travel time or delay distribution, the variability of travel time can be investigated using statistical measures, e.g., percentiles or percent variation (Lomax et al., 2003). Furthermore, the knowledge of the variability of travel time (delay) helps to determine the prediction intervals when dealing with travel time prediction. Without a solid method to estimate the variability of travel times, the prediction of travel times, e.g., for routing purposes, has a low practical value. The model developed in this paper is a further step towards a better method to predict urban travel times.

In this chapter, a link travel time distribution model is proposed. The comparison of the results from the proposed model with those from the VISSIM simulation model shows that the link travel time distribution based on the proposed model can well represent the one from the simulation model. The comparison with field GPS data indicates that model estimated link travel time distributions are not significantly different from field travel time distributions, though middle range and higher travel times are more frequently observed with GPS data than the model predicts for link 11-8 (Figure 5.5 (c)).

The extension of the link travel time distribution to the trip travel time distribution is also discussed. An analytical model of travel time distribution for an urban trip with two intersections taking the stochastic properties of traffic flow and signal coordination into account was for the first time proposed in this chapter. The model assumes that two intersections are fixed-time controlled with a certain offset. Different offset settings (well-coordinated, different levels of mismatch) are investigated under different traffic conditions. Results show that for the case of mismatch 1 - early green -, the shape of the travel time distribution keeps on changing and shifts towards high values when the mismatch level of two intersections increases (from well-coordinated to badly coordinated). This implies that the way two intersections are coordinated has big influence on the travel time distribution, especially in the case of undersaturated intersections. While in oversaturated conditions, the travel time distribution spreads over a big range and shifts to the high values when the level of mismatch increases. The comparison with VISSIM simulation shows that the trip travel time distributions derived from the analytical model can well represent those from VISSIM simulation except there is small discrepancy in low travel times and high travel times. The discrepancy is probably due to both the variable free flow speed in VISSIM and variable demand (stochastic arrivals) at the upstream intersection.

The proposed model was only validated in the undersaturated condition. As for the oversaturated condition, one difficulty is to estimate the overflow queue distribution at the upstream (initial) intersection. One alternative way is to estimate the overflow queue distribution from traffic measures (e.g., measured delays or travel times), which is discussed in chapter 6. Furthermore, this model only considers an urban trip with two intersections. In reality, there can be more intersections within a single trip. The travel time distribution of several intersections can vary depending on the coordination of traffic signals and the effective red time. Finally, intersections in a string often have different cycle green splits. This has not been taken into account in this study, but can rather easily be accounted for in a future, more comprehensive, model.



# Chapter 6

## Urban travel time distribution estimation based on traffic measurements

### 6.1 Introduction

An analytical model of delay distribution for an urban trip with two fixed-time controlled intersections has been developed in chapter 5. The difficulty in applying this model remains the question how to estimate parameters in the model, especially the overflow queue which is a rather stochastic quantity. In the proposed delay distribution model, the overflow queue distribution at the upstream intersection is estimated in an analytical way by applying a Markov chain model with the assumption of a certain arrival distribution (e.g. Poisson distribution) within a certain time period. However, when it comes to the oversaturated condition, the overflow queue distribution has a strong relation with the initial condition and it is rather time dependent and growing over time.

The calibration of parameters in the delay distribution model both in the undersaturated condition and oversaturated condition is an important aspect in applying this model for real time estimation or prediction. On one hand, the calibration of model parameters requires a certain amount of traffic data (e.g., travel times, traffic volumes and signal timings). As the development of traffic monitoring techniques, more and more traffic data is becoming available now. Travel times can be measured by different means such as Automatic Number Plate Recognition (ANPR) cameras (Bertini et al., 2005), GPS equipped vehicles (Hoeschen et al., 2005) and Bluetooth devices (Yegor Malinovskiy et al., 2010). On the other hand, using and fusing all the available data for parameter estimation can be quite computation intensive. Therefore, we have to choose a sample of the available data. We apply two sampling methods - Random sampling (RS) and Latin

Hypercube sampling (LHS) - to obtain delay/travel time measurements of sample trips from all observations (observed travel times or delays). The LHS method is a more efficient way of sampling given that the population distribution is known (N. A. Wahanani et al., 2009). In this chapter, both Least squares and Maximum Likelihood are applied to perform the parameter estimation in section 6.2. The Genetic Algorithm is adopted to find the optimal parameter set both to minimize the square error function and maximize the likelihood function. Based on the estimated parameters, the delay distribution can be reconstructed. In section 6.3, the estimated delay distributions are compared with those from VISSIM simulation. Section 6.4 summarizes the contributions of this chapter.

## 6.2 Parameter estimation methods for the delay distribution model

### 6.2.1 Parameters in the delay distribution model

The delay distribution models for an isolated intersection and an urban trip with two fixed controlled intersections have been developed in chapter 4 and 5, respectively. The proposed delay distribution model both for the undersaturated condition and the oversaturated condition has the formulation as:

$$P(w|n_i) = \alpha(n_i)\delta(w) + \sum_{k=0}^N \beta B(w, w_{2k+1}(n_i), w_{2k+2}(n_i)) \quad (6.1)$$

$$P(w) = \sum_{n_i} P(w|n_i)P(n_i) \quad (6.2)$$

Where  $P(n_i)$  is the overflow queue probability distribution;  $\delta(w)$  is the Dirac delta function which has been introduced in chapter 4 with the following properties:

$$\delta(w) = 0, \quad \text{if } w \neq 0$$

$$\int_{-\infty}^{+\infty} f(w)\delta(w)dw = f(0)$$

$B(w, w_{2n-1}, w_{2n})$  is a box function with the property:

$$B(w, w_{2k+1}, w_{2k+2}) = \begin{cases} 1 & w_{2k+1} < w < w_{2k+2} \\ 0 & \text{otherwise} \end{cases}$$

$w_{2n-1}$ ,  $w_{2n}$  are delay boundaries determined by flow, overflow queue, signal timing (e.g., red phase, cycle time and coordination of intersections in case of an urban corridor) as discussed in chapter 4 and 5;  $\alpha$  and  $\beta$  are model parameters following from the traffic state, e.g. the flow  $q$ , overflow queue  $n_i$ , the red phase  $t_r$  and cycle time  $\tau_C$  with:

$$\alpha = \max\left(1 - \frac{\tau_r + \frac{(n_i + 1)}{s}}{\tau_c(1 - \frac{q}{s})}, 0\right), \beta = \frac{1}{\tau_c(1 - \frac{q}{s})}$$

Among all the parameters in the delay distribution function, the overflow queue probability distribution is the most difficult parameter to be determined. In the analytical model, the overflow queue distribution is estimated using a Markov chain model by assuming a certain arrival distribution (e.g., Poisson arrivals) within a certain time period. In undersaturated conditions, the overflow queue distribution follows the equilibrium distribution after a certain number of cycles. The estimated delay distribution can represent the real delay distribution quite well. However, in oversaturated conditions, the overflow queue distribution is not only dependent on the initial condition but also evolves over time. There is no equilibrium state for the overflow queue distribution. In this case, it is difficult to estimate the delay distribution which can represent the real traffic situation. Therefore, a possible alternative way to be investigated is:

- to estimate the overflow queue distribution from traffic measurements (delays), and
- to reconstruct the delay distribution based on the estimated overflow queue distribution.

## 6.2.2 Parameter estimation methods

As can be seen from Equations (6.1) and (6.2), parameters in these two functions include  $\alpha$ ,  $\beta$ , the delay boundaries in the box function  $w_{2n+1}$  and  $w_{2n+2}$  and the overflow queue distribution  $P(n_i)$ . However,  $\alpha$ ,  $w_{2n+1}$  and  $w_{2n+2}$  are also function of the overflow queue  $n_i$ . The question is whether it is possible to recognize the traffic state which in this case is the overflow queue distribution from the travel time (delay) distribution. Two parameter estimation methods, namely Least Squares (LS) and Maximum Likelihood (ML), are applied to perform the parameter estimation. The Least Squares (LS) and Maximum Likelihood (ML) are widely used for parameter estimation (Myung, 2003; Pollard, 2006; Roberts et al., 2003; Sharma et al., 2003). The idea behind maximum likelihood parameter estimation is to determine the parameters that maximize the probability (likelihood) of the sample data. From a statistical point of view, the method of maximum likelihood is considered to be generally more robust and yields estimators with good statistical properties. The least squares method is simpler and can be seen as a Maximum Likelihood method for normal distributed errors. In other words, MLE methods are versatile and apply to most models and to different types of data. In order to estimate the parameters in the delay distribution functions, a maximum overflow queue is assumed before performing the parameter estimation. The overflow queue distribution is estimated based on the measurements, e.g., the measured delays (travel times), flows and cycle time.

### Least Square (LS) estimation

The objective of the least square method is to adjust the parameters of a model function to

best fit a set of data and to characterize the statistical properties of estimates. Here, the model function is the delay probability function  $P(w)$  with parameters  $\alpha$ ,  $\beta$ , overflow queue probability  $p_0, p_1, \dots, p_n$  and the data set is the measured delays with the probability distribution of  $P_m$ . Therefore, the objective function can be formulated as:

$$\begin{aligned} \min f(\alpha, \beta, p_0, p_1, \dots, p_n) &= \sum (P(w) - P_m)^2 \\ &= \sum_{i=1}^m \left( \sum_{j=0}^n (\alpha(j)\delta(w) + \sum_{k=0}^N \beta B(w_i, w_{2k+1}(j), w_{2k+2}(j))) p(j) - P_m \right)^2 \end{aligned} \quad (6.3)$$

St.  $0 \leq \alpha \leq 1, 0 \leq \beta \leq 1$

$$\begin{aligned} \sum_{j=0}^n p_j &= 1 \\ 0 &\leq p_j \leq 1 \end{aligned}$$

where  $m$  is the maximum number of delays and  $w_m$  is the maximum delay;  $j$  is the number of vehicles in the overflow queue and  $n$  is the maximum overflow queue we assume and can be approximated based on the maximum delay;  $k$  is the number of extra red times that an arriving vehicle needs to wait;  $N$  is the maximum number of red times that the arriving vehicle needs to wait for given the overflow queue  $j$ ;  $P_m$  is the measured delay distribution which in this case is obtained from the VISSIM simulation. As mentioned in the previous subsection, the parameter  $\alpha$  is also a function of the overflow queue. Therefore, the parameter in the objective function to be estimated is the overflow queue distribution.

### **Maximum Likelihood (ML) Estimation**

From the Bayesian point of view, the probability of a certain parameter set  $\Phi$  given observed data  $D$  can be formulated as:

$$P(\Phi | D) = \frac{P(D|\Phi)P(\Phi)}{P(D)} \quad (6.4)$$

Where  $P(D|\Phi)$  is the likelihood to observe  $D$ , given the parameter set  $\Phi$ ,  $P(\Phi)$  is the prior distribution of parameter set  $\Phi$  and  $P(D)$  is the probability to observe  $D$  which can be considered as the normalization factor.

In order to maximize the posterior probability distribution  $P(\Phi/D)$ , one effective way is to maximize the likelihood function  $P(D/\Phi)$  in Equation (6.4) given known probability distribution of data set  $P(D)$ .

In our case, the data set consists of measured delays (travel times) and the parameter set is  $\alpha$ ,  $\beta$  and the overflow queue distribution  $p_0, p_1, \dots, p_n$ . For measured delays  $w_1, w_2, \dots, w_m$ , the dependency among these delays is unlikely to be clear to us. Here we assume they are stochastically independent. The likelihood function can be formulated as:

$$\begin{aligned}
& L(\alpha, \beta, p_0, p_1, \dots, p_n | w_1, w_2, \dots, w_m) \\
& = P(w_1, w_2, \dots, w_m | \alpha, \beta, p_0, p_1, \dots, p_n) \\
& = P(w_1 | \alpha, \beta, p_0, p_1, \dots, p_n) P(w_2 | \alpha, \beta, p_0, p_1, \dots, p_n) \dots P(w_m | \alpha, \beta, p_0, p_1, \dots, p_n)
\end{aligned} \tag{6.5}$$

where  $P(w_1, w_2, \dots, w_m | \alpha, \beta, p_0, p_1, \dots, p_n)$  denotes the probability density function of measured delays  $w_1, w_2, \dots, w_m$  given parameters  $\alpha, \beta, p_0, p_1, \dots, p_n$ . For a single delay  $w_i$ , the probability can be calculated by the following function:

$$\begin{aligned}
& P(w_i | \alpha, \beta, p_0, p_1, \dots, p_n) \\
& = \sum_{j=0}^n [\alpha(j) \delta(w_i) + \sum_{k=0}^N \beta B(w_i, w_{2k+1}(j), w_{2k+2}(j))] p_j
\end{aligned} \tag{6.6}$$

If we combine Equation (6.5) with Equation (6.6), the likelihood function can be rewritten as:

$$L(\alpha, \beta, p_0, p_1, \dots, p_n | w_1, w_2, \dots, w_m) = \prod_{i=1}^m \left\{ \sum_{j=0}^n [\alpha(j) \delta(w_i) + \sum_{k=0}^N \beta B(w_i, w_{2k+1}(j), w_{2k+2}(j))] p_j \right\} \tag{6.7}$$

In practice, it is more convenient to work with scaled logarithm of the likelihood function which is calculated as:

$$\ln L = \sum_{i=1}^m \ln \left[ \sum_{j=0}^n [\alpha(j) \delta(w_i) + \sum_{k=0}^N \beta B(w_i, w_{2k+1}(j), w_{2k+2}(j))] p_j \right] \tag{6.8}$$

The objective function for minimization is formulized as:

$$\begin{aligned}
& \min f(\alpha, \beta, p_0, p_1, \dots, p_n) = \min(-\ln L) \\
& = \min \left\{ -\sum_{i=1}^m \ln \left[ \sum_{j=0}^n [\alpha(j) \delta(w_i) + \sum_{k=0}^N \beta B(w_i, w_{2k+1}(j), w_{2k+2}(j))] p_j \right] \right\}
\end{aligned} \tag{6.9}$$

St.  $0 \leq \alpha \leq 1, 0 \leq \beta \leq 1$

$$\sum_{j=0}^n p_j = 1$$

$$0 \leq p_j \leq 1$$

The objective functions of Least Square estimation and Maximum Likelihood estimation are very complicated and highly nonlinear. Finding the optimal solution for the parameter estimation in an analytical way is not applicable. Therefore, the Genetic Algorithm (GA) (Dias et al., 2002; Whitley, 1994; Yao et al., 1994) is applied to find the optimal solutions for both methods. There are several advantages of applying GA method. First, GA can solve every optimization problem which can be described with the chromosome encoding; secondly, GA is able to solve multi-dimensional, non-differential, non-continuous, and even non-parametrical problems; Thirdly, GA is a heuristic method which has the ability to find a solution at least close to the global optimum. When applying GA for parameter

estimation in our case, the fitness functions are formulated based the LS and ML. The parameter that needs to be estimated is the overflow queue probability distribution. Based on the estimated overflow queue distribution, the delay distribution can be reconstructed using Equations ( 6.1 ) and ( 6.2 ).

## 6.3 Experiment setup

### 6.3.1 Scenarios

In order to estimate the parameters in the delay distribution function, a microscopic simulation tool VISSIM was used to generate the ground truth data (e.g., delays or travel times). An urban corridor with two fixed time controlled intersections was modelled in VISSIM. The cycle time for both intersections is 60s and the effective green time is 24s. The link length between two intersections is about 500m. The free flow speed is 60km/h. The total evaluation period is 10 cycles (600s). Two different traffic conditions are considered:

- *Undersaturated condition*: The input flow is 800veh/h and the degree of saturation is about 0.9.
- *Oversaturated condition*: The input flow is 1050veh/h and the degree of saturation is about 1.2. The delay (travel time) measurement point is placed 300m upstream of the intersection such that the maximum overflow queue won't reach the measurement point.

As discussed in chapter 5, there are two types of mismatch (early green and late green) between two consecutive intersections. In our experiment, we mainly focus on Mismatch 1(the case of early green). Nevertheless, the parameter estimation process can be applied to Mismatch 2 as well. Three levels of mismatch were chosen to be investigated:

- *Level 1 (Mismatch=0)*: Two intersections are well coordinated. There is no mismatch between two intersections;
- *Level 2 (Mismatch=5s)*: The mismatch of traffic signals between two intersections is 5 seconds;
- *Level 3 (Mismatch=20s)*: Two intersections are badly coordinated. The mismatch of traffic signals between two intersections is 20 seconds.

### 6.3.2 Simulation runs

For each scenario, the number of simulation runs needs to be determined in order to obtain a sufficiently smooth distribution as the ground truth distribution. For each simulation run, all delays are recorded and the delay distribution can be derived. The required number of simulation runs depends on the variation of average delay among different simulation runs, the required accuracy and the reliability of the results. In order to estimate the variation of the average delay, a fixed 100 simulation runs was chosen in a pilot

experiment with an average demand of 800veh/h ( $x=0.9$ ). The minimum number of simulation runs can be determined by the following equation:

$$n = \left( \frac{t_{1-\alpha/2} \sigma_d}{\varepsilon_d} \right)^2 \quad (6.10)$$

Where  $n$  is the minimum number of simulation runs required;  $t_{1-\alpha/2}$  is the critical value of the  $t$ -distribution with the confidence level of  $1-\alpha$  (in our experiment, 95% confidence level was chosen);  $\sigma_d$  is the standard deviation of delays (We use the standard deviation of sample average delays from pilot simulation runs).  $\varepsilon_d$  is the accepted error (e.g., we chose  $\varepsilon_d = \mu_d * 5\%$ , where  $\mu_d$  is the mean delay derived from the pilot simulation runs).

By applying Equation (6.10), the required minimum number of simulation runs for the undersaturated condition ( $x = 0.9$ ) and the oversaturated condition ( $x = 1.2$ ) are 185 and 130, respectively. In order to get a sufficiently smooth delay distribution, the number of simulation runs was increased to 300.

### 6.3.3 Sampling strategies for ground truth simulation data

The number of simulation runs we applied is very large such that a smooth ground-truth delay distribution can be obtained. However, using all the data (delays) generated in VISSIM for parameter estimation will lead to the problem of time-consuming computations. Therefore, it is necessary to investigate whether parameters can be well estimated using sampled delays (travel times). In this paper, two sampling methods were applied to obtain the sample delays from the total number of delays generated in VISSIM: Random Sampling (RS) and Latin Hypercube Sampling (LHS).

#### *Random sampling (RS)*

In random sampling, each item or element of the population has an equal chance of being chosen at each draw. A sample is random if the method for obtaining the sample meets the criterion of randomness (each element having an equal chance at each draw). The actual composition of the sample itself does not determine whether or not it was a random sample. For instance, travel times recorded by GPS probe vehicles or Bluetooth devices are just random sample measurements since the total number of vehicle travel times is unknown. However, one should keep in mind that the final estimation results can be biased if the sample measurements cannot represent the population distribution.

#### *Latin Hypercube sampling (LHS)*

The LHS is a stratified-random procedure, provides an efficient way of sampling variables from their distributions. The basic idea is that the LHS involves sampling  $N$  values from the prescribed distribution of each of  $k$  variables  $X_1, X_2, \dots, X_k$ . The cumulative distribution for each variable is divided into  $N$  equiprobable intervals. A value is selected randomly from each interval. The  $N$  values obtained for each variable are paired randomly with the other variables. Unlike simple random sampling, this method ensures a full coverage of

the range of each variable by maximally stratifying each marginal distribution (Helton et al., 2002).

The total number of simulated delays is about 50000 in the undersaturated condition ( $x = 0.9$ ) and 30000 in the oversaturated condition ( $x = 1.2$ ). Table 6.1 indicates the sample percentages for parameter estimation in our experiment.

**Table 6.1: Sample percentages for parameter estimation**

<b>Undersaturation (x=0.9), total measurements=50000</b>			
Sample percentage(%)	0.50%	1%	5%
Number of samples	250	500	2500
<b>Oversaturation (x=1.2), total measurements=30000</b>			
Sample percentage(%)	0.50%	1%	5%
Number of samples	150	300	1500

### 6.3.4 Implementation of GA

There are several issues need to be addressed when applying GA for optimization in our case. First of all, the optimization was done in Matlab which has the built-in software package of GA (Mathworks, 2008). Secondly, the performance of the GA depends on a number of factors such as population size, evaluation of fitness function, selection method, crossover method, mutation method, crossover rate and mutation rate. The population size determines the size of the population at each generation. The larger the population size is, the more points that the GA is able to search and therefore the better the results will be. However, a large population size will lead to a long computation time. There is a trade-off between the performance and the computation time. In our case, the population size was chosen as twice as the number of parameters which is equal to the length of overflow queues. The number of overflow queues is expected to be different in the undersaturated condition and oversaturated condition. The population size was set to be smaller in the undersaturated condition than in the oversaturated condition. Selecting the best options to do the GA optimization involves trial and error. It is also not realistic to try all the combinations of these options. Therefore, four options in the GA (in Matlab) which are crossover function (Five functions are available including 'Scattered crossover', 'Single point crossover', 'Two point crossover', 'Intermediate crossover' and 'Heuristic crossover'), mutation function (Three functions are available including 'Gaussian mutation', 'Uniform mutation' and 'Adaptive feasible mutation'), crossover rate and mutation rate were investigated to obtain the best results. The best combination of these options, which are crossover function of 'Heuristic crossover', mutation function of 'Adaptive Feasible mutation', crossover rate of 0.7 and mutation rate of 0.3, was used to perform the parameter estimation.

### 6.3.5 Performance measures

In order to see whether delay distributions can be well estimated based on the optimized parameters, two aspects are investigated:

- *Comparison of estimated delay distributions with the ground-truth distributions generated in VISSIM*

The estimated delay distributions based on different parameter estimation methods (ML and LS), sampling methods (RS and LHS) and different sample percentages are compared with ground-truth distributions. The objective is to analyse how the aforementioned different combinations influence the estimation results.

- *Robustness of estimation results*

The estimation accuracy based on different percentages of sample measurements is compared with the degree of representation of different percentage sample measurements to the total measurements. The objective is to investigate how robust the estimation results are regarding the incomplete information carried by sampled measurements. The Root Mean Square Error (RMSE) is used as the performance indicator.

$$RMSE_{Model} = \sqrt{\frac{1}{n} \sum_{i=1}^n (P_{Model}(i) - P_{True}(i))^2} \quad (6.11)$$

$$RMSE_{Sample} = \sqrt{\frac{1}{n} \sum_{i=1}^n (P_{Sample}(i) - P_{True}(i))^2} \quad (6.12)$$

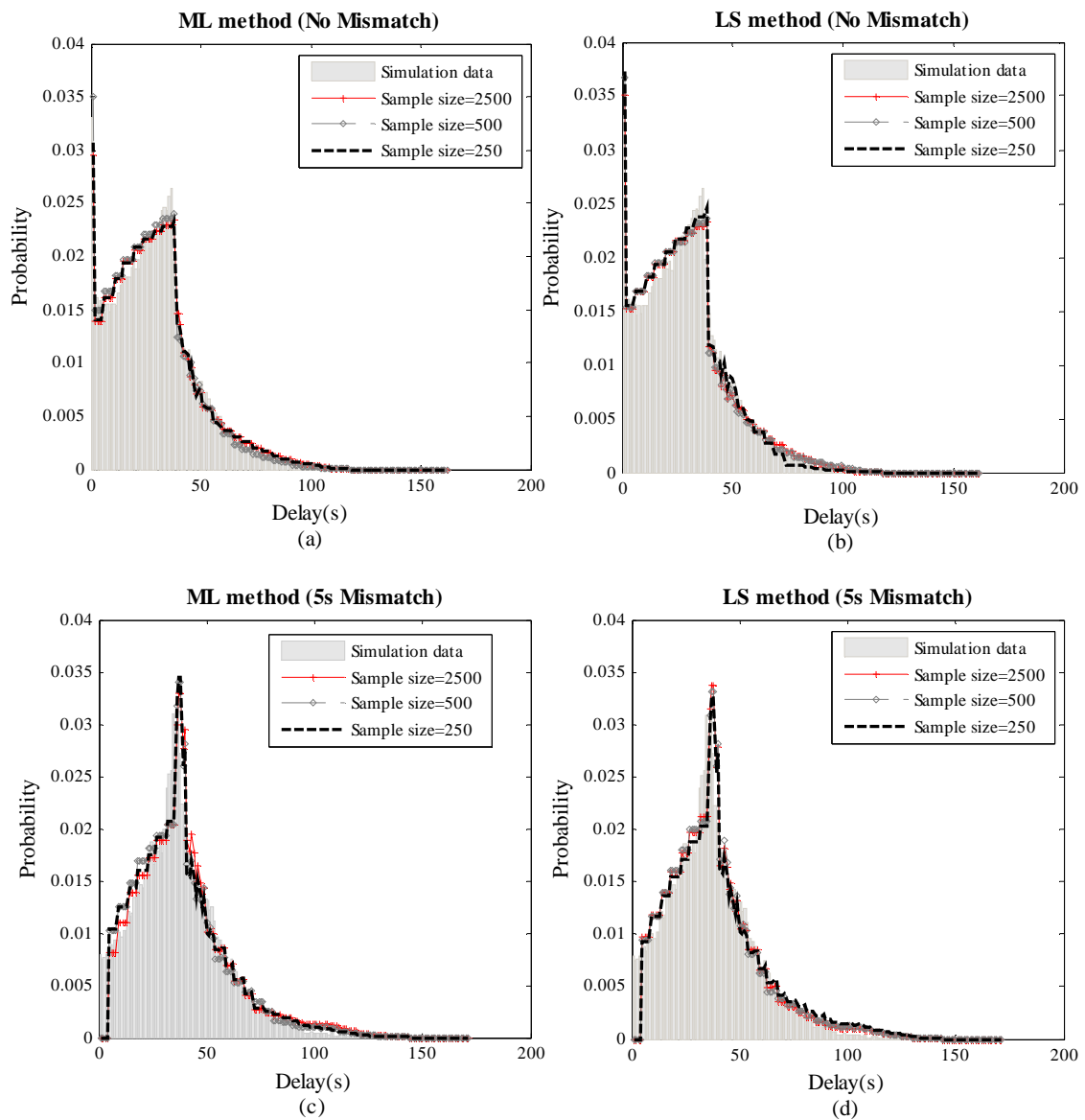
Where,  $RMSE_{Model}$  denotes the  $RMSE$  of the estimated delay distribution based on our proposed model compared with the ground-truth delay distribution;  $RMSE_{Sample}$  denotes the  $RMSE$  of the sample delay distribution compared with the ground-truth delay distribution;  $n$  is the total number of measured delays;  $P_{Model}(i)$  denotes the model-estimated probability of delay in class  $i$ ;  $P_{Sample}(i)$  is the probability of delay in class  $i$  in the sample delay distribution;  $P_{True}(i)$  denotes the probability of delay class  $i$  in the ground-truth delay distribution. For the class size of the delay distribution, 1s has been chosen.

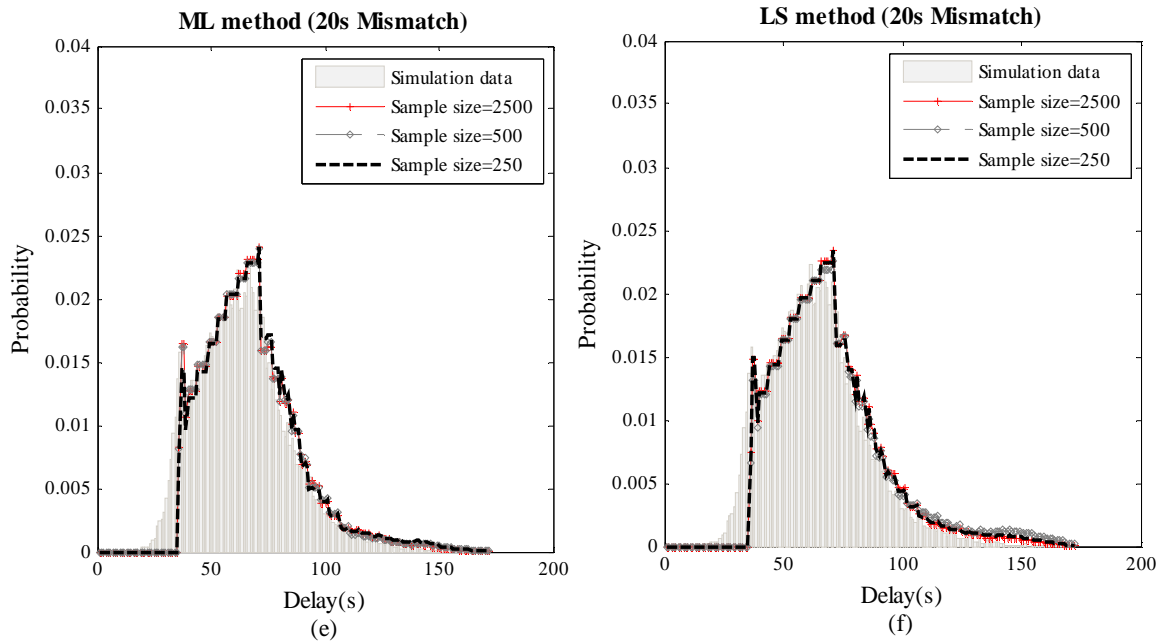
## 6.3.6 Results

### Comparison of delay distributions

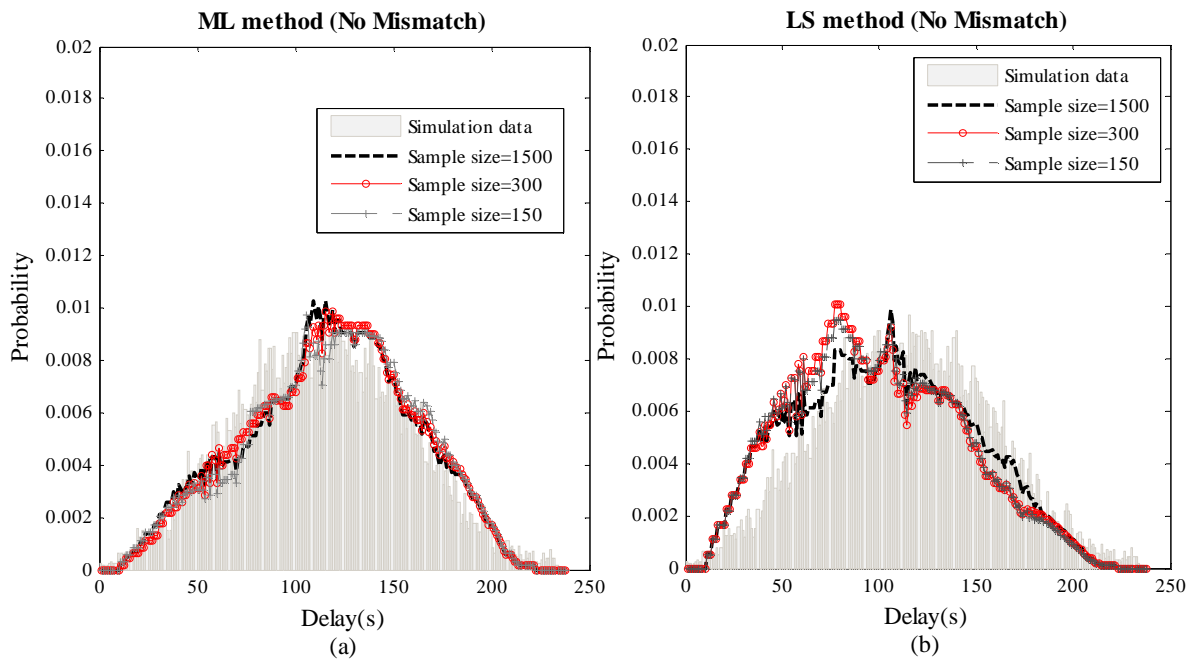
Figure 6.1 illustrates the estimated delay distributions based on the Least-Square (LS) estimation and the Maximum Likelihood (ML) estimation. The Random Sampling (RS) method was applied to obtain sample measurements from the total measurements generated in VISSIM. Figure 6.1 shows estimated delay distributions based on ML method (Figure 6.1 (a), (c), (e)) and LS method (Figure 6.1 (b), (d), (f)) in the undersaturated condition with the degree of saturation of 0.9. As can be seen from Figure 6.1, both the ML method and LS method perform well in the undersaturated condition when two intersections are well coordinated or there is mismatch (5s, 20s). For this case, even with very small sample measurements, e.g., 250 (about 0.5%), the estimated delay distribution can well represent the ground-truth distribution generated from VISSIM. Table 6.2 indicates the performance of these two parameter estimation methods in terms of

RMSE. The ML method performs slightly better than LS method when there is no mismatch. While the LS method performs better when there is mismatch (5s or 20s). Both methods show very small RMSE in the undersaturated condition with different sample sizes. Figure 6.2 illustrates the estimated delay distributions in the oversaturated condition with the degree of saturation of 1.2. As can be clearly seen, the LS method overestimates the low probability values and as a consequence underestimates the higher values. Compared with delay distributions estimated based on LS method, estimated delay distributions based on ML method can better represent the ground-truth even with very small sample measurements of 150 (0.5% ) and 300 (1%), though there is slight discrepancy between estimated distributions and ground-truth distributions. The performance measure of RMSE as indicated in Table 6.2 confirms that the ML method performs better than the LS method in the oversaturated condition.





**Figure 6.1: Comparison of delay distributions derived from simulation data with model estimated delay distributions using ML method (left) and LS method (right) in the undersaturated condition ( $x=0.9$ ) (Sample delays were derived using RS method)**



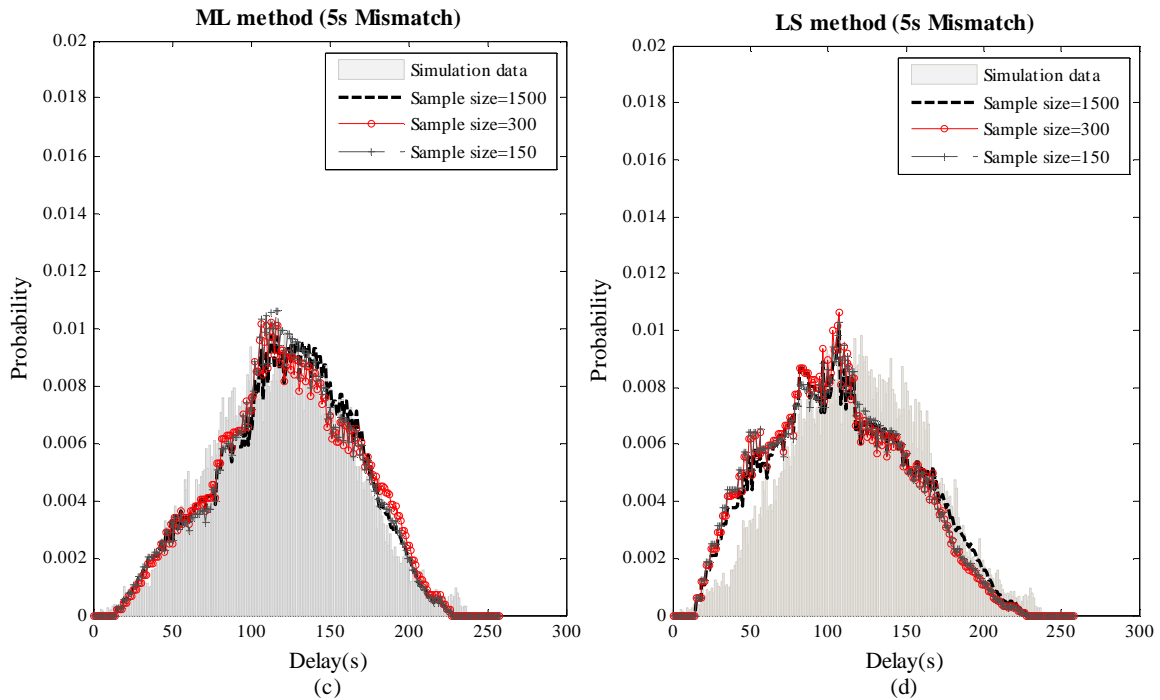


**Figure 6.2:** Comparison of delay distributions derived from simulation data with model estimated delay distributions using ML method (left) and LS method (right) in the oversaturated condition ( $x=1.2$ ) (Sample delays were derived using RS method)

**Table 6.2:** Performance of two parameter estimation methods (ML and LS) in terms of RMSE

ML method(Undersaturation)				RS method(Undersaturation)		
Sample size	No mismatch	mismatch =5s	mismatch =20s	No mismatch	mismatch =5s	mismatch=20s
2500(5%)	0.00096	0.00213	0.00159	0.00102	0.00202	0.00140
500 (1%)	0.00093	0.00215	0.00157	0.00105	0.00204	0.00142
250 (0.5%)	0.00094	0.00211	0.00150	0.00095	0.00204	0.00141
ML method(Oversaturation)				RS method(Oversaturation)		
Sample size	No mismatch	mismatch =5s	mismatch =20s	No mismatch	mismatch =5s	mismatch=20s
1500(5%)	0.00098	0.00084	0.00101	0.00129	0.00124	0.00131
300 (1%)	0.00093	0.00082	0.00081	0.00177	0.00143	0.00212
150 (0.5%)	0.00100	0.00086	0.00087	0.00170	0.00139	0.00161

Figure 6.3 compares the estimated delay distributions based on sample measurements using Latin Hypercube Sampling (LHS) method with those using Random Sampling (RS) method in the oversaturated condition. The grey bars shown in Figure 6.3 (a) and (b) represent the ground-truth distributions when two intersections are well coordinated (no mismatch). As shown in Figure 6.3 (a) and (b), the estimated delay distributions using

both LHS method and RS method are able to represent the ground-truth distributions even with small sample measurements of 300 (1% of total measurements), though a little distortion can be found with RS method when the sample size is very small, e.g., 150 (0.5% of the total measurements). It appears that the estimated delay distributions using the measurements based on LHS method are not significantly better than those based on RS method. The estimation performance in terms of RMSE in Table 6.3 confirms this.

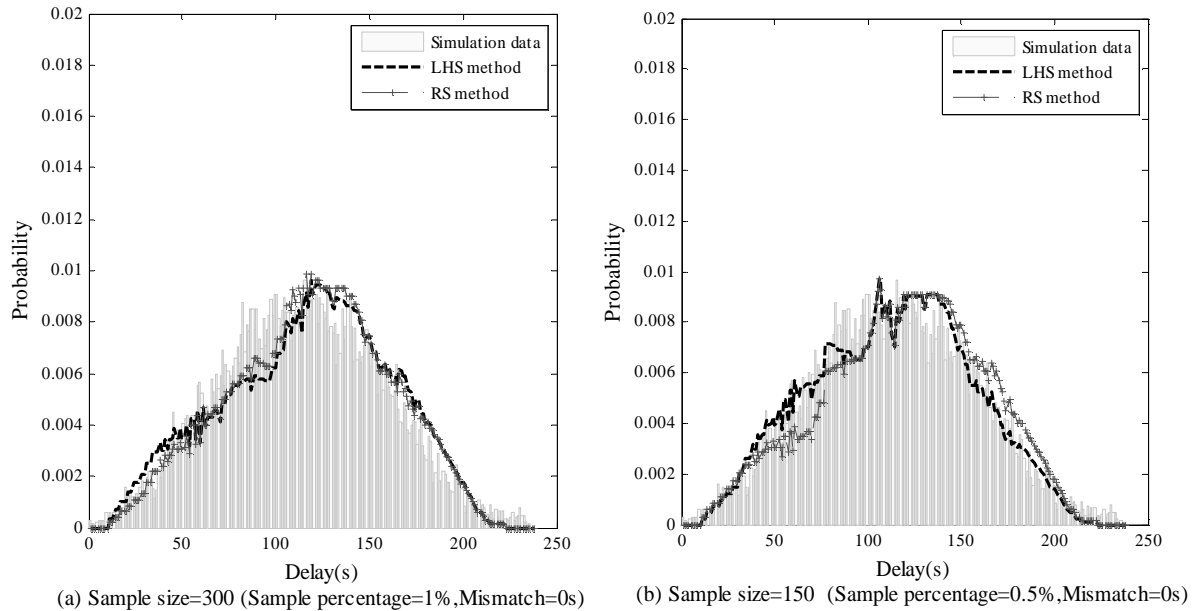


**Figure 6.3: Comparison of delay distributions derived from simulation data with model estimated delay distributions based on LHS and RS in the oversaturated condition (Parameters were estimated using ML method)**

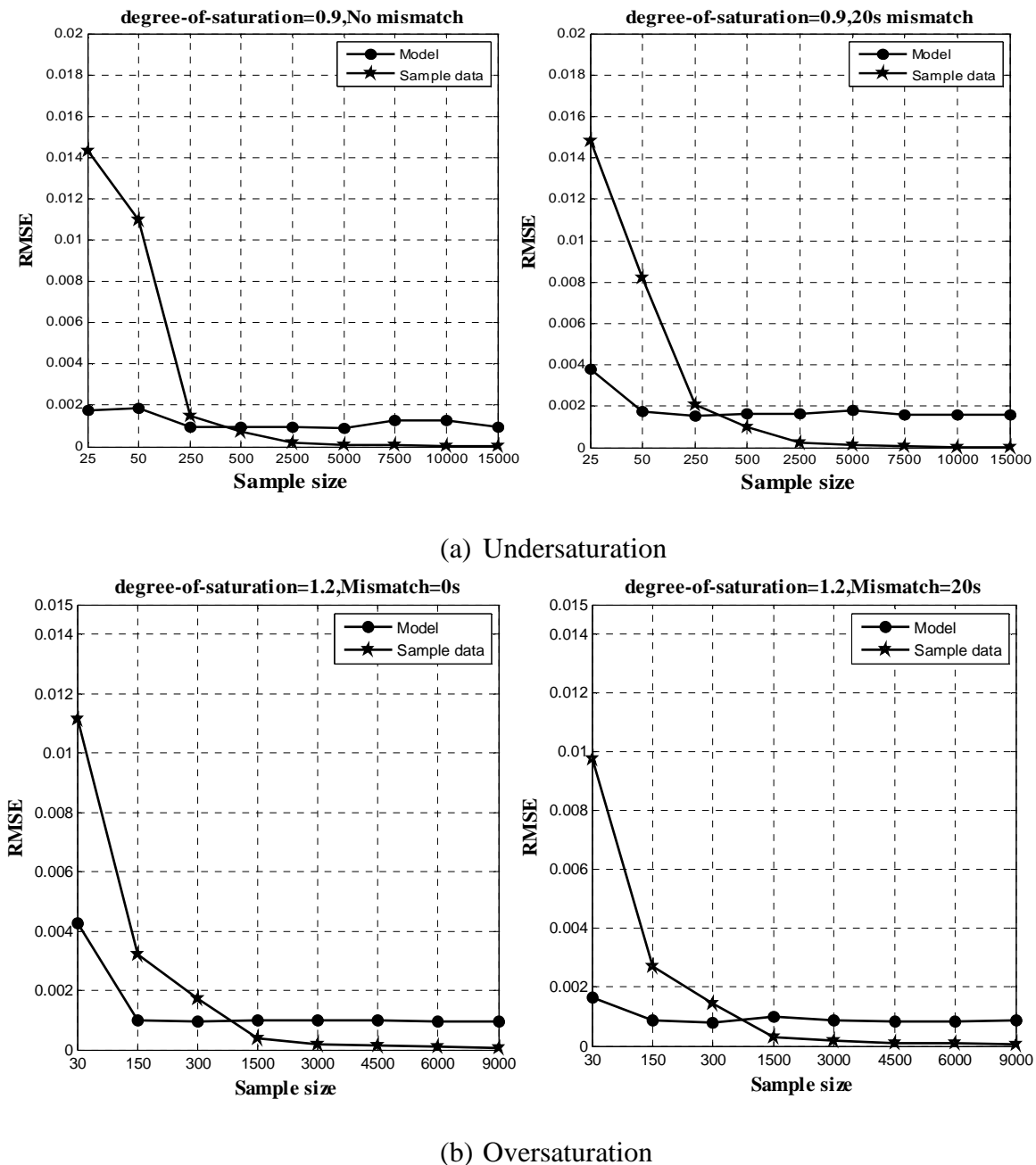
**Table 6.3: Estimation performance of two sampling methods (LHS and RS) in terms of RMSE in the oversaturated condition (Mismatch=0s)**

<i>Sample size</i>	<i>LHS</i>	<i>RS</i>
300 (1%)	0.00103	0.00093
1500(5%)	0.00093	0.00098

### **Robustness of estimation results with different sample percentages**

Figure 6.4 compares the accuracy of the estimated delay distribution in terms of RMSE with that of the random sampled data distribution, which is used for parameter estimation. Different sample sizes were chosen for comparison. The Kolmogorov-Smirnov test shows that all sample delay distributions (from small sample sizes to large sample sizes) we obtained for parameter estimation can statistically represent the ground-truth distribution. From figure 6.4, we can see that the estimation results are quite robust regardless of different sample sizes in both the undersaturated condition (Figure 6.4(a)) and the oversaturated condition (Figure 6.4(b)), as long as the sample size is not too small (e.g., >50 in case of undersaturated condition or >150 in case of oversaturated condition). Even

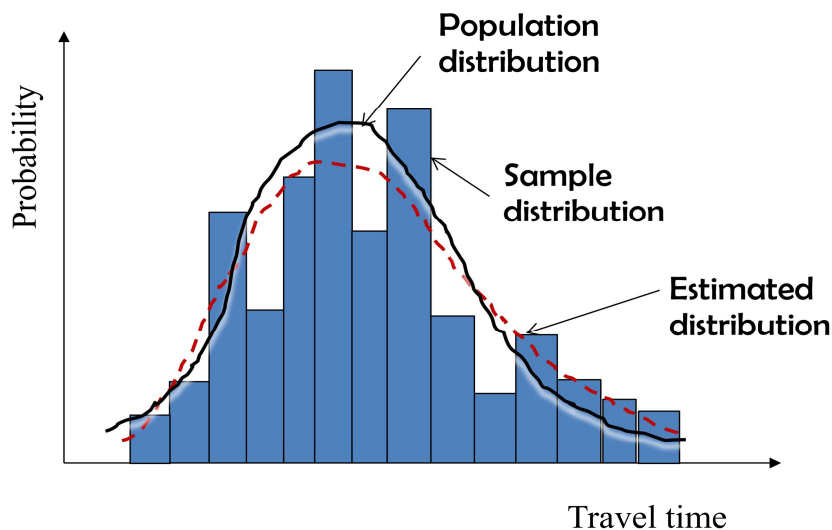
the sample data distribution cannot well represent the ground-truth distribution, e.g., the RMSE of the sample data is very large (see Table 6.4) when the sample size is 25 or 30 (0.05% in the undersaturated condition or 0.1% in the oversaturated condition), the accuracy of estimated delay distribution is still much higher than that of sample data distribution in terms of RMSE. This indicates that the estimation results are quite robust regarding to incomplete information carried by the sample data. The reason for this can be explained by Figure 6.5. The sample distribution is irregular if the sample size is too small. However, the model tries to give a relatively smooth distribution by smoothing the error along the whole range of delays.



**Figure 6.4: Comparison of the accuracy between the estimated delay distributions with sample data distributions in terms of RMSE**

**Table 6.4: RMSE of the sample distribution and the estimated distribution in case of no mismatch**

Undersaturation								
Sample size	25	50	250	500	2500	5000	7500	10000
Sample distribution	<b>0.0143</b>	<b>0.0109</b>	0.0015	0.0007	0.0002	0.0001	0.0001	0.0000
Estimated distribution	0.0018	0.0019	0.0009	0.0009	0.0010	0.0009	0.0013	0.0012
Oversaturation								
Sample size	30	150	300	1500	3000	4500	6000	9000
Sample distribution	<b>0.0111</b>	0.0032	0.0017	0.0004	0.0002	0.0001	0.0001	0.0001
Estimated distribution	0.0043	0.0010	0.0009	0.0010	0.0010	0.0010	0.0009	0.0010

**Figure 6.5: Smoothing effect of the estimated distribution given sample distribution**

## 6.4 Conclusions and discussion

Deriving travel time distributions as discussed in chapter 5 requires proper estimation of parameters in the model, especially the overflow queue distribution. In this chapter, model parameters are estimated based on the traffic measures, e.g., delays (travel times). Two parameter estimation methods, namely ML and LS, are discussed and compared with each other. From the estimation results, the ML method performs much better than the LS method, which is likely to give biased travel time distribution estimation.

In order to see whether model parameters can be estimated based on sample measurements, different sampling methods (LHS and RS) are applied and results show that even with small sample size, e.g., 250 in the undersaturated condition or 150 in the oversaturated condition (0.5%), the travel time distribution can be well reconstructed based on the estimated parameters. The estimation accuracy is not sensitive to different sampling methods.

The investigation of the robustness of parameter estimation indicates that estimation results are quite robust regardless of different sample sizes in both the undersaturated condition and the oversaturated condition, as long as the sample size is not too small and the sample data distribution can statistically represent the true distribution (as indicated in table 6.4 with KS-test). Even the sample data distribution cannot very well represent the ground-truth distribution, for instance, the RMSE of the sample distribution is very large when the sample size is 25 or 30, the accuracy of estimated travel time distribution is still higher than that of sample data distributions. This also indicates that the model can reduce the error due to the small sample size which cannot well represent the ground-truth distribution.

The results obtained in this chapter provide the possibility to calibrate the parameters of the travel time distribution model based on sample observations from field data, for instance, GPS probe vehicle data, camera data or Bluetooth data. Besides, the cycle time (60s) we used in the simulation can be replaced by any other cycle length. The outcomes are independent of cycle time and can be generalized for other signal settings. The next step is to investigate whether travel time distributions can be estimated using observed travel time data.

# Chapter 7

## Application of the model for link travel time distribution prediction

### 7.1 Introduction

The model developed in chapter 4 and 5 provides the possibility to estimate the travel time distribution given traffic flow and traffic control scheme. The results from both the simulation data and the field data show that the travel time distribution can be well estimated for fixed demand within a certain time period. However, in reality, traffic demand varies from period to period within a day. Travel times vehicles experience on an urban road have a certain distribution within a certain time period and this distribution can change from period to period due to different traffic conditions and traffic control schemes. Therefore, it would be useful if it was possible to predict the travel time distribution in such a dynamic and stochastic system. On one hand, the dynamic demand can influence the travel time distribution from time to time. On the other hand, adaptive traffic control schemes can change accordingly due to the time-varying demand, which also has a significant impact on the travel time distribution.

Figure 7.1 shows the relationship of travel time distribution with traffic flow and traffic control. In this chapter, we want to investigate whether the travel time distribution for a certain period can be predicted based on predicted traffic flow and traffic control. Section 7.2 describes the travel time prediction procedure. The cycle time and green split for a certain time period are predicted using a neural network model based on the predicted traffic flow. Thereafter, the travel time distribution is predicted by applying the model we developed in chapter 4 and 5. Sections 7.3 and 7.4 show the model predicted results with VISSIM simulation data and field data, respectively. Finally, section 7.5 summarizes the contribution of this chapter.

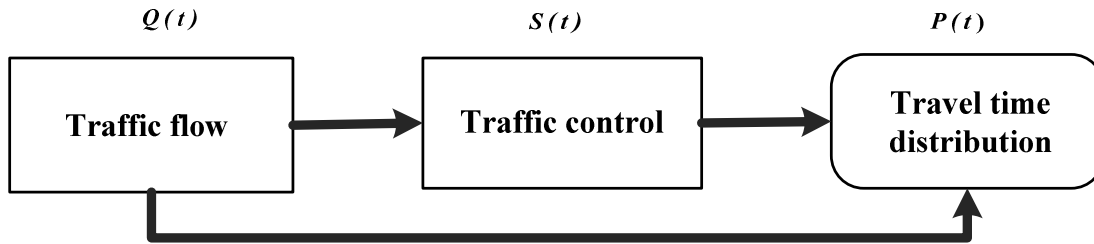


**Figure 7.1: Relationship among travel time distribution, traffic flow and traffic control**

## 7.2 Methodology

### 7.2.1 Traffic flow prediction

Model-based travel time prediction requires the prediction of traffic states in the near (short-term) future. Predicted traffic flows (speeds/densities) are commonly used as the input source of these prediction models. As for the travel time distribution model we developed, traffic demand and traffic control are the pre-requisites. In order to predict the travel time distribution for a short time period, traffic flow needs to be predicted.

In the past decades, different traffic flow prediction models including heuristic method based models (e.g., nonparametric regression, neural network, linear and nonlinear regression, ARIMA) (Cetiner et al., 2010; Kamarianakis et al., 2003; Stathopoulos et al., 2003; Zheng et al., 2006), physical models (e.g., models which are based on traffic process theory) (Ashok et al., 2000) or combination of both types of models (Okutani et al., 1984; Szeto et al., 2009) have been developed. Among all these models, the multivariate models, which can be heuristic method based models or physical models, are capable of capturing the spatial characteristics of the network as well as the temporal revolution of traffic in different location in the network and giving better predictions (Kamarianakis et al., 2003; Stathopoulos et al., 2003). In this chapter, we are not trying to develop a new model to predict traffic flow on the urban road. This is out of the scope of the thesis. We assume that the input flow in our model is the traffic flow predicted by some method such as described above. In the next subsection, a neural network model is proposed to predict the average cycle length and green split for a certain period given predicted traffic flows in case of adaptive control in which traffic demand plays a key role in determining optimal control schemes, e.g., SCATS, SCOOT.

### 7.2.2 Cycle length and green split prediction using a Neural Network model

Different traffic control systems, for instance, fixed-time/pre-timed control, vehicle-actuated control and adaptive control can be applied in an urban network. The fixed /pre-timed control, where the structure and timing of the traffic control process are determined in advance, is the simplest mode of traffic control. For the vehicle-actuated control, the structure and timing of the control program are influenced by the information of individual

vehicles measured by detectors. Compared with the vehicle-actuated control, the adaptive control determines the control process based on the information of the whole traffic situation (e.g., traffic demand). Phase changes based on prediction from traffic measurement at each signalized approach (USDOT, 2005). However, some widely applied dynamic traffic signal control systems, e.g., Scats or Scoot, fall back to nearly fixed time control, for instance, in peak flow situations. The variation of cycle time and green splits is small within a short time period under similar traffic conditions. Therefore, it is feasible to predict the average control scheme (e.g., average cycle time and green split) for a short time period (e.g., 30min) based on the traffic demand in order to apply the travel time distribution model for the purpose of prediction.

A three-layer neural network model is applied to predict the average cycle time and green splits for the SCATS system, which is an adaptive control system. The mathematical formulation of the model is as follows:

**Input layer:**

$$X(t) = \begin{bmatrix} x_1(t) \\ \vdots \\ x_n(t) \end{bmatrix} = \begin{bmatrix} q_1(t) \\ \vdots \\ q_n(t) \end{bmatrix} \quad (7.1)$$

where  $x_i(t)$  denotes the value of the  $i^{th}$  input neuron at time period  $t$ ,  $q_i(t)$  denotes the incoming volume of phase  $i$  at time period  $t$  for intersection  $j$ .  $DS^j(t)$  is the maximum degree of saturation at intersection  $j$ . The reason we chose these parameters as input is that the cycle time is determined by the maximum Degree of Saturation (DS) in SCATS. The green splits are determined by the traffic demand for each phase. One thing we need to mention here is that the traffic demand has nearly linear relationship with the DS. Therefore, the input parameters of traffic flow and DS are interchangeable.

**Hidden layer:**

$$H(t) = \begin{bmatrix} h_1(t) \\ \vdots \\ h_m(t) \end{bmatrix} = \begin{bmatrix} \varphi \left( \sum_{j=1}^n \omega_{j,1}^h q_j(t) + b_1^h \right) \\ \vdots \\ \varphi \left( \sum_{j=1}^n \omega_{j,m}^h q_j(t) + b_m^h \right) \end{bmatrix} \quad (7.2)$$

$\omega_{j,m}^h$  denotes the weight connecting the  $j^{th}$  input neuron and the  $m^{th}$  hidden neuron,  $b_m^h$  denotes a bias with a fixed value for the  $m^{th}$  hidden neuron;  $\varphi$  is the transfer function, for which we chose the hyperbolic tangent function as:

$$\varphi(x) = \tanh(x) \quad (7.3)$$

**Output layer:**

$$Y(t) = \begin{bmatrix} y_1(t) \\ \vdots \\ y_p(t) \end{bmatrix} = \begin{bmatrix} C(t) \\ g_1(t) \\ \vdots \\ g_n(t) \end{bmatrix} = \begin{bmatrix} \Phi \left( \sum_{k=1}^m \omega_{k,1}^o h_k(t) + b_1^o \right) \\ \vdots \\ \Phi \left( \sum_{k=1}^m \omega_{k,p}^o h_k(t) + b_p^o \right) \end{bmatrix} \quad (7.4)$$

where  $y_i(t)$  denotes the value of the  $i^{\text{th}}$  output neuron;  $C(t)$  denotes the predicted cycle time for time period  $t$ ;  $g_i(t)$  denotes the predicted green time of phase  $i$ ;  $\omega_{k,p}^o$  denotes the weight connecting the  $k^{\text{th}}$  hidden neuron and the  $p^{\text{th}}$  output neuron;  $b_p^o$  denotes a bias with a fixed value for the  $p^{\text{th}}$  output neuron;  $\Phi(\cdot)$  is the transfer function and a linear function is commonly used for the output units.

### 7.2.3 Link travel time distribution prediction

The travel time distribution model requires three main inputs: Traffic volume, traffic control information (mainly cycle time and green split) and overflow queue distribution. In the previous sections, traffic volume prediction, cycle time and green split prediction have been discussed. Based on a predicted traffic volume, the existing queue length, and traffic control information, the overflow queue distribution can be predicted by applying the model proposed by Viti (Viti, 2006). Figure 7.2 illustrates the procedure of travel time distribution prediction. Therefore, the predicted travel time distribution  $P_\tau(t)$  can be formulated as:

$$P_\tau(t) = \psi(Q(t), C(t), g(t), P_{n_0}(t)) \quad (7.5)$$

where  $Q(t)$  is the predicted traffic flow at time period  $t$ ;  $C(t)$  and  $g(t)$  are the predicted cycle time and green time during time period  $t$ , respectively;  $P_{n_0}(t)$  is the predicted overflow queue distribution during time period  $t$ ;  $\psi(\cdot)$  is the travel time distribution function developed in chapter 4 and 5.

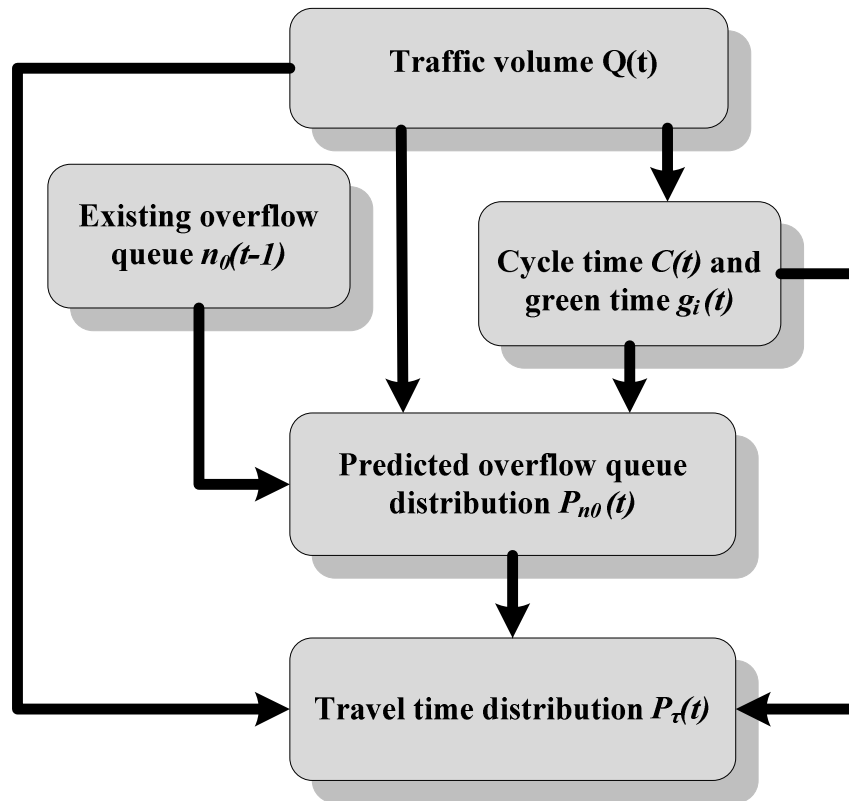


Figure 7.2: Flow chart of travel time distribution prediction

## 7.3 Experiment with VISSIM simulation data

### 7.3.1 Experiment setup

One link with a fixed-time controlled intersection was modelled in VISSIM. The link length is 1000m. The cycle time is 60s with the green time of 24s. No prediction of cycle time and green split is required in this case since the traffic control scheme is fixed. The traffic demand for different periods is indicated in Table 7.1. Traffic was simulated in total 6 periods with each period of 5 cycles (5min) and 15 cycles (15min) for two cases, respectively. The first 5 cycles in the first period is considered as the warm-up period and no simulation data were recorded. The simulation started with low demand (undersaturated condition) and increased to high demand (oversaturated condition) in time period 3. Afterwards, the demand decreased again to undersaturated conditions during periods 4, 5 and 6. Total 500 simulation runs were used and individual travel times were recorded for each simulation run. The prediction was made 5min and 15 min in advance.

**Table 7.1: Traffic demand for total 6 simulation periods (Each period is 5min for case 1 and 15min for case 2)**

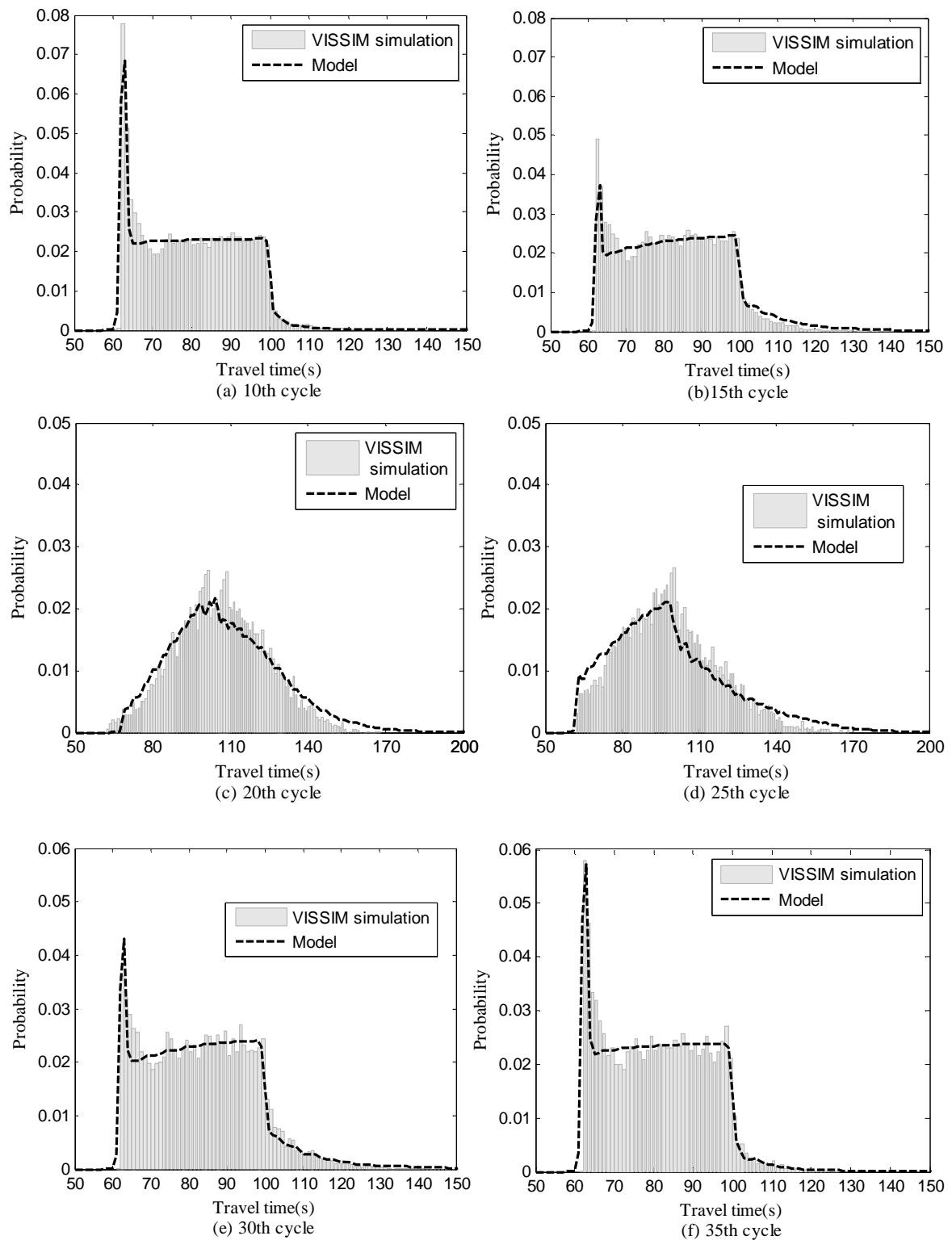
<b>Simulation time period (s)</b>	<i>Case 1</i>	1-600	600-900	900-1200	1200-1500	1500-1800	1800-2100
	<i>Case 2</i>	1-900	900-1800	1800-2700	2700-3600	3600-4500	4500-5400
<b>Traffic demand(veh/h/lane)</b>		650	800	1000	850	750	700

### 7.3.2 Results

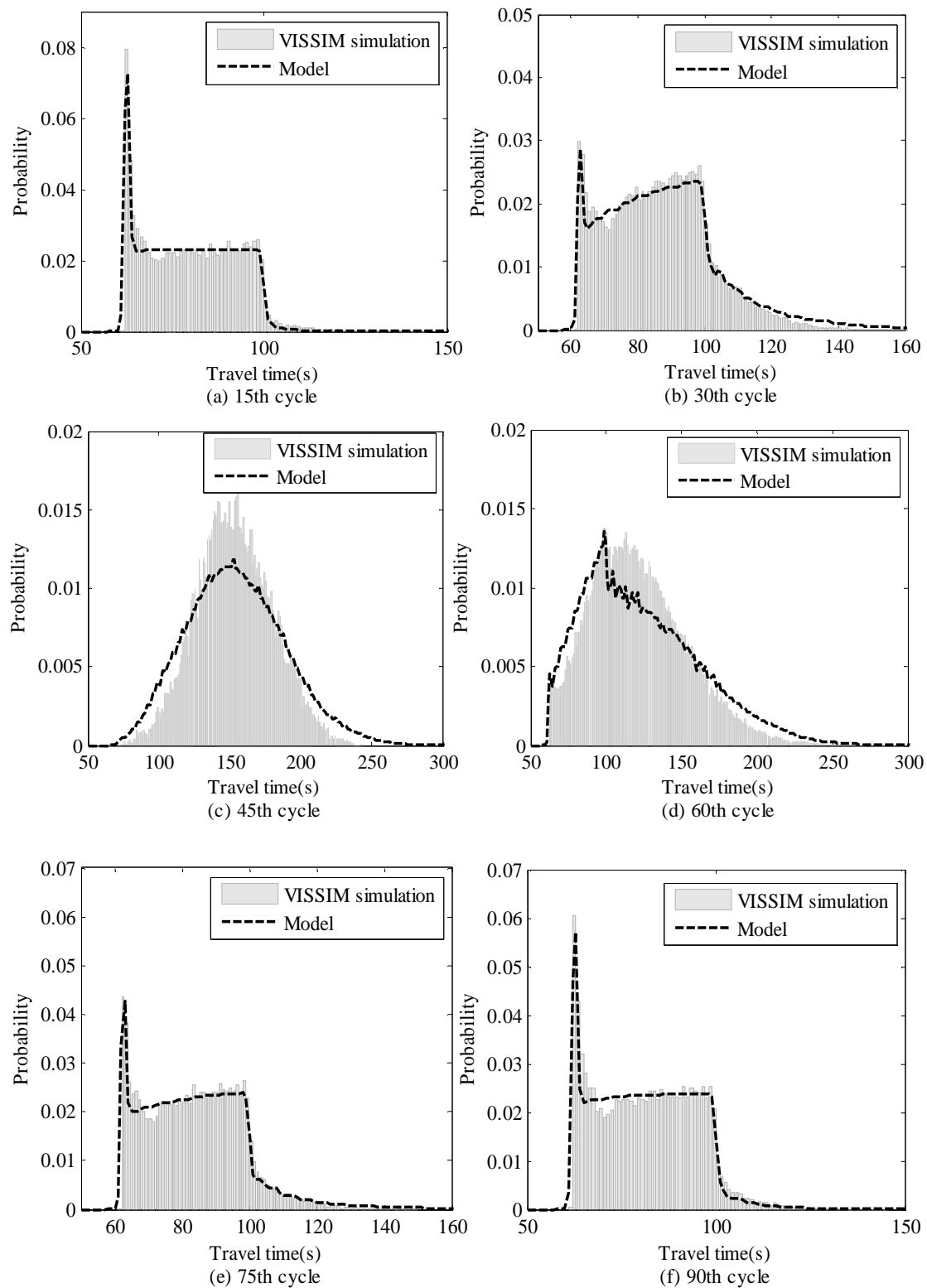
Figure 7.3 shows the link travel time distributions predicted by the proposed model and those obtained from VISSIM simulation for 6 periods with a prediction horizon of 5 min. The travel time distribution changes from period to period due to different traffic demand. Figure 7.3 (a), (b), (e), (f) illustrate that the predicted link travel time distributions can well represent those from the VISSIM simulation in the undersaturated condition during the first two simulation periods and last two simulation periods. When traffic demand increases, the intersection becomes oversaturated. The overflow queue increases from cycle to cycle. The predicted travel time distribution for the oversaturated condition during the last cycle of period 3 is shown in Figure 7.3 (c). It can be seen that the predicted distribution can still represent the true distribution except there are discrepancies in the high travel times and low travel times. When traffic demand decreases in period 4, the shape of travel time distribution is changing from cycle to cycle due to the decreasing overflow queue. The transition from the oversaturated condition to the undersaturated condition can be predicted as shown in Figure 7.3 (d), where the predicted distribution can match the true distribution, though low travel times are slightly more frequently predicted by the model and as a consequence, middle travel times are more frequently observed in the simulation data. From the Kolmogorov-Smirnov test indicated in Table 7.2 with a sample size of 500, the hypothesis that the sample travel time distribution obtained from VISSIM simulation and the predicted travel time distribution draw from the same distribution holds for different time periods.

Figure 7.4 illustrates the comparison of the model predicted travel time distributions with those from VISSIM simulation for a prediction horizon of 15min. In the undersaturated conditions as shown in Figure 7.4 (a) (b) (e) (f), the model can still predict quite accurately even with a longer prediction horizon. However, the predicted distribution for the oversaturated condition shown (Figure 7.4 (c)) overestimates the low values and high values and as a consequence underestimates the middle range delays. The predicted distribution for the transition state (Figure 7.4 (d)) deviates from that of VISSIM simulation significantly, especially for the middle range delays. Nevertheless, the Kolmogorov-Smirnov test (Table 7.2) indicates that the hypothesis can still hold for different prediction periods. The discrepancy between the model-predicted distribution

with that obtained from the VISSIM simulation is probably due to the fact that the overflow queue distribution is more difficult to predict accurately for a longer prediction horizon (e.g., 15min).



**Figure 7.3: Comparison of the model predicted travel time distributions with those recorded in VISSIM (The prediction horizon is 5min)**



**Figure 7.4: Comparison of the model predicted travel time distributions with those recorded in VISSIM (The prediction horizon is 15min)**

**Table 7.2: Komogorov-Smirnov test for a sample size of 500 with different prediction horizons (significance level=0.05)**

<b>Case 1 (Prediction horizon=5min)</b>						
<b>Period</b>	1	2	3	4	5	6
<b>p-value</b>	0.687	0.753	0.422	0.191	0.527	0.334
<b>Hypothesis (H1=H2)</b>	Accepted	Accepted	Accepted	Accepted	Accepted	Accepted
<b>Case 1 (Prediction horizon=15min)</b>						
<b>Period</b>	1	2	3	4	5	6
<b>p-value</b>	0.298	0.796	0.089	0.142	0.664	0.279
<b>Hypothesis (H1=H2)</b>	Accepted	Accepted	Accepted	Accepted	Accepted	Accepted

## 7.4 Experiment with field data

In the previous section, the link travel time distribution can be well predicted given the flow and signal control using simulation data. In this section, model predicted travel time distributions are compared with those from field data. The same route of Shaoshan Road (used in chapter 5) in Changsha city, Hunan province, in China was investigated for this study. Four links (link 13-11, link 11-8 in the northbound direction and link 11-13, link 8-11 in the southbound direction as can be found in Figure 5.5) were selected to perform the travel time distribution prediction. The prediction horizon was chosen to be 30min.

### 7.4.1 Data preparation

#### Travel time data

Travel times were collected by taxis equipped with GPS devices travelling on the Shaoshan Road during the morning peak hour from 8:00AM to 10:00AM on 14<sup>th</sup>, May, 2010. Travel time distributions for both links were obtained every 30min, total 4 periods for each link.

#### Data for cycle time and green splits prediction

The SCATS traffic control system was installed at the intersections on Shaoshan Road. The cycle time and green splits are changing from time to time depending on the traffic demand. Four-phase control has been applied for intersections 13, 11 and 8 which can be found in Appendix E. In the SCATS system, the cycle length is determined by the maximum Degree-of-Saturation (DS). Thus, the maximum DS was also used as the input in the neural network besides the traffic volume. One week data (From 15<sup>th</sup>, May, 2010 to 21<sup>th</sup>, May, 2010) aggregated into 30min interval were used to train the neural network proposed in section 7.2.

### 7.4.2 Cycle time and green splits prediction using SCATS data

Before applying the neural network model proposed in section 7.2.2 for prediction purpose, Bayesian training was applied to train the neural network. Different number of hidden neurons (3, 4, 5, 8, 10) were chosen in order to investigate the sensitivity of the training procedure. When the number of hidden neurons increases, the training error is decreasing. This illustrates that more complex (more neurons) models tend to fit the data better than simple ones. However, the increase of hidden neurons from 5 to 10 just yields marginal improvement in terms of Mean Absolute Percentage Error (MAPE). Therefore, 5 hidden neurons were applied to do the prediction task. Table 7.3 indicates the prediction performance of cycle length and green splits in terms of MAPE for link 13-11 and 11-8.

**Table 7.3: MAPE of cycle length and green splits prediction on link 13-11 and 11-8**

	Link 13-11	Link 11-8
<b>Cycle length</b>	3.23%	3.74%
<b>Green split</b>	3.09%	2.92%

### 7.4.3 Results

Figure 7.5 and 7.6 compare the predicted link travel time distributions with those derived from GPS data on link 13-11(Northbound) and link 11-13, respectively. Total four periods (Each period is 30min) of travel time distribution were investigated. Figures 7.5 and 7.6 (b) (d) (f) (h) on the right side are cumulative distributions. As can be seen from the figures, the predicted distributions can well represent the travel time distributions derived from GPS data. The predicted travel time distributions of link 11-13 in the southbound direction can still represent the GPS travel time distributions, even though the sample size of the GPS travel time measurements is very small for some periods, e.g., 8:30AM-9:00AM, 9:00AM-9:30AM. This can be also confirmed by the Kolmogorov-Smirnov test shown in Table 7.4 and Table 7.5. The performance measures in terms of MAPE for the statistical values of the distribution are indicated in Table 7.6. The MAPEs for these statistical values are quite small. The maximum MAPE of 9.7% can be found with the standard deviation on link 13-11.

Compared with link 13-11 and link 11-13, the predicted travel time distributions for link 11-8 and link 8-11 shown in Figures 7.7 and 7.8 are less accurate. The predicted distributions deviate from the travel time distributions derived from GPS data significantly for some periods, e.g., 9:30-10:00AM of link 11-8, 8:30-9:00AM of link 8-11. The Kolmogorov-Smirnov test of link 11-8 shows the hypothesis that two distributions are the same cannot hold for periods 9:00-9:30AM. As for link 8-11, the hypothesis doesn't hold for periods 8:00-8:30AM and 8:30-9:00AM. However, the MAPEs of links 11-8 and 8-11 indicated in Tables 7.6 and 7.7 are relatively low with the maximum value of 15.8% for

the standard deviation. Nevertheless, it is still difficult to say how general this result is since the GPS sample data are relatively small for all links of interest.

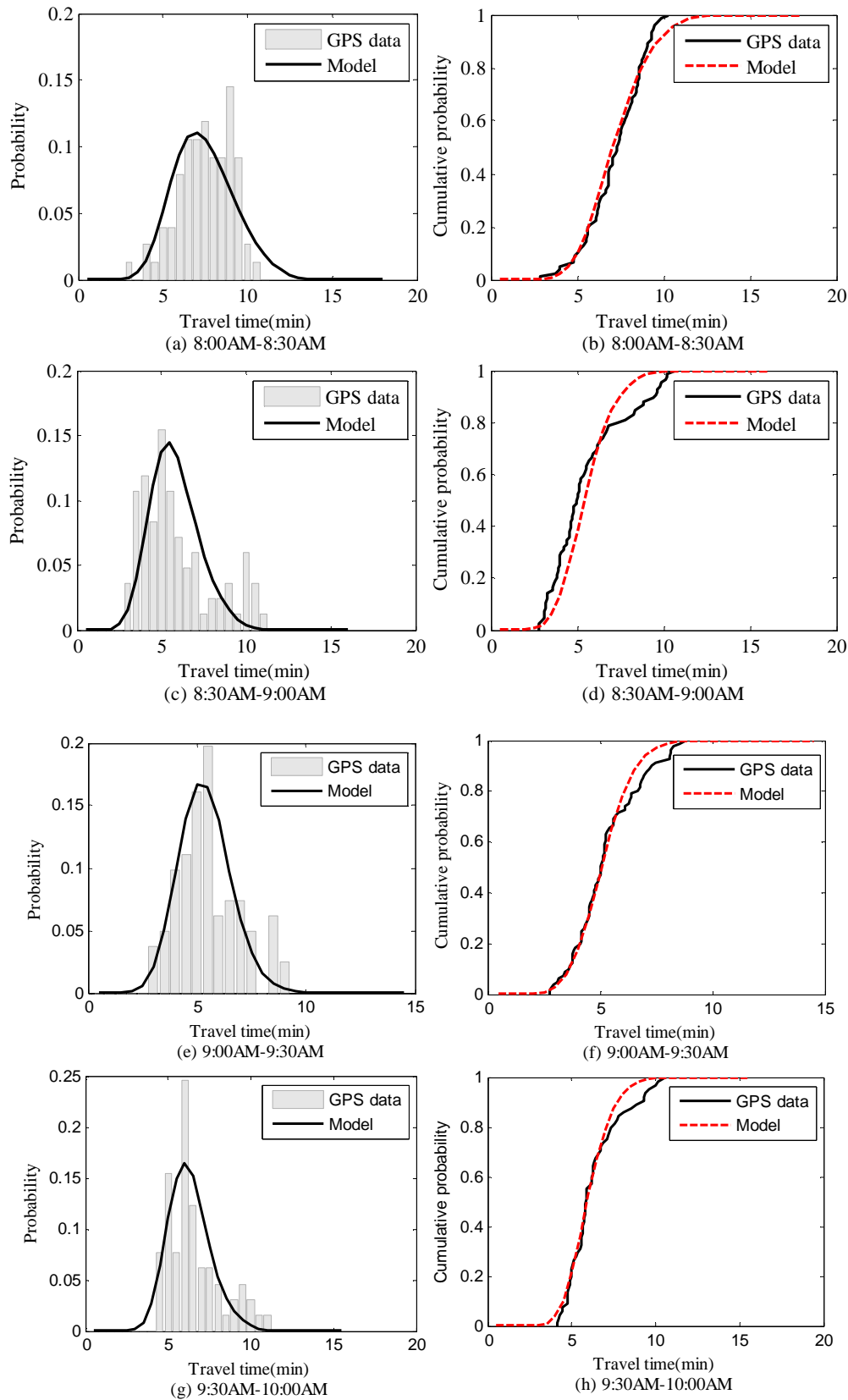


**Figure 7.5: Comparison of the model predicted travel time distributions with those from field GPS data on link 13-11 (Northbound: 8:00AM-10:00AM)**

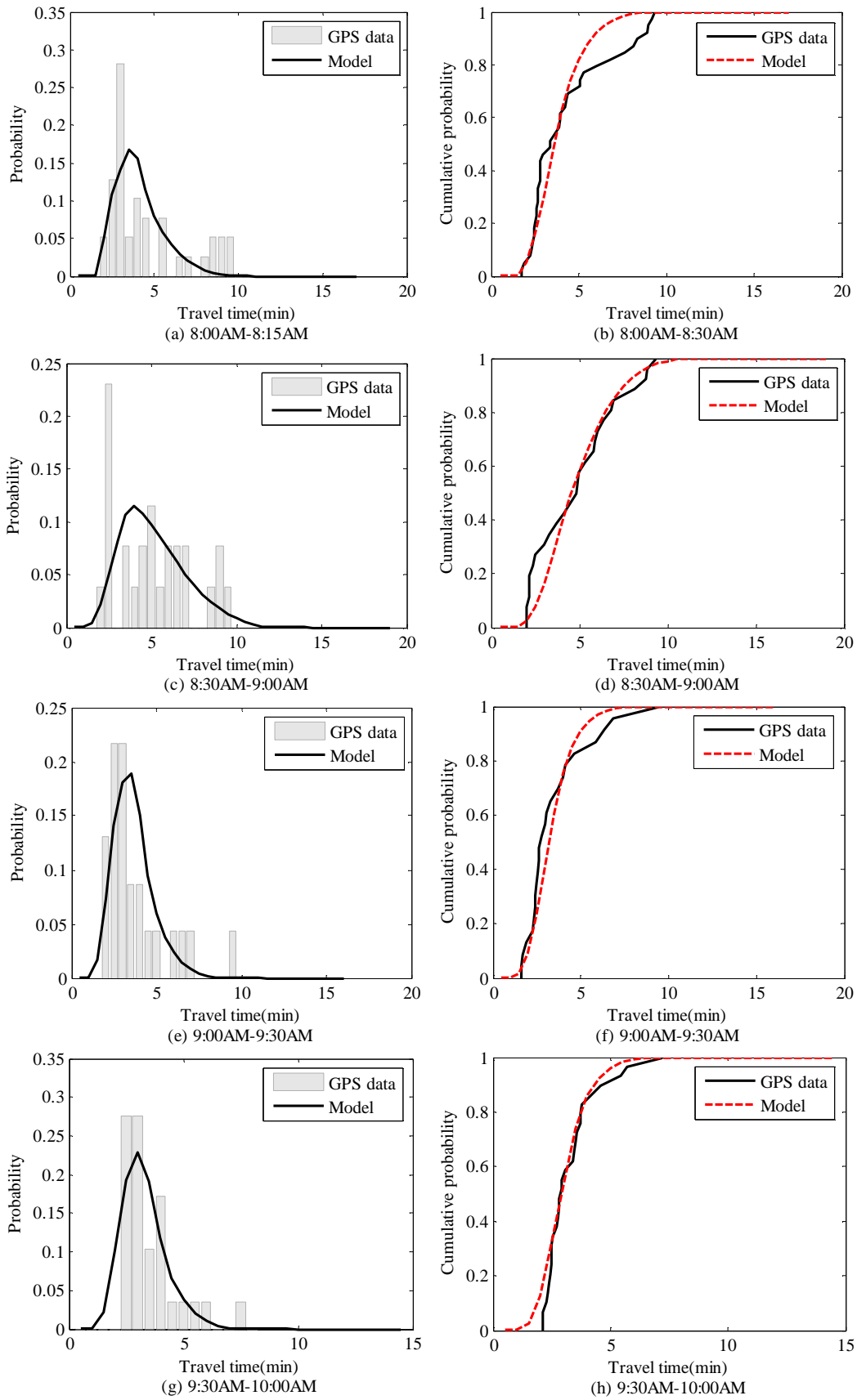


**Figure 7.6: Comparison of the model predicted travel time distributions with those from field GPS data on link 11-13 (Southbound: 8:00AM-10:00AM)**

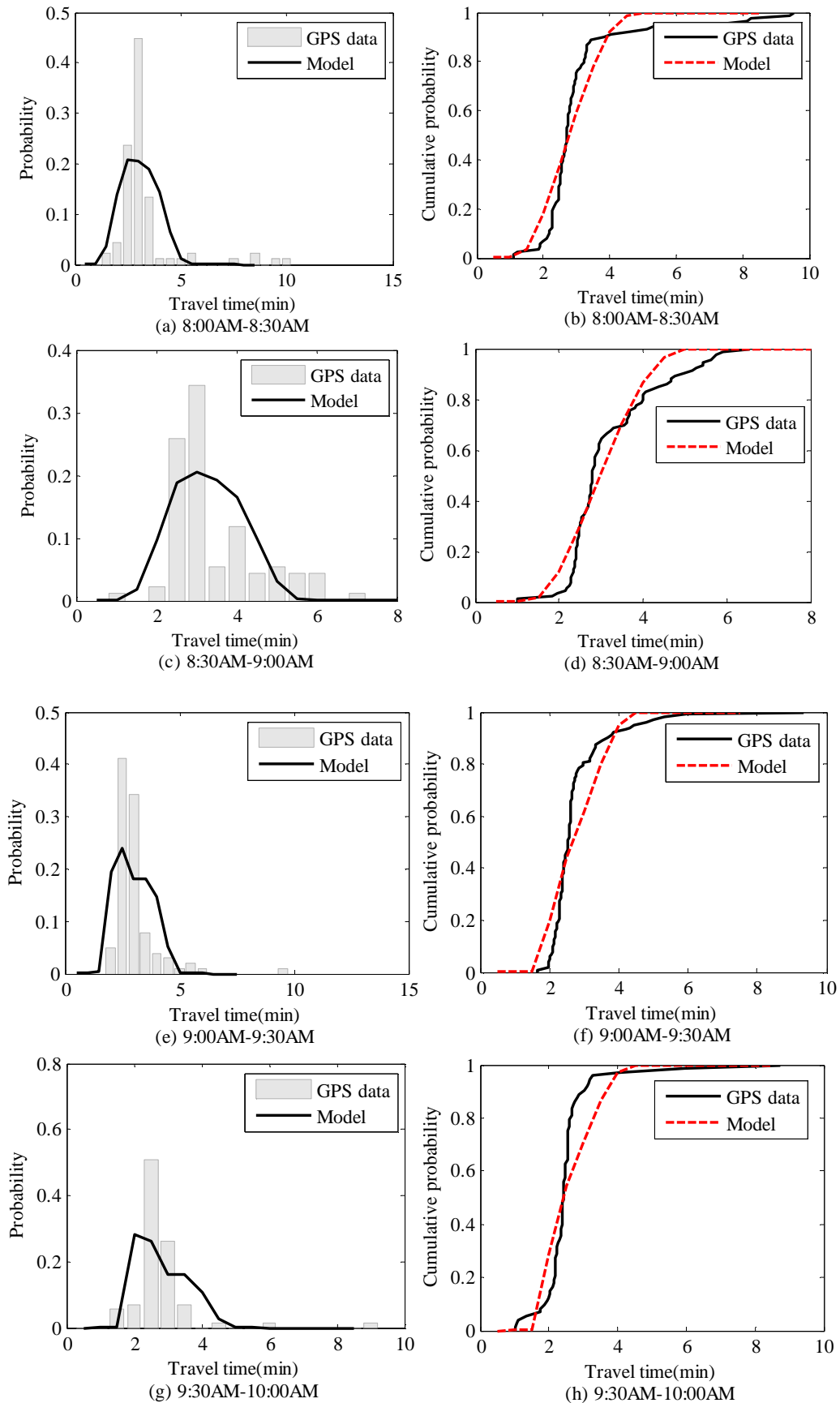


**Figure 7.7: Comparison of the model predicted travel time distributions with those from field GPS data on link 11-8 (Northbound: 8:00AM-10:00AM)**

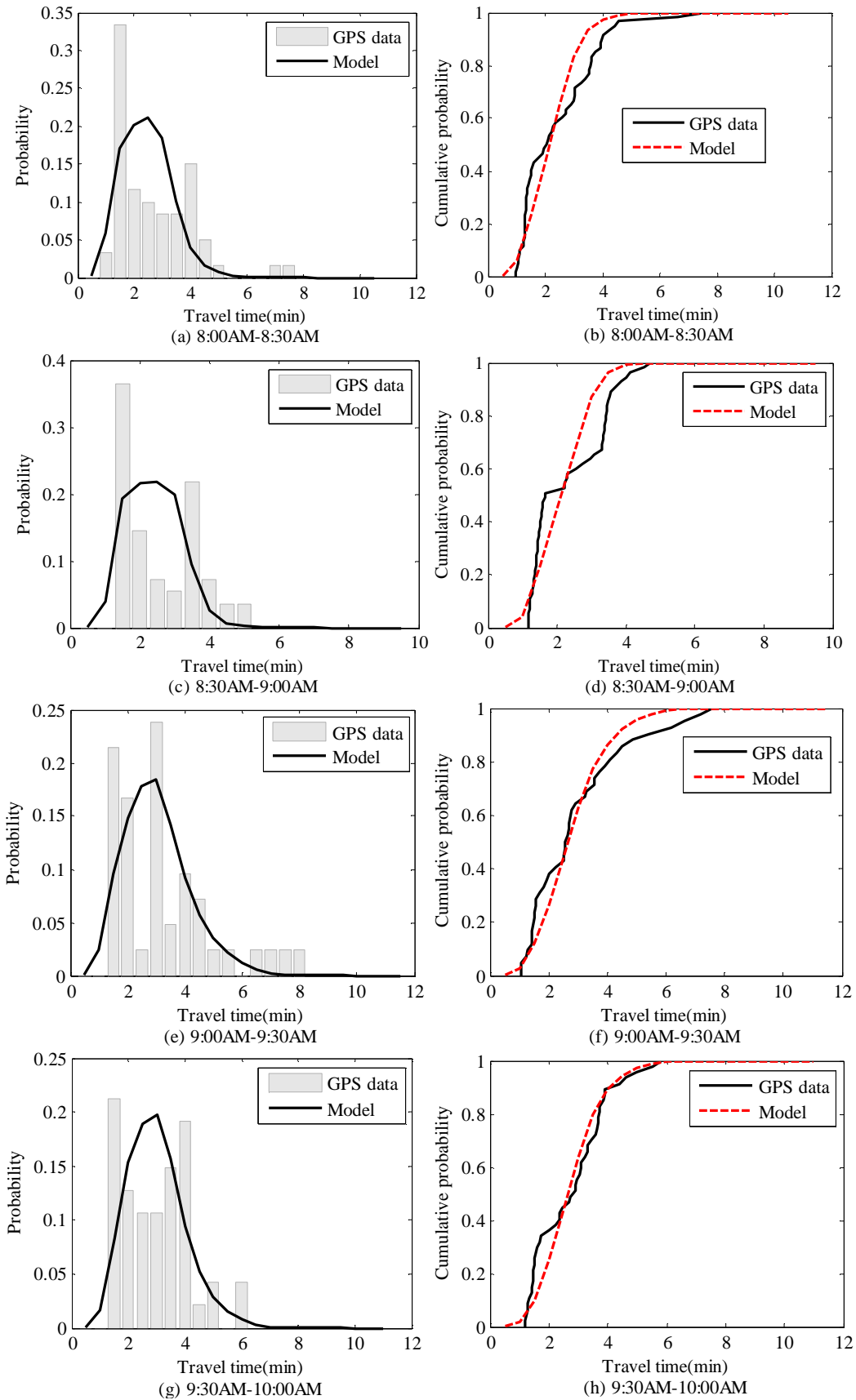


**Figure 7.8: Comparison of the model predicted travel time distributions with those from field GPS data on link 8-11 (Southbound: 8:00AM-10:00AM)**

**Table 7.4: Kolmogorov-Smirnov test of link 13-11 and 11-8 for the Northbound direction (significance level=0.05)**

<b>Link 13-11</b>				
<b>Period</b>	1	2	3	4
<b>p-value</b>	0.388	0.115	0.247	0.481
<b>Number of observations</b>	76	84	81	65
<b>Hypothesis (H1=H2)</b>	Accepted	Accepted	Accepted	Accepted
<b>Link 11-8</b>				
<b>Period</b>	1	2	3	4
<b>p-value</b>	0.058	0.102	0.082	0.001
<b>Number of observations</b>	89	93	98	73
<b>Hypothesis (H1=H2)</b>	Accepted	Accepted	Accepted	Rejected

**Table 7.5: Kolmogorov-Smirnov test of link 11-13 and 8-11 for the Southbound direction (significance level=0.05)**

<b>Link 11-13</b>				
<b>Period</b>	1	2	3	4
<b>p-value</b>	0.213	0.122	0.343	0.288
<b>Number of observations</b>	39	26	23	29
<b>Hypothesis (H1=H2)</b>	Accepted	Accepted	Accepted	Accepted
<b>Link 8-11</b>				
<b>Period</b>	1	2	3	4
<b>p-value</b>	0.009	0.012	0.148	0.113
<b>Number of observations</b>	69	59	65	73
<b>Hypothesis (H1=H2)</b>	Rejected	Rejected	Accepted	Accepted

**Table 7.6: Performance measures in terms of MAPE for 6 periods on link 13-11 and link 11-8 (Northbound)**

<b>Link 13-11</b>					
	<i>Mean</i>	<i>Std.</i>	<i>TT90th</i>	<i>TT50th</i>	<i>TT10th</i>
<b>MAPE(%)</b>	2.1	9.7	6.5	4.2	4.9
<b>Link 11-8</b>					
	<i>Mean</i>	<i>Std.</i>	<i>TT90th</i>	<i>TT50th</i>	<i>TT10th</i>
<b>MAPE(%)</b>	6.0	15.8	7.3	4.5	5.5

**Table 7.7: Performance measures in terms of MAPE for 4 periods on link 11-13 and link 8-11 (Southbound)**

<b>Link 11-13</b>					
	<i>Mean</i>	<i>Std.</i>	<i>TT90th</i>	<i>TT50th</i>	<i>TT10th</i>
<b>MAPE(%)</b>	0.9	8.5	2.7	2.4	3.7
<b>Link 8-11</b>					
	<i>Mean</i>	<i>Std.</i>	<i>TT90th</i>	<i>TT50th</i>	<i>TT10th</i>
<b>MAPE(%)</b>	3.4	6.5	4.4	3.6	2.9

## 7.5 Conclusions and discussion

Urban travel time prediction is an important and challenging topic. Providing predicted travel times, especially the variability (uncertainty) of travel times can help travellers make better route choices. A methodology of urban link travel time distribution prediction is for the first time proposed in this chapter. The traffic control scheme (cycle time and green splits) is predicted using a neural network model. The predicted traffic flow and traffic control scheme are used as model input. By applying the link travel time distribution model proposed in chapter 5, the link travel time distribution is predicted.

The comparison of the model predicted link travel time distribution with that from VISSIM simulation shows that the link travel time distribution predicted by the model can well represent the ground-truth distribution. The comparison with field data indicates that the link travel time distribution can still be predicted reasonably well, e.g., links 13-11 and 11-13. However, the predicted travel time distributions of links 11-8 and 8-11 can represent the observed travel time distributions in 50% of the cases. There is discrepancy between the model predicted travel time distribution and the field travel time distribution. Nevertheless, it is still difficult to say whether the link travel time distribution can be well predicted by the proposed model. First of all, the number of sample travel times collected from the field GPS data is small (<100). This gives an irregular, unsmooth travel time

distribution as can be seen from Figure 7.7 and Figure 7.8. In order to obtain a smooth distribution, more observed travel times are needed. Secondly, travel times collected by the GPS probe vehicles are not complete link travel times. Re-estimating the complete link travel time could also give an error to the field link travel time distribution, though it is not expected to be a significant factor which influences the shape of observed distributions. Thirdly, the length of link 8-11 and 11-8 (700m) is shorter compared with that of link 11-13 and 13-11 (1200m). The influence of the traffic control at the upstream intersection on the arrivals (e.g., filtering and platooning effect) at the downstream intersection is likely more significant for link 8-11 and 11-8. The consequence is that the overflow queue distribution may not be properly estimated, which could lead to the discrepancy between the model estimated distribution and the observed distribution. Finally, vehicles are likely to experience mid-link delay caused by the turning vehicles from side streets which is not considered in the link travel time distribution model. Figure 7.9 shows the speed information collected by GPS taxis on the test corridor. Low speeds due to vehicles turning from the side streets can be clearly observed.

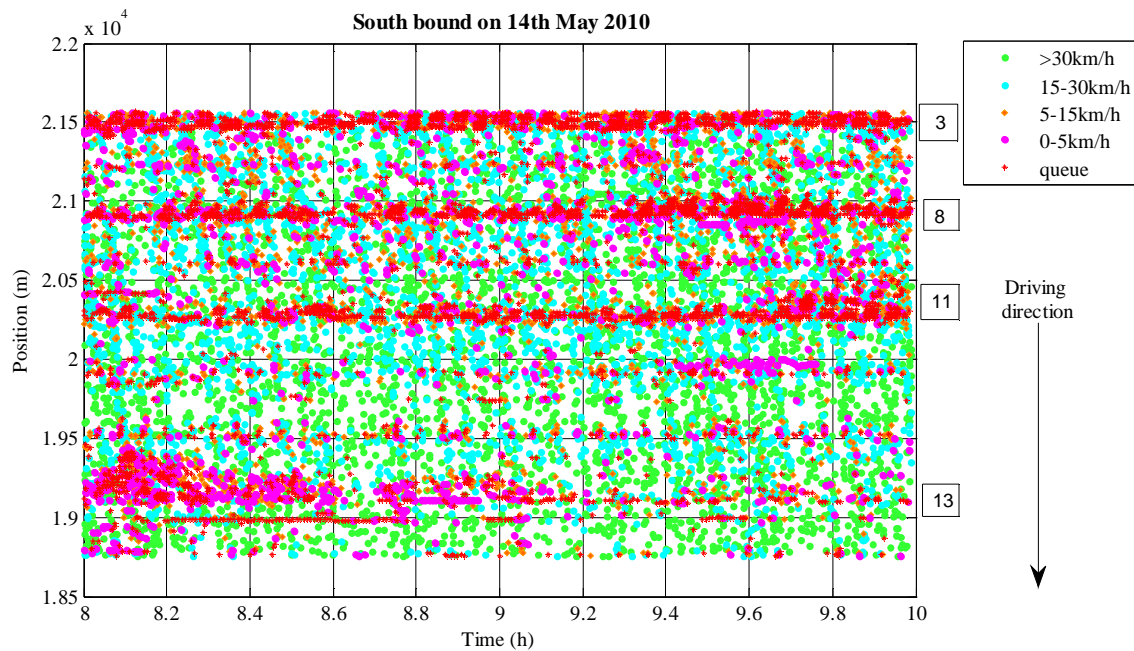


**Figure 7.9: GPS probe vehicle speeds on the test corridor (from south to north: intersections 3->8->11->13)**

Travel time distribution prediction is a difficult subject. The model proposed in this chapter provides the possibility to predict the full link travel time distribution. With the wide application of GPS equipment, GPS probe vehicles become more and more popular to collect traffic data. This gives the opportunity to validate the model with more observed data.



# Chapter 8

## Conclusions and future research

In this thesis, an analytical model has been developed for urban travel time distributions. The model is calibrated and validated using both simulation data and field data. Furthermore, the model has been applied for the travel time distribution prediction. In this chapter, some conclusions which are drawn based on the research carried in this thesis are presented in section 8.1. The applicability of the results for practitioners and some implications for policy makers are indicated in section 8.2 and 8.3, respectively. Finally, section 8.2 gives some recommendations for future research.

### 8.1 Conclusions

Travel time estimation and prediction have been investigated by many researchers as discussed in the literature review in chapter 2. This thesis presents a different way to model urban travel times and travel time variability; more specifically, model the travel time in a probabilistic way instead of the mean travel time. The main contributions of this thesis are the development of an analytical travel time distribution model, calibration and validation of the model and application of the model for the prediction purpose.

#### 8.1.1 Conclusions from the state-of-the-art review

In chapter 2, the current state of practice in modelling urban travel times has been presented. Three aspects of this topic, namely, the urban travel time estimation and prediction, delay estimation at signalized intersections and travel time variability, are studied in the literature review. From the study of current urban travel time estimation and prediction models, it shows that most of these models couldn't perform well and have poor transferability. Most existing approaches, including both model-based and data-driven methods, aim at estimating or predicting the mean travel time. Little or no attention has been paid to the stochastic properties of traffic processes (e.g., stochastic queuing

process at intersections) which often cause uncertainty of the travel time vehicles experience on urban roads. The inability of capturing the uncertainty of the travel time makes these models less suitable to describe the travel time in the urban network.

Delay vehicles experience at intersections is an important component of the travel time on urban roads. The accuracy with which delays can be estimated has a significant influence on the accuracy of final estimated travel times. However, delay models have been developed mainly for the purpose of improving traffic controls at intersections. Therefore, these models try to estimate or predict the mean delay vehicles experience at intersections. As shown in (Viti, 2006), due to the stochastic overflow queues at intersections, delays are uncertain. Given the known average traffic demand and capacity, a wide spread delay distribution can be found. A delay distribution model which can capture the stochastic properties of traffic processes is necessary for estimating or predicting urban travel times.

Travel time reliability (variability) has been widely investigated during the past decades. A number of travel time reliability models and reliability measures have been proposed to describe how reliable travel times are given a certain traffic condition. Different statistical distributions, e.g., normal, log-normal or Weibull distribution, have been applied to model travel time data. However, these distributions hardly have physical meaning. A travel time distribution model which can explain the physical phenomenon of traffic processes is beneficial for the state-of-the-art of modelling urban travel times. This is the main conclusion drawn from the literature review.

### **8.1.2 Empirical analysis of urban travel times**

Travel times are widely accepted as very useful information both for travellers to make route choice or departure time choice and road authorities to improve road network performance. Therefore, different monitoring techniques, for instance, ANPR cameras, probe vehicles, Bluetooth devices, have been developed to measure link/route travel times. In chapter 3, applying these techniques for measuring urban travel times is discussed and some conclusions can be drawn from this chapter:

First of all, ANPR and Bluetooth techniques are quite promising in measuring travel times, especially on freeways. While on urban roads, due to complex road network configurations (e.g., intersections), different traffic processes and travel behaviour, it is difficult to say that these monitoring techniques are qualified for measuring urban travel times. Applying these techniques for measuring urban travel times requires an effective filtering method. In ANPR system in the urban environment, it is difficult to determine whether a vehicle has travelled exactly along the route between A and B without making unexpected stops en-route or choosing alternative routes which have similar or less travel time than the average travel time of this route. A method that can effectively filter these outliers is necessary. As for the Bluetooth system, besides the same problem as discussed before with ANPR, Bluetooth devices transmit signals rather frequently. The Bluetooth-equipped vehicle could be detected at any time within the detection zone and could be

detected several times when it passes a roadside Bluetooth receiver or not be detected at all depending on the driving speed and on the detection range of the Bluetooth device. Furthermore, travel times collected by Bluetooth devices could come from cyclists or pedestrians carrying Bluetooth-enabled devices. How to remove these outliers is critical for applying these techniques in urban settings.

Secondly, probe vehicles equipped with certain positioning devices (e.g., GPS/MEMS integrated system) and with low polling intervals (e.g., 1s, 5s) are able to collect traffic data that are qualified for travel time estimation, even in urban settings. Outliers can be more easily removed from the detailed information. For instance, trajectories can be derived from high-frequency positioning data. Based on the trajectory, it is likely to determine whether a vehicle has travelled exactly the route of interest. On the other hand, a lot of commercial GPS solutions rarely record positions of vehicles with temporal interval smaller than 30s due to the cost of data processing and storage. For instance, taxis equipped with GPS devices are widely used to collect traffic data with polling intervals longer than 30s (e.g., 60s, 300s) in big Chinese cities. As a result, travel times recorded by these mobile sensors are usually not complete link or route travel times. In order to derive complete link/route travel times, methods (e.g., the neural network model as proposed in this thesis) that can accurately estimate the complete link/route travel times are preferable.

Finally, measured travel times provide the ground-truth for developing any travel time estimation or prediction model. They are valuable for building the historical travel time database for the purpose of traffic management and planning. Most importantly, from measured travel times, travel time distribution can be derived which provides more insight into travel time variability and furthermore can be used for travel time prediction purpose.

### **8.1.3 New insight into travel time variability**

On the urban road, the variability (uncertainty) of travel time is largely caused by the variability (uncertainty) of delay vehicles experience at intersections. Delays vehicles experience at a signalized intersection include uniform delays due to traffic control and overflow delays due to high traffic demand. However, delays vary with effects of stochastic properties of traffic flow, stochastic arrivals and departures at the signalized intersection. These stochastic factors are not independent but rather overlap. As a result, delays are uncertain given known traffic condition (traffic flow) and traffic control. Instead, a certain delay distribution can be observed.

The delay distribution model proposed in chapter 4 takes the stochastic properties of traffic processes into account. It allows one to investigate the variability of delay and furthermore variability of travel time on urban roads. The analysis of different arrival processes has revealed that in undersaturated conditions, the delay distribution is not significantly influenced by different arrival processes (e.g., Poisson, binomial). The comparison of delay uncertainty in different traffic conditions shows that the delay is more uncertain in undersaturated conditions than oversaturated conditions. This gives more

insight to travel time estimation and prediction on the urban road. The uncertainty of delay in undersaturated conditions should be particularly taken into account in order to have better estimation or prediction results. This chapter also reveals that the delay distributions for different degrees of saturation are highly overlapping which indicates that a single delay can correspond to different traffic states with certain probabilities and also for a given traffic state, a range of delays can be found.

#### **8.1.4 Urban travel time distribution model**

The investigation of travel time distribution has been done by a lot of researchers in a phenomenological way by calibrating some distribution functions (e.g., log-normal, Gamma) to the observed travel times. However, the character of urban travel times is represented by a specific distribution which can be influenced by different traffic processes (e.g., traffic flow, traffic control). The understanding of fundamental mechanisms of urban travel times can help to better deal with travel time variability, predict travel time variability and furthermore influence travel time variability.

The main contribution of this thesis is the development of an analytical urban link/route travel time distribution model, which distinguishes from the existing models in three aspects. First of all, the proposed model takes into account of traffic demand and supply, stochastic properties of traffic processes on urban signalized roads and traffic control scheme. The physical phenomenon of traffic can be explained by the model. Secondly, the parameters in the model also have physical meanings. For instance, the parameter of the overflow queue distribution can reflect the traffic condition to a certain extent. Furthermore, these parameters can be partially estimated given known traffic demand and supply, traffic control scheme, etc. Finally, this model has transferability and can be applied in different traffic conditions.

The model of travel time distribution for an urban trip with two intersections proposed in chapter 5 assumes that two intersections are fixed-time controlled with a certain offset. Different offset settings (well-coordinated, different levels of mismatch) are investigated under different traffic conditions. Results show that for the case of mismatch 1 – early green -, the shape of the travel time distribution keeps on changing and shifts towards high values when the mismatch level of two intersections increases (from well-coordinated to badly coordinated). This reveals that the way two intersections are coordinated has significant influence on the travel time distribution, especially for undersaturated intersections.

#### **8.1.5 Model calibration**

The application of the proposed model for travel time distribution estimation requires proper calibration (estimation) of parameters. The most important as well as most difficult parameter that needs to be estimated is the overflow queue distribution. The numerical example given in chapter 5 assumes that the arrivals at the intersection and departures from the intersection follow certain distributions (e.g., Poisson distribution, binomial

distribution). The overflow queue distribution is estimated using a Markov chain process model within a certain time period. However, when it comes to the oversaturated condition, the overflow queue distribution has a strong relation with the initial condition and it is rather time dependent and growing over time. Therefore, calibration of these parameters under different traffic conditions is important for the real time application. Chapter 6 applies two parameter estimation methods, namely, Least Squares (LS) and Maximum Likelihood (ML). On one hand, the calibration of model parameters requires a certain amount of traffic data (e.g., travel times, traffic volumes and signal timings). On the other hand, using and fusing all the available data for parameter estimation can be quite computation intensive. Therefore, a sample from the available data is used for parameter estimation.

The estimation results based on simulation data show that both LS method and ML method perform well in the undersaturated condition. While in the oversaturated condition, ML method performs better than LS method, which is likely to give biased travel time distribution estimation. The parameter estimation results based on sample measurements reveal that even with small sample size, parameters can be well estimated both in undersaturated conditions and oversaturated conditions. The travel time distribution can be well reconstructed based on the estimated parameters. The estimation accuracy is not sensitive to different sampling methods (e.g., more stratified or less stratified).

The investigation of the robustness of parameter estimation indicates that estimation results are quite robust regardless of different sample sizes in both the undersaturated condition and the oversaturated condition, as long as the sample size is not too small. Even the sample data distribution cannot very well represent the ground-truth distribution, for instance, the RMSE of the sample distribution is very large, the accuracy of estimated travel time distribution is still higher than that of sample data distributions. This also indicates that the model can reduce the error due to the small sample size which cannot well represent the ground-truth distribution.

### **8.1.6 Model validation**

Chapter 5 provides the validation of the link travel time distribution model and the trip travel time distribution model. Both microscopic simulation and field observations have been used to validate the proposed models.

The comparison of the results from the proposed model with those from the VISSIM simulation model shows that the link travel time distribution based on the proposed model can well represent the one from the simulation model. The comparison with field GPS data indicates that model estimated link travel time distributions are not significantly different from field travel time distributions, though middle range and higher travel times are more frequently observed with GPS data than the model predicts for a certain link.

For the trip travel time distribution model with two fixed time controlled intersections, different situations of signal coordination, for instance, early green and late green as

discussed in chapter 5, were considered. The comparison with VISSIM simulation shows that the trip travel time distributions derived from the analytical model can well represent those from VISSIM simulation except there is small discrepancy in low travel times and high travel times. The discrepancy is probably due to both the variable free flow speed in VISSIM and variable demand (stochastic arrivals) at the upstream intersection.

### 8.1.7 Model prediction

Chapter 7 was dedicated to the prediction method for the urban link travel time distribution by applying the proposed travel time distribution model. Three main inputs are required in the prediction procedure: traffic volume, traffic control and overflow queue distribution. This thesis does not explicitly deal with traffic volume prediction which has been extensively investigated by many researchers as discussed in chapter 7. As for the traffic control scheme, some widely applied dynamic traffic signal control systems, e.g., SCATS or SCOOT, fall back to nearly fixed time control, for instance, in peak flow situations. The variation of cycle time and green splits is small within a short time period under similar traffic conditions. This gives the possibility to predict the traffic control scheme for a short time period. In chapter 7, the average traffic control scheme of SCATS system for a short time period (30 min) is predicted using a neural network model. If the initial queue state is known (e.g., measured by cameras), the overflow queue distribution for the future moment can be predicted using a Markov model.

The comparison of the model predicted link travel time distribution with that from VISSIM simulation shows that with time-varying demand, the link travel time distribution predicted by the model can well represent the ground-truth distribution. The comparison with field GPS data indicate that the link travel time distribution can still be well predicted for certain links. While for other links, the predicted travel time distributions deviate significantly from the field travel time distributions. Nevertheless, it is difficult to say how general this result is. Reasons for this as discussed in chapter 7 are three folds.

- *Lack of sufficient sample observations*: The number of sample travel times collected from the field GPS data is very small (< 90 in 30min). This gives an irregular, unsmooth travel time distribution. In order to obtain a smooth distribution, more observed travel times are needed.
- *Complete link travel time estimation error*: Travel times collected by the GPS probe vehicles are not complete link travel times. Re-estimating the complete link travel time can also give an error to the field link travel time distribution, though it is not expected to be a significant factor which influences the shape of observed distributions.
- *Mid-link delay*: Vehicles turning from the side street could cause extra delay to the through-going vehicles. This is not considered in the link travel time distribution model.

## 8.2 Practical usability of the results

The results presented in this thesis provide several implications for practical applications:

- The travel time distribution models developed in this thesis can be used for travel time assessment. The present navigation systems provide mean travel times for urban routes based on average traffic conditions or only a few probes (e.g., Tomtom does that). The model proposed in this thesis could give an estimation of the whole range of travel times and inform drivers better about routes with high reliability.
- Travel time prediction on urban roads is a difficult subject. The proposed models can be used for urban link/ trip travel time prediction. Chapter 7 already shows the possibility of applying the model for prediction purpose. The full range of link travel times could be predicted for a short time period (e.g., 15min, 30min), though the validation of the prediction procedure using field data is limited by the fact of insufficient field GPS data. More probe vehicles with higher polling frequency (5s or 15s) are necessary in order to validate the prediction method.
- Travel time uncertainty is considered as an important aspect in departure time choice and route choice models. The standard deviation of travel time is usually included in these models to capture the disutility of travel time uncertainty. The effectiveness of using standard deviation lies in the fact that the travel time distribution is normal. However, travel time distributions are rarely normal (more likely skewed) on urban roads. The travel time distribution model developed in this thesis provides the possibility to better incorporate travel time uncertainty into departure time choice and route choice models.

## 8.3 Policy implications

Travel time reliability has been an important subject in the policy agendas in Netherlands. The following implications can be made for practitioners and policy makers:

- The travel time distribution model developed in this thesis provides the possibility to assess travel time reliability in urban areas. The influence of traffic demand, traffic supply, traffic control schemes and stochastic processes on urban travel time reliability can be explicitly considered.
- The fundamental investigation of urban travel time mechanisms provides the possibilities to influence the travel time distribution and as a consequence to influence the travel time reliability from different aspects:
  - Demand: The influence of traffic demand measures (e.g., congestion pricing) on travel time reliability can be quantified.

- Supply: The influence of the change in traffic supply on travel time reliability can be explicitly investigated.
- Traffic control: The traffic control scheme (cycle time, green splits and offsets) can be optimized to provide most reliable link/route.
- Stochastic factors: The stochastic processes at intersections cause the intrinsic uncertainty of travel times on urban roads. These factors should be always considered in urban travel time reliability models.

## 8.4 Recommendations for future research

Based on the conclusions given by the previous section, this final section of the thesis provides the possible directions of future research and some implications of the model application.

### 8.4.1 Recommendations for model development

In chapter 4 and 5, the link travel time distribution model and the trip travel time distribution model were developed. Both models have theoretical background and some assumptions and simplifications were made. Therefore, further research to improve the model can be in the following directions:

- Improvement of the current model from the following aspects:
  - Consider more general signal configuration: The trip travel time distribution model for two intersections assumes that both intersections have the same cycle time and green splits for the convenience of modelling. However, intersections in a string often have different cycle time and green splits. This could be taken into account in future to make the model more generic. Viti (Viti,2006) did something similar for the Markov model for delays in his thesis
  - Consider the overflow queue at the downstream intersection: In the trip travel time distribution model, we only consider the overflow queue distribution at the upstream intersection since we assume both intersections have the same cycle time and green splits. The overflow queue distribution at the downstream intersection could be modelled considering the stochastic departures from the upstream intersection (e.g., time-dependent departure distribution as shown in Viti et al., 2009 and the turning flows coming from the upstream intersection.
- Extension of the travel time distribution model to multiple intersections ( $>2$ ): The trip travel time distribution model only considers two intersections. In reality, more intersections can be included in one trip. The extension of this model to multiple intersections ( $>2$ ) can be beneficial to practical applications.

- Extension of the travel time distribution model to time-dependent control intersections: The model developed in this thesis only considers fixed-time controlled intersections, though the travel time distribution for a certain period can be estimated considering averaged cycle times and green splits as shown in chapters 5 and 7. The overflow queue distribution can be quite different for time-dependent controls as discussed in (Viti, 2006).

### 8.4.2 Recommendations for model calibration and validation

In the thesis, the proposed model is calibrated and validated using both simulation data and field GPS data. Some further improvements are needed in order to apply it in practice.

- Model calibration in different traffic conditions using field data: The main parameter in the delay distribution model is the overflow queue distribution. Chapter 6 shows that it is possible to estimate the overflow queue distribution from traffic measurements. The estimation results from VISSIM simulation data are very promising both in undersaturated conditions and oversaturated conditions. Future research should be devoted to calibrate the model in different traffic conditions using field GPS data.
- The validation of the link travel time distribution model was done both with VISSIM simulation data and field GPS data. Due to the small sample size of GPS data and relatively low polling frequency (30s), the validation results are less convincing. In future, more GPS data with higher polling frequencies (e.g., 1s, 5s) are needed to validate this model. While for the trip travel time distribution model, only VISSIM simulation data were used for the model validation due to the lack of signal coordination information with field data. In future, field data with signal coordination information (e.g., offsets between intersections) are needed to validate the trip travel time distribution model.

### 8.4.3 Recommendations for research direction

Some recommendations for model development, model calibration and validation are given in the previous subsections. Besides, more general research directions can be in the following aspects:

- *Modelling travel time distribution in case of spill back in the network wide*: The probabilistic way of modelling travel times for an urban link can be extended to a network wide taking the spill back into account.
- *Optimization of traffic control*: Traffic control optimization, in a conventional way, is done such that the average delay (travel time) or number of stops can be minimized. The model developed in this thesis can also be incorporated into a traffic control optimization framework considering minimization of both the average delay (travel time) and the variability of delay (travel time).

- *Investigating the influence of traveller compliance and route choice behaviour on the travel time distribution:* The travel time information distributed to travellers has influence on their travel behaviour and as a consequence on the travel time distribution.
- *Travel time distribution model could be imbedded in the macroscopic simulation models.* The travel time distribution model provides the possibility to incorporate uncertainties in macroscopic simulation models.

# Bibliography

- Akcelik, R. (1980). Time-Dependent Expression for Delay, Stop Rate and Queue Length at Traffic Signals. *Australian Road Research Board*, Melbourne.
- Akcelik, R. (1988). The highway capacity manual delay formula for signalized intersections. *ITE Journal*, 58(3):23-27.
- Akcelik, R. and E. Chung (1994). Calibration of the bunched exponential distribution of arrival headways. *Road and Transport Research*, 3(1):42-59.
- Akcelik, R. and N.M. Roupail (1993). Estimation of Delays at Traffic Signals for Variable Demand Conditions. *Transportation Research Part B: Methodological*, 27(2):109-131.
- Asakura, Y. and M. Kashiwadani (1991). Road network reliability caused by daily fluctuation of traffic flow. *Proceedings of the 19th PTRC Summer annual meeting*, Brington, Brington.
- Bajwa, S.U.L., E. Chung and M. Kuwahara (2003). A travel time prediction method based on pattern matching technique. *In proceedings: 21st ARRB and 11th REAAA conference*, Cairns, Australia.
- Bates, J., J.W. Polak, P. Jones and A. Cook (2001). The valuation of reliability for personal travel. *Transportation Research E*, 37:191-229.
- Bertini, R.L., M. Lasky and C.M. Monsere (2005). Validating Predicted Rural Corridor Travel Times from an Automated License Plate Recognition System: Oregon's Frontier Project. *the 8th International IEEE Conference on Intelligent Transportation Systems*, Vienna, Austria.
- Bhaskar, A., E. Chung and A.G. Dumont (2009). Integrating cumulative plots and probe vehicle for travel time estimation on signalized urban network. *9th swiss Transport Research Conference*, Monte Varità.
- Bhaskar, A., E. Chung and A.G. Dumont (2009). Travel time estimation on urban networks with mid-link sources and sinks. *TRB 88th Annual meeting*, Washington D.C.

- Billings, D. and J.S. Yang (2006). Application of the ARIMA Models to Urban Roadway Travel Time Prediction - A Case Study. *IEEE International Conference on Systems, Man, and Cybernetics*, Taipei, Taiwan.
- Bishop, C.M. (1995). Neural network for pattern recognition. *Oxford University Press*, London.
- Brilon, W. and N. Wu (1990). Delays at fix-time traffic signals under time-dependent traffic conditions. *Traffic Engineering and Control*, 31(12):623-631.
- Brilon, W. (2007). Time Dependent Delay at Unsignalized Intersections. *In Proceedings: the 17th International Symposium on Transportation and Traffic Theory* London.
- Cayford, R. and K. Guthrie (2010). Characteristics of Cell Phone Probe Technologies and Field Testing of a Very High Volume Probe System. *89th TRB annual meeting*, Washington D.C., USA.
- Cetiner, B.G., M. Sari and O. Borat (2010). A neural network based traffic-flow prediction model. *Mathematical and Computer Applications*, 15(2):269-278.
- Chang, G.-L. and C.-C. Su (1995). Predicting intersection queue with neural network models. *Transportation Research Part C: Emerging Technologies*, 3(3):175-191.
- Chen, C., A. Skabardonis and P. Varaiya (2003). Travel time reliability as a measure of service *Proceedings of 82nd Transportation Research Board*, Washington D.C.
- Chen, Y., L., Gao, Z., Li and Y., Liu (2007). A new method for urban traffic state estimation based on vehicle tracking algorithm. *IEEE, Intelligent Transportation Systems Conference*, Seattle, WA, USA.
- Chu, L., J.S. Oh and W. RECKER (2005). Adaptive Kalman Filter Based Freeway Travel time Estimation. *84th TRB annual meeting*, Washington D.C., USA.
- Clark, S. (2003). Traffic prediction using multivariate nonparametric regression. *Journal of Transportation Engineering*, 129(2):161-168.
- Daganzo, C.F. (1994). The cell transmission model: A dynamic representation of highway traffic consistent with the hydrodynamic theory *Transportation Research Part B: Methodological*, 28(4):269-287.
- Daganzo, C.F. (1995). The cell transmission model. Part II: Network traffic. *Transportation Research Part B: Methodological*, 29(2):79-93.
- Dale, H.M., S. Porter and I. Wright (1996). Are there Quantifiable benefits from reducing the variability of travel times. *24th European Transport Forum*.
- Davidson, P., J. Hautamaki, J. Collin and J. Takala (2009). Improved Vehicle Positioning in Urban Environment through Integration of GPS and Low-Cost Inertial Sensors. *In Proceedings: ENCGNSS*, Naples, Italy.

- Davis, G., A. Nihan and L. Hamed (1990). Adaptive forecasting of freeway traffic congestion. *Transportation Research Record: Journal of the Transportation Research Board*, 1287:29-33.
- Dharia, A. and H. Adeli (2003). Neural network model for rapid forecasting of freeway link travel time. *Engineering Applications of Artificial Intelligence*, 16(7-8):607-613.
- Dias, A.H.F. and J.A.d. Vasconcelos (2002). Multiobjective Genetic Algorithms Applied to Solve Optimization Problems. *IEEE Transactions on Magnetics*, 38(2):1133-1136.
- Dion, F., H. Rakha and Y.-S. Kang (2004). Comparison of delay estimates at under-saturated and over-saturated pre-timed signalized intersections. *Transportation Research Part B: Methodological*, 38(2):99-122.
- EL FAOUZI, N.-E. and M. MAURIN (2006). Reliability of Travel Time under Log-normal Distribution: Methodological Issues and Path Travel Time Confidence Derivation. *86th TRB Annual Meeting*, Washington D.C., USA.
- Emam, E.B. and H.M. Al-Deek (2006). Using Real-life Dual-Loop Detector Data to Develop New Methodology for Estimating Freeway Travel Time Reliability. *Transportation Research Record: Journal of the Transportation Research Board*, 1959:140-150.
- Friedrich, M., P. Jehlicka and J. Schlaich (2008). Automatic number plate recognition for the observance of travel behaviour. *8th International Conference on Survey Methods in Transport: Harmonisation and Data Comparability*, Annecy, Frankreich.
- Fu, L. and B. Hellinga (2000). Delay Variability at Signalized Intersections. *Transportation Research Record: Journal of the Transportation Research Board*, 1790:215-221.
- Gault, H.E. and I.G. Taylor (1981). The use of the output from vehicle detectors to assess delay in computer-controlled area traffic control systems. *University of Newcastle*, Newcastle, England.
- Godha, S. and M.E. Cannon (2007). GPS/MEMS INS integrated system for navigation in urban areas. *GPS Solut*, 11:193-203.
- Gu, X. and C. Lan (2009). Estimation of Delay and Its Variability at Signalized Intersections. *TRB 88th Annual Meeting*, Washington, D.C., USA.
- Guo, F., H. Rakha and S. Park (2010). A Multi-State Travel Time Reliability Model. *TRB 89th annual meeting*, Washington D.C.
- Hellinga, B., Izadpanah, P., Takada, H., Fu, L.P. (2008). Decomposing travel times measured by probe-based traffic monitoring systems to individual road segments. *Transportation Research Part C*:15.
- Hellinga, B.R. and L. Fu (2002). Reducing bias in probe-based arterial link travel time estimates. *Transportation Research Part C: Emerging Technologies*, 10(4):257-273.

- Helton, J.C. and F.J. Davis (2002). Latin Hypercube Sampling and the Propagation of Uncertainty in Analyses of Complex Systems. *Sandia National Laboratories*,
- Henry Liu and W. Ma (2009). A virtual vehicle probe model for time-dependent travel time estimation on signalized arterials. *Transportation Research Part C*, 17:16.
- Hoeschen, B., D. Bullock and M. Schlappi (2005). A systematic procedure for estimating intersection control delay from large GPS travel time data sets. *In Proceedings: 84th TRB annual meeting*, Washington D.C., USA.
- Hunt, P. B., Robertson, D.I., Bretherton, R. D. and Winton, R. I. (1981). SCOOT-A Traffic Responsive Method of Coordinating Signals. *TRL Laboratory Report 1014*.
- Hurdle, V.F. and S. Bongsoo (2001). Shock wave and cumulative arrival and departure models: partners without conflict. *Transportation Research Record: Journal of the Transportation Research Board*, 1776:159-166.
- Innamaa, S. (2005). Short-term prediction of travel time using neural networks on an interurban highway. *Transportation*, 32:649-669.
- ITE (1995). Canadian Capacity Guide for Signalized Intersections, second ed. *Institute of Transportation Engineers*, District 7, Canada.
- K. Ashok and M.E. Ben-Akiva (2000). Alternative approaches for real-time estimation and prediction of time-dependent origin-destination flows. *Transportation Science*, 34(1):21-36.
- Kamarianakis, Y. and P. Prastacos (2003). Forecasting traffic flow conditions in an urban network: Comparison of multivariate and univariate approaches. *The 82th TRB annual meeting*, Washington D.C., USA.
- Kimber, R.M. and E.M. Hollis (1979). Traffic queues and delays at road junctions. Crowthorne, UK.
- KMJ Consulting, I. (2010). Bluetooth Travel Time Technology Evaluation Using the BlueTOAD.
- Li, Y. and M. McDonald (2002). Link Travel time Estimation using single GPS equipped probe vehicle. *The IEEE 5th international conference on intelligent transportation systems*, Singapore.
- Li, M., Z. Zou and F. Bu (2010). Arterial Travel Time Estimation Using VII Probe Data and Point-based Detection Data. *13th International IEEE Annual Conference on Intelligent Transportation Systems*, Madeira Island, Portugal.
- Lighthill, M.J. and G.B. Whitham, Eds. (1955). On kinematic wave II, a theory of traffic flow on long crowded roads. *Proceedings of the Royal Society of London*.
- Liu, H. (2008). *Travel time prediction for urban networks*. PhD thesis, TRAIL Thesis Series, T2008/12, Delft University of Technology, Delft.

- Liu, H. and M. W. (2009). A virtual vehicle probe model for time-dependent travel time estimation on signalized arterials. *Transportation Research Part C*, 17:11-26.
- Liu, H.X. and W. Ma (2006). Time-dependent Travel Time Estimation Model for Signalized Arterial Network. *86th TRB Annual meeting*, Washington D.C.
- Lo, H.K. (1999). A novel traffic signal control formulation. *Transport Research Part A: Policy and Practice*, 33(6):433-448.
- Lo, H.K. (2001). A cell-based traffic control formulation: strategies and benefits of dynamic timing plans. *Transportation Science*, 35(2):148-164.
- Lo, H.K. and A.H.F. Chow (2004). Control strategies for oversaturated traffic. *Journal of Transportation Engineering*, 130(4):466-478.
- Lomax, T., D. Schrank, S. Tyrners and R. Margiotta (2003). Selecting travel time reliability measures. *Texas Transportation Institute*, Texas, USA.
- Loustau, P., C. Morency and M. Trepanier (2010). Measuring, describing and Modeling travel time reliability. *TRB 89th annual meeting*, Washington D.C.
- Lowrie, P.R. (1982). The Sydney Coordinated Adaptive Traffic System – Principles, Methodology, Algorithms. In *Proceedings: International Conference on Road Traffic Signalling*, London, U.K.
- Mathworks (2008). *Genetic Algorithm and Direct Search Toolbox 2*. <http://www.mathworks.com/>.
- May, A.D. and H.M. Keller (1967). A deterministic queuing model. *Transportation Research* 1(2):117-128.
- Michalopoulos, P.G., G. Stephanopoulos and G. Stephanopoulos (1981). An application of shock wave theory to traffic signal control. *Transportation Research Part B: Methodological*, 15(1):35-51.
- Miller, A.J. (1963). Settings for Fixed-Cycle Traffic Signals. *Operational Research Quarterly*, 14:373-386.
- Modsching, M., R. Kramer and K.t. Hagen (2006). Field trial on GPS Accuracy in a medium size city: The influence of built-up. in *Proceedings of the 3rd workshop on positioning, navigation and communication*, Hannover, Germany.
- Montgomery, F. and A. May (1987). Factors affecting travel times on urban radial routes. *Traffic Engineering and Control*, 28(9):452-458.
- Muller, G., S. Chen and S. Clark (2001). Day-to-Day variability findings. *Seminar on Travel Time Variability*
- Myung, I.J. (2003). Tutorial on maximum likelihood estimation. *Journal of Mathematical Psychology*, 47:90-100.

- N. A. Wahanani, A. Purwaningsih and T. Setiadipura (2009). Latin Hypercube Sampling for uncertainty analysis *Journal of Theoretical and Computational Studies* 8(0408).
- NAM, D.H. and D.R. DREW (1999). Automatic measurement of traffic variables for intelligent transportation systems applications. *Transportation Research Part B: Methodological*, 33:437-457.
- Newell, G.F. (1965). Approximation methods for queues with application to the fixed-cycle traffic light. *SIAM Review*, 7(2):223-240.
- OH, J.S., R. JAYAKRISHNAN and W. RECKER (2003). Section travel time estimation from point detection data. *82nd TRB annual meeting*, Washington D.C., USA.
- Okutani, I. and Y.J. Stephanedes (1984). Dynamic Prediction of Traffic Volume through Kalman Filtering Theory. *Transport Research Part B: Methodological*, 18(1):1-11.
- Olszewski, P.S. (1990). Traffic signal delay model for non-uniform arrivals. *Transportation Research Record: Journal of Transportation Research Board*, 1287:42-53.
- Olszewski, P.S. (1990). Modelling of queue probability distribution at traffic signals. In *Proceedings: the 11th International Symposium on Transportation and Traffic Theory*, Tokyo, Elsevier, New York.
- Olszewski, P.S. (1994). Modeling probability distribution of delay at signalized intersections. *Journal of Advanced Transportation* 28(3):253-274.
- Park, D., L.R. Rilett and G. Han (1999). Spectral basis neural networks for real-time travel time forecasting. *Journal of Transportation Engineering*, 125:515-523.
- Pollard, D. (2006). Nonlinear least-squares estimation. *Journal of Multivariate Analysis*, 97(2):548-562.
- Ranganathan, A. (2004). *The Kevenberg-MARquardt Algorithm*.  
<http://www.sze.hu/~botzheim/LM/The%20Levenberg-Marquardt%20Algorithm.pdf>.
- Richards, P.J. (1956). Shockwaves on the highway. *Operations Research*, 4:42-51.
- Roberts, W.J.J. and F. Sadaoki (2003). Maximum Likelihood Estimation of K-Distribution Parameters via the Expectation-Maximization Algorithm. *IEEE Transactions on Signal Processing*, 48(12):3303-3306.
- Robinson, S. and J.W. Polak (2007). Characterizing the components of urban travel time variability using the k-NN method. *86th TRB Annual meeting*, Washington D.C.
- Robinson, S., Polak, J.W. (2005). Modelling Urban Link Travel Time with Inductive Loop Detector Data by Using the k-NN Method. *Transportation Research Record*, 1935:10.
- SCATS (2006). SCATS Traffic Reporter 6.4.2 user manual. Australia.

- Schrank, D. and T. Lomax (2009). Urban Mobility Report. *Texas Transportation Institute, The Texas A&M University System*, Texas.
- Sharma, M. and R. Agarwal (2003). Maximum likelihood method for parameter estimation in non-linear models with below detection data. *Environmental and Ecological Statistics*, 10:445-454.
- Shlayan, N., L. Ratliff, O. Ayubi and P. Kachroo (2009). Travel time reliability analysis using dynamic message sign recordings. In *Proceedings: 88th TRB annual meeting*, Washington D.C., USA.
- Sisiopiku, V., N. Rouphail and A. Santiago (1994). Analysis of correlation between arterial travel time and detector data from simulation and field studies. *Transportation Research Record: Journal of the Transportation Research Board*, 1457:166-173.
- Skabardonis, A. and N. Geroliminis (2005). Real-time of travel times along signalized arterials. *Proceedings 16th International Symposium on Transportation and Traffic Theory*, University of Maryland, College Park, MD.
- Skabardonis, A. and N. Geroliminis (2008). Real-Time Monitoring and Control on Signalized Arterials. *Journal of Intelligent Transportation Systems: Technology, Planning, and Operations*, 12(2):64 - 74.
- Stathopoulos, A. and M.G. Karlaftis (2003). A multivariate state space approach for urban traffic flow modeling and prediction. *Transport Research Part C: Emerging Technologies*, 11(2):121 -135
- Szeto, W.Y., B. Ghosh, B. Basu and M. O'Mahony (2009). Multivariate Traffic Forecasting Technique Using Cell Transmission Model and SARIMA model. *Journal of Transportation Engineering*, 135(9):658-667.
- Takaba, S., T. Morita, T. Hada, T. Usami and M. Yamaguchi (1991). Estimation and measurement of travel time by vehicle detectors and license plate readers. *Vehicle Navigation and Information Systems*:257-267.
- Takayuki, N. and T. Jun-ichi (2004). Mining Traffic Data from Probe-Car System for Travel time Prediction. *Industry/Government Track Poster*. Washington D.C.
- Tampere, C.M.J. and L.H. Immers (2007). An Extended Kalman Filter Application for Traffic State Estimation Using CTM with Implicit Mode Switching and Dynamic Parameters. In *Proceedings: IEEE conference on Intelligent Transportation Systems*, Seattle, WA, USA.
- Tilahun, N.Y. and D.M. Levinson (2010). A moment of time: reliability in route choice using stated preference. *Journal of Intelligent Transportation Systems*, 14(3):179-187.
- TRB (1997). Highway Capacity Manual 2000. *Transportation Research Board, National Research Council*, Washington D.C.

- TSENG, P.Y., F.-B. LIN and S.L. SHIEH (2005). Estimation of free flow speeds for multilane rural and suburban highways *Journal of the Eastern Asia Society for Transportation Studies*, 6:1484 - 1495.
- Tu, H., J.W.C. van Lint and H.J. van Zuylen (2007). The impact of traffic flow on travel time variability of freeway corridors. *Proceedings of the 86th Transportation Research Board Annual Meeting*, Washington D.C.
- Tu, H., J.W.C. van Lint and H.J. van Zuylen (2008). Travel time reliability modelling on freeways. *Proceedings of the 87th Transportation Research Board Annual Meeting*, Washington D.C.
- Turner, S. and D. Holdener (1995). Probe Vehicle Sample Sizes for Real-Time Information: The Houston Experience. *Proceedings of the Vehicle Navigation & Information Systems Conference*.
- USDOT (2005). Traffic control systems handbook. *Federal Highway Administration*, Washington D.C.
- van Geenhuizen, M.S., H.J. van Zuylen and P. Nijkamp (1998). Limits to predictability.
- van Hinsbergen, C.P.I., A. Hegyi, J.W.C. van Lint and H.J. van Zuylen (2009). Application of Bayesian Trained Neural Networks to Predict Stochastic Travel Times in Urban Networks. *16th ITS World Congress and Exhibition on Intelligent Transport Systems and Services*, Stockholm, Sweden.
- van Hinsbergen, C.P.I. and J.W.C. van Lint (2008). Bayesian combination of travel time prediction models. *Transportation Research Record: Journal of the Transportation Research Board*, 2105:118-126.
- van Hinsbergen, C.P.I., J.W.C. van Lint and H.J. van Zuylen (2009). Bayesian training and committees of State Space Neural Networks for online travel time prediction. *In Proceedings: 88th annual meeting of the Transportation Research Board*, Washington D.C.
- van Zuylen, H.J. and F. Viti (2003). Uncertainty and the Dynamics of Queues at Signalized Intersections. *In Proceedings: CTS-IFAC conference*, Tokyo, Elsevier.
- van Lint, J.W.C. (2004). *Reliable Travel Time Prediction for Freeways*. PhD thesis, TRAIL Thesis Series, T2004/3, Delft University of Technology, Delft.
- van Lint, J.W.C. and v.Z. H.J. (2005). Monitoring and predicting freeway travel time reliability. *Transportation Research Record: Journal of the Transportation Research Board*, 1917:54-62.
- van Lint, J.W.C., S.P. Hoogendoorn and H.J. van Zuylen (2005). Accurate freeway travel time prediction with State-Space Neural Networks under missing data. *Transportation Research Part C*, 13(5-6):347-369.

- van Lint, J.W.C., H.J. van Zuylen and H. Tu (2008). Travel time unreliability on freeways: Why measures based on variance tell only half the story. *Transportation Research Part A: Policy and Practice*, 42(1):258-277.
- van Zuylen, H.J. (2006). A stochastic approach to delays at intersections. *11th meeting of the Euro Working Group on Transportation*, Bari, Italy.
- van Zuylen, H.J. and S.P. Hoogendoorn (2007). A Probabilistic calculation of queue lengths at signalized intersections. *ITS world congress*, Beijing.
- van Zuylen, H.J. and F. Viti. (2007). A Probabilistic Model for Queues, Delays and Waiting Time at Controlled intersections. *TRB 86th Annual Meeting*, Washington D.C., USA.
- Vanajakshi, L.D., B.M. Williams and L.R. Rilett (2009). Improved Flow-Based Travel Time Estimation Method from Point Detector Data for Freeways. *Journal of Transportation Engineering*, 135(1):26-36.
- Viti, F. and H.J. Van Zuylen (2004). Modeling Queues at Signalized Intersections. *Transportation Research Record: Journal of the Transportation Research Board*, 1883:68-77.
- Viti, F. and H.J. van Zuylen (2006). Consistency of random queuing models at signalized intersections. In *Proceedings: 85th TRB annual meeting*, Washington D.C., USA.
- Viti, F. (2006). *The Dynamics and the Uncertainty of Delays at Signals*. PhD thesis, TRAIL Thesis series, Delft University of Technology, Delft.
- Viti, F., C.M.J. Tampere and R. Frederix (2009). Traffic performance of short-distanced traffic lights with probabilistic spillback. In *Proceedings: 88th TRB annual meeting*, Washington D.C., USA.
- Webster, F.V. (1958). Traffic signal settings. *Road Research Laboratory London, Her Majesty Stationary Office*.
- Wei, C.H. and Y. Lee (2007). Development of freeway travel time forecasting models by integrating different sources of traffic data. *IEEE Transactions on Vehicle Technology*, 56(6):3682-3694.
- Whitley, D. (1994). A Genetic Algorithm Tutorial. *Statistics and computing*, 4(2):65-85.
- Wolshon, B. and W.C. Taylor (1999). Analysis of intersection delay under real-time adaptive signal control. *Transportation Research Part C: Emerging Technologies*, 7(1):53-72.
- Wong, H.K. and J.M. Sussman (1973). Dynamic travel time estimation on highway networks. *Transport Research*, 7:355-369.

- Wunnava, S.V., K. Yen, T. Babij, R. Zavaleta, R. Romero and C. Archilla (2007). Travel time estimation using cell phones for highways and roadways. *Department of Electrical and Computer Engineering, Florida International University, Florida*.
- Wu, C.H., C.C. Wei, D.C. Su, M.H. Chang and J.M. Ho (2004). Travel Time Prediction with Support Vector Regression. *IEEE Transactions on intelligent transportation systems*, 5(4):6.
- Yao, L. and W.A. Sethares (1994). Nonlinear Parameter Estimation via the Genetic Algorithm. *IEEE Transactions on Signal Processing*, 42(4):927-935.
- Yegor, M., Y. Wu, Y. Wang and U.K. Lee (2010). Field Experiments on Bluetooth-based Travel Time Data Collection. *89th TRB annual meeting, Washington D.C., USA*.
- Yeon, J., L. Elefteriadou and S. Lawphongpanich (2008). Travel time estimation on a freeway using Discrete Time Markov Chains. *Transportation Research Part B: Methodological*, 42(4):325-338.
- You, J. and T.J. Kim (2000). Development and evaluation of a hybrid travel time forecasting models. *Transport Research Part C: Emerging Technologies*, 8(1-6):231-256.
- Yusuf, I.T. (2010). The factors for free flow speed on urban arterials- Empirical evidences from Nigeria. *Journal of American Science*, 6(12):1487-1497.
- Zheng, W., D.-H. Lee and Q. Shi (2006). short-term Freeway Traffic Flow Prediction: Bayesian Combined Neural Network Approach. *Journal of Transportation Engineering*, 132(2):114-121.
- Zheng, F. and H.J., Van Zuylen (2010). Comparison of Urban Link Travel Time Estimation Models based on Probe Vehicle Data. In *proceedings: 7th International Conference on Traffic and Transportation Studies*, Kunming, China.
- Zheng, F., H.J., Van Zuylen and Y.S., Chen (2010). An investigation of urban link travel time estimation based on probe vehicle data. In *proceedings: 89th annual meeting of Transportation Research Board*, Washington D.C.
- Zheng, F. and H.J., Van Zuylen (2010). Uncertainty and Predictability of Urban Link Travel Time: A Delay Distribution Based Analysis. *Transportation Research Record: Journal of the Transportation Research Board*, 2192:136-146.
- Zheng, F. and H.J., Van Zuylen (2011). Estimating the delay distribution function for an urban trip based on sample measurements. In *proceedings: 90th annual meeting of Transportation Research Board*, Washington D.C.
- Zheng, F. and H.J., Van Zuylen (2011). Modelling Travel Time Variability Based on Delay Distribution for Signalized Urban Trips. *Transportation Research Record: Journal of the Transportation Research Board* (Accepted).

# Appendix A

## GPS position and speed accuracy

---

**Note.** In the thesis, GPS probe vehicle data were used as ground truth for model calibration and validation. A short discussion of GPS data for travel time estimation has been discussed in chapter 3. This appendix provides more detailed information about GPS position and speed accuracy.

---

A GPS system consists of three segments: space segment (satellites), control segment (control stations), user segment (GPS receivers). A GPS receiver calculates its position by precisely timing the signals sent by GPS satellites high above the Earth. Each satellite continually transmits messages that include the time the message was transmitted, precise orbital information, the general system health and rough orbits of all GPS satellites. The receiver uses the messages it receives to determine the transit time of each message and computes the distance to each satellite. These distances along with the satellites' locations are used with the possible aid of trilateration, depending on which algorithm is used, to compute the position of the receiver. Many GPS units show derived information such as direction and speed, calculated from position changes<sup>1</sup>. There are many issues related to the GPS system. This appendix mainly provides information about GPS position accuracy and speed accuracy.

### A.1 Positioning accuracy

#### A.1.1 GPS positioning accuracy<sup>1</sup>

The accuracy of GPS position can be influenced by several factors: selectivity availability, satellite geometry, satellite orbits, multipath effect, atmospheric effects, satellite and receiver clock errors and etc.

##### Selectivity availability

The selectivity availability (SA) is an artificial falsification of the time in the signal transmitted by the satellite. The implementation of SA was to intentionally degrade the autonomous real-time positioning accuracy available to unauthorized users for security reasons. With SA turned on, nominal horizontal and vertical errors can be up to about 100m and 150m. On May 2, 2000, the U.S. government deactivated SA, resulting in a much-improved GPS position accuracy of 20m or even less.

### Satellite geometry

The accuracy of the computed GPS position is also affected by the geometric location of the GPS satellites as seen by the receiver. Good satellite geometry is obtained when the satellites are spread out in the sky. For instance, if a receiver sees 4 satellites and all are arranged for example in the north-west, this leads to a “bad” geometry. In the worst case, no position determination is possible at all, when all distance determinations point to the same direction. Even if a position is determined, the error of the positions may be up to 100 – 150 m. If, on the other hand, the 4 satellites are well distributed over the whole firmament, the determined position will be much more accurate. Figure A.1 and A.2 show geometrical alignment of satellites for the two-dimensional case.

If the two satellites are in an advantageous position, from the view of the receiver they can be seen in an angle of approximately 90 degrees to each other. The signal runtime cannot be determined absolutely precise as explained earlier. The possible positions are therefore marked by the grey circles. The point of intersection A of the two circles is a rather small, more or less quadratic field (square area), the determined position will be rather accurate.

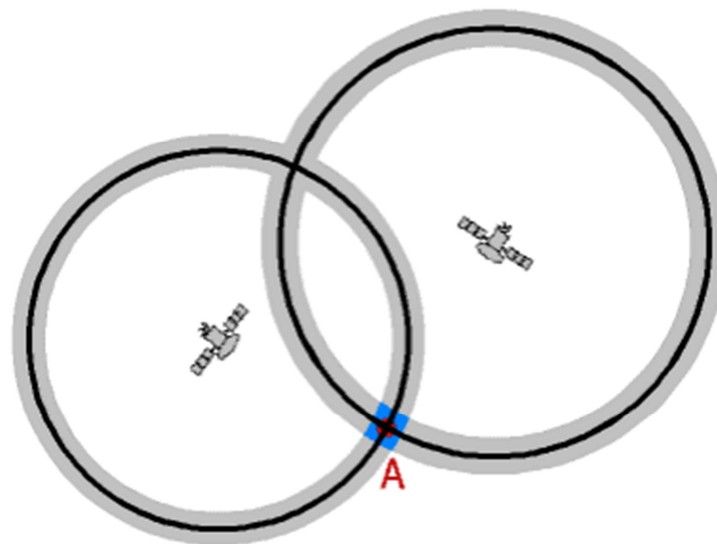


**Figure A.1 Good geometrical alignment of two satellites<sup>1</sup>**

<sup>1</sup> Source: <http://www.kowoma.de/en/gps/satellites.htm>

If the satellites are more or less positioned in one line from the view of the receiver, the plane of intersection of possible positions is considerably larger and elongated. The determination of the position is less accurate.

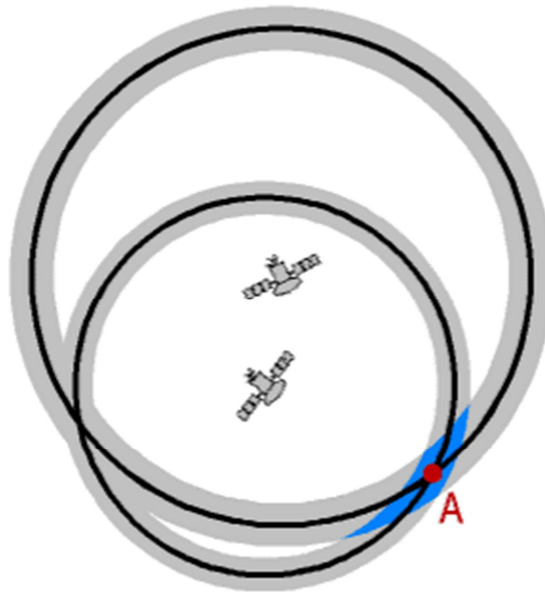


**Figure A.2 Bad geometrical alignment of two satellites<sup>1</sup>**

### **Satellite orbits**

Usually, satellites are positioned in very precise orbits. However, slight shifts of the orbits are possible due to gravitation forces. The orbit data are controlled and corrected regularly and are sent to the receivers in package of ephemeris data. Therefore, the influence on the position determination is low with a resulting error due to satellite orbits of not more than 2m.

### **Multipath effects**

The multipath effect is caused by reflection of satellite signals on objects. The reflected signal takes more time to reach the receiver than the direct signal. For GPS signals, this effect mainly appears in the neighbourhood of large buildings or other elevations, especially in the urban environment.

### **Atmospheric effects**

Another source of inaccuracy is the reduced speed of propagation in the troposphere and ionosphere. While radio signals travel with the velocity of light in the outer space, their propagation in the ionosphere and troposphere is slower.

### **Satellite and receiver clock errors and rounding errors**

The GPS satellite clocks, although highly accurate, are not perfect. The remaining inaccuracy of the time still leads to an error of about 2 m in the position

determination. Rounding and calculation errors of the receiver sum up approximately to 1 m.

The errors of the GPS position are summarized in the following table. The individual values are no constant values, but are subject to variances. All numbers are approximate values. All these effects lead to a total error of about  $\pm 15\text{m}$ .

**Table A.1: Typical GPS position accuracy with SA deactivated<sup>1</sup>**

Factors	Error (m)
Shifts in the satellite orbits	$\pm 2.5$
Multipath effect	$\pm 1$
Ionospheric effects	$\pm 5$
Tropospheric effects	$\pm 0.5$
Clock errors of the satellites' clocks	$\pm 2$
Calculation and rounding errors	$\pm 1$

### A.1.2 DGPS positioning accuracy<sup>2</sup>

The accuracy of GPS positioning can be improved by applying the technique called differential GPS (DGPS), which enables civil receivers to achieve accuracies in the range of decimetres to a few meters. The basic idea is that a second stationary GPS receiver is used for correcting the measurements of the first receiver. If the position of the stationary receiver is known very accurately, by means of a long wave transmitter a correction signal can be sent which is received and analysed by a receiver connected to the mobile GPS. Some countries around the world have established networks of GPS reference stations around their coastal areas, which continuously broadcast real-time DGPS corrections. Basically, there are three types of DGPS service systems: a single station-based DGPS service system (Maritime DGPS service), wide-area differential GPS (WADGPS) and multisite RTK system.

In the maritime DGPS service system, each reference station operates independently of the other stations in the network to serve users within its coverage area. This service requires a beacon receiver connected to a GPS receiver that accepts the Radio Technical Commission for Maritime Service (RTCM) corrections. The coverage depends on the transmitter power output, the atmospheric noise, the receiver sensitivity, the characteristics of the propagation path or conductivity. The coverage is greater over water than inland.

Real-time DGPS with a single reference station has the disadvantage that the positioning accuracy tends to deteriorate as the user moves away from the reference station. To overcome this problem, a system based on a number of widely separated reference stations

<sup>2</sup> Source: El-Rabbany, A (2006). *Introduction to GPS: the global Positioning System*. Artech House, London.

known as WADGPS has been developed. This system involves a set of ground reference stations that cover a wide geographical area, e.g., coverage of large, inaccessible regions using fewer reference stations.

The multisite RTK service could provide the positioning accuracy at subdecimetre-level. The idea behind multisite RTK positioning is based on using a network of reference stations to create raw GPS measurements for a virtual reference station, which is located close to the mobile, or the rover, receiver. Once created, the virtual reference station measurements are transmitted to the mobile receiver, where the normal single reference station RTK positioning can be performed. The RTK positioning with a single reference station is limited to a distance of 15 to 20 km. With this service, four GPS reference stations could cover an entire city or even a number of small adjacent cities.

## A.2 GPS speed accuracy

The results and discussions about the accuracy of GPS speed measurements provided in this appendix are mainly cited from Al-Gaadi's work<sup>3</sup>. The initial motivation of their work is to see how accurate the GPS speed measurements are for the agricultural operations. However, their results are also valuable for other applications.

In their study, a passenger vehicle was equipped with a hand-held GPS receiver to provide GPS speed data and a pulse transmitter to obtain vehicle's wheel speed. GPS-derived speed data was compared with the speed measurements based on wheel speed data (reference speed) and errors in GPS speed measurements were determined. Different ground speed values: 5, 10, 15, 20, 25, 30, 40 and 50km/h were chosen to do the comparison. Some results and discussions are given based on their experiment:

1. For all GPS data points, the average speed measurement accuracy is 1.27 km/h (6.9%). A maximum error of 0.51km/h and 5.54 km/h were found with 50 percentile and 95 percentile data points, respectively.
2. The magnitude of error in tested GPS speed measurement is not proportional to the magnitude of vehicle ground speed.
3. In their experiment, they found that the GPS accuracy is significantly degraded at sudden big changes of vehicle speed. E.g., an error of -80.16% was produced due to a vehicle speed reduction from 18.65 to 11.19 km/h with 10s. This result also implies that the accuracy of acceleration calculated from GPS speed measurements can not be guaranteed, especially for the high acceleration.
4. If no big sudden change of vehicle speed occurs, the average accuracy of GPS speed measurement is less than 1km/h except for 15km/h data set with an average accuracy of 1.72km/h. They found that the average error is less than 5.3% with all data sets, except for the 15km/h data set with an error of 9.92%.

---

<sup>3</sup> Al-Gaadi, K.A. (2005). Testing the accuracy of autonomous GPS in ground speed measurement. *Journal of Applied Sciences*,5(9):1518-1522.



# Appendix B

## Formulation of overflow queue distribution

---

**Note.** The overflow queue at an isolated intersection (at the upstream intersection in case of an urban trip with two intersections as discussed in chapter 5) is not constant but rather stochastic. This stochastic overflow queue has a big influence on the delay distribution. The derivation of the overflow queue distribution is not discussed in chapter 4 and 5. This appendix provides the detailed formulation of the overflow queue distribution model (cited from Viti).

---

Let  $Q_{max}$  be the maximum value of the queue length, which can be stored in the considered road section,  $q_{max}$  and  $d_{max}$  respectively the maximum number of arrivals and departures possible within a cycle,  $Q_{ij}$  be the transition matrix, which represents the probability that the queue length moves from a state  $i$  at time  $t-1$  to state  $j$  at time  $t$ . If  $j \neq 0$ , this probability is expressed by:

$$Q_{ij}(t) = \begin{cases} \Pr(j = i + q_t - d_t) & \forall j \geq i - d_t, q_t \in [0, q_{max}], d_t \in [0, d_{max}] \\ 0 & \text{otherwise} \end{cases} \quad (\text{B.1})$$

Since queues are constrained to be non-negative, when the departures are larger than the sum of the arrivals and the queue at the starting of the cycle, the queue at the end of the green phase will be zero. Obviously, part of this green phase will not be used by any vehicle. According to this consideration the chance of a queue  $i$  to become zero is computed with the following condition:

$$Q_{i0}(t) = \begin{cases} \sum_{k=0}^{d_t-i} \Pr(k - q_t = 0) & \forall i \leq d_t, q_t \in [0, q_{\max}] \\ 0 & \text{otherwise} \end{cases} \quad (\text{B.2})$$

If the departures are deterministic, Equation (B.2) computes the probability for a specific queue length  $j$  in the transition matrix from each couple  $(i, a_t)$ . If departures  $d_t$  are stochastic, given the range of possible departures  $[0, d_{\max}]$  and the assumption of independence of departure and arrival distributions, the transition probability from a state  $i$  to a state  $j$  is given by:

$$Q_{ij}(t) = \sum_{d_t=0}^{d_{\max}} Q_{ij}(t, d_t) \Pr(d_t) \quad (\text{B.3})$$

Every time step  $t$  is uniquely determined once an initial condition  $Q_0$  is assumed. This value, as said, can be a specific value or a stochastic variable. In both conditions the initial condition can be expressed by a vector of initial queue probabilities  $\Pr_{Q_0}(0) = \{ \Pr_0(0), \Pr_1(0), \Pr_2(0), \dots, \Pr_{Q_{\max}}(0) \}$  where the deterministic case can be seen as a special case of this vector where probability is 1 for the deterministic value and zero for the others. Since the queue probability distribution at every time  $t-1$  and the transition matrix  $q_{ij}$  are, as defined, independent, the probability of each state  $j$  is given by:

$$\Pr(Q_o = j, t) = \sum_{i=0}^{Q_{\max}} \Pr(Q_o = i, t-1) \cdot Q_{ij}(t) \quad (\text{B.4})$$

# Appendix C

## Derivation of boundary delays in the trip travel time distribution function in oversaturated conditions

---

**Note.** The detailed derivation of boundary delays  $w_{2n+1}$  and  $w_{2n+2}$  in the delay distribution function for the oversaturated condition is not presented in chapter 5. Therefore, this appendix provides more detailed derivation for readers who are interested. The boundary delays here refer to the delays at the transition moments when a vehicle arrives just before these moments can pass the intersection, whereas the following vehicle needs to wait for the red time.

---

### C.1 Mismatch 1 (early green)

In oversaturated conditions, the delay as the function of arrival time is derived as:

$$W = \begin{cases} \left\{ \tau_r + \frac{n_0 + 1}{s} + \left\lfloor \frac{n_0 + q(t - t_0) + 1}{s\tau_g} \right\rfloor \tau_r \right\} - \left(1 - \frac{q}{s}\right)(t - t_0), & \text{if } n_0 + q(t - t_0) + 1 - \left\lfloor \frac{n_0 + q(t - t_0) + 1}{s\tau_g} \right\rfloor s\tau_g < s\tau'_g \\ \left\{ 2\tau_r + \frac{n_0 + 1}{s} + \left\lfloor \frac{n_0 + q(t - t_0) + 1}{s\tau_g} \right\rfloor \tau_r \right\} - \left(1 - \frac{q}{s}\right)(t - t_0), & \text{else} \end{cases} \quad (\text{C.1})$$

As for the oversaturated condition, the number of extra red times that a vehicle arriving at time  $t$  needs to wait at the upstream intersection can be directly derived from Equation (C.1). The more generic expression is:

$$n = \left\lfloor \frac{q(t-t_0) + n_0 + 1}{s\tau_g} \right\rfloor \quad (\text{C.2})$$

From Equation (C.2), we can see that when a vehicle arriving within the time interval of one cycle time, the minimum number of extra red times this vehicle needs to wait at the upstream intersection can be derived as:

$$N_{\min} = \left\lfloor \frac{n_0 + 1}{s\tau_g} \right\rfloor \quad (\text{C.3})$$

And the maximum number of extra red times is given by:

$$N_{\max} = \left\lfloor \frac{q\tau_c + n_0 + 1}{s\tau_g} \right\rfloor \quad (\text{C.4})$$

If the value within  $\lfloor \cdot \rfloor$  is an integer, the maximum delay will be experienced by the vehicle arriving at the end of the cycle. Otherwise, the maximum delay will appear before the end of the cycle ( $t < t_0 + \tau_c$ ) in oversaturated conditions.

When vehicles arrive at the downstream intersection, there are two cases:

- *Passing the downstream intersection without delay;*
- *Passing the downstream intersection with a certain delay.*

Whether vehicles need to wait for the red time at the downstream intersection depends on whether the number of vehicles in front of this vehicle plus the vehicle itself can be released within the green time  $\tau_g'$  at the downstream intersection.

1) If  $0 \leq n_0 + q(t-t_0) + 1 - \left\lfloor \frac{n_0 + q(t-t_0) + 1}{s\tau_g} \right\rfloor s\tau_g < s\tau_g'$ , vehicles experience no delay at the downstream intersection. Vehicles just experience delays at the upstream intersection. Given the initial moment of the calculation  $t_0$ , in our approach, it is the beginning of the red time. For this case, the transition moments (discontinuity of the delay as function of  $t_n$ ) appear when:

$$n_0 + q(t_n - t_0) + 1 - ns\tau_g = 0$$

Each transition moment can be derived as:

$$t_n = \begin{cases} t_0 & n = N_{\min} \\ t_0 + \frac{ns\tau_g - n_0 - 1}{q} & N_{\min} < n \leq N_{\max} \end{cases} \quad (\text{C.5})$$

2) If  $n_0 + q(t - t_0) + 1 - \left\lfloor \frac{n_0 + q(t - t_0) + 1}{s\tau_g} \right\rfloor s\tau_g \geq s\tau'_g$  vehicles experience delays at both the upstream and downstream intersections, the transition moments appear when:

$$n_0 + q(t'_n - t_0) + 1 - ns\tau_g = s\tau'_g$$

Each transition moment can be expressed as:

$$t'_n = t_0 + \frac{ns\tau_g + s\tau'_g - n_0 - 1}{q} \quad N_{\min} \leq n < N_{\max} \quad (\text{C.6})$$

An example is shown in Figure C.1. The ‘star’ points are the transition moments when the vehicles needs to wait for another red time at the upstream intersection; The ‘dot’ points are transition moments that vehicles arrive at the downstream intersection right after the signal turns red. As can be seen in Figure C.1, after the transition moments (dots), the delay is decreasing linearly as the function of arrival time and the other transition moments (stars) can be ignored because all these transition moments are within the delay evolution trend starting from the dot transition moments. However, this is only for the case of the same red time both for the upstream intersection and the downstream intersection. In case of different red times, the star transition moments can be above or below the trend line starting from the dot transition moments as described above. The example given in the following considers two situations:

(a)  $n_0 + 1 - \left\lfloor \frac{n_0 + 1}{s\tau_g} \right\rfloor s\tau_g < s\tau'_g$ : The first vehicle arriving right after the beginning of the red time can leave the downstream without delay. For this case, the delay the vehicle arriving at the beginning of the red time equals to:

$$W = \tau_r + \frac{n_0 + 1}{s} + \left\lfloor \frac{n_0 + 1}{s\tau_g} \right\rfloor \tau_r = \left(1 + \left\lfloor \frac{n_0 + 1}{s\tau_g} \right\rfloor\right) \tau_r + \frac{n_0 + 1}{s} = (1 + N_{\min})\tau_r + \frac{n_0 + 1}{s} \quad (\text{C.7})$$

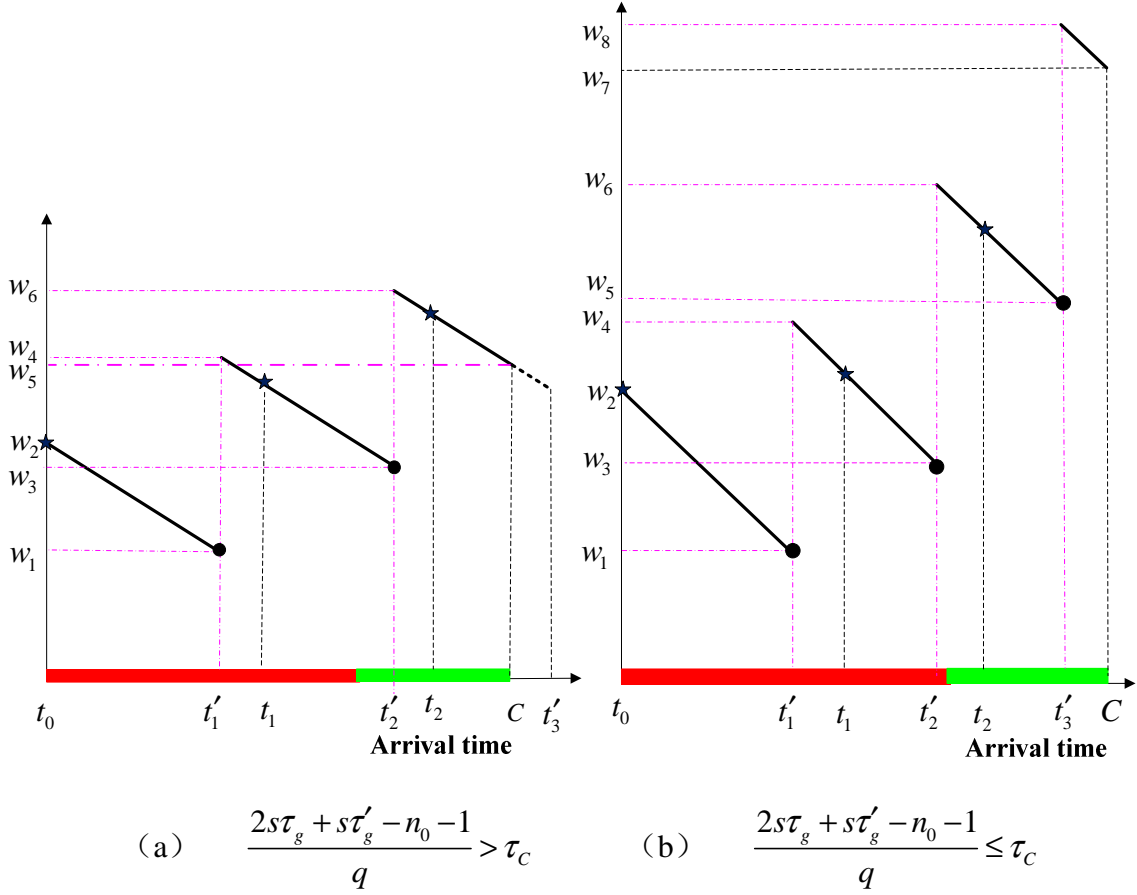


**Figure C.1: Delay as a function of arrival time with two intersection coordinated in the oversaturated condition**

**Transition 1:**  $t_0$

$$W_2 = (1 + N_{\min})\tau_r + \frac{n_0 + 1}{s}$$

**Transition 2:**  $t'_1 = \frac{N_{\min}s\tau_g + s\tau'_g - n_0 - 1}{q} + t_0$

$$\begin{aligned} W_1 &= (1 + N_{\min})\tau_r + \frac{n_0 + 1}{s} - \frac{N_{\min}s\tau_g + s\tau'_g - n_0 - 1}{q} \left(1 - \frac{q}{s}\right) \\ &= N_{\min}\tau_c + \tau_r + \tau'_g + \frac{n_0 + 1 - N_{\min}s\tau_g - s\tau'_g}{q} \end{aligned}$$

$$W_4 = W_1 + \tau_r = N_{\min}\tau_c + 2\tau_r + \tau'_g + \frac{n_0 + 1 - N_{\min}s\tau_g - s\tau'_g}{q}$$

**Transition 3:**  $t'_2 = \frac{(1 + N_{\min})s\tau_g + s\tau'_g - n_0 - 1}{q} + t_0$

$$\begin{aligned}
 W_3 &= (2 + N_{\min})\tau_r + \frac{n_0 + 1}{s} - \frac{(1 + N_{\min})s\tau_g + s\tau'_g - n_0 - 1}{q} \left(1 - \frac{q}{s}\right) \\
 &= (1 + N_{\min})\tau_c + \tau_r + \tau'_g - \frac{(1 + N_{\min})s\tau_g + s\tau'_g - n_0 - 1}{q} \\
 W_6 &= W_3 + \tau_r = (3 + N_{\min})\tau_r + \frac{n_0 + 1}{s} - \frac{(1 + N_{\min})s\tau_g + s\tau'_g - n_0 - 1}{q} \left(1 - \frac{q}{s}\right) \\
 &= (1 + N_{\min})\tau_c + 2\tau_r + \tau'_g - \frac{(1 + N_{\min})s\tau_g + s\tau'_g - n_0 - 1}{q}
 \end{aligned}$$

**Transition 4:** if  $t'_3 = \frac{(2 + N_{\min})s\tau_g + s\tau'_g - n_0 - 1}{q} > \tau_c$  (see Figure C.1 (a))

$$t_3 = \tau_c$$

$$W_5 = (3 + N_{\min})\tau_r + \frac{n_0 + 1}{s} - \tau_c \left(1 - \frac{q}{s}\right)$$

if  $t'_3 = \frac{(2 + N_{\min})s\tau_g + s\tau'_g - n_0 - 1}{q} \leq \tau_c$  (see Figure C.1 (b))

$$\begin{aligned}
 W_5 &= (3 + N_{\min})\tau_r + \frac{n_0 + 1}{s} - \frac{(2 + N_{\min})s\tau_g + s\tau'_g - n_0 - 1}{q} \left(1 - \frac{q}{s}\right) \\
 &= (2 + N_{\min})\tau_c + \tau_r + \tau'_g - \frac{(2 + N_{\min})s\tau_g + s\tau'_g - n_0 - 1}{q}
 \end{aligned}$$

$$W_8 = W_5 + \tau_r$$

$$= (2 + N_{\min})\tau_c + 2\tau_r + \tau'_g - \frac{(2 + N_{\min})s\tau_g + s\tau'_g - n_0 - 1}{q}$$

$$W_7 = (4 + N_{\min})\tau_r + \frac{n_0 + 1}{s} - \tau_c \left(1 - \frac{q}{s}\right)$$

(b)  $n_0 + 1 - \left\lfloor \frac{n_0 + 1}{s\tau_g} \right\rfloor s\tau_g \geq s\tau'_g$ : The initial overflow queue is so large that the first vehicle arriving right after the start of the red time at the upstream intersection has to wait for the red time at the downstream intersection. For this case, the delay the vehicle arriving at the beginning of the red time equals to:

$$W = (2 + N_{\min})\tau_r + \frac{n_0 + 1}{s} \tag{C.8}$$

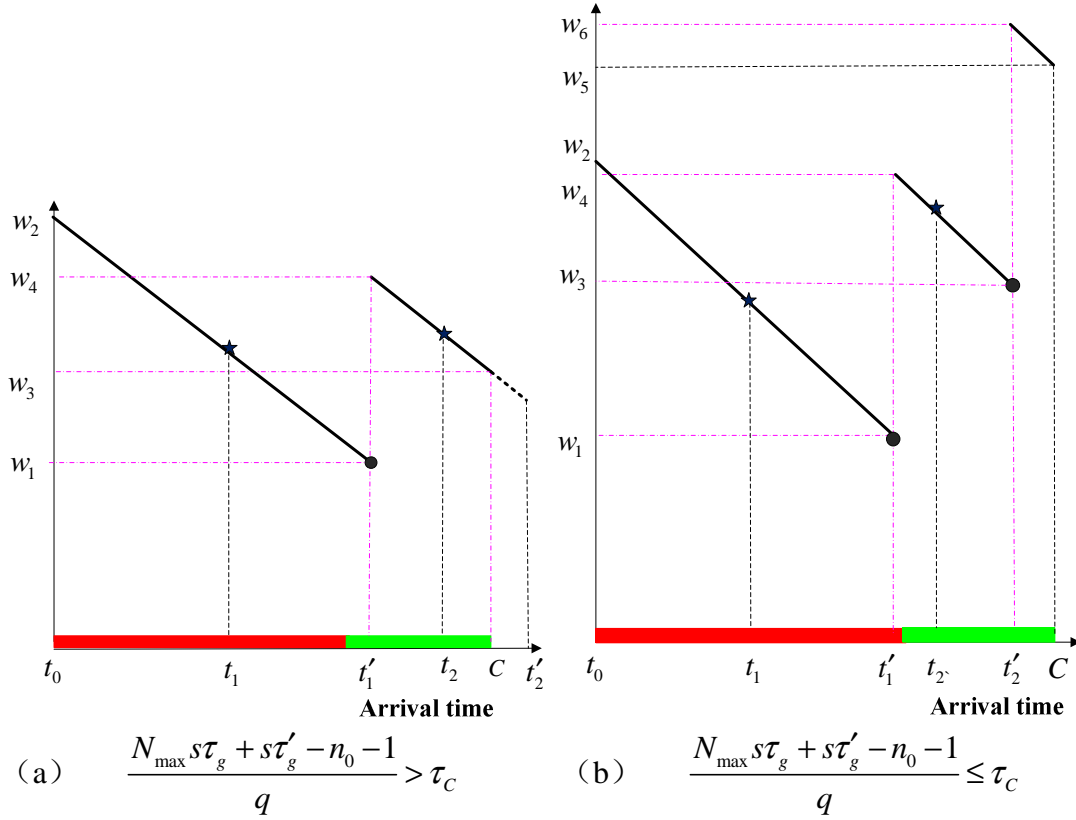


**Figure C.2: Delay as a function of arrival time with two intersections coordinated in the oversaturated condition**

**Transition 1:**  $t_0$

$$W_2 = (2 + N_{\min})\tau_r + \frac{n_0 + 1}{s}$$

**Transition 2:**  $t'_1 = \frac{(1 + N_{\min})s\tau_g + s\tau'_g - n_0 - 1}{q} + t_0$

$$\begin{aligned} W_1 &= (2 + N_{\min})\tau_r + \frac{n_0 + 1}{s} - \frac{(1 + N_{\min})s\tau_g + s\tau'_g - n_0 - 1}{q} \left(1 - \frac{q}{s}\right) \\ &= (1 + N_{\min})\tau_C + \tau_r + \tau'_g - \frac{(1 + N_{\min})s\tau_g + s\tau'_g - n_0 - 1}{q} \end{aligned}$$

$$\begin{aligned} W_4 &= W_1 + \tau_r = (3 + N_{\min})\tau_r + \frac{n_0 + 1}{s} - \frac{(1 + N_{\min})s\tau_g + s\tau'_g - n_0 - 1}{q} \left(1 - \frac{q}{s}\right) \\ &= (1 + N_{\min})\tau_C + 2\tau_r + \tau'_g - \frac{(1 + N_{\min})s\tau_g + s\tau'_g - n_0 - 1}{q} \end{aligned}$$

**Transition 3:** if  $t'_2 = \frac{(2 + N_{\min})s\tau_g + s\tau'_g - n_0 - 1}{q} > \tau_C$  (see Figure C.2 (a))

$$W_3 = (3 + N_{\min})\tau_r + \frac{n_0 + 1}{s} - \tau_C \left(1 - \frac{q}{s}\right)$$

if  $t'_2 = \frac{(2 + N_{\min})s\tau_g + s\tau'_g - n_0 - 1}{q} \leq \tau_C$  (see Figure C.2 (b))

$$W_3 = (3 + N_{\min})\tau_r + \frac{n_0 + 1}{s} - \frac{(2 + N_{\min})s\tau_g + s\tau'_g - n_0 - 1}{q} \left(1 - \frac{q}{s}\right)$$

$$= (2 + N_{\min})\tau_C + \tau_r + \tau'_g - \frac{(2 + N_{\min})s\tau_g + s\tau'_g - n_0 - 1}{q}$$

$$W_6 = W_3 + \tau_r$$

$$= (2 + N_{\min})\tau_C + 2\tau_r + \tau'_g - \frac{(2 + N_{\min})s\tau_g + s\tau'_g - n_0 - 1}{q}$$

$$W_5 = (4 + N_{\min})\tau_r + \frac{n_0 + 1}{s} - \tau_C \left(1 - \frac{q}{s}\right)$$

For more general expression, the delay for each transition point can be calculated as:

(1) If  $n_0 + 1 - \left\lfloor \frac{n_0 + 1}{s\tau_g} \right\rfloor s\tau_g < s\tau'_g$  &  $\frac{N_{\max}s\tau_g + s\tau'_g - n_0 - 1}{q} > \tau_C$

$$W_{2n+1} = \begin{cases} n\tau_C + \tau_r + \tau'_g - \frac{ns\tau_g + s\tau'_g - n_0 - 1}{q} & N_{\min} \leq n < N_{\max} \\ (n+1)\tau_r + \frac{n_0 + 1}{s} - \tau_C \left(1 - \frac{q}{s}\right) & n = N_{\max} \end{cases} \quad (\text{C.9a})$$

$$W_{2n+2} = \begin{cases} (n+1)\tau_r + \frac{n_0 + 1}{s} & n = N_{\min} \\ (n-1)\tau_C + 2\tau_r + \tau'_g - \frac{(n-1)s\tau_g + s\tau'_g - n_0 - 1}{q} & N_{\min} < n \leq N_{\max} \end{cases} \quad (\text{C.9b})$$

(2) If  $n_0 + 1 - \left\lfloor \frac{n_0 + 1}{s\tau_g} \right\rfloor s\tau_g < s\tau'_g$  &  $\frac{N_{\max}s\tau_g + s\tau'_g - n_0 - 1}{q} \leq \tau_C$

$$W_{2n+1} = \begin{cases} n\tau_C + \tau_r + \tau'_g - \frac{ns\tau_g + s\tau'_g - n_0 - 1}{q}, & N_{\min} \leq n \leq N_{\max} \\ (n+1)\tau_r + \frac{n_0 + 1}{s} - \tau_C \left(1 - \frac{q}{s}\right) & n = N_{\max} + 1 \end{cases} \quad (\text{C.10a})$$

$$W_{2n+2} = \begin{cases} (n+1)\tau_r + \frac{n_0+1}{s} & n = N_{\min} \\ (n-1)\tau_C + 2\tau_r + \tau'_g - \frac{(n-1)s\tau_g + s\tau'_g - n_0 - 1}{q} & N_{\min} < n \leq N_{\max} + 1 \end{cases} \quad (\text{C.10b})$$

$$(3) \text{ If } n_0 + 1 - \left\lfloor \frac{n_0 + 1}{s\tau_g} \right\rfloor s\tau_g \geq s\tau'_g \text{ \& } \frac{N_{\max}s\tau_g + s\tau'_g - n_0 - 1}{q} > \tau_C$$

$$W_{2n+1} = \begin{cases} n\tau_C + \tau_r + \tau'_g - \frac{ns\tau_g + s\tau'_g - n_0 - 1}{q} & N_{\min} + 1 \leq n < N_{\max} \\ (n+1)\tau_r + \frac{n_0+1}{s} - \tau_C(1 - \frac{q}{s}) & n = N_{\max} \end{cases} \quad (\text{C.11a})$$

$$W_{2n+2} = \begin{cases} (n+1)\tau_r + \frac{n_0+1}{s} & n = N_{\min} + 1 \\ (n-1)\tau_C + 2\tau_r + \tau'_g - \frac{(n-1)s\tau_g + s\tau'_g - n_0 - 1}{q} & N_{\min} + 1 < n \leq N_{\max} \end{cases} \quad (\text{C.11b})$$

$$(4) \text{ If } n_0 + 1 - \left\lfloor \frac{n_0 + 1}{s\tau_g} \right\rfloor s\tau_g \geq s\tau'_g \text{ \& } \frac{N_{\max}s\tau_g + s\tau'_g - n_0 - 1}{q} \leq \tau_C$$

$$W_{2n+1} = \begin{cases} n\tau_C + \tau_r + \tau'_g - \frac{ns\tau_g + s\tau'_g - n_0 - 1}{q} & N_{\min} + 1 \leq n \leq N_{\max} \\ (n+1)\tau_r + \frac{n_0+1}{s} - \tau_C(1 - \frac{q}{s}) & n = N_{\max} + 1 \end{cases} \quad (\text{C.12a})$$

$$W_{2n+2} = \begin{cases} (n+1)\tau_r + \frac{n_0+1}{s} & n = N_{\min} + 1 \\ (n-1)\tau_C + 2\tau_r + \tau'_g - \frac{(n-1)s\tau_g + s\tau'_g - n_0 - 1}{q} & N_{\min} + 1 < n \leq N_{\max} + 1 \end{cases} \quad (\text{C.12b})$$

## C.2 Mismatch 2 (late green)

In case of mismatch 2, the delay as the function of arrival time is given by:

$$W = \left\{ \tau_r + \tau_m + \frac{n_0 + 1}{s} + \left\lfloor \frac{n_0 + q(t - t_0) + 1}{s\tau_g} \right\rfloor \tau_r \right\} - t(1 - \frac{q}{s}) \quad (\text{C.13})$$

Vehicles departing from the upstream intersection right after the traffic light turns to green will experience extra delay due to the late start of green phase at the downstream intersection. The transition moments can be derived from Equation (C.14) as:

$$t_n = \begin{cases} t_0 & n = N_{\min} \\ t_0 + \frac{ns\tau_g - n_0 - 1}{q} & N_{\min} < n \leq N_{\max} \end{cases} \quad (C.14)$$

$N_{\min}$ ,  $N_{\max}$  are the minimum number of extra red time and maximum number of extra red time that vehicles need to wait at the upstream intersection, respectively, which are given by Equations(C.3) and (C.4).

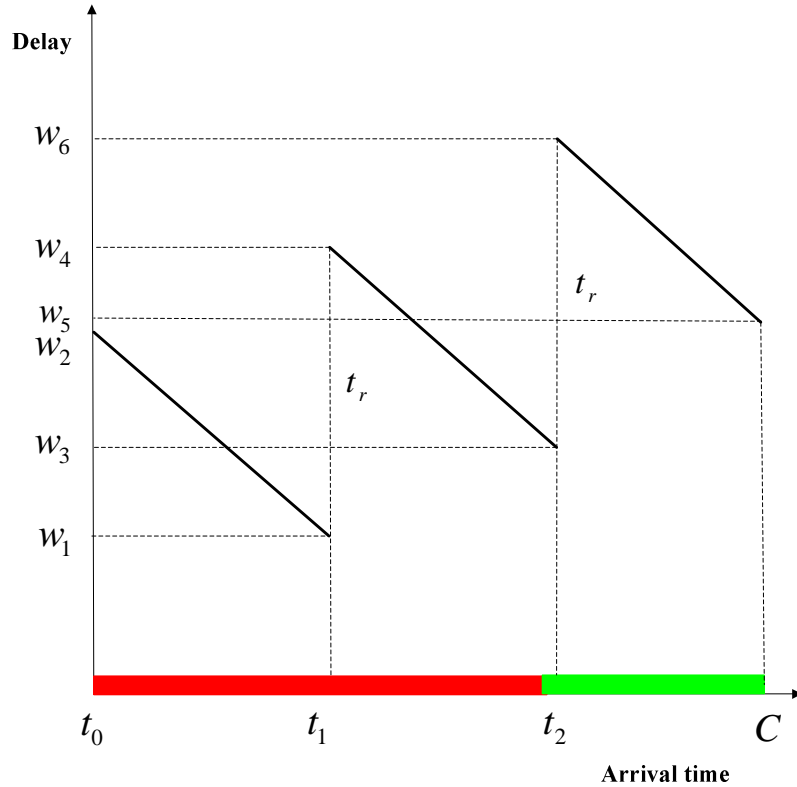


**Figure C.3: Delay as a function of arrival time with two intersections coordinated in the oversaturated condition**

**Transition 1:  $t_0$**

When the vehicle arrives at the beginning of the red time  $t_0$ , the delay equals to the red time plus the time to release the queue in front of this vehicle plus the coordination mismatch at the downstream intersection, which is given by:

$$W_2 = (1 + N_{\min})\tau_r + \tau_m + \frac{n_0 + 1}{s}$$

**Transition 2:  $t_1 = \frac{(1 + N_{\min})s\tau_g - n_0 - 1}{q} + t_0$**

$$\begin{aligned}
W_1 &= (1 + N_{\min})\tau_r + \tau_m + \frac{n_0 + 1}{s} - (1 - \frac{q}{s}) \left( \frac{(1 + N_{\min})s\tau_g - n_0 - 1}{q} \right) \\
&= (1 + N_{\min})\tau_C + \tau_m - \frac{(1 + N_{\min})s\tau_g - n_0 - 1}{q}
\end{aligned}$$

$$W_4 = W_1 + \tau_r = (1 + N_{\min})\tau_C + \tau_r + \tau_m - \frac{(1 + N_{\min})s\tau_g - n_0 - 1}{q}$$

**Transition 3:**  $t_2 = \frac{(2 + N_{\min})s\tau_g - n_0 - 1}{q} + t_0$

$$\begin{aligned}
W_3 &= (2 + N_{\min})\tau_r + \tau_m + \frac{n_0 + 1}{s} - (1 - \frac{q}{s}) \left( \frac{(2 + N_{\min})s\tau_g - n_0 - 1}{q} \right) \\
&= (2 + N_{\min})\tau_C + \tau_m - \frac{(2 + N_{\min})s\tau_g - n_0 - 1}{q}
\end{aligned}$$

$$\begin{aligned}
W_6 &= W_3 + \tau_r = (2 + N_{\min})\tau_C + \tau_m - \frac{(2 + N_{\min})s\tau_g - n_0 - 1}{q} + \tau_r \\
&= (2 + N_{\min})\tau_C + \tau_r + \tau_m - \frac{(2 + N_{\min})s\tau_g - n_0 - 1}{q}
\end{aligned}$$

**Transition 4:**  $t_3 = \tau_C$

$$W_5 = (3 + N_{\min})\tau_r + \tau_m + \frac{n_0 + 1}{s} - \tau_C \left( 1 - \frac{q}{s} \right)$$

From the given example, a more generic expression can be derived as:

$$W_{2n+1} = \begin{cases} (n+1)\tau_C + \tau_m - \frac{(n+1)s\tau_g - n_0 - 1}{q} & N_{\min} \leq n < N_{\max} \\ (n+1)\tau_r + \tau_m + \frac{n_0 + 1}{s} - \tau_C \left( 1 - \frac{q}{s} \right) & n = N_{\max} \end{cases} \quad (\text{C.15a})$$

$$W_{2n+2} = \begin{cases} (1+n)\tau_r + \tau_m + \frac{n_0 + 1}{s} & n = N_{\min} \\ n\tau_C + \tau_m + \tau_r - \frac{ns\tau_g - n_0 - 1}{q} & N_{\min} < n \leq N_{\max} \end{cases} \quad (\text{C.15b})$$

# Appendix D

## Comparison of link travel time in case of a vertical queue and shock wave

---

**Note.** In order to see whether the shock wave has influence on the calculation of link travel time, this appendix provides detailed analysis of the delay as a function of arrival time in D.1. Afterwards, the comparison of the link travel time between the vertical queue and shock wave is given in D.2. The derivation of the delay as a function of arrival time for the case of shock wave is based on the assumption of a triangular fundamental diagram.

---

### D.1 Delay calculation in case of shock wave

#### **Case 1: No initial queue exists at the beginning of the red phase**

For the sake of simplicity, we assume the triangular fundamental diagram as illustrated in Figure D.1.  $k_j$  is the jam density,  $k_s$  is the capacity density,  $k_q$  is the arrival flow density,  $s$  is the capacity flow,  $q$  is the arrival flow,  $L_s$  is the effective length of a stopped vehicle, the following relationship can be derived:

$$L_s = \frac{1}{k_j} \quad (\text{D.1})$$

The difference of delay between the preceding vehicle and the following vehicle is given by:

$$\Delta d = \frac{L_s}{w} - \frac{L_s}{u_w} \quad (\text{D.2})$$

Where  $w$  is the congested wave speed from the standing still state to the queue discharging state which can be derived as:

$$w = \frac{s}{k_j - k_s} \quad (\text{D.3})$$

$u_w$  is the shock wave speed from the free flow state to the standing still state which is given by:

$$u_w = \frac{q}{k_j - k_q} \quad (\text{D.4})$$

Where  $k_q = \frac{q}{s} k_s$

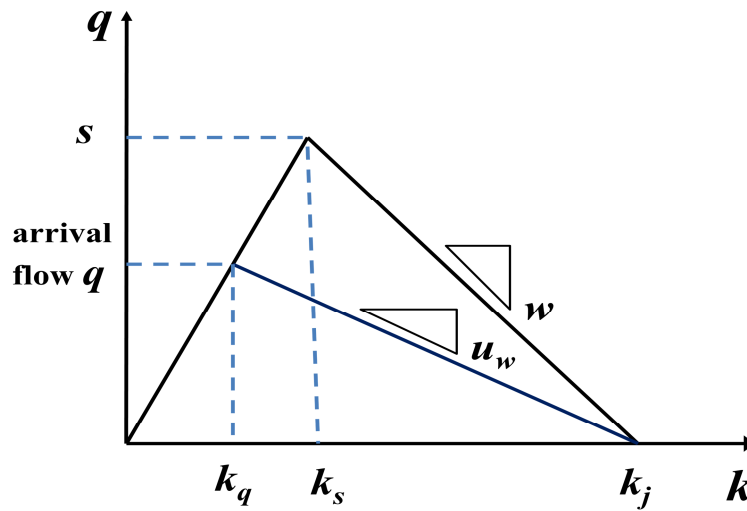


**Figure D.1: Flow density diagram**

Let's assume there is no queue at the beginning of the red phase ( $t=0$ ) and no spillback during the whole analysis period. For a given time instant  $t$  when vehicles arriving at the back of the queue (in case of shock wave), the total arrivals between time instant  $0$  and  $t$  can be calculated as :

$$A(t) = qt \quad (\text{D.5})$$

Therefore, the delay can be derived as:

$$\begin{aligned}
W(t) &= \tau_r + \Delta d * A(t) = \tau_r + \left(\frac{L_s}{w} - \frac{L_s}{u_w}\right)qt = \tau_r + \left(\frac{k_j - k_s}{s} - \frac{k_j - k_q}{q}\right)\frac{1}{k_j}qt \\
&= \tau_r + \left(\frac{k_j - k_s}{s} - \frac{k_j - \frac{q}{s}k_s}{q}\right)\frac{1}{k_j}qt = \tau_r + \left(\frac{q}{s}t - \frac{k_s qt}{k_j s} - t + \frac{k_s qt}{k_j s}\right) \\
&= \tau_r - \left(1 - \frac{q}{s}\right)t
\end{aligned} \tag{D.6}$$

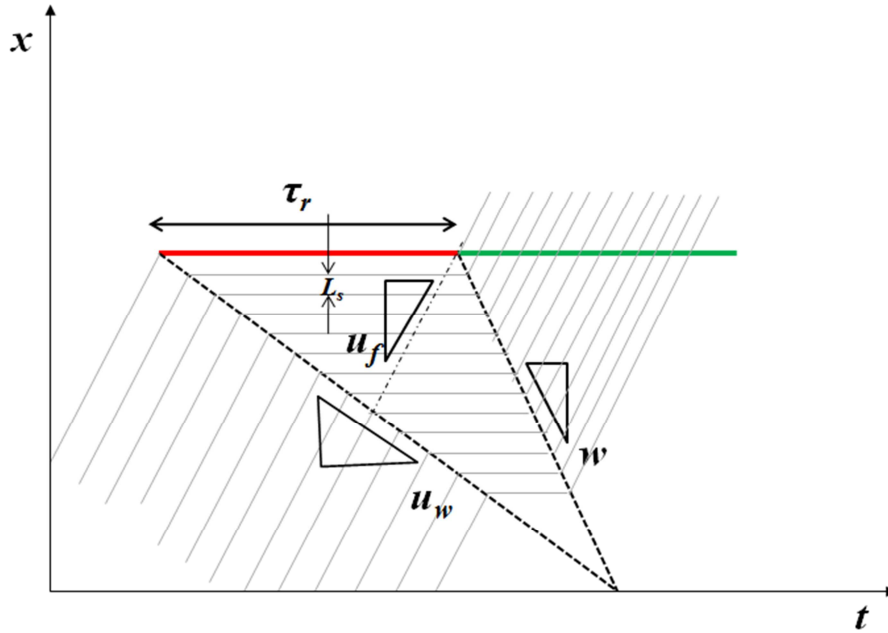


**Figure D.2: Space-time diagram at a signalized intersection**

### **Case 2: Initial overflow queue $n_0$ at the beginning of the red phase**

In the absence of queues, all vehicles would depart following the trajectory AB as shown in Figure D.3. Therefore, the queuing delay is the area of  $W_q$ . When a vehicle arrives at the beginning of the red phase ( $t=0$ ), there is an initial queue  $n_0$ . For this case, the delay  $W_0$  is composed of two parts:

$$W_0 = \tau_r + d \tag{D.7}$$

Where  $d$  is the queuing delay due to the initial overflow queue at the beginning of the red phase, which can be calculated as:

$$\begin{aligned}
d &= \frac{(n_0 + 1)L_s}{u_f} + \frac{(n_0 + 1)L_s}{w} = (n_0 + 1)\left(\frac{1}{u_f} + \frac{1}{w}\right)L_s \\
&= (n_0 + 1)\left(\frac{k_s}{s} + \frac{k_j - k_s}{s}\right)\frac{1}{k_j} \\
&= \frac{n_0 + 1}{s}
\end{aligned} \tag{D.8}$$

By substituting  $d$  in Equation (D.7) with Equation (D.8), we can derive the delay at the beginning of the red phase as:

$$W_0 = \tau_r + \frac{n_0 + 1}{s} \quad (\text{D.9})$$

The delay as a function of arrival time (the moment when the vehicle joins the end of the queue) in this case can be calculated as:

$$W(t) = W_0 + \Delta d * A(t) = \tau_r + \frac{n_0 + 1}{s} - \left(1 - \frac{q}{s}\right)t \quad (\text{D.10})$$

From Equations (D.6) and (D.10), we can see that the delay as a function of arrival time in case of a shock wave is consistent with what we have discussed in chapter 4 and chapter 5. The difference is the definition of the arrival time. In case of a vertical queue, the arrival time  $t$  refers to the arrival moment at the stop line. While for the shock wave case, it refers to the arrival moment at the back of the queue.

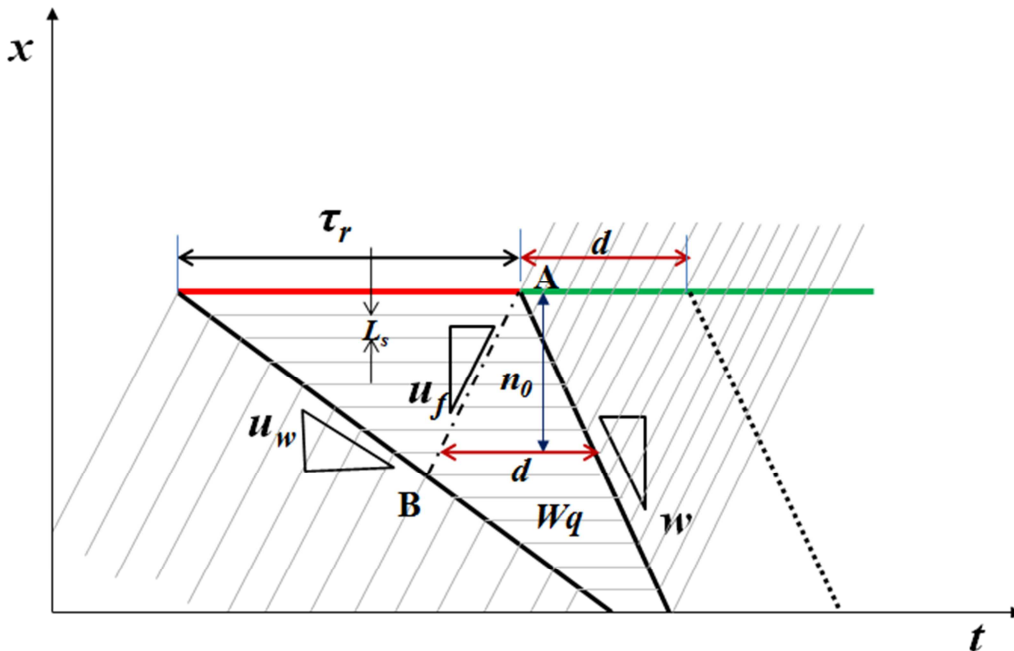


**Figure D.3: Space-time diagram at a signalized intersection in case of an initial queue  $n_0$**

The validity of the above comparison of the delay as a function of arrival time between vertical queue and shock wave is limited by the assumption of triangular fundamental diagram. Different fundamental diagram could result in different conclusions. However, when calculating the complete link travel time, the assumption of triangular fundamental diagram is not necessary. Hurdle (Hurdle et al., 2001) compared the delay estimated from the shock wave model and the cumulative arrival and departure model on freeways. They showed that these two models are compatible, yielding identical estimates of travel times

and delay. D.2 shows more detailed comparison of the complete link travel time in case of a vertical queue and shock wave.

## D.2 Comparison of link travel time between a vertical queue and shock wave

Figure D.4 shows trajectories of vehicles passing a link in case of a vertical queue (Figure D.4 (a)) and shock wave (Figure D.4 (b)).  $x_0$  is the start of the link and  $x_l$  is the end of the link (stop line). We assume arrival moments at the upstream of the link are uniformly distributed within a cycle time; The First-In-First-Out holds for all arriving vehicles and vehicles approach and depart from the intersection with instant acceleration and deceleration. For the case of a vertical queue, a vehicle entering the upstream of the link at time instant  $t_0$  will pass the stop line of the downstream intersection at time instant  $t_0'$ . The same goes for vehicles entering at time instances  $t_1, t_2, \dots, t_n$  and passing the stop line of the downstream intersection at time instances  $t_1', t_2', \dots, t_n'$ . The link travel time of a vehicle entering at time instant  $t_i$  for the case of vertical queue can be calculated as:

$$TT_{VQ}(t_i) = t_i' - t_i, \quad i = 0, 1, 2, \dots, n \quad (D.11)$$

Where  $TT_{VQ}(t_i)$  is the link travel time of a vehicle entering the upstream of the link at time instant  $t_i$  in case of a vertical queue;  $t_i'$  is the time instant when the vehicle passing the stop line of the downstream intersection.

For the case of shock wave, the link travel time of a vehicle entering at time instant  $t_i$  at the upstream of the link can be calculated as:

$$TT_{SW}(t_i) = T_i' - t_i, \quad i = 0, 1, 2, \dots, n \quad (D.12)$$

Where  $TT_{SW}(t_i)$  is the link travel time of a vehicle entering the upstream of the link at time instant  $t_i$  in case of shock wave;  $T_i'$  is the time instant when the vehicle passing the stop line of the downstream intersection.

Let's assume that when a vehicle enters the upstream of link at time  $t_0$  will arrive at the beginning of the red time at the downstream intersection and there is no queue, the travel time of this vehicle is given by:

$$TT_{VQ}(t_0) = t_0' - t_0 = \tau_r + \frac{x_1 - x_0}{u_f} \quad (D.13)$$

$$TT_{SW}(T_0) = T_0' - t_0 = \tau_r + \frac{x_1 - x_0}{u_f} \quad (D.14)$$

The link travel time of a vehicle entering at time instant  $t_i$  ( $T_i$  in case of shock wave) at the upstream of the link can be calculated as:

$$\begin{aligned}
 TT_{VQ}(t_i) &= t'_i - t_i = TT_{VQ}(t_0) + i(t'_i - t'_{i-1} - (t_i - t_{i-1})) \\
 &= TT_{VQ}(t_0) + i\left(\frac{1}{s} - \frac{1}{q}\right)
 \end{aligned}
 \tag{D.15}$$

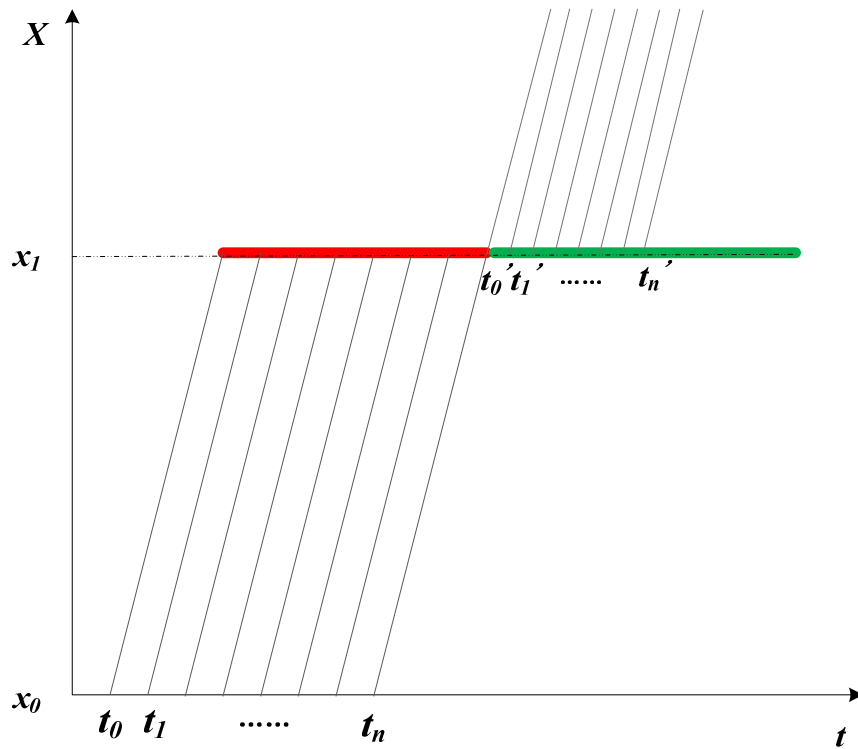
$$TT_{SW}(T_i) = T'_i - T_i = TT_{SW}(t_0) + i(T'_i - T'_{i-1} - (T_i - T_{i-1}))
 \tag{D.16}$$

Where  $T_i - T_{i-1} = \frac{L_s}{u_w} + \frac{L_s}{u_f} = \frac{1}{q}$ ,  $T'_i - T'_{i-1} = \frac{L_s}{w} + \frac{L_s}{u_s} = \frac{1}{s}$ ,  $u_f$  is the free flow speed of arriving vehicles and  $u_s$  is the platoon departure speed.

Therefore, Equation (D.16) can be rewritten as:

$$TT_{SW}(T_i) = T'_i - T_i = TT_{SW}(T_0) + i\left(\frac{1}{s} - \frac{1}{q}\right)
 \tag{D.17}$$

From Equations (D.13), (D.14), (D.15), (D.17), we can see that the link travel time for the case of a vertical queue is consistent with that of shock wave under the assumption of a triangular fundamental diagram.



(a) Vertical queue

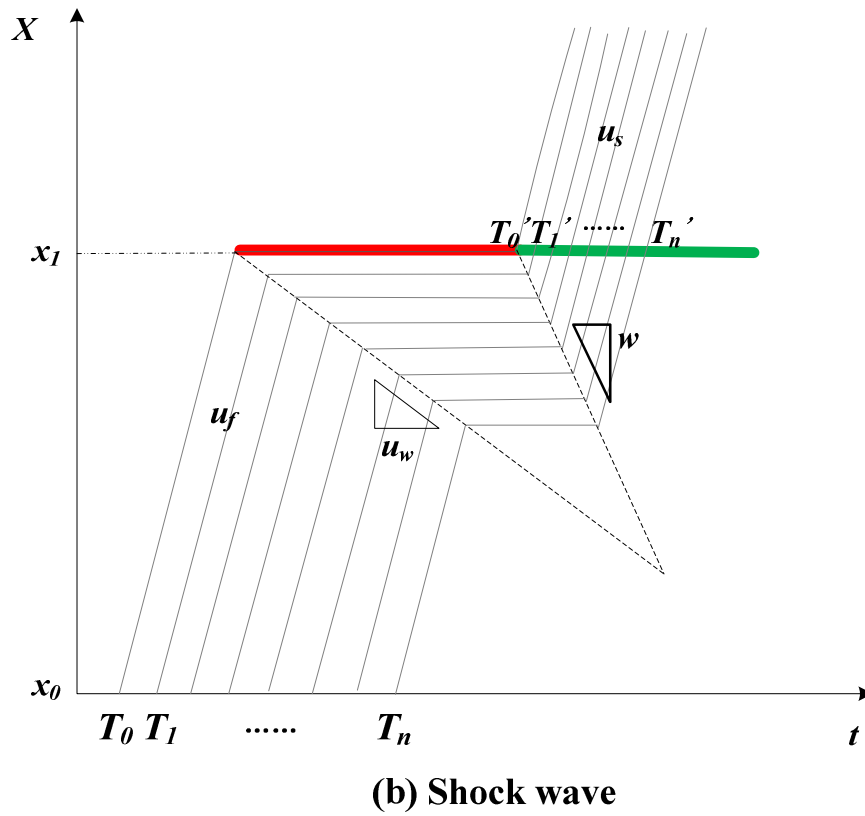


Figure D.4: Space-time diagram of vehicles passing one link in case of a vertical queue (a) and shock wave (b)



# Appendix E

## Test area

---

**Note.** Throughout this thesis, travel times measured by GPS probe vehicles were used for analysis. This appendix provides more information about the test area where GPS travel times were collected.

---

The city Changsha is the capital of Hunan Province. It is located in the southwest of China. More than 5000 taxis and private cars equipped with GPS devices are travelling in the urban network every day. Every 30s, information about vehicle positions, speeds and time stamps is sent to the monitoring centre. Figure E.1 illustrates the test corridor we selected for our research. Total three bidirectional links and four signalized intersections are considered. We name the intersections and links with numbers for the simplicity purpose. The intersections are 3, 8, 11 and 13 as shown in figure E.1. The northbound links include:

- Link 13-11
- Link 11-8
- Link 8-3

The southbound links include:

- Link 3-8
- Link 8-11
- Link 11-13

The intersections on the test road are controlled by an adaptive control system called SCATS system. The cycle time and green splits change from time to time according to traffic demand.



Figure E.1: The test road in Changsha city, Hunan Province, China

# Appendix F

## Complete link travel time estimation from GPS data

---

**Note.** Chapter 3 proposes a Neural Network model to estimate complete link travel times from GPS data. However, due to the fact that there is no ground-truth data and insufficient real-life GPS data to train the Neural network model, we applied a method proposed by Li (Li et al., 2010) to estimate the complete link travel times. The estimated travel times are used for the validation purpose in chapters 5 and 7.

---

Figure F.1 illustrates an example of a probe vehicle traversing different links. The information of probe vehicle positions, time stamps and speeds is recorded. The method proposed by Li (Li et al., 2010) is basically an interpolation process. The estimation results show that this method is quite accurate with Root Mean Square Percentage Error of 5.9% for estimating the average link travel time when the probe vehicle penetration rate is 5%. As shown in Figure F.1,  $t_1(i)$ ,  $t_2(i)$ ,  $t_3(i)$ ,  $t_4(i)$  are time stamps of probe vehicle  $i$ ;  $v_1(i)$ ,  $v_2(i)$ ,  $v_3(i)$ ,  $v_4(i)$  are instant speeds of probe vehicle  $i$ . In order to derive the complete link travel time of link 2, time stamps  $t_{up}(i)$ ,  $t_{down}(i)$ , which are the start moment when the probe vehicle passes the stop line at the upstream intersection and the end moment when the probe vehicle passes the stop line at the downstream intersection, need to be estimated. The start moment passing the stop line at the upstream intersection can be estimated using Equation (F.1) and (F.2) as:

$$\hat{a}_{t_1 \rightarrow t_2}(i) = \frac{v_2(i) - v_1(i)}{2(d_2 + d_1)} \quad (\text{F.1})$$

$$t_{up}(i) = t_2(i) - \frac{1}{\hat{a}_{t_1 \rightarrow t_2}(i)} (v_2(i) - \sqrt{v_2(i)^2 - 2\hat{a}_{t_1 \rightarrow t_2}(i)d_2}) \quad (F.2)$$

Similarly, the end moment arriving at the stop line of the downstream intersection can be estimated as:

$$\hat{a}_{t_3 \rightarrow t_4}(i) = \frac{v_4(i) - v_3(i)}{2(d_3 + d_4)} \quad (F.3)$$

$$t_{down}(i) = t_4(i) - \frac{1}{\hat{a}_{t_3 \rightarrow t_4}(i)} (v_4(i) - \sqrt{v_4(i)^2 - 2\hat{a}_{t_3 \rightarrow t_4}(i)d_4}) \quad (F.4)$$

Therefore, the complete link travel time of probe vehicle  $i$  passing link 2 is derived as:

$$TT(i) = t_{down}(i) - t_{up}(i) \quad (F.5)$$

Where  $\hat{a}_{t_1 \rightarrow t_2}(i)$  and  $\hat{a}_{t_3 \rightarrow t_4}(i)$  are the average acceleration of probe vehicle  $i$  between point 1 and point 2, point 3 and point 4, respectively;  $d_1$ ,  $d_2$  are the distances from start moment to point 1 and point 2;  $d_3$ ,  $d_4$  are the distances from the end moment to point 3 and point 4.

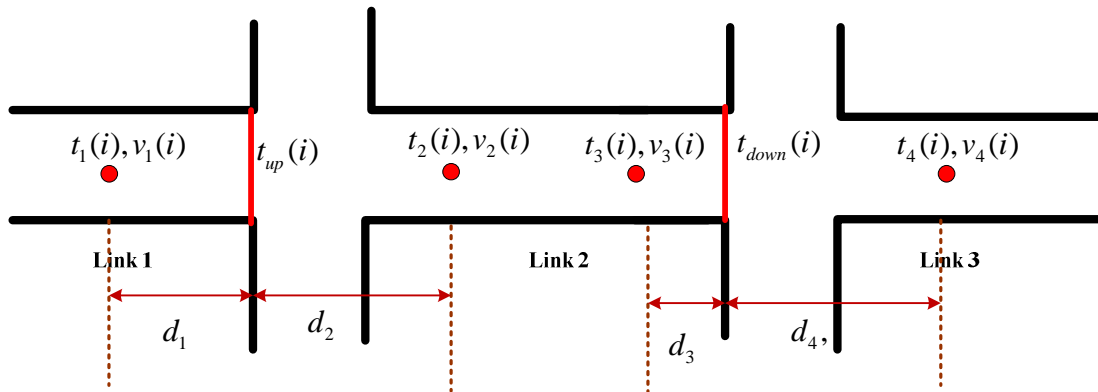


Figure F.1 Calculation of complete link travel time

# Summary

Urban travel times are intrinsically uncertain due to a lot of stochastic characteristics of traffic, especially at signalized intersections. A single travel time does not have much meaning and is not informative to drivers or traffic managers. The range of travel times is large such that certain travel times can occur for congested conditions as well as off-peak situations. Therefore, it is better to consider the whole distribution of travel times. The knowledge of travel time variability (uncertainty) is in fact important both in the evaluation of Dynamic Traffic Management measures and traveller's choices. Particularly in the Netherlands, one of the policy goals is to improve the door-to-door travel time reliability. Providing travel time variability information can help different types of travellers make better route choice decision for different purposes. Risk-averse travellers tend to choose more reliable routes even if they have higher mean travel times. While for opportunity-seekers, routes with lower mean travel times but higher uncertainty are more appealing.

## *Travel time variability in urban areas*

The importance of travel time variability in urban networks has received more and more attention during the past years. However, the investigation of travel time variability as done by most researchers is just in a phenomenological descriptive way by fitting some distribution functions (e.g., log-normal, gamma) to observed travel times. The problem arises when applying these distributions to different traffic conditions since they are only calibrated for a specific traffic situation. The character of urban travel times is represented by a specific probability distribution which can be influenced by different traffic processes (e.g., traffic flow, traffic control). The understanding of fundamental mechanisms of urban travel times can help to better deal with travel time variability, predict travel time variability and furthermore influence travel time variability. Therefore, this thesis focuses on developing a theoretical travel time distribution model which can explain these mechanisms and can be generalized to different traffic conditions.

## *Link travel times from probe vehicles*

We started our research by obtaining 'ground truth' field link travel time data. These data

are valuable for model calibration and validation. Different monitoring techniques (ANPR cameras, probe vehicles, Bluetooth devices) for measuring urban travel times were compared. We focused on estimating the complete link travel time from the GPS probe vehicle data with low polling frequencies (e.g., 30s, 1 min). Due to the fact that the available data are the positions of probe vehicles at fixed time intervals, which means that travel times directly obtained from GPS data are likely to be partial link or route travel times, we need to estimate the complete link/route travel times from GPS data. Three methods were applied in this study, namely, the distance-proportion method, Hellinga's method and an Artificial Neural Network (ANN) model. The estimation results showed that the ANN method gives the best performance.

### ***Verification of the travel time distribution model***

On urban roads, the variability of the delay at intersections is the main source of travel time variability. We started developing an analytical delay distribution model for a single fixed-time controlled intersection. The model considers stochastic properties of traffic flow, and stochastic arrivals and departures at the intersection. The influence of stochastic arrivals on the delay distribution has been particularly investigated by looking at different arrival distributions, e.g., Poisson, Binomial. In the undersaturated condition, different arrival distributions have marginal influence on the delay distribution. The comparison of delay variability in different traffic conditions shows that the delay is more uncertain in undersaturated conditions than in oversaturated conditions. This gives more insight into travel time estimation and prediction on urban roads. The uncertainty of delay in undersaturated conditions should be particularly taken into account in order to have better estimation and prediction results.

We extended the delay distribution model from a single intersection to multiple intersections. The signal coordination between two intersections is explicitly modelled. Different offset settings from well-coordinated to badly coordinated situations were investigated under different traffic conditions. Furthermore, the free flow travel time distribution has been incorporated into the delay distribution model in order to derive a complete travel time distribution. The numerical results show that the shape of the travel time distribution keeps on changing and shifts towards high values when the mismatch level of two intersections increases (from well coordinated to badly coordinated). This reveals that the way two intersections are coordinated has significant influence on the travel time distribution, especially in undersaturated conditions.

### ***Model calibration and validation***

We compared the travel time distributions from the theoretical model with those from VISSIM simulation data and field GPS data. The comparison results show a very good agreement. The model-estimated travel time distributions can well represent the travel time distributions derived from VISSIM simulation data. The model-estimated link travel time distribution has been compared with that from field GPS data and results show that,

for certain links, the model-estimated link travel time distribution can still represent the real distribution quite well. While for other links, a significant discrepancy between these two distributions can be observed. This discrepancy can be attributed to two reasons: insufficient sample observations with potential estimation errors and mid-link delay which is likely to be observed in the field whereas it is not included in the model.

As a further step, we investigated the possibilities of calibrating the model by observed travel times. The overflow queue is the most important stochastic parameter in the mathematical model for the delay and travel time distribution. In order to estimate the overflow queue distribution, two parameter estimation methods (Least-Squares (LS) and Maximum Likelihood (ML)) have been applied to estimate the overflow queue distribution from traffic measurements (e.g., measured delays or travel times). The Genetic Algorithm was used to find the quasi-optimal solutions for these two methods. The estimation results based on VISSIM simulation data have shown that both the LS method and the ML method can perform well in undersaturated conditions. While in the oversaturated condition, ML method performs better than LS method, which is likely to give biased travel time distribution estimations. The parameter estimation results based on sample delays have revealed that, even with a small sample size, parameters could still be well estimated both in undersaturated conditions and oversaturated conditions. The estimation accuracy is not sensitive to different sampling methods (e.g., Random Sampling or Latin Hypercube Sampling). We also investigated the robustness of parameter estimation. The results show that parameters can be well estimated regardless of different sample size in both the undersaturated condition and the oversaturated condition, as long as the sample size is not too small.

### ***Prediction of travel time distributions***

We applied the model for travel time distribution prediction using both the VISSIM simulation data and the real-life data. The field data was collected in Changsha, China. The prediction procedure requires three input variables, namely, traffic volume, traffic control, and overflow queue distribution. In the field test area, the intersections are controlled by a SCATS system, which is an adaptive network control system. The cycle time and green splits vary from time to time. Therefore, the average traffic control scheme (mainly cycle time and green splits) of the SCATS system for a short time period (30min) is predicted using a neural network model. The overflow queue distribution is predicted by assuming certain arrival distribution (e.g., Poisson, Binomial) and departure distribution (e.g., Binomial) at the upstream intersection using a Markov chain model. The comparison of the model-predicted link travel time distribution with that from VISSIM simulation has shown that the link travel time distribution predicted by the model can well represent the ground-truth distribution of VISSIM with time-dependent traffic demand. The comparison with field GPS data indicates that the link travel time distribution can still be predicted reasonably well for certain links.

### *A new vision of urban travel time*

To conclude, the travel time distribution model developed in this thesis provides a new way to describe and understand travel time variability on urban roads. The proposed model can be easily transferred to different traffic conditions, and can be applied for travel time distribution prediction which is more meaningful for the urban network with a lot of uncertainties involved. By creating the understanding of the fundamental mechanism of travel times on urban roads, it provides the possibilities to influence the travel time variability on urban roads.

# Samenvatting

Stedelijke reistijden zijn intrinsiek onzeker door een groot aantal variabele verkeerskarakteristieken met name bij geregelde kruispunten. Een enkele reistijd is van weinig betekenis en is niet informatief voor automobilisten of verkeersmanagers. Afzonderlijke reistijden lopen dusdanig uiteen dat specifieke reistijden zowel tijdens de spits als er buiten kunnen voorkomen. Daarom is het beter om uit te gaan van de volledige verdeling van reistijden. Het kennis hebben van de variabiliteit (onzekerheid) van reistijden is van belang voor zowel het evalueren van dynamisch verkeersmanagement als ook reizigerskeuze. In Nederland in het bijzonder is het één van de beleidsdoelen om de deur-tot-deur reistijdbetrouwbaarheid te verbeteren. Het aanbieden van informatie over de reistijdvariabiliteit kan daarnaast ook verschillende typen reizigers helpen bij het maken van betere routekeuzen voor verschillende reisdoelen. Risicomijdende reizigers zijn geneigd om te kiezen voor meer betrouwbare routes zelfs als deze routes gemiddeld genomen een hogere reistijd hebben. Dit terwijl voor opportunisten routes met een lagere gemiddelde reistijd en hogere onzekerheid aantrekkelijker zijn.

## *Reistijdvariabiliteit in stedelijke gebieden*

Het belang van reistijdvariabiliteit in stedelijke netwerken heeft meer en meer aandacht gekregen gedurende de afgelopen jaren. Echter, door de meeste onderzoekers wordt reistijdvariabiliteit enkel geanalyseerd op fenomenologische, beschrijvende wijze door een verdelingsfunctie (bv. lognormaal, gamma) te fitten op de geobserveerde reistijden. Wanneer deze verdelingsfuncties worden toegepast op verschillende verkeerscondities ontstaan echter problemen, aangezien zij enkel voor een specifieke verkeerssituatie zijn gekalibreerd. Het karakter van stedelijke reistijden wordt gerepresenteerd door een specifiek verdelingsfunctie welke beïnvloedt wordt door verscheidene verkeersprocessen (bv. verkeersafwikkeling, verkeersregeling). Het begrijpen van de onderliggende mechanismen van stedelijke reistijden verbetert het omgaan met reistijdvariabiliteit, alsmede het voorspellen en beïnvloeden van reistijdvariabiliteit. Deze dissertatie focust daarom op het ontwikkelen van een theoretisch model voor de reistijdverdeling welke deze onderliggende mechanismen kan verklaren en welke gegeneraliseerd kan worden naar verschillende verkeerscondities.

### ***Linkreistijden van probe vehicles***

We zijn het onderzoek begonnen met het verzamelen van *ground truth* linkreistijdgegevens uit het veld. Deze data zijn waardevol voor modelkalibratie en –validatie. Verschillende monitoringstechnieken (automatische nummerplaat herkenning camera's, *probe vehicles*, Bluetooth apparaten) voor het meten van stedelijke reistijden zijn onderling vergeleken. We hebben gefocust op het schatten van complete linkreistijden op basis van laagfrequente GPS data (bv. 30 seconde, 1 minuut) van *probe vehicles*. De beschikbare data beslaan dan de posities van de *probe vehicles* op vastgestelde tijdsintervallen. Daardoor zullen de reistijden welk direct volgen uit deze GPS data doorgaans betrekking hebben op een gedeelte van de link of route. De complete link- en routereistijden moeten geschat worden op basis van deze data. In deze studie zijn drie methoden hiervoor gebruikt, namelijk de *distance-proportion* methode, Hellinga's methode en met behulp van een artificiële neurale netwerk (ANN). De schattingsresultaten laten zien dat de ANN het beste resultaat oplevert.

### ***Verificatie van het reistijdverdelingsmodel***

Op stedelijke wegen is de variabiliteit van de vertraging bij kruispunten de voornaamste bron van reistijdvariabiliteit. Wij zijn daarom begonnen met het ontwikkelen van een analytisch model voor de vertragingverdeling bij een enkel *fixed-time controlled* kruispunt. Het model houdt rekening met stochastische verkeerskenmerken en stochastische aankomsten en vertrekken. De invloed van stochastische aankomsten bij het kruispunt is in het bijzonder onderzocht door te kijken naar verschillende aankomstverdelingen, zoals poisson en binomiaal. Er is gevonden dat voor *onverzadigde* condities verschillende aankomstverdelingen slechts een marginale invloed hebben op de vertragingverdeling. Het vergelijken van de vertragingvariabiliteit laat zien dat de grootte van de vertraging onzekerder is bij *onverzadigde* condities dan bij *oververzadigde* condities. Dit geeft nieuwe inzichten aan reistijdschatting en –voorspelling op stedelijke wegen. De vertragingonzekerheid tijdens *onverzadigde* condities zou meegenomen moeten worden om tot betere schattings- en voorspellingsresultaten te komen.

Het vertragingverdelingsmodel is vervolgens uitgebreid van een enkel kruispunt naar meerdere kruispunten. De afstemming van verkeerslichtregelingen op twee kruispunten is expliciet gemodelleerd. De verschillende mate van afstemming, variërend van goed gecoördineerd tot slecht gecoördineerd, zijn onderzocht onder verschillende verkeerscondities. Daarnaast is de verdeling van de vrije reistijd opgenomen in het vertragingverdelingsmodel om zo te komen tot de complete reistijdverdeling. De numerieke resultaten tonen aan hoe de vorm van de reistijdverdeling continue verandert en groter wordt naarmate de *afstemming* van de twee kruispunten slechter wordt (van goed gecoördineerd tot slecht gecoördineerd). Hieruit blijkt dat de wijze waarop twee kruispunten zijn gecoördineerd met name in *onverzadigde* condities een significante invloed uitoefent op de reistijdverdeling.

### ***Modelkalibratie en -validatie***

We hebben de reistijdverdelingen vanuit het theoretisch model vergeleken met VISSIM simulatiedata en GPS veld data. Deze vergelijking toont heel goede overeenkomsten. De model geschatte reistijdverdelingen komen goed overeen met de reistijdverdeling verkregen van VISSIM simulatiedata. Uit de vergelijking tussen de model geschatte reistijdverdelingen en de GPS veld data blijkt dat voor bepaalde wegvakken het model goede resultaten geeft terwijl voor andere links grote verschillen te zien zijn. Deze verschillen hebben twee oorzaken: onvoldoende observaties welke kunnen resulteren in schattingsfouten en vertragingen in het midden van de link welke waarschijnlijk zijn in het veld, echter niet gemodelleerd worden.

In een volgende stap is gekeken naar de mogelijkheden om het model te kalibreren aan de hand van geobserveerde reistijden. De *overloop* wachtrij, de wachtrij die overblijft aan het eind van de groenfase, is de voornaamste stochastische parameter in het model voor het bepalen van de vertraging- en reistijdverdeling. Om deze *overloop* wachtrijverdeling te schatten, zijn twee schattingsmethoden (*least-squares* (LS) en *maximum likelihood* (ML)) toegepast, gebruikmakend van verkeersmetingen (bv. gemeten vertragingen of reistijden). Een genetisch algoritme is gebruikt om quasi-optimale oplossingen te vinden voor deze beide methoden. Modelschattingen gebaseerd op VISSIM simulatiedata geven goede resultaten in *onverzadigde* condities zowel bij de LS methode als de ML methode. In *oververzadigde* condities geeft de ML methode echter betere resultaten dan de LS methode welke de reistijdverdeling structureel over- of onderschat. Deze parameterschattingen gebaseerd op trekkingen uit de vertragingverdeling laat zien dat, zelfs met weinig trekkingen, parameterwaarden nauwkeurig geschat kunnen worden bij zowel *onverzadigde* als *oververzadigde* condities. De nauwkeurigheid van de schattingen hangt daarbij niet af van de wijze waarop deze trekkingen worden gedaan (bv. willekeurig of *latin hypercube sampling*). Ook is gekeken naar de robuustheid van de parameterschattingen. De resultaten tonen aan dat de parameterwaarden goed geschat kunnen worden ongeacht het aantal trekkingen, zolang het aantal niet te laag is, voor zowel *onverzadigde* als *oververzadigde* condities.

### ***Voorspellen van reistijdverdelingen***

Het model is toegepast voor het voorspellen van de reistijdverdeling gebruikmakend van VISSIM simulatiedata en velddata. De velddata zijn verzameld in de stad Changsha, China. De voorspellingsprocedure maakt gebruik van drie invoervariabelen, namelijk de verkeersvolume, verkeersregeling en de *overloop*wachtrijverdeling. In het gebied waar de velddata zijn verzameld, worden de kruispuntregelingen gestuurd door het SCATS systeem; een netwerk regelsysteem. De cyclustijden en groentijden variëren in de tijd afhankelijk van de verkeerscondities. Het gemiddelde verkeersregelschema (voornamelijk cyclustijden en groentijden) van het SCATS systeem voor een korte periode (30 min) wordt daarom voorspeld met een neurale netwerk model. De *overloop*wachtrijverdeling wordt voorspeld met een *Markov keten* model waarbij veronderstellingen worden gemaakt

over de aankomstenverdeling (bv. poisson, binomiaal) en de vertrekverdeling (bv. binomiaal) bij het kruispunt stroomopwaarts. De reistijdverdeling op een wegvak, zoals voorspeld door het model, komt goed overeen met de verdeling volgend uit de VISSIM simulatie met een dynamische vervoersvraag. Een vergelijking met de GPS veld data laat zien dat de reistijdverdeling op een wegvak redelijk goed voorspeld kan worden voor sommige wegvakken.

### *Een nieuwe kijk op stedelijke reistijden*

We kunnen als conclusie trekken dat het reistijdverdelingsmodel ontwikkeld in dit proefschrift een nieuwe manier verschaft om reistijdvariabiliteit op stedelijke netwerken te beschrijven en te begrijpen. Het ontwikkelde model kan eenvoudig toegepast worden bij verschillende verkeerscondities en kan gebruikt worden voor het voorspellen van reistijdverdelingen welk meer van belang is op stedelijke netwerken gegeven de grote mate van onzekerheden. Door inzicht te brengen in de onderliggende mechanismen welk de reistijden op stedelijke wegen bepalen, creëert deze dissertatie de mogelijkheden om de reistijdvariabiliteit op deze stedelijke wegen te verbeteren.

(Dutch translation provided by Adam Pel)

# 概述 (Summary in Chinese)

随着经济的不断发展，全球交通拥堵问题也越来越严重。因此，各个国家不断在高速路和城市路网中实施各种交通管理策略以改善交通状况，例如，匝道控制、高峰时段车道、限速、交叉口信号控制、出行信息服务系统等。在评价城市路网交通性能的各种指标中，其中一个很重要的指标就是行程时间。行程时间可以直观地反映道路交通运行状况（拥堵还是畅通）。从本质上来说，城市道路行程时间是一个不可确定的变量。这主要归因于城市路网中交通的随机特性，尤其是在交通信号控制路口处存在众多不可预测性因素。单个行程时间对于出行者和道路交通管理部门来说没有太大意义，而且包含的信息量也不够。倘若行程时间范围很大，以至于在拥挤交通状态下某些出行者经历的行程时间也可能在非拥堵（平峰时段）状态下出现。因此，相比之下考虑整个行程时间分布更有意义。掌握行程时间可变性（Travel Time Variability）对于动态交通管理措施的评价和出行者的出行选择行为都是非常重要的。在荷兰，提高门对门的行程时间可靠度已列入了交通政策目标之一。为出行者提供行程时间可变性信息可以帮助不同类别的出行者更好地做出路径选择。一些比较保守的出行者可以选择更可靠的路径，即使该路径的平均行程时间要长一些。而对于那些冒险型（乐观型）的出行者来说，平均行程时间短但不确定性高的路径更有吸引力。

## **城市路网行程时间可变性**

在过去几十年中，城市路网行程时间可变性的重要性得到了越来越多的关注。然而，对于行程时间可变性（不确定性）的研究绝大部分仅限于用现象逻辑学的方法用某些分布函数（例如，对数-正态分布函数，伽马函数）来拟合实测的行程时间数据。由于这些函数模型仅仅在某些特定交通状况下进行过校正，并不能适用于其他不同的交通状况。城市道路行程时间的特性可以用一个特殊的概率分布函数来表示。这一分布函数受不同交通过程（traffic process，例如，交通流、交通控制）的影响。充分理解城市道路行程时间的基本机理可以更好地应对行程时间可变性，预测行程时间可变性，更重要的是影响行程时间可变性（例如，提高行程时间可靠度）。因此，本文的研究重点是建立一个适用于不同交通状况的行程时间分布的理论模型。

## **基于浮动车的行程时间估计**

本文首先着手分析用于获取“真实”路段行程时间数据的技术和方法。实际行程时间数据对于行程时间分布模型的校正和验证都是非常有价值的。目前，用于行程时间数据采集技术主要包括自动车牌识别技术、浮动车技术、蓝牙检测技术等。本

文的重点放在 GPS 浮动车采集技术上, 主要研究如何从 GPS 浮动车采集的数据中估计完整的路段行程时间。由于 GPS 浮动车采集的数据包括采样位置和采样时刻, 这些采样位置可以在道路的任何位置 (如道路中、路口处)。这就意味着直接从 GPS 数据中获得的只是部分路段行程时间, 因而需要采用有效的估计方法获得完整的路段或路径行程时间。本文应用了 3 种不同方法, 即路程比例法 (distance-proportion method)、Hellinga 方法、人工神经网络法 (ANN)。从估计准确度来看, 人工神经网络法的精度最高。

### **城市道路行程时间分布模型**

在城市道路中, 交叉口的延误可变性是整个行程时间可变性的主要来源之一。本文提出了一个针对固定信号配时交叉口的解析延误分布模型。该模型充分考虑了交通流的随机特性、交叉口的车辆到达和离开随机过程。其中, 重点研究了车辆的随机到达分布 (例如, 泊松分布, 二项式分布) 对交叉口延误概率分布的影响。在非饱和和交通状态下, 不同车辆到达分布对于延误分布的影响很小。而对不同交通状态下延误可变性的比较显示: 在非饱和交通状态下的延误比在过饱和交通状态下的延误更具不确定性。这就意味着在非饱和交通状态下, 要得到更准确的行程时间估计或预测, 模型中必须重点考虑延误的不确定性。

本文进一步将单一交叉口的延误分布模型扩展到多交叉口延误分布模型。该模型充分考虑了在不同交通状况下交叉口之间的协调控制, 例如相邻交叉口的相位差设置 (从完全协调控制到不协调控制)。除此之外, 通过将自由流行程时间分布函数和延误分布函数相结合, 本文提出了一个完整的行程时间分布模型。数值计算结果显示, 当相邻交叉口的相位不匹配率增加时 (也即从完全协调控制到不协调控制), 行程时间分布函数的形状不断发生变化, 并且一直沿着更高行程时间方向移动。这也意味着相邻交叉口之间的协调控制方式对于行程时间分布有很大影响, 尤其是在非饱和交通状况下。

本文将基于理论模型的行程时间分布与基于 VISSIM 仿真数据以及实际 GPS 数据的行程时间分布进行了比较。比较结果显示两者之间基本一致 (理论模型和 VISSIM 仿真数据, 理论模型和实际 GPS 数据)。其中, 理论模型估计的行程时间分布能够很好地吻合 VISSIM 仿真得到的行程时间分布。对于实际数据, 某些路段模型估计的行程时间分布能够较好地表示实际 GPS 行程时间分布。而对于另一些路段, 两者之间存在一定的偏差。导致这一偏差的因素主要包括: 1. 实际样本量不足, 而且可能存在误差; 2. 路段延误 (mid-link delay): 理论模型没有考虑路段延误, 只考虑交叉口延误。

### **模型校正和验证**

理论模型建立后, 下一步就是校正模型参数。本文研究了如何通过实测行程时间数据来校正模型参数。在交叉口延误和道路行程时间分布的数学模型中, 最主要的随机参数是二次排队 (overflow queue) 概率分布。为了估计二次排队概率分布, 本文采用了两种参数估计方法, 即最小二乘法 (Least-Squares) 和极大似然估计法 (Maximum Likelihood)。同时, 应用遗传算法求出目标函数 (LS 和 ML) 的准优

解。基于 VISSIM 仿真数据的参数估计结果显示，在非饱和交通状况下，这两种方法的估计精度都较高。而在过饱和交通状况下，ML 的估计精度明显要比 LS 高。LS 参数估计法得到的估计结果往往存在很大的偏差。基于样本数据的参数估计（这里指的是 ML 方法）表明：即使使用少量的样本数据，不管在非饱和交通状况下还是过饱和交通状况下，都能较准确地估计模型参数。参数估计的精度不受采样方法的影响，如随机采样（RandomSampling）或拉丁超立方体采样（Latin Hypercube Sampling）。同时，本文对于参数估计方法的鲁棒性（robustness）也进行了研究。结果表明：只要用于参数估计的样本数量（延误或行程时间）不是很小，不管在非饱和交通状态下还是过饱和交通状态下，参数估计的精度跟样本量的大小之间没有直接关系。

### **行程时间分布预测**

本文还应用该理论模型来预测路段行程时间分布。其中，预测数据分别来自于 VISSIM 仿真软件和实际采集的数据（数据采集地点：长沙）。整个预测过程需要 3 个输入变量：交通流量、交通控制方式以及二次排队概率分布。在测试路网区域内，交叉口是由 SCATS 系统控制的。该系统是一个自适应路网控制系统。信号周期和绿灯相位随着时间不断变化。因此，本文应用神经网络模型来预测短期（30 分钟）SCATS 系统的平均交通控制方式（主要是指平均信号周期和绿灯相位）。溢出车辆排队概率分布则通过马可夫链模型（Markov chain）预测得到的，同时假设某一随机到达分布函数（如：泊松分布，二项式分布）和随机离开分布函数（如：二项式分布）。将模型预测的路段行程时间分布与 VISSIM 仿真的行程时间分布行进比较，结果显示：在动态交通需求情况下，理论模型预测的行程时间分布与 VISSIM 仿真获得的行程时间分布能很好地吻合。对于实际数据中的某些路段，模型预测的路段行程时间分布也能较好地吻合 GPS 浮动车获取的行程时间分布。

综上所述，本文提出的行程时间分布模型为描述和理解城市道路行程时间可变性（可靠性）提供了全新的途径。该模型可以方便地应用于不同交通状况，并且适用于行程时间分布预测，这对于充满不确定性的城市道路来说更有意义。



## About the author: curriculum vitae and list of publications



Fangfang Zheng was born in Pujiang, Zhejiang Province, China, in 1981. She started her bachelor study in 1999 at the school of Information Science and Technology of Southwest Jiaotong University, Chengdu. She received her Bachelor degree in July, 2003. Afterwards, she was recommended to continue her master study at the college of Traffic and Transportation in Southwest Jiaotong University. In 2006, she completed her master thesis and obtained the MSc degree. Thereafter, she started to work in the college of Traffic and Transportation. In 2007, she started her part-time PhD study in Traffic Engineering at the College of Traffic and Transportation.

In March 2008, she started her PhD research in Transportation and Planning, at the Faculty of Civil Engineering and Geosciences, Delft University of Technology, the Netherlands. Her study is funded by the China Scholarship Council (CSC) and University Foundation of Delft (UfD). During her stay at TU Delft, she worked on the subject of urban travel time modelling, especially on the reliability of urban travel times, for which she participated in a Trail Course for PhD students called 'Reliability of Transportation' as one of the lecturers. She also published several Journal papers based on her research work and presented in various conferences. In the conference of Mobil.TUM 2009 in Munich, she presented a paper and for which she won the prize of 'best presentation'.

After her PhD, she will continue her scientific career in the College of Traffic and Transportation in Southwest Jiaotong University, China.

The following publications by the author have been accepted or are still under review: (papers that are presented at multiple conferences are only included once in this list)

### **Journal publications**

1. Zheng, F. and van Zuylen, H.J. (2011). Modeling Travel Time Variability Based on Delay Distribution for Signalized Urban Trips. *Accepted for publication in Transportation Research Record: Journal of the Transportation Research Board.*
2. Zheng, F. and van Zuylen, H.J. (2011). Urban link travel time estimation based on sparse probe vehicle data: an Artificial Neural Network model vs. an analytical model. *Submitted for publication in Transportation Research Part C: Emergency technology (under review)*
3. Zheng, F. and van Zuylen, H.J. (2010). Uncertainty and Predictability of Urban Link Travel Time: A Delay Distributon Based Analysis. *Transportation Research Record: Journal of the Transportation Research Board*, 2192:136-146.

### **Book chapter**

4. van Zuylen, H.J., Zheng, F. and Chen, Y.S. (2010). Using Probe vehicle data for traffic state estimation in signalized urban networks. *International series in operation research and management science: Traffic data collection and its standardization*, Springer.

### **Peer-reviewed conference proceedings**

5. Zheng, F. and van Zuylen, H.J. (2011). Modeling Travel Time Variability Based on Delay Distribution for Signalized Urban Trips. In *proceedings: 90th annual meeting of Transportation Research Board*, Washington D.C.
6. Zheng, F. and van Zuylen, H.J. (2011). Estimating the delay distribution function for an urban trip based on sample measurements. In *proceedings: 90th annual meeting of Transportation Research Board*, Washington D.C.
7. Zheng, F. and van Zuylen, H.J. (2011). Calibration of an urban travel time distribution model. In *proceedings: 2nd International Conference on Models and Technologies for Intelligent Transportation Systems*, Leuven, Belgium.
8. Zheng, F. and van Zuylen, H.J. (2011). Reistijdverwachting voor een stedelijke rit, DVM congres ANWB Verkeerskunde, Rotterdam, the Netherlands.
9. Zheng, F., van Zuylen, H.J. and Chen, Y.S. (2010). An investigation of urban link travel time estimation based on probe vehicle data. In *proceedings: 89th annual meeting of Transportation Research Board*, Washington D.C.
10. Zheng, F. and van Zuylen, H.J. (2010). Uncertainty and Predictability of Urban Link

- Travel Time: A Delay Distribution Based Analysis. In *proceedings: 89th annual meeting of Transportation Research Board*, Washington D.C.
11. Zheng, F. and van Zuylen, H.J. (2010). Comparison of Urban Link Travel Time Estimation Models based on Probe Vehicle Data. In *proceedings: the 7th International Conference on Traffic and Transportation Studies*, Kunming, China
  12. Zheng, F. and van Zuylen, H.J. (2010). Reconstruction of Delay Distribution at Signalized Intersections based on Traffic Measurements. In *proceedings: the IEEE conference on Intelligent Transportation System*, Madeira, Portugal
  13. Zheng, F. and van Zuylen, H.J. (2010). Estimating urban travel time distribution using probe vehicle data. In *Proceedings: 11<sup>th</sup> Trail congress and knowledge Market*. Rotterdam, the Netherlands
  14. Zheng, F., van Zuylen, H.J. and Chen, Y.S. (2009). Investigating the feasibility of urban link travel time estimation based on probe vehicle data. In *proceedings: the 2<sup>nd</sup> International Conference on Traffic Engineering*, Chengdu, China
  15. van Zuylen, H.J., Zheng, F. and Chen, Y.S. (2008). Using Probe vehicle data for traffic state estimation in signalized urban networks. In *proceedings: the international workshop on data collection and its standardization*, Barcelona.
  16. van Zuylen, H.J., Zheng, F. and Chen, Y.S. (2008). Using Probe vehicle data for traffic state estimation in signalized urban networks. In *proceedings: 10<sup>th</sup> Trail Congress and Knowledge Market*. Rotterdam, the Netherlands



# TRAIL Thesis Series

The following list contains the most recent dissertations in the TRAIL Thesis Series. For a complete overview of more than 100 titles see the TRAIL website: [www.rsTRAIL.nl](http://www.rsTRAIL.nl).

The TRAIL Thesis Series is a series of the Netherlands TRAIL Research School on transport, infrastructure and logistics.

Zheng, F., *Modelling Urban Travel Times*, T2011/9, July 2011, TRAIL Thesis Series, the Netherlands

Vlassenroot, S.H.M., *The Acceptability of In-vehicle Intelligent Speed Assistance (ISA) Systems: from trial support to public support*, T2011/8, June 2011, TRAIL Thesis Series, the Netherlands

Kroesen, M., *Human Response to Aircraft Noise*, T2011/7, June 2011, TRAIL Thesis Series, the Netherlands

Nielsen, L.K., *Rolling Stock Rescheduling in Passenger Railways: applications in short-term planning and in disruption management*, T2011/6, May 2011, TRAIL Thesis Series, the Netherlands

Qing, O., *New Approach to Fusion of Heterogeneous Traffic Data*, T2011/5, May 2011, TRAIL Thesis Series, the Netherlands

Walta, L., *Getting ADAS on the Road: actors' interactions in Advanced Driver Assistance Systems deployment*, T2011/4, April 2011, TRAIL Thesis Series, the Netherlands

Lin, S., *Efficient Model Predictive Control for Large-Scale Urban Traffic Networks*, T2011/3, April 2011, TRAIL Thesis Series, the Netherlands

Oort, N. van, *Service Reliability and Urban Public Transport Design*, T2011/2, April 2011, TRAIL Thesis Series, the Netherlands

Mahmod, M.K.M., *Using Co-Operative Vehicle-Infrastructure Systems to Reduce Traffic Emissions and Improve Air Quality at Signalized Urban Intersections*, T2011/1, March 2011, TRAIL Thesis Series, the Netherlands

Corman, F., *Real-Time Railway Traffic Management: dispatching in complex, large and busy railway networks*, T2010/14, December 2010, TRAIL Thesis Series, the Netherlands

Kwakkel, J., *The Treatment of Uncertainty in Airport Strategic Planning*, T2010/13, December 2010, TRAIL Thesis Series, the Netherlands

Pang, Y., *Intelligent Belt Conveyor Monitoring and Control*, T2010/12, December 2010, TRAIL Thesis Series, the Netherlands

Kim, N.S., *Intermodal Freight Transport on the Right Track? Environmental and economic performances and their trade-off*, T2010/11, December 2010, TRAIL Thesis Series, the Netherlands

Snelder, M., *Designing Robust Road Networks: a general design method applied to the Netherlands*, T2010/10, December 2010, TRAIL Thesis Series, the Netherlands

Hinsbergen, C.P.IJ. van, *Bayesian Data Assimilation for Improved Modeling of Road Traffic*, T2010/9, November 2010, TRAIL Thesis Series, the Netherlands

Zuurbier, F.S., *Intelligent Route Guidance*, T2010/8, November 2010, TRAIL Thesis Series, the Netherlands

Larco Martinelli, J.A., *Incorporating Worker-Specific Factors in Operations Management Models*, T2010/7, November 2010, TRAIL Thesis Series, the Netherlands

Ham, J.C. van, *Zeehavenontwikkeling in Nederland: naar een beter beleidsvormingsproces*, T2010/6, August 2010, TRAIL Thesis Series, the Netherlands

Boer, E. de, *School Concentration and School Travel*, T2010/5, June 2010, TRAIL Thesis Series, the Netherlands

Berg, M. van den, *Integrated Control of Mixed Traffic Networks using Model Predictive Control*, T2010/4, April 2010, TRAIL Thesis Series, the Netherlands

Top, J. van den, *Modelling Risk Control Measures in Railways*, T2010/3, April 2010, TRAIL Thesis Series, the Netherlands

Craen, S. de, *The X-factor: a longitudinal study of calibration in young novice drivers*, T2010/2, March 2010, TRAIL Thesis Series, the Netherlands

Tarau, A.N., *Model-based Control for Postal Automation and Baggage Handling*, T2010/1, January 2010, TRAIL Thesis Series, the Netherlands

---

Knoop, V.L., *Road Incidents and Network Dynamics: effects on driving behaviour and traffic congestion*, T2009/13, December 2009, TRAIL Thesis Series, the Netherlands

Baskar, L.D., *Traffic Control and Management with Intelligent Vehicle Highway Systems*, T2009/12, November 2009, TRAIL Thesis Series, the Netherlands

Konings, J.W., *Intermodal Barge Transport: network design, nodes and competitiveness*, T2009/11, November 2009, TRAIL Thesis Series, the Netherlands

Kusumaningtyas, I., *Mind Your Step: Exploring aspects in the application of long accelerating moving walkways*, T2009/10, October 2009, TRAIL Thesis Series, the Netherlands

Gong, Y., *Stochastic Modelling and Analysis of Warehouse Operations*, T2009/9, September 2009, TRAIL Thesis Series, the Netherlands